Synthesis and Exploration of Catalytic and Biochemical Aspects of Molybdenum Complexes in Macroligand Environment

A thesis submitted in partial fulfillment of
the requirement for the degree of

Doctor of Philosophy

By

JEENA JYOTI BORUAH

Registration No. 030 of 2010

Department of Chemical Sciences
School of Sciences
Tezpur University
Tezpur, Assam

June, 2013

Dedicated to -

My Beloved Parents

ABSTRACT

Synthesis and Exploration of Catalytic and Biochemical Aspects of Molybdenum Complexes in Macroligand Environment

ABSTRACT

The thesis presents an account of the findings of investigation on synthesis, characterization and catalytic activity of some new peroxide containing macro complexes of molybdenum(VI), immobilized on polymer supports. The thesis also deals with the studies on interaction of the water soluble polymeric compounds with certain enzymes. The contents of the thesis have been distributed over seven chapters.

Chapter 1 gives a general introduction describing the outline and scope of the present study in the light of known chemistry and biochemistry of molybdenum in general, peroxomolybdenum(VI) (pMo) compounds in particular. The advantages associated with immobilization of metal complexes on insoluble cross-linked resin as well as water soluble polymers are being highlighted. Attention has been drawn to the fact that there is a dearth of information on preparation and application of well-defined polymer supported peroxometallates, despite the enormous progress in the field of metal containing polymers.

In **Chapter 2**, details regarding the materials used and techniques employed for characterization of compounds are presented. Reaction protocols used for evaluation of catalytic activity of the macro complexes as well as, methods for investigating effect of the compounds on various enzyme functions are given.

Chapter 3 deals with the synthesis of dioxomonoperoxo compounds of molybdenum(VI) immobilized on amino acid functionalized Merrifield resin of the type $[MoO_2(O_2)(L)_2]^{2-}$–MR [L = valine (**MRVMo**) (**3.1**) or alanine (**MRAMo**) (**3.2**) and

MR = Merrifield resin]. The fun(tionalized polymers, **MRV** and **MRA** were prepared by reacting the chloromethylated po) /styrene cross-linked with 2% DVB with the respective amino acid in methanol and using)yridine as a base. The reaction of **MRV** or **MRA** with H_2MoO_4 in presence of 30% H_2O_2 afforded the compounds **MRVMo** (**3.1**) and **MRAMo** (**3.2**).

Preparation and characterization of a new supported complex $[MoO_2(O_2)(CN)_2]$-PAN [PAN = poly(acrylonitrile)] (**PANMo**) (**3.3**) is also reported herein. Synthesis was achieved by reacting H_2MoO_4 with 30% H_2O_2 and the macromolecular ligand, PAN at near neutral pH.

The synthesized compounds were characterized by elemental analysis (CHN, AAS and energy dispersive X-ray spectroscopy), spectral studies (UV-Vis, IR, ^{13}C NMR and ^{95}Mo NMR), thermal (TGA) as well as scanning electron micrographs (SEM). A structural feature common to each of the immobilized compound was observed to be the presence of pMo species in its dioxomonoperoxo form. In the compounds, **MRVMo** (**3.1**) and **MRAMo** (**3.2**), the pMo moieties are unidentately co-ordinated via O (carboxylate) atoms of the pendant amino acid ligands. In case of the compound **PANMo** (**3.3**), the pMo moieties are anchored to the polymeric chain through N atom of nitrile groups. All these compounds are stable and non-hygroscopic in the solid state and can be stored dry in closed containers at < 30 °C.

In **Chapter 4,** facile synthesis of a family of peroxomolybdate(VI) complexes attached to water soluble polymeric matrices such as poly(acrylate), poly(methacrylate), poly(acrylamide) and poly(vinylsulfonate) are described. The one-pot synthesis of the compounds was achieved under fairly mild reaction condition by reacting H_2MoO_4 with 30% H_2O_2 and the respective water soluble macromolecular ligand at pH ca. 5. In

addition, it was essential to maintain the temperature at $\leq 4\ ^{o}C$ and the required time (1 h) and limiting water to that contributed by 30% H_2O_2 and alkali hydroxide solution.

The characterization of the compounds were primarily achieved by elemental analysis, spectral studies and other physico-chemical techniques as described under Chapter 3. It is noteworthy that in the soluble macrocomplexes, pMo groups are bound to the polymer chain as oxodiperoxo moieties, $[Mo_2O_2(O_2)_4(carboxylate)]$-PA [PA = poly(sodium acrylate)] **(PAMo)** (**4.1**), $[MoO(O_2)_2(carboxylate)]$-PMA [PMA = poly(sodium methacrylate)] **(PMAMo)** (**4.2**), $[MoO(O_2)_2(amide)]$-PAm [PAm = poly(acrylamide)] **(PAmMo)** (**4.3**) and $[MoO(O_2)_2(sulfonate)]$-PS [PS = poly(sodium vinylsulfonate)] **(PSMo)** (**4.4**), in contrast to the compounds immobilized on insoluble polymers, where they occur as oxomonoperoxomolybdenum(VI) species. In the compounds, **PMAMo** (**4.2**), **PAmMo** (**4.3**) or **PSMo** (**4.4**), the monomeric pMo units are linked to the polymer chain via unidentately co-ordinated O (carboxylate), N (amide) or O (sulfonate) atoms respectively whereas, in **PAMo** (**4.1**), a bridged bidentate co-ordination of the pendant carboxylate group leads to formation of dimeric tetraperoxo molybdate structure.

Chapter 5 comprises of two sections. In **Section A**, the findings of our investigation on activity of insoluble pMo compounds, $[MoO_2(O_2)(valine)_2]^{2-}$–MR (**3.1**), $[MoO_2(O_2)(alanine)_2]^{2-}$–MR (**3.2**) and $[MoO_2(O_2)(CN)_2]$-PAN (**3.3**) as efficient heterogeneous catalysts in selective oxidation of organic sulfides and dibenzothiophene(DBT) with H_2O_2 as terminal oxidant have been documented. The water soluble complexes, $[Mo_2O_2(O_2)_4(carboxylate)]$-PA (**4.1**), $[MoO(O_2)_2(carboxylate)]$-PMA (**4.2**), $[MoO(O_2)_2(amide)]$-PAm (**4.3**) and $[MoO(O_2)_2(sulfonate)]$-PS (**4.4**), on the other hand served as homogeneous catalysts in sulfide oxidation and the results are incorporated in **Section B**.

A series of structurally diverse sulfides and dibenzothiophene (DBT) undergo clean and selective oxidation to sulfoxide or sulfone by H_2O_2, at room temperature with high turnover frequency (TOF), under adjusted reaction conditions in presence of each of the polymer bound pMo compounds used as catalyst. The synthetic protocols are operationally simple, high yielding, halogen free and environmentally acceptable. All the catalysts, irrespective of being heterogeneous or homogeneous, showed excellent chemoselectivity towards sulfur group of substituted sulfides with oxidation prone functional groups such as allylic, vinylic, benzylic or alcoholic groups. The heterogeneous catalysts, **3.1-3.3** could be regenerated and reused for at least up to six cycles of reaction without loss of their catalytic activity as well as product selectivity. Catalytic activity of the homogeneous catalysts, **4.1-4.4**, on the other hand gradually decreases with increasing number of cycles. The data obtained from the study thus demonstrated that the heterogeneous catalysts exhibit superior catalytic activity over homogeneous analogues both in terms of yield as well as recyclability.

Chapter 6, which is distributed over two sections, describes the activity of the supported pMo complexes in oxidative bromination of organic substrates. The results included in **Section A** demonstrated that the polymer supported complexes $[MoO_2(O_2)(valine)_2]^{2-}$–MR (**3.1**), $[MoO_2(O_2)(alanine)_2]^{2-}$–MR (**3.2**) and $[MoO_2(O_2)(CN)_2]$-PAN (**3.3**) with monoperoxomolybdate moieties heterogeneously catalyzed the oxidative bromination of a variety of activated aromatics to afford the corresponding bromo organics in presence of H_2O_2, in impressive yield. The reaction takes place under environmentally clean condition in aqueous-organic medium, at ambient temperature with KBr or Et_4NBr as bromide source, instead of elemental bromine. The catalysts could be easily recovered and reused for subsequent reaction cycles.

It is noteworthy that the water soluble polymeric compounds with diperoxomolybdate species **4.1-4.4**, as apparent from the data presented in **Section B**, could also efficiently mediate oxidative bromination of organic substrates in absence of H_2O_2 in aqueous-organic media, in contrast to the insoluble supported monoperoxomolybdenum complexes, **3.1-3.3** which were ineffective in bromination on their own.

The bromination activity of supported pMo compounds, **3.1-3.3** and **4.1-4.4** in water was explored as well, by using method of de Boer et al. with phenol red as substrate. The reaction was monitored spectrophotometrically as the product bromophenol blue was formed with absorption at 592 nm with a gradual decrease in absorbance of the peak at 433 nm due to loss of phenol red. The homogeneous pMo compounds, **4.1-4.4** can stoichiometrically brominate phenol red by utilizing half of its coordinated peroxides under physiological pH, an essential requirement of a biomimetic model. A mechanistic pathway has been proposed based on the above results.

In **Chapter 7**, the results of our investigation on some of the biologically important activities of the water soluble polymer bound complexes, **4.1-4.4** and free monomeric compounds, $[MoO(O_2)_2(glycine)(H_2O)]$ (**DMo_1**) (**7.1**) and $[MoO(O_2)_2(asparagine)(H_2O)]$ (**DMo_2**) (**7.2**), are documented. We endeavoured to draw comparison between the two types of pMo compounds, macro as well as neat, with respect to their tested properties. The effect of catalase, the ubiquitous enzyme that catalyze the degradation of H_2O_2 in the intercellular peroxisomes, on the pMo compounds have been examined. From the rates of degradation of the compounds under the effect of catalase, it was clear that the polymer bound pMo species were nearly 100 fold weaker as substrate to catalase compared to its natural substrate H_2O_2. On the other hand, the monomeric pMo complexes, **DMo_1** (**7.1**) and **DMo_2** (**7.2**) were observed to undergo rapid

degradation, with loss of peroxide within approximately 5 min of incubation with catalase. The relatively higher resistance of the peroxomolybdenum moiety in the macro ligand environment to catalase action is likely to be a consequence of additional stability imparted to the compounds by the polymeric support through immobilization.

The stability of water soluble polymer bound pMo compounds, **PAMo (4.1)**, **PMAMo (4.2)**, **PAmMo (4.3)** and **PSMo (4.4)** has been examined in solution of a wide range of pH values. The evidences gathered by determining their peroxide content, monitoring the absorbances in the electronic spectra as well as ^{13}C and ^{95}Mo NMR at specified time intervals, revealed that the compounds remain stable in solution of acidic as well as higher pH for at least 12 h.

It has been observed that pMo compounds are potent inhibitors of membrane associated phosphohydrolases: alkaline phosphatase (ALP) and acid phosphatase (ACP). The enzyme inhibitory effects of the compounds were studied by using standard enzyme assay systems with p-nitrophenyl phosphate (p-NPP) as substrate. Glycine buffer (pH =10.0) and acetate buffer (pH = 4.6) were used in assays for ALP and ACP, respectively. The half-maximal inhibitory concentration (IC_{50}) for each inhibitor were graphically determined which gave rise to a 50% suppression of the original enzyme activity and kinetic parameters (V_{max} and K_m) were determined by using Lineweaver-Burk plots. The two classes of compounds with their IC_{50} and K_i values varying in the range of < 2 μM (for ACP) to 50 μM (for ALP) exhibit distinct mechanistic preferences as phosphatase inhibitors. The polymer bound pMo complexes, **4.1-4.4** behave as classical non-competitive inhibitors whereas the neat mononuclear pMo complexes, **DMo_1 (7.1)** and **DMo_2 (7.2)** are mixed type of inhibitors of ALP and ACP. The two classes of enzymes however, responded differently towards the inhibitor species as evident from the IC_{50} and

K_i values, which were more than 20 orders of magnitude lower for ACP than those observed for ALP.

The major part of the results of studies described in **Chapters 3-7** have been published and the rest is under communication.

Declaration

I hereby declare that the thesis entitled "***Synthesis and Exploration of Catalytic and Biochemical Aspects of Molybdenum Complexes in Macroligand Environment***" being submitted to the Department of Chemical Sciences, Tezpur University, is a record of original research work carried out by me. Any text, figures, results or designs that are not of own devising are appropriately referenced in order to give credit to the original author(s). All sources of assistance have been assigned due acknowledgement. I also declare that neither this work as a whole nor a part of it has been submitted to any other university or institute for any other degree, diploma or award.

Jeena Jyoti Boruah

Place: Tezpur (Jeena Jyoti Boruah)

Date: 31/5/13

TEZPUR UNIVERSITY

(A Central University Established by an Act of Parliament)

NAPAAM, TEZPUR-784028

DISTRICT :: SONITPUR :: ASSAM :: INDIA

Ph: 03712-267004
03712-267005
Fax: 03712-267006
03712-267005

I certify that the thesis entitled "***Synthesis and Exploration of Catalytic and Biochemical Aspects of Molybdenum Complexes in Macroligand Environment***" submitted to the Tezpur University in the Department of Chemical Sciences under the School of Sciences, in partial fulfillment for the award of the degree of Doctor of Philosophy in Science is a record of research work carried out by Miss Jeena Jyoti Boruah under my supervision and guidance.

All help received by her from various sources have been duly acknowledged.

No part of this thesis has been submitted elsewhere for award of any other degree.

N. S. Islam

Place: Tezpur University
Date: May 31, 2013

(Prof. Nashreen S. Islam)
Professor
Department of Chemical Sciences
School of Sciences

Acknowledgement

First and foremost, I extend my heart-felt regards and deepest appreciation to my esteemed research guide Prof. Nashreen S. Islam, Department of Chemical Sciences, Tezpur University, whose profound learning, life long research experience and venerable scientific temperament help me to carry out my research work. Her hard work, dedication towards research and indomitable spirit has not only boosted me to carry out my present research work with great confidence, vigour and vision but will always be remembered as constant source of motivation and inspiration in every walk of my life.

I take this opportunity with great pleasure to express my sincere gratitude to our honourable and distinguished Prof. M. K. Chaudhuri, Vice-Chancellor, Tezpur University for his constructive suggestions and rock solid institute building attitude, by dint of which every research scholar can avail state-of the art laboratory facilities and a scientific work environment in the institute premise itself.

I am also indebted to the authorities of Tezpur University who have extended co-operation and support to me and the entire community of the Department of Chemical Sciences for allowing me to use the administrative and technical facilities for my research work.

I convey my heartiest thanks and gratitude to Prof. N. Karak, Head, Department of Chemical Sciences along with all the faculty members of the Department of Chemical Sciences for their precious advice and help during the course of my research work.

I deeply acknowledge Prof. S. K. Dolui, and Dr. Ruli Borah, members of my doctoral research committee for their constant support, suggestions and inspirations during the entire course of my research.

I am always grateful to Prof. R. C. Deka, Department of Chemical Sciences, specially because of his immense help with my theoretical work. It gives me immense pleasure to thank Dr. Pankaj Bharali and Kusum Kumar Bania for his selfless advice, fruitful discussions, and ever readiness to help who will remain ever green in my heart.

I would like to offer my sincere thanks to Dr. Biren Gohain, Dr. Binoy Saikia, Nipu Dutta, Rajen Borah, Raju Kumar Borah, Sankur Phukan, Biraj Borah, Arup Chakrabarty, Monoranjan Sarma, Ratan Baruah, Prakash Kurmi for assisting me in handling different analytical instruments. I also acknowledge Hemantada, Prafulla, and Babita for their corporation and help.

I take this opportunity to sincerely acknowledge Tezpur University for the institutional Fellowship and Council of Scientific & Industrial Research (CSIR) for

providing financial assistance in the form of Senior Research Fellowship (SRF) which buttressed me to perform my work comfortably.

A heartfelt bouquet of appreciation goes to my senior lab mates Dr. Pankaj Hazarika, Dr. Diganta Kalita and Dr. Siva Prasad Das for their manifold help and active co-operation over all these years. My special thanks go to the present group members Seshadri and Sandhya for their constant inspiration, friendship and help during my research work.

My life at Tezpur University would not have been so productive, enjoyable, lovable and memorable had it not been for my ever inquisitive, energetic and active friends that have become a very important part of my life. I take this opportunity to sincerely appreciate and reciprocate the warmest and heartfelt best wishes with all my friends especially Kalyanda, Papia, Parishmita, Pinky, Mamon, Arup, Binodda, Harekrishnada, Subratada, Surajitda, Isha, Gautam, Biplab, Amar, Ankur, Buddha, Rashmi, Bornali, Rasna, Ujjal, Dhrubajyoti, Satyajit, Vijoy, Murshid, Iftikar, Swaswat, Pankaj, Prasanta, Shreemoyee, Anisha, Rekha, Sweety, Chandamika, Monalisha, Subhi, Dipshikhaba, Nimisha, Jutikaba, Biswajit, Mithu, Chinmoy, Arandao and all other research scholars.

Last but not the least, I would like to acknowledge the love and endless support of my dear parents who have always inspired me right from my childhood, celebrated all of my success, picked me up at times of distress, instilled in me confidence for life time. My true love goes to for my brother, Dhruba and little sister Renika, who cheer me up throughout my research work to make it worthwhile. I have no any words to express my gratitude to Dhan Mama, Halen Mami, Setona mahi, Bhadra moha, Purna uncle and Hiranya aunty whose encouragement and inspiration lift me uphill to this phase of my life. I cannot but take pleasure in thanking my niece Bijaylakshmi and Rajlakshmi keeping me always cheer up during my Ph. D. tenure.

Thank God, and thank you all who have directly or indirectly contributed towards my successful completion of the thesis work.

Department of Chemical Sciences
Tezpur University
Date: 31/5/13

Jeena Jyoti Boruah
(Jeena Jyoti Boruah)

CONTENTS

Page no.

List of Abbreviations

ACP	acid phosphatase
ALB	albumin
ALP	alkaline phosphatase
CTS	chitosan
DBT	dibenzothiophene
DMF	dimethyl formamide
CSDVB	cross-linked poly(styrene-divinyl benzene)
DNA	deoxyribonucleic acid
DTG	differential thermogravimetry
DX	dextran
EDTA	ethylenediaminetetraacetic acid
EDX	energy dispersive X-Ray analysis
GC	gas chromatography
HIV	human immunodeficiency virus
HMPA	hexarnethylphosphoric triamide
HMPT	hexamethylphosphorous triamide
HPLC	high Performance Liquid Chromatography
IC_{50}	half-maximal inhibitory concentration
IR	infra red
insRTK	insulin receptor tyrosine kinase
LMCT	ligand to metal charge transfer
MPS	methyl phenyl sulfide
MR	Merrifield resin
NMR	nuclear magnetic resonance
ODS	oxidative desulfurization
PA	poly(sodium acrylate)
PAA	polyacrylic acid
PAm	poly(acryl amide)
PAN	poly(acrylonitrile)
PAV	$Na_3[V_2O_2(O_2)_4$(carboxylate)]–PA
PEG	poly(ethylene glycol)

PEI	polyethyleneimine
PEO	poly(ethylene oxide)
PMA	sodium polymethacrylate
PMAA	*poly(methacrylamide)*
PMMA	poly(methylmethacrylate)
pMo	peroxomolybdate
PNs	polyphosphazenes
polyP	polyphosphates
POX	polyoxazoline
PS	poly(styrene)
PSNa	poly(sodium vinyl sulfonate)
pic	picolinato
p-NPP	p-nitrophenyl phosphate
p-NP	p-nitrophenol
PTC	phase transfer catalyst
pV	peroxovanadate
PVA	polyvinyl alcohol
P(4-VP)	poly(4-vinyl pyridine)
pW	peroxotungstate
PTPase	phosphotyrosine phosphatase
RT	room temperature
RNA	ribonucleic acid
SEM	Scanning electron microscopy
TEAB	Tetraethylammoniumbromide
TG	thermogravimetry
TLC	thin layer chromatography
TMB	*1,3,5-trimethoxybenzene*
TOF	turnover frequency
TON	turnover number
V-BPO	vanadium bromoperoxidase
V-HPO	vanadium haloperoxidase
WSP	Water soluble polymer
XG	xanthan gum

List of Tables

List of Figures

List of Schemes

CHAPTER 1

INTRODUCTION

1.1 Preamble

Modification of organic polymers by attaching transition metal complexes constitutes one of the most thriving areas of current research. Materials with unique properties are usually obtained by having a metal complex or a metal as part of a macromolecule.[1-6] Anchoring of peroxometallates to water soluble polymers has recently been recognized as a promising new field.[7] Peroxo complexes have been for the past several decades object of intense investigation, due to their potential catalytic, biochemical and therapeutic applications.[8-14] A facile route to newer members of peroxometal containing macromolecules opens the possibility of finding novel catalysts and biologically active agents. The work presented in this thesis is therefore, focused on synthesis, characterization and exploration of biochemical as well as catalytic activity of some new peroxide containing macrocomplexes of molybdenum (VI).

In this Chapter we present a concise review of the following interrelated areas relevant to the work embodied in the thesis:

(i) Immobilization of metal complexes on insoluble cross-linked resin as well as water soluble polymer matrices.

(ii) Selected aspects of molybdenum co-ordination chemistry and biological significance of Mo and its compounds.

(iii) Peroxo compounds of molybdenum – chemistry, importance in catalysis and their biochemical relevance.

1.2 Metals and metal complexes bound to macromolecules – General aspects

Anchoring of an active transition metal complex to a functionalized polymer is fascinating from the perspective of designing effective catalysts as well as modeling of complex biomolecules and bioprocesses. Polymers containing metals or metal complexes have emerged as a new generation of material in the light of their extensive applications in diversified fields including, catalysis, medicine, ecology, hydrometallurgy, ultra-high strength and superconducting materials, liquid crystals, electronics device and waste water treatment.[1-6,15,16]

Besides carbon, the main elements in chain or network forming organic macromolecules are O, N, P, S and Si.[17] Organic macromolecules are generally limited in most cases by their low thermal stability and relatively weak ability to take part in such important processes as binding interactions, activation of small molecules, electron transfer processes and therapeutic effects.[17] Therefore, development of new materials incorporating other elements is of fundamental importance. Various combinations of metal complexes or metals with organic, inorganic and semi-organic macromolecules exist.[17] Several methods have been employed for this purpose such as adsorption, encapsulation, covalent and coordination bonding and ion exchange and gel immobilization.[19,20]

The polymeric matrix may bind with the metal complexes either through monodentate binding or by either intra or inter polydentate binding. The polymer support usually contributes to coordination unsaturation of a central metal ion and at the same time prevents aggregation of active sites, and must be chemically and thermally stable.[19] Diverse approaches to prepare polymer supported complexes as well as a variety of names for supporting processes such as immobilization, anchoring, attachment

"heterogenization of homogeneous complexes" have been proposed.[19] According to the classification proposed by Wohler, a metal complex[21] or metal can be part of a macromolecular chain or network by any of the following ways:

Type I: Binding of metals at a macromolecule – "Macromolecular Metal Complexes"

In this type, as shown in Fig. 1.1, a metal ion, a metal complex or metal chelate is attached to a linear or cross-linked organic polymer via a covalent, a coordinative (at the metal), a complex (at the ligand of the complex), an ionic or π-type bonds (Fig. 1.1) to form the macromolar metal complex. Besides these, binding at the surface of a carrier or the end group of a macromolecule are other possible modes of attachment of the metal to the polymer.

Type II: Ligand of metal complexes as part of a macromolecular chain – "Ligand Macromolecular Complexes"

This class of macromolecular metal complexes (Fig. 1.2) can be obtained by polyreactions of either a multifunctional ligand/metal complex or a multifunctional ligand metal complex precursor. Instead of direct synthesis of polymer metal complexes from low molecular precursors, a macromolecular ligand can be prepared first which is then metallated in a second step.

Type III: Metal complexes or metals as part of a linear or crosslinked macromolecule via the metal – "Metal Macromolecular Complexes"

In this type, homochain or heterochain polymers with covalent bonds to the metal, coordinative bonds between metal ions and a polyfunctional ligand (coordination

polymers), π-complexes in the main chain with a metal, cofacially stacked polymer metal complexes and different types (polycatenanes, polyrotaxanes, dendrimers with metals) are dealt (Fig. 1.3).

Type IV: "Macromolecule Incorporated Metal Complexes"

New composite materials have been synthesized by physical incorporation and stabilization of metal clusters or metal complexes in macromolecular environment (Fig. 1.4) and have become an important field.

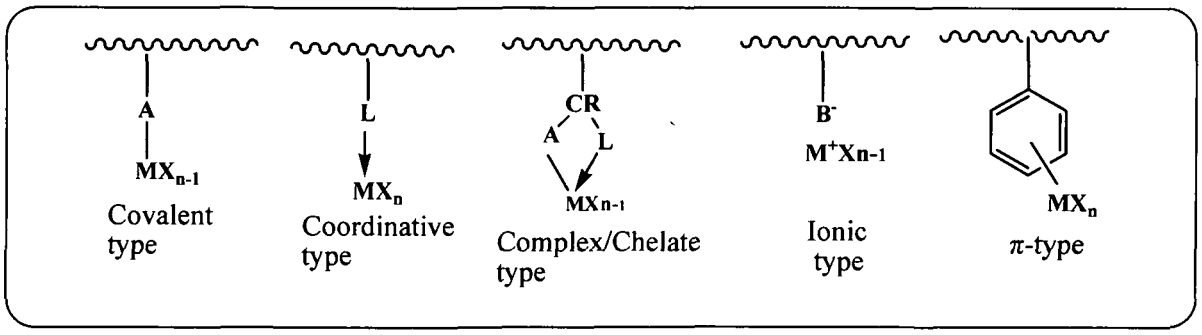

Fig. 1.1 Type I: Metal ions, complexes, chelates at macromolecules.[21]

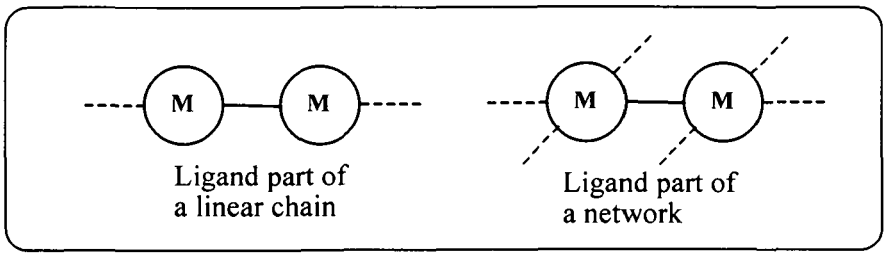

Fig. 1.2 Type II: Ligand of metal complexes, chelates as part of linear or crosslinked macromolecules.[21]

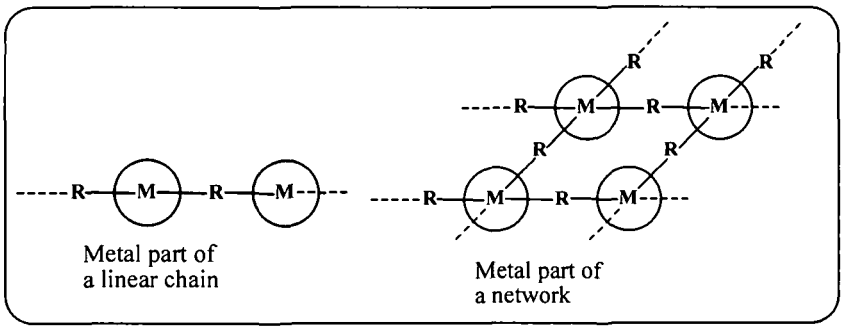

Fig. 1.3 Type III: Metals as part of a linear chain or network.[21]

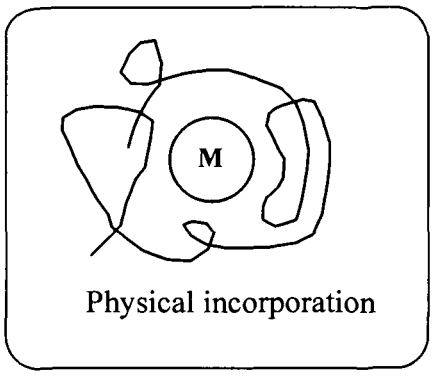

Fig. 1.4 Type IV: Physical incorporation of metal complexes, chelates.[21]

Different polymeric materials, natural and synthetic, prepared both by addition and condensation polymerization, are reported as matrices to anchor complexes (Table 1.1). The great variety of possible combinations of metal complexes with the available macroligands are summarized in Table 1.1. The interaction of metal complexes MX_n to macromolecule may occur either through monodentate binding or by either intra or inter polydentate binding. In the case of linear or branched organic polymer the macromolecular metal complexes are soluble in organic solvents and their structure can be identified rather easily. The solubility of bridged macromolecular metal complexes decreases and they are more stable and have less defined structure. The complexes with intermolecular bridge bonds are insoluble and difficult to characterize. The active transition metal complex may be supported on insoluble or soluble polymeric supports as discussed below in section 1.2.1 and 1.2.2 with each type of the support being associated with some advantages as well as disadvantages.

Table 1.1 The summary of combinations of metal complexes and macroligands, as well as catalyzed reactions most commonly used in practice[22]

Polymer support	Functional group	MX_n	Catalysed reaction
Phosphinated CSDVB	$-PPh_2$	$RhCl(PPh_3)$ $[CODRhCl]_2$ $Rh(CO)_2(PPh_3)_2$ $PdCl_2(PPh_3)$ $RuCl_2(CO)_2(PPh_3)_3$ $RhHCO(PPh_3)_3$ $[COdRhCl]_2$ $Cocl_2(PPh_3$ $Mo(CO)_2(PPh)_2$ $Fe(CO)_4PPh_3$	Hydrogenation Hydroformylation Deuterium/hydrogen exchange Isomerisation Oligomerisation Cyclooligomerisation
CSDVB	Dipy Cp $NH_2CH_2CH_2NH_2$	$Pd(OCOCH_3)_2$ $CpTiCl_3$ $Pt(PhCN)_2Cl$	Hydrogenation
PA	-	Ni(napht)	PhA hydrogenation
PEI/SiO2	NH	Pd^0	nitrobenzene
PE-gr-P4VP	Py	$PdCl_2(PhCN_2)$	p-Nitrochlorobenzene hydrogenation
PMMA	$-COOCH_3$	Pd^0	Nitrocompound hydrogenation
PTFE	-	Au^0	Deuterium/hydrogen exchange
CSDVB	$-NMe_2$	MCl_2(Pt,Ru)	Hydrosilylation
PE-gr-PAAc	-COOH	Co(AcAc)	Cyclohexene oxidation
PAN	-C≡N	$M(AcAc)_2$(M= Mn,Co)	Ethyl benzeneIsoprpyl benzene oxidation
Polystyrene-co-divinyl-benzene-2-Me-5-VP)	N-	Cu^{2+}	
CSDVB		Co,Ni,VO, CO, Fe, Mn,phtalocyanines	Cyclohexene oxidation
PEG	- OCH_2CH_2 -	MCl_2(M= Co, Mn, Cu) Co^{2+} ,Cu^{2+}	Teralin oxidation H_2O_2 oxidation
Poly(2-vinylpyridine-co-styrene)		Fe^{3+},Co^{2+},phthalocyanines	H_2O_2 oxidation
Phosphate cellulose	$-PO_2OH$	V^{5+},Mo^{5+}	Cyclohexene epoxidation
Chloromethylated CSDVB		Dithiocarbamate, Mo^{5+}	Olefin epoxidation
P4VP	-N	Cu^{2+}	Dialkylphenol oxidation
Polyvinylamine	$-NH_2$	Co^{2+}, Fe^{3+},	Thiol oxidation

Continued...

		Cu^{2+},phthalocyanines	
P4VP	-N	Cu^{2+}	Ascorbic acid oxidation
PMMA	C=O	$TiCl_4$,VCl_4	Ethylene polymerisation
PE-gr-PAAI	-OH	$Ti(OBu_4)_4$	Ethylene polymerisation
PE-gr-P4VP	-N -N	$TiCl_3$ $CoCl_2$	Stereospecific propylene polymerisation 1,4-cis-butadiene polymerisation
Copolymer of styrene and acrylic acid	-COOH	$Ni(napht)_2$	1,4-cis-butadiene polymerisation
PE-gr-PAAc	-COOH -COOH	$Ni(CH_3COO)_2$ Ni^{2+}, V^{4+}	Ethylene polymerisation "Relay-race" ethylene copolymerisation
Triple copolymer of ethylene propylene and P4VP	-N	$CoCl_2$, $NiCl_2$	Butadiene di and oligomeerisation
PS	-	$AlCl_3$,$TiCl_4$	Styrene and ethyl styrene polymerisation
PE-grPAAI	-OH	$MoCl_5$,WCl_5,Cu^{2+}	PhA polymerisation
CSDVB-P4VP	-N	Cu^{2+}	Oxidative polycondensation of phenols
PE-gr-PAAc	-COOH	$Co(OCOCH_3)_2$	Phenol formaldehyde oligomers solidification
CSDVB	Cp	$CpCo(CO)_2$	Fischer-Tropsch synthesis
PEI	-NH	$RhCl_3$	Methanol carbonylation
PVAI	-OH	Cu^{2+}	2,4 dinitrophenyl acetate hydrolysis
CSDVB		$TiCl_4$	Etherification Alkylation, acetalisation
Copolymer of styrene and AAc	-COOH	Cp_2TiCl_2	Reduction of nitrogen to ammonia
Thioacetalderivatives of poly(4-amino-styrene)	$-CH_2$ $-NH_2$	$-Mo(NMe_2)_4$ -	Nitrogen reduction Photocatalytic hydrogen formation
PEI	-NH	Rh^{3+}	Formation of H_2 from H_2O
CSDVB	-	Mg,Mn,Fe,Ru,Pthalocyanines	Isomerisation of quadricycalne to norbornadiene
Poly[$Ru(DiPy)_3^{2+}$	-	-	Chemically modified electrodes
P4VP/Carbon	-N	Cu^{2+}	Electrochemical reduction of O_2 to H_2O
Poly[$Ru(Dipy)_3^{2+}$-4VP/Pt	-	-	Photodiodes (Chemically modified photoelectrods)

1.2.1 Metal complexes supported on insoluble polymeric support

The cross-linked copolymers of styrene and divinylbenzene, first introduced by Merrifield in 1963 during his pioneering work on solid-phase peptide synthesis.[23,24] is one of the most extensively used polymeric materials in the synthesis of supported metal compounds due to its ready availability, low cost, mechanical robustness, chemical inertness, and facile functionalization.[25] Functionalization of Merrifield resin (**MR**) through the aromatic ring with different functional groups provided the potential anchoring sites for metal complexes.[26-29] The polymer is often prepared commercially by copolymerization of styrene and divinylbenzene with active monomers such as chloromethylstyrene or bromomethylstyrene (Scheme 1.1).[25] Depending upon the requirement, different percentages as well as types of cross-linking agents have been incorporated into the polystyrene resins.[25] The 2% cross-linked micro-porous or gel type polystyrene resins used as support requires solvent swelling for reagents to access internal functional groups.[25,30] In order to overcome the need to swell the supports in a compatible solvent, macro-porous resins which typically contain greater than 10-15% levels of the

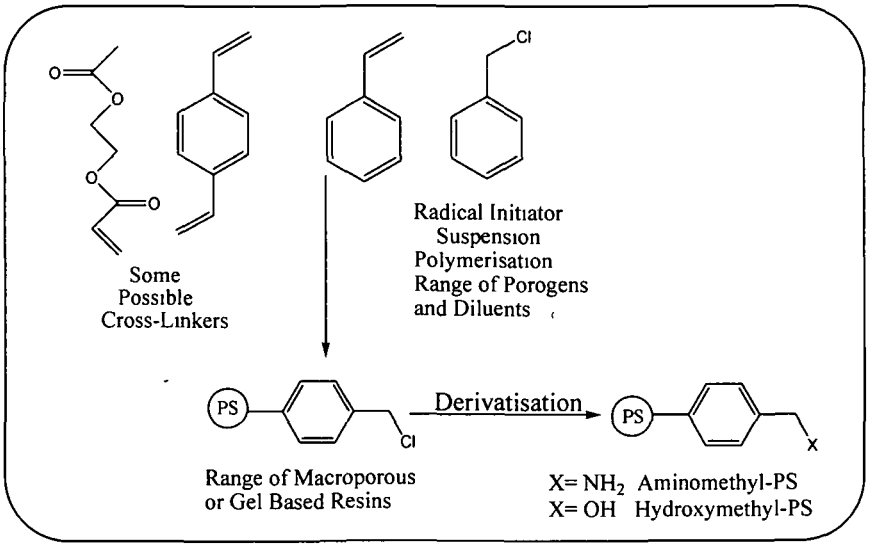

Scheme 1.1 Synthesis and derivatization of PS-based supports[25]

cross-linker, may be used. These however sometimes suffer from poor loading capacity and brittleness.[25] As a consequence, to rule out some of the above limitations, 1 or 2% cross-linked polystyrene resins have been modified with suitable functionals.[25] TentaGel and ArgoGel are the example of this type where poly(ethylene glycol) (PEG) has been grafted onto the polystyrene backbone.[25] The cross-linked copolymers of styrene with butadiene and divinylbenzene are also used extensively.[31]

Ion exchange resins are commonly based on cross-linked poly(styrene divinylbenzene) copolymers bearing ion-exchanging functional groups such as sulfonate, carboxylate, amine, etc. as shown in Scheme 1.2.[32,33] Compared to other insoluble support, ion-exchange resins usually offer considerable advantages as catalysts carriers such as reasonable stability, defined amounts of anchoring sites, easy immobilization procedure, ease of handling, particle size allows quantitative recovery by simple filtration, catalyst efficiency comparable to homogeneous reactions, ease of catalyst recycle, negligible to low metal leaching, compatible with many reaction solvents, including water, adaptable to the engineering of reactors, etc.[32] There are number of reports available on use of metal complexes supported on ion exchange resin in different chemical reactions such as oxidation,[34-36] hydrogenations,[37-39] hydroformylations,[40,41] carbonylations,[42] polymerizations.[32,43,44]

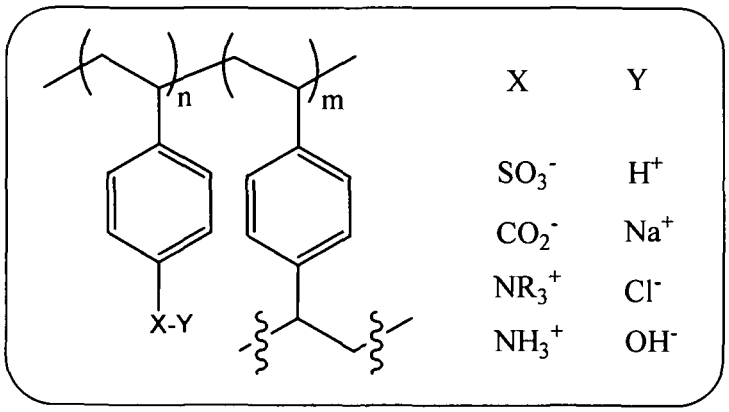

Scheme 1.2 Cross-linked poly(styrene divinylbenzene) copolymers bearing ion-exchanging functional groups[32]

1.2.1.1 Polymer immobilized metal complexes as catalysts

The reaction of appropriate polymers and reagents with catalytically active groups often confers catalytic activity to the polymer and generates a functional polymer.[19]There has been an increasing demand of application of polymer-supported catalysts in the production of bulk organic substances.[19,20] The catalytic properties of immobilized metal complexes are controlled by a number of factors such as the nature and distribution of attached transition metal ions and the character of the polymer support, together with unreacted functional groups of the polymer after fixation and activation of metal complexes.[22] Besides these, the cross-linking level in the polymer-support also offers different activity as well as selectivity of the anchored-metal complexes.[22,45] The use of polymer groups as ligands permits the ligand surroundings to be varied and regulation of the catalytic properties of the complexes become possible because of the flexibility of the macromolecular chains and their ability to adopt various conformations. Depending on the chemical nature of initial components, immobilized complexes can be soluble or insoluble in the reaction mixtures, therefore it is possible to transform homogeneous into heterogeneous catalysts and vice versa, which is a remarkable feature of such systems.[22] In fact, immobilized catalysts combine the main features of homogeneous, heterogeneous and enzymatic catalysts such as high activity and selectivity, specific character and stability in operation which enhances their efficiency.[19]

The so-called "heterogenized homogeneous catalysts", offer the advantage of ease of separation from reaction mixture and reuse applications by recycling which lead to significant reduction in problems of waste disposal.[46] Also, catalyst reuse increases the overall productivity and cost effectiveness of chemical transformations while minimizing their environmental impact, ultimately contributing considerably to the sustainability of

chemical processes which follows most of the "principles of green chemistry".[32,47,48] Table 1.1 summarizes the use of different polymeric supports with metal centers in various catalytic reactions.[22]

The poly(styrene) based resins have greatly influenced the activity of supported catalysts, which has been the subject of several reviews.[25,32,46,49-51] A **MR** supported palladium catalyst reported by Jang and co-workers[25,52] (Fig. 1.5) was highly effective in the Suzuki coupling of a number of organoboranes with alkenyl bromides, iodobenzene, and aryl triflates. Subsequently, Miyaura[25,53] has reported another recoverable PS-bound palladium catalyst which was efficient in cross-coupling reactions and successfully extended the range of applicable substrates. The first instance of an amino acid complex of Cu(II) bonded to cross-linked poly(styrene-divinylbenzene) resin was reported by Petit et al[54] although, the complexes were not examined for any catalytic activity. Pd(II) and Ru(III) complexes anchored to a L-valine functionalized cross-linked poly(styrene-divinylbenzene) resin was reported by Valodkar et al.[55,56] The Pd(II) based complex behaved as a versatile and recyclable catalysts for the hydrogenation of 1-octene, cyclohexene, acetophenone and nitrobenzene.[55] On the other hand, Ru(III) based complex acts as catalyst in epoxidation of styrene, norbornylene, cyclooctene and cyclohexene in

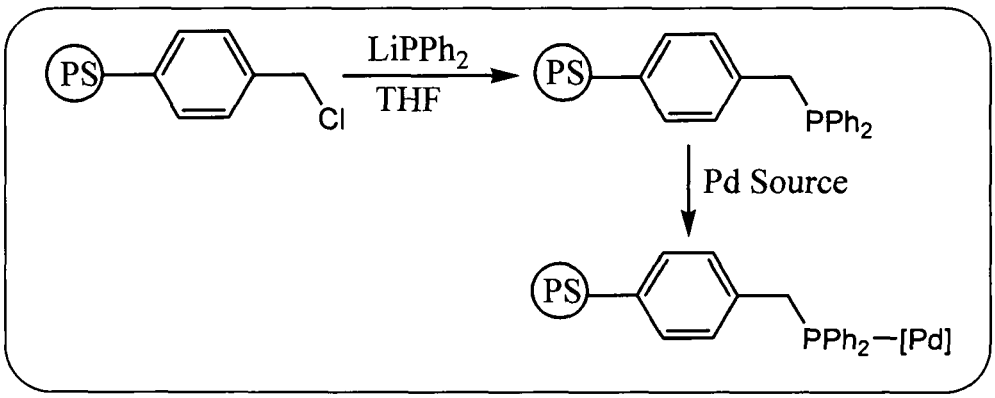

Fig. 1.5 Preparation of Merrifield resin supported palladium catalyst.[25]

presence of tert-butyl hydroperoxide as the terminal oxidant.[56] An *in situ* generated PS-supported rhodium complex reported by Jun and co-workers, catalyzed the reaction of benzyl alcohols with terminal alkenes to give ketones.[25,57] Significant improvement was also observed in turnover number of Heck reaction catalyzed by PS-supported 1,2-bis(diisopropylphosphino)benzene Pd(II) complex over its solution analogue as well as Pd-$(OAc)_2/PPh_3$.[25,58] A number of PS-supported ruthenium complexes reported by Grubbs have been shown to efficiently catalyze olefin metathesis reactions.[59] A PS supported $Pd(PPh_3)_4$ hydrogenation catalyst that reduced alkenes and alkynes under mild reaction condition was reported by Nayak et al.[60] The first successful supported Jacobsen's Mn(Salen) complex was reported in 1996 by Salvadori that afforded asymmetric epoxidation of styrene.[25,61]

Redox polymers are a class of chemically active metal containing polymers which undergo reversible redox processes.[62] The co-ordination chemistry of the redox active site plays a major role in these polymers. Redox active polymers had found application in the quantitative redox of metal ions and organic substrates[63] via the columnar procedure devised by Jones in 1963. Since then a multitude of oxidation and reduction have been performed by redox polymers. Catalysts of the Zeigler-Natta type such as complexes of Ti, Zr, Hf, V, Mo, Co, Ni, Cr, etc. immobilized on polymers in combination with organoaluminium compounds are active catalysts for unsaturated substrate reductions.[62]

Oxidation of a plethora of substrates such as catechol, amines, hydrocarbons, selective epoxidation, hydroformylation of olefins and etherification etc., have been achieved by using dioxygen as the oxidant in the presence of polymer supported complexes of W(VI), V(V) and Mo(VI).[64-72] Reports are available on catalytically active O_2 bound macromolecules consisting of metals viz., Cr, Mn, Fe, Co, Mo.[65] Features of the polymeric ligand affect the kinetics and even directions of these reactions. For example

macrocomplex of Co^{2+}-polyethyleneimine (PEI) are known to reversibly bind oxygen with formation of a μ-peroxo adduct stable in aqueous solution at room temperature[73] whereas, immobilized Cu^{2+} compounds are most often used for O_2 activation.[74]

Metal catalyzed organic oxidations using dilute H_2O_2 as terminal oxidant, has been gaining tremendous importance especially for large scale process, mainly owing to the recognition of H_2O_2 as an ideal environmentally benign and clean oxidising agent.[75,76] The most widely investigated polymer supported system are W(VI)/H_2O_2, V(V)/ROOH, Mo(VI)/ROOH.[65] D. C. Sherrington and his co-workers[64-67] reported few polymer immobilized V(V), Mo(VI) and W(VI) complexes supported on chloromethylated poly(styrene), poly(glycidyl-methacrylate) and polybenzimidazole based chelating resins which could catalyze alkene epoxidation. Mo(VI) and V(V) catalysts immobilized on ethylene-propylene rubber and cross-linked poly(ethylene oxide) grafted with poly(acrylic acid), poly(methacrylic acid), poly(4-vinyl pyridine) and poly(vinyl alcohol) as the support, developed by Stamenova and co-workers[77] effectively catalyzed styrene epoxidation by ethylbenzene hydroperoxide. Maurya and co-workers[78-80] [Fig. 1.6(a)] synthesized a number of PS supported V(V), Mo(VI) and W(VI) compounds which catalyzed oxidation of organic substrates such as phenol, styrene, sulfide as well as bromide by H_2O_2. In a recent report of Gupta and co-workers[46,81] [Fig. 1.6(b)], polymer-supported Schiff base (N_2O_2 donor set) complexes based on Ti(IV), Mo(VI), Mn(III), Cr(VI) and Fe(III) have used as active catalysts in the oxidation of alkanes/alkenes in presence of hydrogen peroxide and a variety of other oxidants.

We have come across only three reports dealing with peroxomolybdates immobilized on insoluble polymeric supports.[79,82,83] By using 2-(3-pyrazolyl)pyridine functionalized Merrifield resin and Schiff base functionalized chloromethylated polystyrene-divinylbenzene as support, Thiel and co-workers[82] as well as Maurya et al.,[79]

respectively, reported pMo complexes which were active in catalytic oxidation of olefin. The amberlyst supported pMo complexes reported by Tamami et al.[83] on the other hand served as stoichiometric oxidants for a variety of organic compounds such as alcohols, α-hydroxy acids, thiols, hydroquinones, benzylamines, phosphines and sulfoxides.

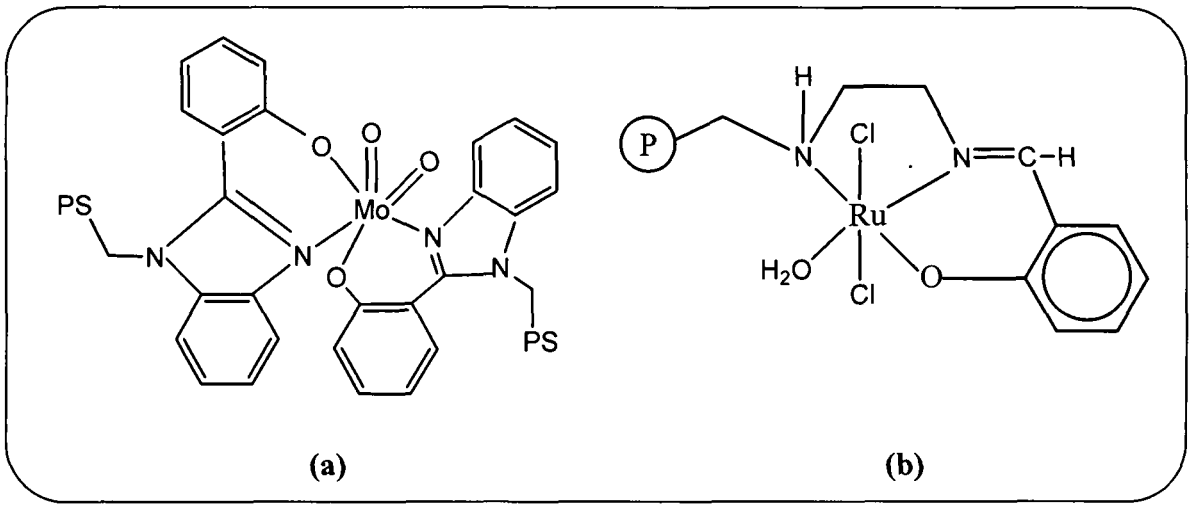

Fig. 1.6 Poly(styrene-divinylbenzene) (P or PS) supported (a) molybdenum(VI)[78] and (b) ruthenium(III)[81] Schiff base complexes.

1.2.1.2 Macrocomplexes as biomimetic models

Recent progress in the field of biomimetic catalysis has amply demonstrated that enzymes, the biological polymeric catalysts, can be mimicked and the processes of nature can be modeled.[62] Immobilized complexes can be considered as models of biological catalysts because they can carry out multicenter activation of a substrate like the metal enzyme catalysis.[18,84]

The polymer bound metal complexes were shown to act as model for several metalloenzymes including catalase, peroxidase, cytochrome P450, myoglobin,

hemoglobin, vitamin B_{12}, proteolytic and other enzymes.[19,22,85] The most important success in activation of molecular oxygen was achieved for immobilized complexes of Fe^{3+}, Mn^{3+} and Co^{3+} with porphyrins and pthalocyanines.[86,87] These are studied as model systems of metal enzymes for cytochrome P450, myoglobin and hemoglobin.[86,87] Polymer ligands, like protein globins, are capable of resisting dimerization of active complexes through matrix isolation.

Complexes of poly(4-vinylpyridine) (P-4VP) with Co-dimethylglyoxime has been employed as a model of vitamin B_{12}.[19] Metallo derivatives of anionic tetrasulphonated tetraphenylporphyrin (MTPPS, M = Mn(III), Fe(III) and Co(III)) immobilized on cationically functionalized divinylbenzene (DVB) – cross-linked polystyrene (PS) were shown by others to exhibit peroxidase-like activity.[88] Polymer-metal chelates were also found to exhibit catalase like behaviour, whereas metal complexes of the monomer from which the polymer was derived were devoid of such activity.[62] Enzyme catalase is an effective catalyst for H_2O_2 decomposition. Catalase-type activity of Cu^{2+} complexes immobilized on CSDVB modified by Schiff bases was studied extensively.[22] There are many heterogenized enzymatic systems, obtained by immobilization of catalase on synthetic polymers, which decompose H_2O_2 to H_2O and O_2.[22]

1.2.2 Metal complexes anchored to water soluble polymers (WSP) – General aspects

The utility of water soluble macromolecular metal complexes in diverse fields including catalysis,[19,89] separation processes,[90-92] biomedical[93-95] and environmental applications[96-98] are increasingly being recognized in recent years. Coordination

compounds of metal ions with soluble macromolecular ligands are interesting with respect to bio-inorganic chemistry as well.[19] Since for natural macromolecules, such as proteins, enzymes and DNA, water is the basic solvent, water-soluble functional polymers find relevance in designing biomimetic models.[97,98,99] Also, there is a great deal of contemporary interest in the use of environmentally benign solvent such as water in organic synthesis particularly in the context of green chemistry.[47,97]

The most important requirements for technological application of these polymers include: high hydrophilicity, an easy and cost effective route of synthesis, an adequate molecular weight distribution, chemical stability and high affinity to bind metal ions.[1] The water soluble polymers are essentially polychelatogens with functional groups able to form co-ordinate bonds with metals.[1] There are various types of soluble polymers bearing different functional groups available which are used as support for metal anchoring (Fig. 1.7).[24] The commonly occurring ligands in these polychelatogens, as shown in Table 1.1. are: amines, carboxylic acids, amides, alcohols, amino acids, pyridines, thiourea.[1,100] The most usual route for synthesis of WSP are through addition polymerization and functionalization of polymers by polymer-analogous reactions.[1]

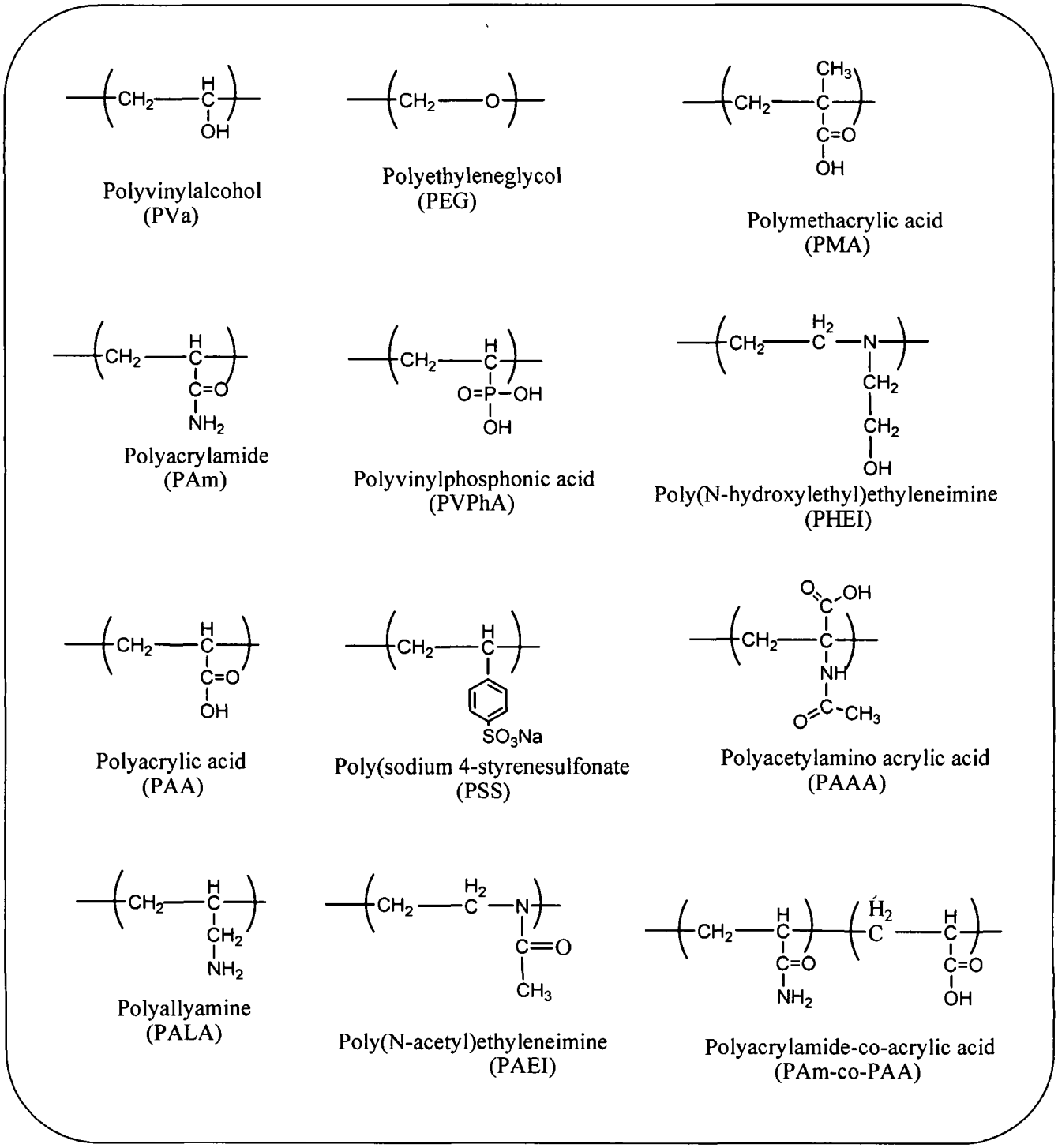

Fig. 1.7 Different water-soluble polymers used for metal ion interaction.

1.2.2.1 Catalytic applications of WSP – bound metal complexes

Use of WSP in catalysis is relatively a newer concept.[97] Notwithstanding the myriad advantages of insoluble supports there are several limitations in the use of these resins due to the heterogeneous nature of the reaction conditions.[24] The problems associated with insoluble polymer support include nonlinear kinetic behavior, unequal distribution or access to the chemical reaction, solvation problems associated with the nature of the support, and synthetic difficulties in transferring standard organic reactions to the solid phase.[24] A way to overcome some of these problems is to use low molecular weight soluble linear polymers as supports which reinstate the familiar reaction conditions of classical organic chemistry.[24,51,101,102] In fact, transition metal complexes attached to soluble non-cross linked polymer is essentially a homogeneous catalyst with macromolecular ligands. One of the advantageous aspects of use of the soluble polymer support is that the chemical reactions performed on such polymers can be monitored by high resolution solution phase ^{1}H and ^{13}C NMR spectroscopy.[103,104]

Traditionally, soluble polymers till recently have received less attention as polymeric supports compared to their insoluble counterparts due to the difficulty in isolation of the polymer from all other reaction components. In practice however, the recovery of soluble polymer supported catalyst can be achieved effectively by temperature or solvent-induced precipitation followed by filtration.[24,51] Most frequently, the homogeneous polymer solution is simply diluted with an appropriate solvent that induces precipitation of the support, followed by filtration to isolate the polymer.[24,51] Besides the solvent-induced precipitation technique, crystallization, dialysis and centrifugation methods could also be applied for the separation of polymer from reaction mixtures.[24,51]

The discoveries of Merrifield and Letsinger in the 1960's[105,106] in the field of peptide and oligopeptide synthesis by using soluble polymers to recover catalysts and ligands revolutionized the synthesis of biomolecules.[107] They provided impetus for research in industrial and academic laboratories that was directed toward developing immobilized or heterogenized homogeneous catalysts. The first example where a soluble polymer was used as an alternative to a cross-linked insoluble polymeric resin to support a chiral ligand, was reported in 1976 by Bayer and Schurig.[108] A DIOP (4,5-bis(diphenylphosphinomethyl)-2,2-dimethyl-1,3-dioxolane) ligand was attached to a linear polystyrene. The resulting polystyrene-bound version of DIOP was allowed to react with $HRh(CO)\text{-}(PPh_3)_3$, and the resulting polymer-bound Rh complex was used to hydroformylate styrene. An important progress in soluble polymer support occurred with the report of Janda and co-workers on supported chiral catalysts for asymmetric dihydroxylation of olefins, in the year 1996.[109]

Among the various types of soluble polymers, poly(ethylene glycol) (PEG) and non-cross-linked polystyrene are some of the most often used examples in the preparation of soluble polymer-supported catalysts.[24] PEG is also known as poly(ethylene oxide), poly(oxyethylene) and polyoxirane which is formed from the polymerization of ethylene oxide.[24,110] The modified poly(ethylene oxide) catalyst is widely used in catalysis for hydrogenation,[111,112] Sharpless asymmetric dihydroxylation reaction,[109,113] hydroformylation,[114] Wacker oxidation,[115,116] hydroxylation of aromatic compounds[117] and epoxidation.[24,118] Additionally, PEG is also well known for its ability to act as a phase transfer catalyst.[24,119] For instance, anchoring of rhodium to PEG was reported which catalyze hydrogenation of various olefins in water.[111] Among the first soluble macromolecular metal complexes to be used as catalyst were modified linear polystyrenes.[108,120,121] Catalysts such as preformed Rh or Pd complexes were loaded on

chemically modified non-cross-linked polystyrene which catalyzed hydrogenation or hydroformylation of alkene.[51,122] Polycarboxylic acid and its derivative are often used to synthesize soluble ligands and complexes. In this aspect, reports are available on manganese, cobalt, iron, copper or chromium complexes anchored on polyacrylic acid for autooxidations of cumene to cumene hydroperoxide.[123-125] Furthermore, a poly(acrylic acid)-Rh(II) complex was reported which have very high catalytic activity for the hydrogenation of olefins in homogeneous solution. Besides polyacrylic acid, poly(pentenoic acid) has also been used to produce phosphine containing ligands.[126] Polyacrylamide modified with optically active phosphine containing ligands and Rh catalyst were used for asymmetric hydrogenation of prochiral amides.[127,128] Significantly, to the best of our knowledge water soluble polymers were used for the first time in our laboratory to obtain a series of pV and pW containing macro complexes.[129,130] These complexes, in addition to exhibit unique biorelevant properties, also served as efficient and recoverable oxidants in oxidative bromination of organic substrates.

1.2.2.2 Biological applications of WSP—metal complexes

Apart from the utility of the soluble macromolecular metal complexes in catalysis, the use of water soluble polymer–metal adducts opened new strategies in the development of pharmaceutical formulations and other biological applications.[131] Polymers as drug carriers have been investigated to achieve efficient delivery of the drug molecule to the targeted cell. The application of such metal bound polymeric materials offer numerous advantages to the drug molecule such as controlled release, prolongation of drug life-span, acceleration of drug absorption, and drug targeting[132] which may otherwise be highly toxic with poor assimilation and absence of selective action.[133] The pharmacokinetics of the high molecular weight materials can be tailored by altering the molecular weight,

conformation and molecular weight distribution of the polymer; by selecting the appropriate composition.[133]

A large number of polymeric materials are used in the formulation of different dosage, novel delivery systems and biomedical applications including PVA,[134,135] PAm,[136] PAA,[134,137] POX,[134,138] polyP,[134] derivatives of PMA,[139] synthetic poly(aminoacids),[140,141] PEO,[142] polyamides,[143] and polyamines,[143] XG,[134] CTS derivatives,[134,144] DX,[134,145] cellulose ethers,[134] ALB,[134] and starch or starch based derivatives.[134,146,147] Lee and Rashidova[148] studied the biological activity, toxicity, immunological response and the pharmacokinetics of several polymer metal complexes of N-vinylpyrrolidone and derivatives of N-2-hydroxypropylmethacrylamide with transition metals. The effect of the macroligand type, polyacid behaviour, and the comparison of the biological properties between the polymer–metal complexes and the polymer bases were performed. A remarkable improvement has been achieved in case of platinum based anti-cancer drugs by anchoring it to soluble polymers.[149,150] Dicarboxylato and dihydroxylatoplatinum(II) chelates,[151] diaminocyclohexyl platinum[152] are used as anti-cancer agent. Such polymer-drug conjugates can increase the effectiveness of an anticancer drug compared to their low molecular weight analogues.

Rivas and his co-workers introduced Ag(I) based water-soluble complexes supported on poly(4-ethylene azide) N-alkylated, poly(diallyl dimethyl ammonium chloride) (PDDA) or poly[((3-methacryloyl amino) propyl) tri methyl ammonium chloride] (PMPTA) which served as bactericidal agent against both Gram-positive and Gram-negative bacteria.[131] Nandi and co-workers[153] studied the bactericide activity of metal ions and polymer–metal complexes with Co^{2+}, Zn^{2+} and Cu^{2+} whereas Nonaka and co-workers[154] studied the bactericide activity of resins containing the triethylamine and thiols as side groups and the metal ions Ag^{+}, Cu^{2+} and Zn^{2+} for *E. coli* and *S. aureus*.

It is observed that the polymer based anti-bacterial agents being non-volatile, chemically stable, can reduce the loss associated with volatilization, photolytic decomposition, and transportation.[155,156]

Hosseinkhani et al.[132] reported cationic polymers including poly(L-lysine), polyethylenimine (PEI), poly(ami-doamine) dendrimers, and polymer micelles for the delivery of genes and drugs into cells. Their results suggest that a polymer-metal complex significantly enhanced the gene expression of cells *in vivo* treated with dextran or pullulan-plasmid DNA complexes.[132] In view of the afore mentioned advancements, it appears likely that metal containing polymers would be a rich source of potential future therapeutic agents.[157] A survey of literature however reveals that screening of peroxo-metal incorporated soluble macromolecules, including compounds of molybdenum, for their biochemical potential have so far received scant attention.

1.3 Co-ordination chemistry of molybdenum and its biological significance

Molybdenum with the ground state electron configuration [Kr] $5s^1 4d^5$ belongs to the periodic Group VI. Molybdenum is the only second row element that is essential for most living organisms.[158] The element was first discovered in 1778 by a Swedish chemist named Carl William Scheele[159,160] and the name Molybdenum was derived from a Greek word "molybdos".[161]

Molybdenum has a chemical versatility that is useful to biological systems and is redox active under physiological conditions.[162] In order to understand its role in catalysis and its interaction with complex biomolecules an understanding of the basic co-ordination chemistry of the metal with simpler ligands is a primary pre-requisite. The co-ordination chemistry of Mo appears to be highly complex among the transition elements due to several reasons[163] such as:

(i) Possibility of a wide variety of stereochemistries, as its co-ordination number varies between 4 to 12;

(ii) Oxidation states can range from 2- to 6+ in complexes;

(iii) The ability of Mo to form compounds with most inorganic and organic ligands, with a particular preference for oxygen, sulfur, fluorine, and chlorine donor atoms;

(iv) Mo shows the tendency to form a bi and polynuclear compounds containing bridging oxide and chloride ligands and/or Mo – Mo bonds.

Molybdenum is very similar, with respect to many molecular properties, to tungsten, the third member of Group 6, but different from the first member, chromium. The pronounced similarity, in the chemistry of molybdenum and tungsten follow from two principal factors: (i) analogous valence electron configurations in all oxidation states of nearly all compounds, and (ii) virtually identical radii – atomic and ionic radii for a given oxidation state – arising from the lanthanide contraction.[164,165] Nevertheless, there also exist clear differences, some in reactivity and others based on electronic structure such as ionization and redox potentials[166] and relativistic effects on structural properties[167] between the elements.[164]

A wide variety of compounds are formed by molybdenum (VI) ion with d^0 configuration such as oxides, halides, sulfides, oxohalides, isopolymetallates, heteropolymetallates, selenides and tellurides.[160,163,165] Molybdenum trioxide, MoO_3 is the ultimate product of heating the molybdenum or other compounds in oxygen with 6+ oxidation state.[163] When MoO_3 is dissolved in aqueous alkali, the resulting solution contains simple or normal molybdates such as Na_2MoO_4.[160] On the other hand, if these solutions are made strongly acidic, yellow precipitates of molybdic acid, $MoO_3.2H_2O$ is formed.[160] Moreover, careful adjustment of acidity, concentration and temperature, often

coupled with slow crystallization produced isopolymolybdates which are characterized as dimolybdate, $[Mo_2O_7]^{2-}$; hexamolybdate, $[Mo_6O_{19}]^{2-}$ and octamolybdate, $[Mo_8O_{26}]^{2-}$.[160,168,169] Among the heteropolymolybdates(VI), Keggin and Dawson complexes of general formula $[X^{n+}Mo_{12}O_{40}]^{(8-n)-}$ and $[(X^{n+})_2Mo_{18}O_{62}]^{(16-2n)-}$, respectively are important.[163,170] Besides these, molybdenum forms a very diverse polymolybdate(VI) in association with other oxo ligands such as squarate ($C_2O_4^{2-}$), methoxide, malate, phosphate and arsenate anion.[163] Molybdenum(VI) forms hexafluoride, MoF_6 as well as oxohalides of formula MoO_2X_2, (X= F, Cl, Br, I).[163,171,172] Apart from oxohalides, a wide variety of oxo molybdenum(VI) compounds formed containing MoO_2^{2+} or MoO^{4+} structural unit with different organic ligands such as acac,[163,173] DMF,[174] HMPT,[175] Schiff base,[176-179] amino acids,[180,181] etc.[] Molybdenum(VI) is also found in different forms of thiomolybdates such as MoO_3S^{2-}, $MoO_2S_2^{2-}$, $MoOS_3^{2-}$ and MoS_4^{2-} formed from MoO_4^{2-} by successive replacement of oxygen atoms by sulfur atoms which act as useful reagents for the preparation of metal-sulfur cluster as well as ligands.[160,182]

Molybdenum in 5+ oxidation state with d^1 configuration forms an extensive range of mono- and dinuclear oxo complexes containing MoO^{3+}, MoO_2^{+} or $Mo_2O_3^{4+}$ core.[163,183] Fluoro and chloro complexes of molybdenum of the type MoF_5, MoF_6^{-}, MoF_8^{3-}, $MoCl_5$ and $MoOCl_3$ are found to exist in this oxidation state.[160,163,171,173] These halides are susceptible to hydrolysis and react with oxygen to form different oxygen-containing complexes.[160] The tetravalent molybdenum with d^2 configuration forms different oxides, halides, sulfides and oxohalides and is thought to be the biologically most important oxidation state.[160,184-186] Molybdenite (MoS_2) is a sulfur containing molybdenum(IV) ore which is most stable sulfide and commercially important.[160] In molybdenum enzymes it seems, not in details, that the Mo atom cycles back and forth from Mo^{IV} to Mo^{VI} via oxygen atom transfer as shown in equation 1.1:[163]

$$Mo^{IV}O + Sub \rightleftharpoons Mo^{VI} + OSub \quad \text{--- (1.1)}$$

Molybdenum with lower oxidation state such as III to II formed only few complexes of halides and sulfides such as MoX_3 (where X= F, Cl, Br, I), MoX_2 (where X= Cl, Br, I), MoS, etc. along with compounds containing metal – metal bonds e.g. $Mo_2(O_2CR)_4$ and $Mo_2(OR)_6$.[160,163,171,173]

Among the numerous transition metal-oxo compounds, molybdenum is one of the most studied element as an oxygen atom transfer agent due to its presence in many isopoly and heteropoly anions, as well as its importance in several enzymatic systems.[187] Oxidation of phosphines, alcohols, olefins and alkanes are some of the oxygen atom transfer reactions by Mo=O complexes.[187] It is pertinent here to mention that vast majority of pterin based molybdoenzymes possesses Mo=O unit in their active site and are often referred to as oxomolybdenum enzymes (Fig. 1.8).[188,189]

The trace element molybdenum forms the catalytic centre of a large variety of molybdenum containing enzymes[190] which are ubiquitous.[162,191-194] In biology molybdenum is a component of fertilizer and nutrient formulations.[159] There are at least 50 such enzymes now known[190,192] which are not only important to their host organisms for metabolism and energy generation but also the products from the catalytic cycles in which these enzymes participate have major impact in the nitrogen, sulfur, carbon and arsenic cycles.[191]

On the basis of cofactor composition and catalytic function, molybdenum-dependent enzymes can be grouped into two categories:[190] (i) bacterial nitrogenase containing an iron–sulphur-cluster-based iron–molybdenum cofactor (FeMo-co) in the active site, and (ii) pterin-based molybdenum enzymes. The second category is further

divided into three families viz. (a) xanthine oxidase, (b) sulphite oxidase, and (c) dimethyl sulphoxide reductase (DMSOR), each of which has a distinct active-site structure (Fig. 1.8).[162,190] Table 1.2 summarize representative examples of the reactions catalyzed by different molybdoenzymes.[192] In order to mimic the activity of these molybdoenzymes several molybdenum based bioinspired functional model has been developed.[191] However, no such report is available which can clearly described the reactivity of the enzyme functions.[191]

Table 1.2 Representative examples of the reactions catalyzed by molybdoenzymes[192]

Enzyme	Reaction catalyzed
Carbon monoxide oxidoreductase (dehydrogenase)	$CO + H_2O \rightleftharpoons CO_2 + 2H^+ + 2e^-$
Dimethyl sulfoxide reductase	$Me_2SO + 2H^+ + 2e^- \rightleftharpoons Me_2S + H_2O$
Nitrate reductase	$NO_3^- + 2H^+ + 2e^- \rightleftharpoons NO_2^- + H_2O$
Arsenite oxidase	$H_2AsO_3^- + H_2O \rightleftharpoons HAsO_4^{2-} + 3H^+ + 2e^-$
Sulfite oxidase	$SO_3^{2-} + H_2O \rightleftharpoons SO_4^{2-} + 2H^+ + 2e^-$
Xanthine oxidase	Xanthine $+ H_2O \rightleftharpoons$ uric acid $+ 2H^+ + 2e^-$
Aldehyde oxidoreductase	$RCHO + H_2O \rightleftharpoons RCO_2H + 2H^+ + 2e^-$

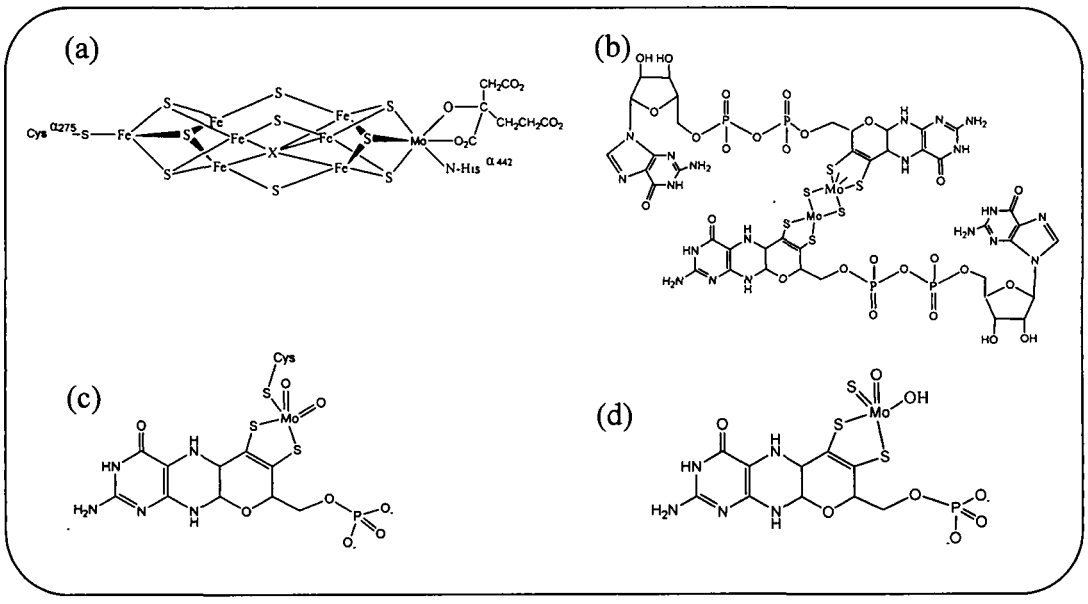

Fig. 1.8 Chemical structures of (a) FeMo-co (b) Mo–bis-MGD or (DMSOR) (c) sulphite oxidase (d) xanthine oxidase.[190]

Molybdenum concentration in the human body is found to be about 0.07 mg per kilogram of weight.[195] It occurs in higher concentrations in the liver and kidney and in lower concentrations in the vertebrae.[196] In body, it acts as a cofactor for a limited number of enzymes such as sulfite oxidase, xanthine oxidase, and aldehyde oxidase although, molybdenum deficiency has not been observed in healthy people.[197]

An exciting development which has raised status of molybdenum to an element of therapeutic importance is the findings of Goto et al.[198] in 1992, followed by the report of Shechter and co-workers,[8] on the ability of molybdate to mimic the biological action of insulin like vanadate. Molybdenum compounds, such as Na_2MoO_4 and cis-MoO_2L_2 [L = maltol (3-hydroxy-2-methyl-4-pyrone)] were effective in lowering the blood glucose and free fatty acid levels.[199] Molybdate has been known as an anti-diabetic agent and potent inhibitor of phosphatases viz., tyrosine phosphatase,[200] acid phosphatases,[201,202] alkaline phosphatases[201,203] and glucose-6-phosphatases.[204,205] Molybdate is also known to inhibit the enzyme ATP sulfurylase which activates sulfate for participation in biosynthetic pathways.[159] The efficacy of a Mo(VI) maltolato species, $[Mo^{VI}(O)_2(ma)_2]$, ma = maltolato(-), in STZ-induced diabetic rats is close to its V(IV) counterpart, in a chronic treatment.[199,206,207] In another report it was found that ammonium tetrathiomolybdate can be used in the therapy of chronic Cu poisoning and is recommended for Wilson's disease in humans.[199,208] Moreover, anti-tumor activity of molybdenum compounds such as $Mo_7O_{24}^{6-}$ anion, hexabis(isopropylammonium) heptamolybdate trihydrate and 2,5-dihydroxybenzoate molybdenum(VI) complex has been confirmed.[209] Additionally, 12-molybdophosphoric acid are finding applications as biomedical agents including antitumoral, anticoagulant, antibacterial, antiviral agents.[210] Most importantly, trace levels of molybdenum are reported to be not harmful to animals or human beings.[211] Acute

toxicity of molybdenum compounds has been investigated only in experimental animals.[211]

One of the most fascinating domains of molybdenum chemistry is its peroxo chemistry. Interest in the peroxo transition metal complexes in general, seem to be never diminishing.

1.4 Peroxo compounds of molybdenum – Chemistry and importance

It has been appreciated for at least 140 years that characteristic color reactions may occur when hydrogen peroxide is added to solutions of transition metal derivatives.[212] Numerous peroxo transition metal compounds have been synthesized since then as such systems are attractive as potential catalysts both from industrial as well as biological perspectives.[8-13,201,213-217] The bonding of molecular oxygen to transition metal complexes has been a subject of increasing interest because it represents a basic step in understanding the function of oxygen–carrying and –activating metalloproteins in biological systems.[218-220] According to the rationalization made by Vaska,[221] transition metal peroxides involve covalently bound dioxygen resembling O_2^{2-} in peroxo configuration. The peroxo moiety around the metal center may be co-ordinated in two distinctly different ways viz. non-bridging and bridging.[9] The non-bridging type may be co-ordinated by η^1 and η^2 fashion.[9] The μ-peroxo structure, named following the definition made by Vaska,[221,222] that can bind two metals in bimetallic complexes have a variety of mode of co-ordination (Fig. 1.9).[222] A common characteristic of these complexes is the O-O distance, which occurs between 1.4 and 1.52 Å (1.49 for O_2^{2-}), and the corresponding infrared frequency ν(O-O), which lies between 800 and 950 cm^{-1}.

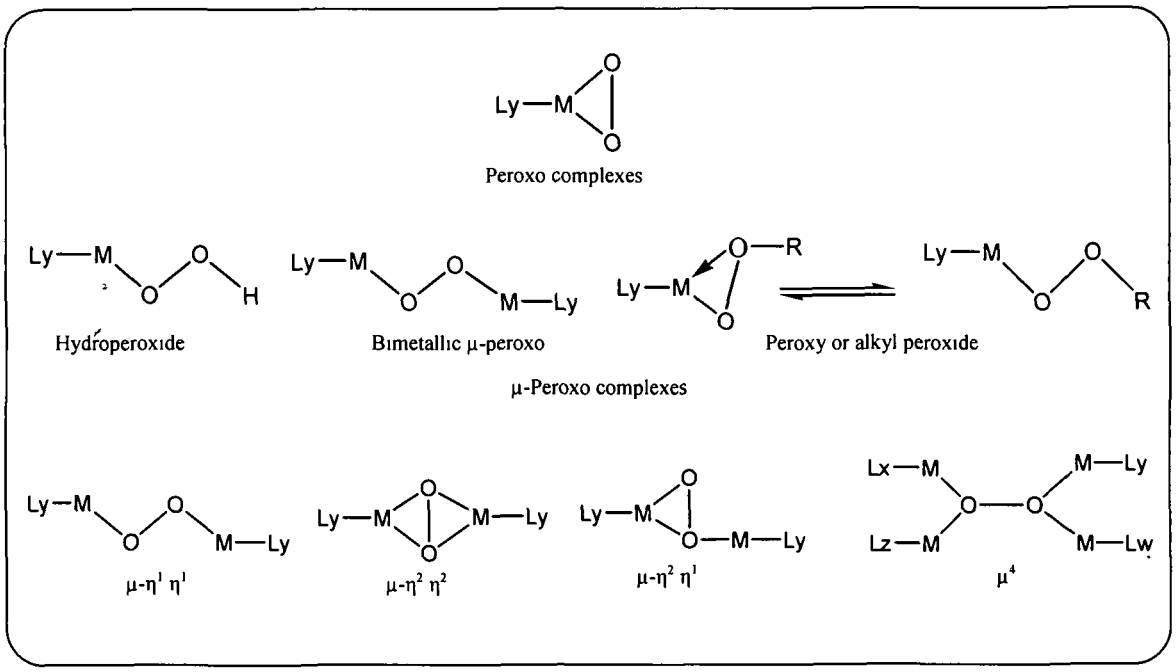

Fig. 1.9 Structural classification of metal-dioxygen complexes.[222]

The d^0 peroxo complexes of vanadium, molybdenum and tungsten, which have clear structural and isoelectronic relationships, are tuned towards their use as an important class of stoichiometric or catalytic oxidizing or oxo-transfer agent in variety of organic oxidations such as epoxidation of alkenes,[223-226] oxidation of sulfides and sulfoxides,[227-233] primary and secondary alcohols[234,235] as well as halide oxidation[236-240] (Fig. 1.10). Besides these, the active involvement or relevance of these peroxometallates in haloperoxidase,[236,238,240-242] their insulino-mimetic,[13,213,243-248] anti-neoplastic[249-251] and enzyme inhibitory activity[200,242,252,253] have been emphasized in the literature which increases the biological significance of this class of compounds.

Molybdenum is capable of forming a number of peroxo species, ranging from mono to tetra peroxomolybdates, depending upon the concentration of molybdenum, hydrogen peroxide and pH of the medium[9,254,255] owing to which the aqueous pMo chemistry appears to be rather complex. Besides these, molybdenum is capable of forming di or

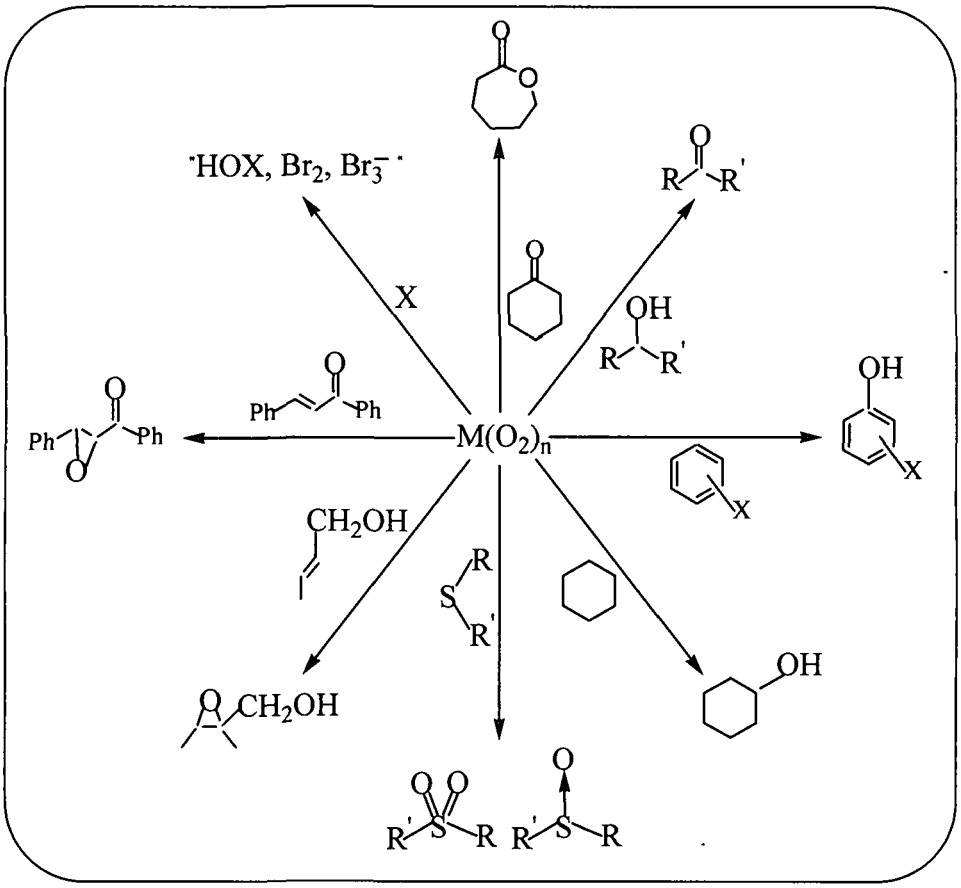

Fig. 1.10 Selected oxidations of organic compounds by peroxometal complexes,[256] M= V, Mo or W.

polynuclear peroxomolybdate species.[9,257] Red tetraperoxomolybdate anion, $[Mo(O_2)_4]^{2-}$ is formed in mildly alkaline solution (pH 7-9) by the addition of excess H_2O_2 to solutions of MoO^{2-}.[9,212] However, in solution the species is unstable above pH = 9; below pH = 5 they are progressively converted into tetraperoxodimolybdate anion.[9]

$$2[Mo(O_2)4]^{2-} + 5H_2O \rightleftharpoons [Mo_2O_3(O_2)_4(H_2O)_2]^{2-} + 2OH^- + 4H_2O_2 \quad \text{---- (1.2)}$$

Salts of triperoxomolybdate anion has been claimed, e.g. $Cs_2[MoO_7]$[258] but there is no convincing evidence that these are pure species, and $(Hpy)_2[MoO_7]$ have been shown to be $(Hpy)_2[Mo_2O_3(O_2)_4(H_2O)_2].H_2O$.[259] The only confirmed "triperoxomolybdate" is the salt reported as $(Hpy)_2[Mo_2O_{11}].2H_2O_2$ and later shown to contain bridging hydroperoxo ligands, $[MoO(O_2)_2(OOH)]_2^{2-}$.[9,260]

Peroxomolybdate species formed in aqueous solution have been characterized by several techniques viz., ^{95}Mo-NMR spectroscopy,[254,255] ^{17}O-NMR spectroscopy,[261,262] Raman spectroscopy[263,264] and by electrospray ionization mass spectrometry (ESI-MS).[262,265] Structure and reactivity of peroxo molybdenum complexes have also been theoretically investigated.[266]

A large number of diperoxomolybdate complexes of the type $[MoO(O_2)_2L_{ax}L_{eq}]^{0/-1/-2}$ with a pentagonal bipyramidal structure have been reported.[9] In such complexes, the oxo and one L ligand (or donor atom of a bidentate ligand) occupy axial positions, and the two η^2-peroxo groups and the remaining L are occupying the equatorial position. A series of such types of peroxo complexes are given in Table 1.3. However, the ligands L may also function as bridging groups in binuclear species and are summarized in Table 1.4.

Table 1.3 Structurally characterized oxoperoxo complexes of molybdenum(VI), $[MoO(O_2)_2L_{ax}L_{eq}]^{n-}$ (n=0,1,2)[9]

L_{ax}	L_{eq}	n	Ref.
H_2O	H_2O	0	267
H_2O	hmpt	0	175
Py	hmpt	0	175
½(bipy)	½(bipy)	0	268
½(tbbpy)	½(tbbpy)	0	269
H_2O	Hgly	0	181
H_2O	Hpro	0	181
F^-	F^-	2-	270
½(cit)	½(cit)	2-	271
½(pic[N])	½(pic[O])	1-	272

Table 1.4 Structurally characterized dimeric oxodiperoxo complexes of molybdenum(VI), $[MoO(O_2)_2L_{ax}L_{eq}]_2^{2-}$ [9]

L_{ax}	L_{eq}	Ref.
H_2O	μ-O	273
½(μ-OOH)	½(μ-OOH)	274
½(μ-F^-)	F^-	275
¼(μ_4-tart)	¼(μ_4-tart)	264

A significant contribution to the existing wealth of organic oxidants is the important class of molybdenum-peroxo complexes of the type, $[MoO(O_2)_2Lx]$ (L = py, hmpa, dmf, H_2O and so on; x =1,2) introduced by Mimoun et al. in 1969 (Fig. 1.11).[276] The neutral seven-coordinated diperoxomolybdenum complexes were obtained by treatment of a solution of MoO_3 in 30% H_2O_2 with organic bases.[9] Since then, a large number of apparently analogous complexes have been reported with different ligands such as water, amides, ureas, phosphoramides, amino acids, pyridine, pyridine-N-oxides, phosphine and arsine oxides and bidentate 2,2'-bipyridine, 2,2'-bipyridine N,N'-dioxide, picolinate and its N-oxide, 1,10-phenantbroline, phenylenediamine and ethanolamine, octamethylpyrophosphoric triamide, (S)-dimethyllactamide, etc.[9]

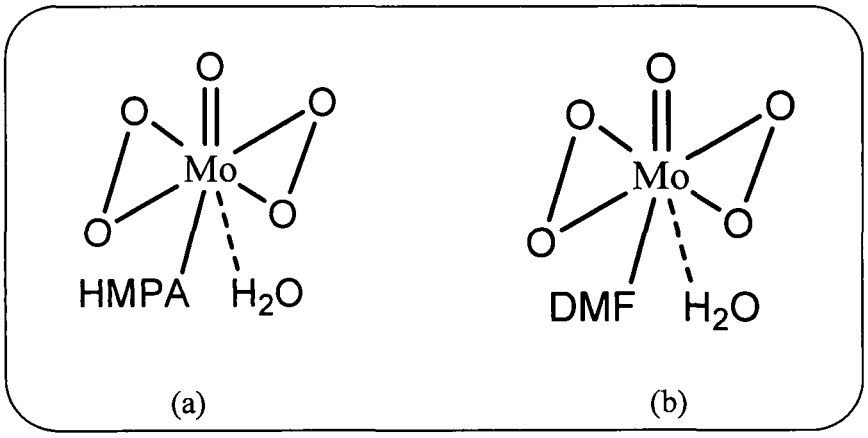

Fig. 1.11 Structures of Mimoun type complexes (a) $[MoO(O_2)_2(HMPA)(H_2O)]$ and (b) $[MoO(O_2)_2(DMF)(H_2O)]$.[277]

The Mimoun type complexes are highly soluble in both polar and nonpolar solvents. Thus the neutral compounds and appropriate salts of the monoanions have been widely used as both stoichiometric and catalytic oxidants in organic oxidations.[9] Epoxidation of alkene,[223-226] oxidation of primary and secondary alcohols to aldehydes and ketones respectively,[234,235] oxidation of sulfides and sulfoxides to sulfoxides and sulfones,[227-233] and oxidation of indoles,[278] furans[279] and phenacetin[280] are few of the examples of stoichiometric oxygen transfer reactions by this class of compounds. It is notable that most of these investigation has been carried out with $[MoO(O_2)_2(hmpt)]$, however, other complexes are also effective.[9] Cass et al.[228] examined the use of Mimoun type[277] complexes $MoO(O_2)_2(L)(H_2O)$, (L = pyridine N-oxide or pyrazole) to oxidize a wide variety of substituted sulfides and found that the procedure offers several major advantages such as control over the degree of oxidation of products, excellent chemoselectivity toward the sulfur group of substituted sulfides and sulfoxides.[266] Jacobson et al.[272] synthesized and structurally characterized quite a few oxo-diperoxo-picolinato molybdenum complexes and used these in alcohol oxidation.[34,281] Bortolini et al.[282] also studied the oxo-diperoxo-picolinate complexes of molybdenum for oxidation of alcohol to aldehyde. In the case of one substrate, 20% epoxidation occurs along with 80% aldehyde formation.[281,282] Bhattacharyya and co-workers[283,294] reported oxo-monoperoxo-molybdenum complexes of the type $[MoO(O_2)(QO)_2]$ as well as its diperoxo analogues $[MoO(O_2)_2.2QOH]$ and $[MoO(O_2)_2(QO)]^-$ using 8-quinolinolate (QO) anion as ancillary ligand.[283] The complexes act as efficient catalysts in the oxidation of alcohols and sulfides.[283,284] They have also reported a few oxo and oxoperoxomolybdate(VI) complexes coordinated with derivatives of hydroxamic acid which have high potential and selectivity as catalyst in the epoxidation of olefin.[281] It is notable that Mo containing analogue of W based 'Venturello's complex', $(NMe_4)_2[PhPO_3\{MoO(O_2)_2\}_2\text{-}(H_2O)]$ was

prepared, and its catalytic ability in epoxidation was examined.[285,286] However, the compound was found to be much less efficient than the tungsten systems even in harsh reaction conditions.[281]

Besides these mononuclear oxodiperoxo complexes of molybdenum (VI), several binuclear pMo complexes having pseudotrigonal bipyramidal oxo diperoxo polyhedra were reported.[257] In such complexes, the two fragments, $MoO(O_2)_2$ were joined together by a bridging ligand e.g., μ-O group.[257] In addition, isopolyperoxo and heteropolyperoxo complexes of molybdenum (VI) such as $A_4[Mo_3O_7(O_2)_4].2H_2O$ (A= K^+ and NH_4^+) with pseudotrigonal bipyramidal oxo diperoxo polyhedra are known.[258,287]

Oxomonoperoxo complexes of molybdenum(VI) of $MoO(O_2)L_4$ type generally exhibit the pentagonal-bipyramidal geometry as observed for the diperoxo species but with two equatorial ligands replacing one of the peroxo groups.[9,288] $[MoO(O_2)(dipic)(hmpt)]$ is an example of this type. Dioxomonoperoxo molybdenum(VI) complexes of the type $[Mo(O)_2(O_2)L]$, where L = diethylene triamine, 2,2,2-triethylenetetraamine and 2,3,2-triethylenetetraamine, have been reported.[289] In the context of existing literature, the number of isolated and characterized monoperoxomolybdate complexes are relatively fewer in comparison to its diperoxo counterpart.[7]

The nature of the coordinating ligand has a dramatic effect on the reactivity of the peroxometallates of V(V), Mo(VI), W(VI) and other transition metal complexes. Depending upon the ligand, the reactivity may shift from polar to radical oxidants even when the metal is the same. In case of monoperoxo complexes containing bidentate ligands it is evident that the reactivity of the complexes decrease when the negative charge on the metal is increased.[290] In fact, it is observed that the ability to decompose selected monoperoxovanadium complexes decreases on decreasing the electron-donating

properties of the different ligands.[290] Furthermore, from the study on peroxo complexes of different metals containing the same ligand it was observed that the stronger the oxygen-oxygen bond, the easier is the electron transfer to the complex. Therefore, peroxo vanadium and chromium complexes, in which the O-O stretching frequency is the largest, are reduced at lower potentials than molybdenum and tungsten derivatives.[290] This fits with the common notion that radical oxidations are more frequent when peroxo chromium and vanadium complexes are used. Thus it appears that in simple oxidations, an increase of the electron-donating character of the ligands may decrease the reactivity.[290] Thus the activity of pMo complexes as stoichiometric or catalytic agent have been fine-tuned with ligands and various correlations have been made involving the electronic and other properties of the ligand.[291-293]

The pMo species has been observed to catalyze oxidative bromination of organic substrates in acidic medium.[237] The peroxo-metal mediated oxidative bromination has been garnering tremendous interest as such a process is actually a functional model of the activity of vanadium-dependent enzymes, haloperoxidases.[241,294] The haloperoxidases oxidize halide by utilizing peroxide to the corresponding halogenating species, which subsequently halogenates organic substrates (Org)[241,294] (Scheme 1.3). The primary oxidized intermediate is still not known with certainity, although for bromide it is thought to be an equivalent of hypobromous acid, bromine, tribromide or an enzyme-bound bromonium ion-type species.[241,294,295] They are referred to as chloroperoxidases, bromoperoxidases or iodoperoxidases depending on the most electronegative halogen they can oxidize.

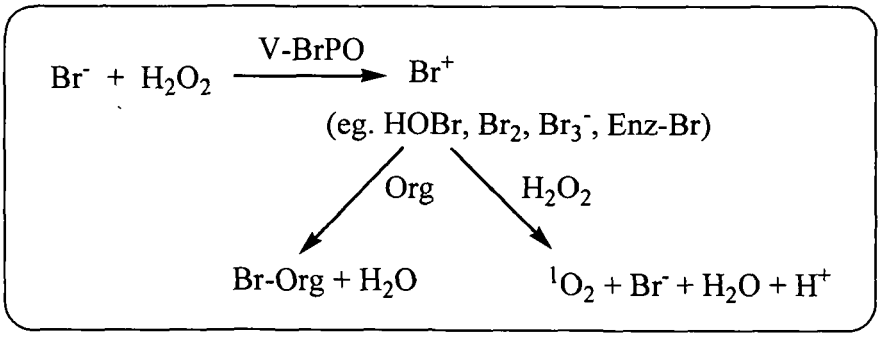

Scheme 1.3 Overall reaction scheme of V-BPO[296]

Vanadium bromoperoxidase (V-BPO) involved in the biosynthesis of many brominated marine natural products ranging from halogenated indoles, terpenes, acetogenins, phenols etc. to volatile halogenated hydrocarbons that are produced on a very large scale.[296,297] In many cases these halogenated marine metabolites possess biological activities of pharmacological interest, including antifungal, antibacterial, antiviral, and anti-inflammatory activities.[296] The haloperoxidase proteins have been isolated and characterized irrespective of their origin from all the different classes of marine algae or fungi, including *Ascophyllum nodosum* (brown algae), and *Corallina officinalis* (red algae) or *Curvularia inaequalis* (fungi).[296] It is intriguing to note that these proteins exhibit a dual activity from peroxidases to phosphatases on the removal of vanadate.[298,299]

Numerous mechanistic studies have been performed to elucidate the catalytic cycle of the V-BPO enzymes. Various vanadium based biomimetic functional models have been developed which are mainly based on monoperoxovanadium[300] or triperoxodivanadium species.[241,301,302] Schiff-base complexes of V(V), aqueous solution of cis-dioxovanadium(V) (VO_2^+) in acidic medium, a V_2O_5 and H_2O_2 system, KBr in excess H_2O_2 in presence of vanadyl sulphate in phosphate buffer were all found to be effective in bromination of organic substrates and were studied in detail as functional mimic of the enzyme. However, despite the progress made in understanding various aspects of activity of V-BPO, the exact mechanistic details of the enzyme function is yet to be fully unraveled.

Along with the biochemical interest on the activity of V-BPO, there have been on-going efforts devoted to establish catalytic protocols with synthetic V-BPO mimics. The need for ecologically benign catalytic systems for the synthesis of bromoorganics is increasingly being felt since, traditional bromination procedures require the elemental

bromine and chlorinated solvents, which are toxic, corrosive and hence hazardous pollutants.[303-307]

Apart from vanadate and peroxovanadate, a few other transition metal systems such as $MeReO_3$,[308] MoO(oxalate),[238] $MoO_3(aq)$[237] and $WO_3(aq)$[237] catalyze the oxidation of bromide by hydrogen peroxide and are thus treated as functional mimics of V-BPO.[306] A tungstate-exchanged layered double hydroxide (LDH) has also been studied as a heterogeneous catalyst in oxidative bromination of olefins by H_2O_2 system.[309] The molybdate exchanged LDH catalyzed oxidative bromination of aromatic substrates.[310] Bhattacharjee et al.[311] reported the formation of β-bromostyrene in presence of Na_2MoO_4 by using KBr and H_2O_2 in aqueous medium.

However, a great deal of effort is still required to develop peroxometallates with definite prospect for application as safer alternative synthetic catalyst for organic bromination reactions. For instance, unlike V-BPO which functions most efficiently at near neutral pH,[294] most of the model complexes were found to be catalytically active only in acid medium and required the use of chlorinated solvent. It is therefore, significant to note that success has been achieved by other workers of the laboratory where the present work has been carried out, in synthesizing a series of pV compounds with bridging μ-peroxo group of the type $[V_2O_2(O_2)_3.(L)_3].H_2O$ (L = amino acid or dipeptide),[312,313] as well as a polymer-anchored peroxovanadate compound.[129] which could act as powerful oxidants of bromide with good activity at physiological pH thus mimicking the enzyme V-BPO. The μ-peroxo vanadium compounds however, undergo rapid degradation in solution with loss of its high bromination activity.[312] Moreover, a set of dinuclear and mononuclear pW compounds with amino acids and peptides as auxiliary ligands[314] as well as polymer[315] supported pW complexes could serve as efficient oxidants of bromide at neutral pH, and act as catalyst in bromide oxidation in presence of H_2O_2.

Interestingly, the enzyme V-BPO not only oxidized halides but also several bicyclic sulfides to corresponding sulfoxides with high enantioselectivity.[241] The sulfoxides constitute an important class of synthetic intermediates for the construction of variety of chemically and pharmacologically important molecules including anti-ulcer (proton pump inhibitor), antibacterial, antifungal, antihypertensive, and cardiotonic agents.[316-319] Furthermore oxidative desulfurization involving oxidation of sulfides to sulfone is emerging as a promising procedure for removal of sulfur from fuel and industrial products.[320-323] Thus the contemporary interest in the process of selective oxidation of sulfides to sulfoxides or sulfone spurred the development of a vast variety of useful reagents and transition metal catalysts including vanadium,[324-326] molybdenum,[234,319,327,328] tungsten,[319, 327,329,330] copper,[331] manganese,[332,333] titanium,[323,334] iron,[335,336] rhenium,[337] etc. Nevertheless, most of the reported protocols suffer from serious limitations such as non-selectivity, high cost, over oxidation, toxicity of the catalyst. Most of the protocols also require the use of other additives and harmful chlorohydrocarbon solvents. It is worth mentioning the important work of Noyori et al.[330] where oxidation of sulfides to sulfoxide and sulfone with H_2O_2 could be achieved by using Na_2WO_4 under solvent and halide free conditions. However, a phosphonic acid promoter and an acidic quaternary ammonium salt are required along with the catalyst. Moreover, homogeneous reaction conditions of the protocol prevented catalyst recovery and recycling.[330]

There has been lot of emphasis in recent years to find new and strategically important synthetic processes using greener ingredients and a robust and recyclable catalyst that provides higher atom utilization to minimize waste and pollution level.[32,47,48] The use of solid catalysts under heterogeneous conditions, which allows easy recovery of the catalyst are considered ideal for such reactions.[47,338,339] Selective oxidation of sulfide has been carried out with a large number of supported reagents and catalysts.[340-342] Fuerte

et al.[343] reported dioxomolybdenum(VI) complexes supported on USY-zeolite and mesoporous MCM-41 as recyclable heterogeneous catalysts, which selectively catalyzed the oxidation of sulfides to sulfoxides or sulfones. However, the catalysts lose their sulfoxide selectivity at higher conversion and overoxidation of sulfide to sulfone occurs. The important findings of a comparative study carried out by Gomez and co-workers[344] with different oxidant and support to understand the role of support in selectivity of sulfoxidation, demonstrated that acid support (amberlyst) gave sulfoxide selectively, basic support (basic alumina) increased the proportion of sulfone formed.[345] Some of these systems however, are associated with the drawback of gradual leaching of the catalytic species during the repeated catalytic cycles. It is important in this context that a poly(acrylonitrile) supported pW catalyst developed in our laboratory, served as an efficient recoverable heterogeneous catalyst to selectively oxidize sulfides to sulfoxides or sulfones by H_2O_2 under mild reaction conditions.[346] A perusal available literature shows that in spite of the advantages associated with immobilization of active catalyst on polymer support, there appears to be very little information available on application of peroxometal compounds supported on polymers in organic oxidations in general.

In addition to the interesting catalytic or stoichiometric oxidizing activity exhibited by the pMo complexes, this class of compounds display properties of clinical relevance. The peroxo compounds of molybdenum (pMo) and tungsten (pW), besides peroxovanadates (pV), are now recognized as potential insulin mimics.[8] It has been reported that peroxomolybdates formed in the solution of molybdate with hydrogen peroxide stimulate all or most of the insulin bioeffects in rat adipocytes generated renewed interest in these systems.[8,198] Peroxomolybdates are also active in normalizing blood glucose levels in streptozotocin-induced diabetic rats.[8] Mikalsen et al.[200] reported that permolybdate formed in solution is potent inhibitor of protein tyrosine phosphatases.

A great deal of recent effort has been directed towards developing pV based therapeutic agents, despite the fact that most of the synthetic pV compounds are unstable under physiological condition and end with radical formation when subjected to redox processes[1,13] which limits their pharmaceutical potential. In contrast, although there has been ample evidences to show that pMo species formed in a solution of Mo-H_2O_2 are hydrolytically stable and are relatively less toxic,[8] the biochemical potential of pMo complexes remains relatively unexplored.

From the foregoing non-exhaustive discussion it is evident that despite the enormous progress in the domain of polymer supported metal complexes, and multitude of pMo complexes synthesized and studied in recent years, very few reports exist on design, synthesis and application of pMo compounds immobilized on polymer matrices. Furthermore, no information is available on peroxomolybdate anchored to water soluble polymers.

In line with the scope highlighted above, in the present research programme, we have endeavored to establish viable synthetic routes to new pMo complexes supported on insoluble as well as soluble polymer matrices. Strong focus of this work involves investigating the catalytic activity of the macrocomplexes with respect to organic oxidations and testing of some of the key bio-relevant properties of the soluble complexes viz., hydrolytic stability and their interaction with certain enzymes. Our effort has been directed basically towards two major goals: (i) to develop newer reagents and methodologies for organic oxidations under environmentally acceptable reaction conditions, and (ii) to generate peroxomolybdates with biologically important characteristics.

Chapters **3** to **7** of the thesis present interpretative accounts of the findings of our investigations on the afore mentioned aspects of peroxomolybdenum chemistry. Each of

these Chapters has been so designed as to make it a self-contained one with brief introduction, sections on experimental, results and discussion, and conclusion followed by relevant bibliography. Most of the new results have been either published or are under communication.

REFERENCES

1. Rivas, B.L., et al. *Prog. Polym. Sci.* **36**, 294--322, 2011.

2. Nasef, M.M., & Güven, O. *Prog. Polym. Sci.* **37**, 1597--1656, 2012.

3. Ko, D.Y., et al. *Prog. Polym. Sci.* **38**, 672--701, 2013.

4. Michalska, Z.M., et al. *J. Mol. Catal. A: Chem.* **156**, 91--102, 2000.

5. Buchmeiser, M.R., et al. *Macromol. Symp.* **164**, 187--196, 2001.

6. Tsuchida, E., & Nishide, H. *Adv. Polym. Sci.* **24**, 1--87,1977.

7. Conte, V., & Floris, B. *Dalton Trans.* **40**, 1419--1436, 2011.

8. Li, J., et al. *Biochemistry* **34**, 6218--6225, 1995.

9. Dickman, M.H., & Pope, M.T. *Chem. Rev.* **94**, 569--584, 1994.

10. Sheldon, R.A. & Kochi, J.K. *Metal Catalyzed Oxidations of Organic Compounds*, Academic Press, New York, 1981.

11. Bolm, C. *Coord. Chem. Rev.* **237**, 245--256, 2003.

12. Mimoun, H., et al. *J. Am. Chem. Soc.* **108**, 3711--3718, 1986.

13. Thompson, K.H., & Orvig, C. *J. Chem. Soc., Dalton Trans.* 2885--2892, 2000.

14. Szymanska, A., et al. *Polyhedron* **60**, 39--46, 2013.

15. Akelah, A. & Moet, A. *Functionalized polymers and their Applications,* Chapman & Hall, London, 1990.

16. Zhu, C., et al. *Chem. Rev.* **112**, 4687--4735, 2012.

17. Wöhrle, D. & Pomogailo, A.D. (ed.). *Metal Complexes and Metals in Macromolecules: Synthesis, Structure and Properties*, Wiley-VCH Verlag GmbH & Co. KGaA, Weinheim, 2003.

18. Likhtenshtein, G.I. *Chemical Physics of Redox Metalloenzyme Catalysis*, Springer, Heidelberg, 1988.

19. Bekturov, E.A. & Kudaibergenov, S.E. *Catalysis by Polymers*, WILEY-VCH Verlag GmbH & Co. KGaA, Weinheim, 2002.

20. Lisichkin, G.V. & Yuffa, A. Ya. *Geterogennye Metallokompleksnye Katalizatory (Heterogeneous Metal-Complex Catalysts)*, Nauka, Moscow, 1981.

21. Wohrle, D. Metal-Containing Macromolecules, in *Handbook of Polymer Synthesis*, H.R. Kricheldorf et al., eds., 2nd ed., Marcel Dekker, New York, 2005, 666-742.

22. Pomogailo, A.D. *Catalysis by Polymer Immobilised Metal Complexes*, Gordon and Breach Science Publishers, Amsterdam, 1998.

23. Merrifield, R.B., et al. *J. Am. Chem. Soc.* **85**, 2149--2154, 1963.

24. Dickerson, T.J., et al. *Chem. Rev.* **102**, 3325--3344, 2002.

25. McNamara, C.A., et al. *Chem. Rev.* **102**, 3275--3300, 2002.

26. Millar, J.R., et al. *J. Chem. Soc.* 2779--2784, 1963.

27. Farrall, M.J., & Frechet, J.M.J. *J. Org. Chem.* **41**, 3877--3882, 1976.

28. Hodge, P., et al. *Polymer* **26**, 1701--1707, 1985.

29. Letsinger, R.L., et al. *J. Am. Chem. Soc.* **86**, 5163--5165, 1964.

30. Hodge, P. *Chem. Soc. Rev.* **26**, 417--424, 1997.

31. Prazejus, H. in *Catalyst containing supported complexes*, Y.I. Yermakov, eds., Instityte of catalysis, Novosibirsk, 1978.

32. Barbaro, P., & Liguori, F. *Chem. Rev.* **109**, 515--529, 2009.

33. Helfferich, F. *Ion Exchange*, McGraw-Hill Book Company, New York, 1962.

34. Sacco, H.C., et al. *J. Chem. Soc., Perkin Trans. 2* 181--190, 2001.

35. Bahramian, B., et al. *Appl. Catal. A: Gen.* **301**, 2006, 169--175.

36. Mirkhani, V., et al. *Monatsh. Chem.* **138**, 1303--1308, 2007.

37. Selke, R. *J. Mol. Catal.* **37**, 227--234, 1986.

38. Toth, I., & Hanson, B.E. *J. Mol. Catal.* **71**, 365--371, 1992.

39. Toth, I., et al. *J. Organomet. Chem.* **396**, 363--373, 1990.

40. Kuntz, E.G. *Chemtech.* **17**, 570--575, 1987.

41. Diwakar, M.M., et al. *J. Mol. Catal. A: Chem.* **232**, 179--186, 2005.

42. Yoneda, N., & Hosono, Y. *J. Chem. Eng. Jpn.* **37**, 536--545, 2004.

43. Li, Z., et al. *Appl. Catal. A: Gen.* **292**, 61--67, 2005.

44. Hong, S.C., & Matyjaszewski, K. *Macromolecules* **35**, 7592--7605, 2002.

45. Drago, R.S., et al. *Inorg. Chem.* **20**, 2461--2466, 1981.

46. Gupta, K.C., et al. *Coord. Chem. Rev.* **253**, 1926--1946, 2009 and references there in.

47. Anastas, P.T. & Warner, J.C. *Green Chemistry: Theory and Practice*, Oxford University Press, New York, 1998.

48. Sheldon, R.A. *Green Chem.* **10**, 359--360, 2008.

49. Maurya, M.R. *Curr. Org. Chem.* **16**, 73--88, 2012.

50. da Silva, J.A.L., et al. *Coord. Chem. Rev.* **255**, 2232--2248, 2011.

51. Bergbreiter, D.E. *Chem. Rev.* **102**, 3345--3384, 2002.

52. Jang, S.-B. *Tetrahedron Lett.* **38**, 1793--1796, 1997.

53. Inada, K., & Miyaura, N. *Tetrahedron* **56**, 8661--8664, 2000.

54. Petit, M.A., & Jozefonvicz, J. *J. Appl. Polym. Sci.* **21**, 2589--2596, 1977.

55. Valodkar, V.B., et al. *J. Mol. Catal. A: Chem.* **202**, 47--64, 2003.

56. Valodkar, V.B., et al. *React. Funct. Polym.* **56**, 1--15, 2003.

57. Jun, C.-H., et al. *Tetrahedron Lett.* **40**, 8897--8900, 1999.

58. Wang, P.W., & Fox, M.A. *J. Org. Chem.* **59**, 5358--5364, 1994.

59. Nguyen, S.T., & Grubbs, R.H. *J. Organomet. Chem.* **497**, 195--200, 1995.

60. Nayak, S.D., et al. *J. Catal.* **92**, 327--339, 1985.

61. Minutolo, F., et al. *Tetrahedron Lett.* **37**, 3375--3378, 1996.

62. Skorobogaty, A., & Smith, T.D. *Coord. Chem. Rev.* **53**, 55--226, 1984.

63. Erdey, L., et al. *Talanta* **4**, 25--32, 1960.

64. Sherrington, D.C., & Simpson, S. *React. Polym.* **19**, 13--25, 1993.

65. Sherrington, D.C., & Simpson, S. *J. Catal.* **131**, 115--126, 1991.

66. Miller, M.M., et al. *J. Chem. Soc., Perkin Trans. 2* 2091--2096, 1994.

67. Miller, M.M., & Sherrington, D.C. *J. Catal.* **152**, 368--376, 1995.

68. Bedioui, F., et al. *Acc. Chem. Res.* **28**, 30--36, 1995.

69. Maslinska-Solich, J., et al. *React. Polym.* **19**, 191--199, 1993.

70. Bhaduri, S., & Khwaja, H. *J. Chem. Soc., Dalton Trans.* **25**, 415--418, 1983.

71. De, B.B., et al. *Macromolecules* **27**, 1291--1296, 1994.

72. Naughton, M.J., & Drago, R.S. *J.Catal.* **155**, 383--389, 1995.

73. Drago, R.S., & Gaul, J.H. *Inorg. Chem.* **18**, 2019--2023, 1979.

74. Masuda, S., et al. *J. Polym.* **180**, 1681--1690, 1979.

75. Noyori, R., et al. *Chem. Commun.* 1977--1986, 2003.

76. Lane, B.S., & Burgess, K. *Chem. Rev.* **103**, 2457--2474, 2003.

77. Stamenova, R.T., et al. *J. Appl. Polym. Sci.* **42**, 807--812, 1991.

78. Maurya, M.R., et al. *J. Mol. Catal. A: Chem.* **273**, 133--143, 2007.

79. Maurya, M.R., et al. *React. Funct. Polym.* **66**, 808--818, 2006.

80. Maurya, M.R., et al. *React. Funct. Polym.* **63**, 71--83, 2005.

81. Dalal, M.K., & Ram, R.N. *J. Mol. Catal. A: Chem.* **159**, 285--292, 2000.

82. Hinner, M.J., et al. *Z. Anorg. Allg. Chem.* **629**, 2251--2257, 2003.

83. Tamami, B., & Yeganeh, H. *Eur. Polym. J.* **35**, 1445--1450, 1999.

84. Bertini, I., Drago, R.S. & Luchinat, C. *The Coordination Chemistry of metalloenzyme*, D. Reidel Publishing Company, Dordrecht, Holland, 1983.

85. Andreini, C., et al. *J. Biol. Inorg. Chem.* **13**, 1205--1218, 2008.

86. Nolte, R.J.M., et al. *J. Am. Chem. Soc.* **108**, 2751--2752, 1986.

87. Tyeklar, Z., & Karlin, K.D. *Acc. Chem. Res.* **22**, 241--248, 1989.

88. Vinodu, M.V., & Padmanabhan, M. *Proc. Indian Acad. Sci.(Chem. Sci.)* **113**, 1--9, 2001.

89. Samuelson, O. Ion exchange separations, in *analytical chemistry*, Academic Press, New York, 1980.

90. Hosoya, K., et al. *J. Chromatogr. A* **979**, 3--10, 2002.

91. Kirsh, Y.E., et al. *Sep. Purif. Technol.* **22-23**, 559--565, 2001.

92. Hester, J.F., et al. *J. Membr. Sci.* **208**, 375--388, 2002.

93. Vihola, H., et al. *Eur. J. Pharm. Sci.* **16**, 69--74, 2002.

94. Murthy, N., et al. *J. Control. Release* **89**, 365--374, 2003.

95. Twaites, B.R., et al. *J. Control. Release* **97**, 551--566, 2004.

96. Pustam, A.N., & Alexandratos, S.D. *React. Funct. Polym.* **70**, 545--554, 2010.

97. Okhapkin, I.M., et al. *Adv. Polym. Sci.* **195**, 177--210, 2006.

98. Haupt, K., & Mosbach, K. *Chem. Rev.* **100**, 2495--2504, 2000.

99. Wulff, G. *Chem. Rev.* **102**, 1--28, 2002.

100. Rivas, B.L., & Geckeler, K.E. *Adv. Polym. Sci.* **102**, 171--188, 1992.

101. Zhao, X.-Y., & Janda, K.D. *Tetrahedron Lett.* **38**, 5437--5440, 1997.

102. Jr. Wentworth, P., & Janda, K.D. *Chem.Commun.* 1917--1924, 1999.

103. Sherrington, D.C. *Chem. Commun.* 2275--2286, 1998.

104. Henderson, H.C., et al. *Polymer* **35**, 2867--2873, 1994.

105. Merrifield, R.B. *Angew. Chem. Int. Ed.* **24**, 799--810, 1985.

106. Letsinger, R.L., & Wagner,T.E. *J. Am. Chem. Soc.* **88**, 2062--2063, 1966.

107. Angeletti, R.H., Bonewald, L.F., & Fields, G.B. *Six year study of peptide synthesis,* 1997, **289**, 780.

108. Bayer, E., & Schurig, V. *Chemtech.* **6**, 212--214, 1976.

109. Han, H., & Janda, K.D. *J. Am. Chem. Soc.* **118**, 7632--7633, 1996.

110. Gravert, D.J., & Janda, K.D. *Chem. Rev.* **97**, 489--510, 1997.

111. Nuzzo, R.G., et al. *J. Am. Chem. Soc.* **101**, 3683--3685, 1979.

112. Fan, Q.-H., et al. *Tetrahedron: Asymmetry* **12**, 1241--1247, 2001.

113. Sharpless, K.B., et al. *J. Org. Chem.* **57**, 2768--2771, 1992.

114. Haumann, M., et al. *Appl. Catal. A* **225,** 239--249, 2002.

115. Alper, H., et al. *Tetrahedron Lett.* **26**, 2263--2264, 1985.

116. Rico, I., et al. *J. Chem. Soc., Chem. Commun.* 1205--1206, 1987.

117. Karakhanov, E.A., et al. *Catal. Lett.* **3**, 31--36, 1989.

118. Dallmann, K., et al. *J. Mol. Catal. A: Chem.* **178**, 43--46, 2002.

119. Kimura, Y., & Regen, S.L. *J. Org. Chem.* **47**, 2493--2494, 1982.

120. Jongsma, T., et al. *Polymer* **33**, 161--165, 1992.

121. Challa, G. *J. Mol. Catal.* **21**, 1--16, 1993.

122. Bergbreiter, D.E., et al. *Angew. Chem. Int. Ed.* **39**, 1039--1042, 2000.

123. Jin, J.-J., et al. *React. Polym.* **23**, 95--100, 1994.

124. Teranishi, T. et al. *React. Funct. Polym.* **37**, 111--119, 1998.

125. Hsu, Y.F., & Cheng, C.P. *J. Mol. Catal. A: Chem.* **136**, 1--11, 1998.

126. Ajjou, A.N., & Alper, H. *J. Am. Chem. Soc.* **120**, 1466--1468, 1998.

127. Malmstrom, T., & Andersson, C. *Chem. Commun.* 1135--1136, 1996.

128. Malmstrom, T., & Andersson, C. *J. Mol. Catal. A: Chem.* **157**, 79--82, 2000.

129. Kalita, D., et al. *React. Funct. Polym.* **68**, 876--890, 2008.

130. Das, S.P., et al. *RSC Adv.* **2**, 7248--7261, 2012.

131. Rivas, B.L., et al. *Polym. Int.* **58**, 1093--1114, 2009.

132. Hosseinkhani, H., & Hosseinkhani, M. *Current Drug Safety* **4**, 79--83, 2009.

133. Lee, V.A., et al. *J. Controlled Release* **14**, 61--70, 1990.

134. Kadajji, V.G., & Betageri, G.V. *Polymers* **3**, 1972--2009, 2011.

135. Reneker, D.H., et al. *J. Appl. Phys.* **87**, 4531--4547, 2000.

136. Drobnik, J. & Rypacek, F. Soluble Synthetic Polymers in Biological Systems, in *Polymers in Medicine*, Springer-Verlag, Berlin, New York, 1984, **57**, 1-50.

137. Polymers for Pharmaceutical Applications, in *Lubrizol Pharmaceutical Bulletin 1*, Lubrizol, Wickliffe, OH, USA, 2011.

138. Adams, N., & Schubert, U.S. *Adv. Drug Deliv. Rev.* **59**, 1504--1520, 2007.

139. Carpino, L.A., et al. *Makromol. Chem.* **177**, 1631--1635, 1976.

140. Neri, P., et al. *J. Med. Chem.* **16**, 893--897, 1973.

141. Antoni, G., et al. *Biopolymers* **13**, 1721--1729, 1974.

142. Ajisaka, K., & Iwashita, Y. *Biochem. Biophys. Res. Commun.* **97**, 1076--1081, 1980.

143. Ferrutti, P. *Il Farmaco. De. Sci.* **32,** 220--236, 1977.

144. Khan, T.A., & Khiang, P.K. *J. Pharm. Pharm. Sci.* **5**, 205--212, 2002.

145. Lévesque, S.G., & Shoichet, M.S. *Biomaterials* **27**, 5277--5285, 2006.

146. Vilivalam, V.D., et al. *Pharm. Sci. Technol. Today* **3**, 64--69, 2000.

147. Milojevic, S., et al. *J. Controlled Release* **38**, 75--84, 1996.

148. Lee, V.A., & Rashidova, S.S. *Abstr. 36th IUPAC Int. Symp. Macromol.*, Seoul, Korea 1996, 513.

149. Haxton, K.J., & Burt, H.M. *J. Pharm. Sci.* **98**, 2299--2316, 2009.

150. Avichezer, D., et al. *React. Polym.* **36**, 59--69, 1998.

151. Neuse, E.W., et al. *Polym. Adv. Technol.* **13**, 884--894, 2002.

152. Sood, P., et al. *Bioconjugate Chem.* **17**, 1270--1279, 2006.

153. Nandi, M.M., et al. *Ind. J. Chem. Sect. A: Inorg.* **27**, 687--690, 1998.

154. Nonaka, T., et al. *J. Appl. Polym. Sci.* **62**, 1651--1659, 1996.

155. Rivas, B.L., et al. *Prog. Polym. Sci.* **28**, 173--208, 2003.

156. Kanazawa, A., et al. *Antimicrob. Agents. Chemother.* **38**, 945--952, 1994.

157. Abd-El-Aziz, A.S., Carraher, C.E., Pittman, C.U., Sheats, J.E., & Zeldin, M., eds., Macromolecules Containing Metal and Metal-Like Elements, in *Biomedical Applications*, John Wiley & Sons Inc., Canada, 2004, **3**, 6.

158. Crichton, R.R. *Biological Inorganic Chemistry: An Introduction,* Elsevier, Netherlands, 2008, 279.

159. Howe-Grant, M. (ed.) *Kirk-Othmer Encyclopedia of Chemical Technology*, 4th ed., John Wiley & Sons, New York, 1995, 16, 925-962.

160. Greenwood, **N.N.** & Earnshaw, A. *Chemistry of the Elements*, 2nd ed., Butterworth-Heineman, Oxford, 1997, 1002-1039.

161. Lide, D.R. (ed.), *Handbook of Chemistry and Physics*, 81st ed., CRC Press, Boca Raton, 2000.

162. Hille, R. *Trends Biochem. Sci.* **27**, 360--367, 2002.

163. Cotton, F.A., Wilkinson, G., Murillo, C.A. & Bochmann, M. *Advanced Inorganic Chemistry*, 6th ed., Wiley India (P) Ltd., New Delhi, 2008, 920-974.

164. Holm, R.H., et al. *Coord. Chem. Rev.* **255**, 993--1015, 2011.

165. Sebenik, R.F., Burkin, A.R., Dorfler, R.R., Laferty, J.M., Leichtfried, G., Meyer-Grunow, H., Mitchell, P.C.H., Vukasovich, M.S., Church, D.A., Vanriper, G.G., Gilliland, J.C. & Thielke, S.A. Molybdenum and Molybdenum Compounds, in *Ullmann's Encyclopedia of Industrial Chemistry*, Wiley-VCH Verlag GmbH & Co. KGaA, Weinheim, 2012, **23**, 522-566.

166. Oyerinde, O.F., et al. *Inorg. Chim. Acta* **361**, 1000--1007, 2008.

167. Emsley, J. *The Elements*, Oxford University Press, Oxford, 1998.

168. Niven, M.L., et al. *J. Chem. Soc., Dalton Trans.* 2007--2011, 1991.

169. Roman, P., et al. *Polyhedron* **11**, 2027--2038, 1992.

170. Keggin, J.F. *Proc. R. Soc.Lond. A* **144**, 75--100, 1934.

171. Braithwaite, E.R. & Haber, J. (ed.). *Molybdenum: An Outline of its Chemistry and Uses*, Elsevier, Amsterdam, 1994, 662.

172. Rollinson, C.L. Chapter 36 in *Comprehensive Inorganic Chemistry*, Pergamon Press, Oxford, 1973, **3,** 623-769.

173. Chen, G.J.J., et al. *Inorg. Chem.* **15**, 2612--2615, 1976.

174. Kristallogr, Z. *NCS* **222**, 215--216, 2007.

175. Le Carpentier, J.-M., et al. *Acta Crystallogr., Sect. B: Struct. Crystallogr. Cryst. Chem.* **B28**, 1278--1288, 1972.

176. Lyashenko, G., et al. *Dalton Trans.* 5655--5665, 2009.

177. Ngan, N.K., et al. *Polyhedron* **33**, 235--251, 2012.

178. Judmaier, M.E., et al. *Inorg. Chem.* **51**, 9956--9966, 2012.

179. Takjoo, R., et al. *J. Coord. Chem.* **66**, 345--357, 2013.

180. Djordjevic, C., et al. *Inorg. Chem.* **36**, 1798--1805, 1997.

181. Djordjevic, C., et al. *Inorg. Chim. Acta* **104**, L7--L9, 1985.

182. Greaney, M.A., & Stiefel, E.I. *J. Chem. Soc., Chem. Commun.* 1679--1680, 1992.

183. Basu, P., et al. *Inorg. Chem.* **34**, 405--407, 1995.

184. Calderazzo, F., et al. *J. Chem. Soc., Dalton Trans.* 655--658, 1993.

185. Bissessur, R., et al. *J. Chem. Soc., Chem. Commun.* 1582--1585, 1993.

186. Muller, A., et al. *Angew.Chem. Int. Ed.* **19**, 875--882, 1980.

187. Arzoumanian, H. *Coord. Chem. Rev.* **178–180**, 191--202, 1998.

188. Hill, R. *Chem. Rev.* **96**, 2757--2816, 1996.

189. Hille, R. *Biochim. Biophys. Acta* **1184**, 143--169, 1994.

190. Schwarz, G., et al. *Nature* **460**, 839--847, 2009.

191. Majumdar, A., & Sarkar, S. *Coord. Chem. Rev.* **255**, 1039--1054, 2011.

192. Enemark, J.H., et al. *Chem. Rev.* **104**, 1175--1200, 2004.

193. Johnson, M.K., et al. *Chem. Rev.* **96**, 2817--2840, 1996.

194. Sugimoto, H., et al. *Chem. Commun.* **49**, 4358--4360, 2013.

195. Holleman, A.F. & Wiberg, E. *Inorganic chemistry*, Academic Press, San Diego, 2001, 1384.

196. Barr, R.Q. Molybdenum in *Van Nostrand's Encyclopedia of Chemistry*, G.D. Considine, eds., Wiley-Interscience, New York, 2005, 1038–1040.

197. Russell, R. & Beard, J.L. *Dietary reference intakes for Vitamin A, Vitamin K, Arsenic, Boron, Chromium, Copper, Iodine, Iron, Manganese, Molybdenum, Nickel, Silicon, Vanadium and Zinc*, National Academy Press, Washington, 2001, 420-441.

198. Goto, Y., et al. *Biochem. Pharmacol.* **44**, 174--177, 1992.

199. Lord, S.J., et al. *Can. J. Chem.* **77**, 1249--1261, 1999.

200. Mikalsen, S.-O., & Kaalhus, O. *J. Biol. Chem.* **273**, 10036--10045, 1998.

201. Stankiewicz, P.J., & Gresser, M.J. *Biochemistry* **27**, 206--212, 1988.

202. VanEtten, R.L., et al. *J. Am. Chem. Soc.* **96**, 6782--6785, 1974.

203. Morales, L., et al. *J. Mex. Chem. Soc.* **56**, 80--84, 2012.

204. Nordlie, R.C., & Arion, W.J. *J. Biol. Chem.* **239**, 1680--1685, 1964.

205. Nishigori, H, & Toft, D. *Biochemistry* **19**, 77--83, 1980.

206. McNeill, J.H., et al. *J. Med. Chem.* **35**, 1489--1491, 1992.

207. Levina, A., & Lay, P.A. *Dalton Trans.* **40**, 11675--11686, 2011.

208. Haywood, S., et al. *Brit. J. Nutr.* **79**, 329--331, 1998.

209. Mitsui, S., et al. *Biomed. Pharmacother.* **60**, 353--358, 2006.

210. Mioc, U.B., et al. *Solid State Ionics* **176**, 3005--3017, 2005.

211. Jelikic-Stankov, M., et al. *J. Trace Elem. Med. Biol.* **21**, 8--16, 2007.

212. Connor, J.A., & Ebsworth, E.A.V. *Adv. Inorg. Chem. Radiochem.* **6**, 279--381, 1964.

213. Nxumalo, F., Tracey, A.S., Detich, N., Gresser, M.J. & Ramachandran, C. in *Vanadium Compounds. Chemistry, Biochemistry and Therapeutic Applications*, A.S. Tracey, & D.C. Crans, eds., Oxford University Press, New York, 1998, 259.

214. Chaudhuri, M.K. *J. Mol. Catal.* **44**, 129--141, 1988.

215. Mimoun, H. *The Chemistry of Functional Groups, Peroxides;* Patai, S., ed., Wiley, New York, 1983, 463-474.

216. Sharpless, K.B. *Chemtech* **15**, 692--700, 1985.

217. Itoh, T., et al. *J. Am. Chem. Soc.* **101**, 159--169, 1979.

218. Kadish, K.M., et al. *Inorg. Chem.* **22**, 3490--3492, 1983.

219. Fuhrhop, J.-H. *Angew. Chem. Int. Ed.* **15**, 648--659, 1976.

220. Swedo, K.B., & Enemark, J.H. *J. Chem. Educ.* **56**, 70, 1979.

221. Vaska, L. *Acc. Chem. Res.* **9**, 175--183, 1976.

222. Conte, V. & Bortolini, O. Transition metal peroxides. Synthesis and role in oxidation reactions, in *the chemistry of Peroxides,* Z. Rappoport, ed., John Wiley & Sons Ltd, England, 2006, **2**, 1053-1128.

223. Mimoun, H., et al. *Tetrahedron* **26**, 37--50, 1970.

224. Sharpless, K.B., et al. *J. Am. Chem. Soc.* **94**, 295--296, 1972.

225. Afsharpour, M., et al. *Appl. Catal. A* **327**, 205--210, 2007.

226. Mimoun, H. *Catal. Today* **1**, 281--295, 1987.

227. Campestrini, S., et al. *J. Org. Chem.* **53**, 5721--5724, 1988.

228. Batigalhia, F., et al. *Tetrahedron* **57**, 9669--9676, 2001.

229. Sheikhshoaie, I., et al. *Polyhedron* **28**, 733--738, 2009.

230. Bagherzadeh, M., et al. *Inorg. Chim. Acta* **361**, 2019--2024, 2008.

231. Gamelas, C.A., et al. *Tetrahedron Lett.* **49**, 4708--4712, 2008.

232. Gharah, N., et al. *Inorg. Chim. Acta* **362**, 1089--1100, 2009.

233. Tundo, P., et al. *Catal. Commun.* **11**, 1181--1184, 2010.

234. Jacobson, S.E., et al. *J. Org. Chem.* **44**, 921--924, 1979.

235. Di Furia, F., et al. *J. Mol. Catal.* **19**, 81--84, 1983.

236. Reynolds, M.S., et al. *Inorg. Chim. Acta* **263**, 225--230, 1997.

237. Meister, G.E., & Butler, A. *Inorg. Chem.* **33**, 3269--3275, 1994.

238. Reynolds, M.S., et al. *Inorg. Chem.* **33**, 4977--4984, 1994.

239. Butler, A. & Baldwin, A.H. Vanadium Bromoperoxidase and Functional Mimics, in *Metal Sites in Protein and Models: Phosphatases, Lewis Acids and Vanadium*, H.A.O. Hill, P.J. Sadler & A.J. Thomson, eds., Springer, Germany, 1997, 109-132.

240. Colpas, G.J., et al. *J. Am. Chem. Soc.* **118**, 3469--3478, 1996.

241. Butler, A. *Coord. Chem. Rev.* **187**, 17--35, 1999.

242. Crans, D.C., & Shin, P.K. *J. Am. Chem. Soc.* **116**, 1305--1315, 1994.

243. Shechter, Y., et al. *Coord. Chem. Rev.* **237**, 3--11, 2003.

244. Sakurai, H., et al. *Coord. Chem. Rev.* **226**, 187--198, 2002.

245. Maniatakou, A., et al. *J. Inorg. Biochem.* **103**, 859--868, 2009.

246. Shaver, A., et al. *Mol. Cell. Biochem.* **153**, 5--15, 1995.

247. Sarkar, A.R., & Mandal, S. *Met Based Drugs* **7**, 157--164, 2000.

248. Holder, A.A. *Annu. Rep. Prog.Chem., Sect. A* **106**, 176--185, 2010.

249. Thompson, H.J., et al. *Carcinogenesis* **5**, 849--851, 1984.

250. Scrivens, P.J., et al. *Mol. Cancer Ther.* **2**, 1053--1059, 2003.

251. Thomadaki, H., et al. *J. Inorg. Biochem.* **105**, 155--163, 2011.

252. Crans, D.C., et al. *Chem. Rev.* **104**, 849--902, 2004.

253. Huyer, G., et al. *J. Biol. Chem.* **272**, 843--851, 1997.

254. Campbell, N.J., et al. *J. Chem. Soc., Dalton Trans.* 1203--1208, 1989.

255. Nardello, V., et al. *Inorg. Chem.* **34**, 4950--4957, 1995.

256. Conte, V., et al. *J. Mol. Catal. A: Chem.* **113**, 175--184, 1996.

257. Sergienko, V.S. *Crystallogr. Rep.* **53**, 18--46, 2008.

258. Arkhipov, A.V., et al. *Russ. J. Inorg. Chem.* **24**, 936--938, 1979.

259. Griffith, W.P. *J. Chem. Soc.* 5345--5350, 1963.

260. Mitschler, A., et al. *J. Chem. Soc., Chem. Commun.(London)* 1260--1261, 1968.

261. Taube, F., et al. *J. Chem. Soc., Dalton Trans.* 4451--4456, 2002.

262. Howarth, O.W., Pettersson, L., Andersson, I. Aqueous Peroxoisopolyoxometalates, in *Polyoxometalate Chemistry from Topology via Self-Assembly to Applications*, M.T. Pope & A. Müller, Editors, Kluwer Academic Publishers, United States of America, 2002, 145-159.

263. Krishnan, C.V., et al. *Chin. J. Polym. Sci.*. **27**, 11--22, 2009.

264. Dengel, A.C., et al. *J. Chem. Soc., Chem. Commun.* 555--556, 1986.

265. Feyel, S., et al. *Dalton Trans*. 4010--4016, 2004.

266. Sensato, F.R., et al. *J. Org. Chem.* **68**, 5870--5874, 2003.

267. Shoemaker, C.B., et al. *Acta Crystallogr. Sect. C Cryst. Struct. Commun.* **C41**, 347--350, 1985.

268. Schlemper, E. O., et al. *Polyhedron.* **3**, 377--380, 1984.

269. Herrmann, W. A., et al. *Chem. Ber.* **123**, 1963--1970, 1990.

270. Stomberg, R. *J. Crystallogr. Spectrosc. Res.* **18**, 659--669, 1988.

271. Flanagan, J., et al. *Inorg. Chim. Acta* **96**, L23--L24, 1985.

272. Jacobson, S.E., et al. *Inorg. Chem.* **17**, 3055--3063, 1978.

273. Stomberg, R. *Acta Chem. Scand.* **22**, 1076--1090, 1968.

274. Einstein, F.W.B., & Penfold, B.R. *Acta Crystallogr. (Supplement)* **16**, A35, 1963.

275. Stomberg, R. *J. Less-Common Met.* **144**, 109--116, 1988.

276. Mimoun, H., et al. *Bull. Soc. Chim. Fr.* **5**, 1481--1492, 1969.

277. H. Mimoun, *Angew. Chem. Int. Ed. Engl.* **21**, 734--750, 1982.

278. Chien, C.S., et al. *Chem. Pharm. Bull.* **33**, 1843--1848, 1985.

279. Chien, C.S., et al. *Chem. Pharm. Bull.* **33**, 5071--5074, 1985.

280. Brewer, G.A., & Sinn, E. *Inorg. Chem.* **20**, 1823--1830, 1981.

281. Maiti, S.K., et al. *Inorg. Chem.* **45**, 9843--9857, 2006.

282. Bortolini, O., et al. *J. Org. Chem.* **52**, 5467--5469, 1987.

283. Maiti, S.K., et al. *Inorg. Chem. Commun.* **7**, 823--828, 2004.

284. Maiti, S.K., et al. *New J. Chem.* **29**, 554--563, 2005.

285. Csanyi, L.J., & Jaky, K. *J. Catal.* **127**, 42--50, 1991.

286. Griffith, W.P., et al. *J. Chem. Soc., Dalton Trans.* 3131--3138, 1995.

287. Stomberg, R., & Olson, S. *J. Alloys Compd.* **237**, 39--44, 1996.

288. Moller, E.R., & Jorgensen, K.A. *Acta Chem. Scand.* **45**, 546--548, 1991.

289. Tarafder, M.T.H., et al. *Polyhedron* **11**, 795--798, 1992.

290. Conte, V., et al. *J. Phys. Org. Chem.* **9**, 329--336, 1996.

291. Conte, V., et al. *Inorg. Chim. Acta* **272**, 62--67, 1998.

292. Ghiron, A.F., & Thompson, R.C. *Inorg. Chem.* **29**, 4457--4461, 1990.

293. Conte,V., & Di Furia, F. *Catylic Oxidations with Hydrogen Peroxide as Oxidant*, G. Strukul, ed., Kluwer Academic Publishers, The Netherlands, 1992, 223.

294. Butler, A., et al. *Chem. Rev.* **94**, 625--638, 1994.

295. Wischang, D., et al. *Coord. Chem. Rev.* **255**, 2204--2217, 2011.

296. Butler, A., & Carter-Franklin, J.N. *Nat. Prod. Rep.* **21**, 180--188, 2004.

297. Faulkner, D.J. *Nat. Prod. Rep.* **17**, 7--55, 2000.

298. Crans, D.C., et al. *Coord.Chem. Rev.* **255**, 2178--2192, 2011.

299. Rehder, D., et al. *Coord.Chem. Rev.* **237,** 53--63, 2003.

300. Pecoraro, V.L., Slebodnick, C. & Hamstra, B. *Vanadium Compounds. Chemistry, Biochemistry and Therapeutic Applications.*, A.S. Tracey & D.C. Crans, eds., Oxford University Press, New York, 1998, 157.

301. Sakurai, H., & Tsuchiya, K. *FEBS Lett.* **260**, 109--112, 1990.

302. Clague, M.J., & Butler, A. *J. Am. Chem. Soc.* **117**, 3475--3484, 1995.

303. Podgorsek, A., et al. *Angew. Chem. Int. Ed.* **48**, 8424--8450, 2009.

304. Kikushima, K. et al. *Tetrahedron* **66**, 6906--6911, 2010.

305. Kavala, V., et al. *J. Org. Chem.* **70**, 4267--4271, 2005.

306. Sels, B.F, et al. *J. Am. Chem. Soc.* **123**, 8350--8359, 2001.

307. Clark, J.H. *Green Chem.* **1**, 1-8, 1999.

308. Espenson, J.H., et al. *J. Am. Chem. Soc.* **116**, 2869--2877, 1994.

309. Sels, B.F., et al. *J. Catal.* **216**, 288--297, 2003.

310. Choudary, B.M., et al. *Catal. Commun.* **5**, 215--219, 2004.

311. Sinha, J. et al. *Chem. Commun.* **19**, 1916--1917, 2001.

312. Sarmah, S., et al. *Polyhedron* **23,** 1097--1107, 2004.

313. Sarmah, S., et al. *Mol. Cell. Biochem.* **236**, 95--105, 2002.

314. Hazarika, P., et al. *Polyhedron* **25**, 3501--3508, 2006.

315. Boruah, J.J., et al. *Polyhedron* **52**, 246--254, 2013.

316. Lai, K.C., et al. *N. Engl. J. Med.* **346**, 2033--2038, 2002.

317. Baker, D.E. *Rev. Gastroenterol. Disord.* **1**, 32--41, 2001.

318. Schmied, R., et al. *Circ. Res.* **68**, 597--604, 1991

319. Kaczorowska, K., *Tetrahedron* **61**, 8315--8327, 2005.

320. Guoxian Yu., et al. *Energy Fuels* **19**, 447--452, 2005.

321. Mei, H., et al. *Fuel* **82**, 405--414, 2003.

322. Zhu, W., et al. *J. Mol. Catal. A Chem.* **347,** 8--14, 2011.

323. Hulea, V., et al. *J. Catal.* **198**, 179--186, 2001.

324. Di Furia, F., et al. *Tetrahedron Lett.* **17**, 4637--4638, 1976.

325. Conte, V., et al. *Pure Appl. Chem.* **81**, 1265--1277, 2009.

326. Gregori, F., et al. *J. Mol. Catal. A: Chem.* **286**, 124--127, 2008.

327. Gresley, N.M., et al. *J. Mol. Catal.* A **117**, 185--198, 1997.

328. Romanelli, G.P., et al. *Catal. Commun.* **12**, 726--730, 2011.

329. Koo, D.H., et al. *Org. Lett.* **7**, 5015--5018, 2005.

330. Sato, K., et al. *Tetrahedron* **57**, 2469--2476, 2001.

331. Ayala, V., et al. *J. Mol. Catal. A: Chem.* **221**, 201--208, 2004.

332. Xie, F., et al. *J. Mol. Catal. A: Chem.* **307**, 93--97, 2009.

333. Barker, J.E., & Ren, T. *Tetrahedron Lett.* **46**, 6805--6808, 2005.

334. Iwamoto, M., et al. *Microporous Mesoporous Mater.* **48**, 271--277, 2001.

335. Egami, H., & Katsuki, T. *J. Am. Chem. Soc.* **129**, 8940--8941, 2007.

336. Baciocchi, E., et al. *J. Org. Chem.* **69,** 3586--3589, 2004.

337. Stanger, K.J., et al. *J. Mol. Catal. A: Chem.* **243**, 158--169, 2006.

338. Horvath, I.T., & Anastas, P.T. *Chem. Rev.* **107**, 2169--2173, 2007.

339. Anastas, P.T., et al. *Appl. Catal. A.* **221**, 3--13, 2001.

340. Fraile, J.M., et al. *Chem. Commun.* 1807--1808, 1998.

341. Raju, S.V.N., et al. *Chem. Commun.* 1969--1970, 1996.

342. Kholdeeva, O.A., et al. *J. Mol. Catal. A: Chem.* **158**, 417--421, 2000.

343. Fuerte, A., et al. *J. Mol. Catal. A: Chem.* **211**, 227--235, 2004.

344. Gomez, M.V., et al. *Green Chem.* **9**, 331--336, 2007.

345. Bharadwaj, S.K., et al. *Tetrahedron Lett.* **50**, 3767--3771, 2009.

346. Das, S.P., et al. *J. Mol. Catal. A: Chem.* **356**, 36--45, 2012.

CHAPTER 2

Materials and Methods

This chapter gives a brief account of the materials used and the various analytical and physicochemical techniques employed for the characterization of the ligands and the supported peroxometal complexes. Procedural details regarding the synthesis of the complexes and their activity studies are described in their respective chapters.

2.1 CHEMICALS

The chemicals used were all reagent grade products. The sources of chemicals are given below:

Acetone, acetonitrile, methanol, ethylacetate, petroleum ether, diethyl ether, dichloromethane, silica gel (60-120 mesh), 50% hydrogen peroxide, 30% hydrogen peroxide, aniline (v/v) (RANKEM), DL-alanine, L-valine, aminophenol (CDH, New Delhi, India), molybdic acid, sodium hydroxide, sodium sulfate, resorcinol, salicylaldehyde, pyrogallol, catechol, acetanilide, nitroaniline, methanol, acetonitrile (E. Merck, India), poly(sodium acrylate) (Mw= 2100) (Fluka), poly(sodium methacrylate) (Mw = 4000), poly(sodium vinyl sulfonate) (Mw = 4000), alkaline phosphatase from rabbit intestine (ALP), acid phosphatase from wheat thylakoid membrane (ACP), catalase, p-nitrophenyl phosphate (p-NPP), chloromethylated poly(styrene-divinylbenzene) (2.5 mmol g^{-1} Cl loading, 2% DVB) (**MR**), methyl phenyl sulfide (MPS), ethyl phenyl sulfide (EPS), dimethyl sulfide (DMS), dibutyl sulfide (DBS), butyl propyl sulfide (BPS), dibenzothiophene (DBT), phenylvinyl sulfide (PVS),

2-(phenylthio)ethanol (PTE), dihexyl sulfide (DHS), diphenyl sulfide (DPS), benzyl phenyl sulfide (BPS), allyl phenyl sulfide (APS) (Sigma-Aldrich Chemical Co., Milwaukee, USA) and sodium thiosulphate, potassium hydrogen phosphate, potassium dihydrogen phosphate, glycine, oxine, and $MgCl_2$ (SD Fine Chemicals, Mumbai, India). **$[MoO(O_2)_2(glycine)(H_2O)]$** (**$DMo_1$**) and **$[MoO(O_2)_2(asparagine)(H_2O)]$** (**$DMo_2$**) were synthesized according to a previously reported procedure.[1] Polyacrylamide (PAm) was prepared by solution polymerization technique using iron(II) ammonium sulfate and hydrogen peroxide as redox initiator.[2] The resin, **MR** was pretreated with aqueous dioxane (50:50 (v/v)) and finally washed with methanol and dried under vacuum at 90 °C for 8 h before chemical functionalization. The water used for solution preparation was deionized and distilled.

2.2 ELEMENTAL ANALYSES

2.2.1 Molybdenum

2.2.1.1 Gravimetry[3]

Molybdenum was estimated by precipitation as molybdenum oxinate, $MoO_2(C_9H_6ON)_2$ by adopting the following procedure.

An accurately weighed amount of the water soluble compounds **PAMo** (**4.1**) or **PMAMo** (**4.2**) or **PAmMo** (**4.3**) or **PSMo** (**4.4**) was dissolved in 20 mL distilled water in a 250 mL beaker and then acidified with a few drops of dilute M - sulfuric acid. To the mixture, 5 mL of 2 M ammonium acetate was added and diluted it to 50-100 mL followed by heating upto boiling. The molybdenum was precipitated by the addition of 3% solution of oxine in dilute acetic acid until the supernatant liquid becomes perceptibly yellow. The

mixture was then boiled gently and stirred for 3 minutes. The precipitate was then filtered through a constant-weighed sintered glass crucible and washed with hot water until free from the reagent. After washing, it was dried to constant weight at 130-140 °C.

In case of insoluble compound **PANMo (3.3)**, an accurately weighed amount of the compound was treated with H_2SO_4 (4 N) to detach the anchored molybdenum from the polymer matrix. The mixture was filtered and the residue containing the solid polymer was washed several times with H_2SO_4 (4 N) for complete removal of the metal. The solid residue was discarded and the filtrate and the washings were transferred to a 250 mL beaker. Subsequently, molybdenum was estimated by following the procedure as mentioned above for compound **4.1-4.4**.

In case of insoluble peroxomolybdate complexes immobilized on amino acid functionalized Merrifield resin, **MRVMo (3.1)** and **MRAMo (3.2)**, an accurately weighed amount was first ignited in a Bunsen flame to remove the polymer. Subsequently, the residue was acid digested followed by evaporation to dryness. To the dry mass, 20 mL of distilled water was added and estimated the molybdenum content by following the procedure as mentioned for the compounds **4.1-4.4**.

2.2.2.2 EDX analysis and Atomic absorption spectroscopy *(AAS)*

Molybdenum content was also determined by using Energy Dispersive X-Ray (EDX) analysis and atomic absorption spectroscopy *(AAS)*.

2.2.2 Peroxide[4-6]

2.2.2.1 Permanganometry[4]

To a freshly prepared solution of 7N sulfuric acid containing *ca.* 4 g of boric acid, an accurately weighed amount of a peroxomolybdate compound was added. Boric acid

was used to form perboric acid to prevent any loss of active oxygen. The resulting solution was then titrated with a standard potassium permanganate solution. This method is suitable for determination of peroxide content in peroxomolybdenum(VI) compounds.

1 mL of 1N $KMnO_4$= 0.01701 g of H_2O_2

2.2.2.2 Iodometry[5]

An accurately weighed amount of the peroxomolybdenum(VI) compound was added to a freshly prepared 2 N sulfuric acid solution containing an appropriate amount of potassium iodide (~1 g in 100 mL) and a pinch of sodium bicarbonate with constant stirring. The mixture was kept at dark for *ca.* 15 min in CO_2 atmosphere. The liberated iodine was then titrated with a standard sodium thiosulfate solution by adding 2 mL freshly prepared starch solution when the color of the iodine was nearly discharged. The liberated iodine was titrated against standard sodium thiosulfate solution until it turned into pale yellow. Subsequently, a few drops (1-5 mL) of 1% starch solution was added and the solution was turned into deep purple colour. Finally, it was titrated until the solution became colourless and the final reading was observed.

1 mL of 1N $Na_2S_2O_3$ = 0.01701 g of H_2O_2

This method gives the total amount of peroxide present in the compound.

2.2.2.3 By standard Ce(IV) solution[6]

An accurately weighed amount of a peroxomolybdate(VI) compound was added to 0.7 N sulfuric acid solution in the presence of an excess of boric acid. Peroxide was then estimated by titrating with a standard Ce(IV) solution.

2.2.3 Carbon, Hydrogen and Nitrogen

The compounds were analyzed for carbon, hydrogen and nitrogen by Perkin Elmer 2400 series II at the Department of Chemical Sciences, Tezpur University.

Carbon and nitrogen content was also determined from EDX analysis.

2.2.4 Chlorine

The chlorine content in the compounds was determined by EDX analysis.

2.2.5 Sulfur

The sulfur content in the compounds was determined by EDX analysis.

2.2.6 Sodium

Sodium content in the compounds was determined by EDX analysis and AAS.

2.3 PHYSICAL AND SPECTROSCOPIC MEASUREMENTS

2.3.1 pH measurement

pH of the reaction solutions, whenever required were measured by using a Orion VSTAR52, and also by E. Merck Universal indicator pH 0-14 paper.

2.3.2 Electronic spectra

The diffuse reflectance UV–Vis spectra of solid samples are recorded using a Hitachi U-3400 spectrophotometer equipped with a diffuse reflectance accessory with an integrating sphere of 60 mm inner diameter using $BaSO_4$ as standard.

The UV-Vis absorption spectra in solution were recorded in a Cary model Bio 100 spectrophotometer, equipped with a peltier controlled constant temperature cell in 1 cm quartz cuvettes. All the absorbance values are denoted as, e.g., A_{405}, A_{592}, A_{320} at the wavelengths indicated.

2.3.3 Infrared (IR) spectra

The infrared (IR) spectra were recorded in KBr pellets using a Nicolet model impact 410 FTIR spectrophotometer in the range 4000-400 cm^{-1}.

2.3.4 Surface morphology analysis by Scanning Electron Microscope (SEM)

The surface morphology of the samples was analyzed by using the JEOL JSM-6390LV Scanning Electron Micrograph attached with energy dispersive X-ray detector. The samples were mounted on SEM mounts with carbon tape and coated with a thin layer of evaporated platinum. Scanning was done at 1–20 μm range and images were taken at a magnification of 15–20 kV. Data were obtained using INCA software. The standardization of the data analysis is an integral part of SEM-EDX instrument employed.

2.3.5 Atomic Absorption Spectroscopy (AAS)

Atomic Absorption Spectrometry was done in Thermo iCE 3000 series Atomic absorption spectrophotometer model analyst 200.

2.3.6 Surface area analyses

Dinitrogen adsorption/desorption measurements were performed at 77.3 K on Quantachrome model Nova 4200e porosimeters. Surface area measurements utilized a

five point adsorption isotherm collected over 0.05 to 0.35 p/p^{o} and analyzed via the BET method[7] and pore volume were determined by BJH model.[8]

2.3.7 ^{1}H NMR spectra

The ^{1}H NMR spectra were recorded on JEOL JNM-ECS400 spectrophotometer using deuterated chloroform. The chemical shifts are referenced with respect to TMS = δ 0 ppm. The values are given in ppm. The abbreviations s, d, m and br are used to depict the singlet, doublet, multiplet and broad absorption signals respectively in ^{1}H-NMR spectrum.

2.3.8 ^{13}C NMR spectra

The ^{13}C NMR spectra for all the peroxomolybdenum complexes, **3.1-3.3** and **4.1-4.4** were recorded in a JEOL JNM-ECS 400 spectrometer at carbon frequency 100.5 MHz.

The ^{13}C NMR spectra for **MR**, **MRV**, **MRA**, **MRVMo** (**3.1**) and **MRAMo** (**3.2**) were recorded in the spectrometer at carbon frequency 100.5 MHz, 4096 X-resolution points, number of scans 2300, 75 ms of acquisition time, 30° pulse length and 0.4 s of relaxation delay with ^{1}H NMR decoupling method by swelling in (CCl_4 / DMSO-d) (80:20, v/v).

The ^{13}C NMR spectra for PAN and **PANMo** (**3.3**) were recorded at carbon frequency 100.5 MHz, 32768 X-resolution points, number of scans 10000, 1.04 s of acquisition time and 2.0 s of relaxation delay with ^{1}H NMR decoupling method in (DMSO-d + DMF) (1:4).

For the water soluble polymer bound peroxomolybdenum complexes, **4.1-4.4**, the ^{13}C NMR spectra were recorded at a carbon frequency of 100.5 MHz, 131 072 X-resolution

points, number of scans 8000, 1.04 s acquisition time, and 2.0 s relaxation delay with the ^{1}H NMR decoupling method in D_2O.

The ^{13}C NMR spectra of organic sulfides, sulfoxides and sulfones were recorded in $CDCl_3$ as solvent.

In all cases the deuterated solvents provide the lock signal.

2.3.9 ^{95}Mo NMR spectra

The ^{95}Mo NMR spectra were recorded in JEOL JNM-ECS400 spectrometer and Bruker AV 400 MHz FT-NMR at a molybdenum frequency of 26.07 MHz with sample in a 10 mm spinning tube with a sealed coaxial tube. For the water soluble polymer bound peroxomolybdenum complexes (**4.1-4.4**), D_2O is used to provide the lock signal and for the peroxomolybdenum complexes anchored to water insoluble polymer, polyacrylonitrile, (DMSO-d + DMF) (1:4) was used, where DMSO-d provided the lock signal. Again, in case of immobilized peroxomolybdate on amino acid functionalized Merrifield resin, (CCl_4 / DMSO-d) (80:20, v/v) was used as a solvent, where DMSO-d provided the lock signal. The spectra for the complexes **MRVMo** and **MRAMo** were recorded by swelling the compounds in CCl_4. The chemical shift data are recorded as negative values of ppm (δ) in the low-frequency direction with reference to 1 M $Na_2MoO_4.2H_2O$ solution at 298 K.

2.3.10 GC analysis

GC analysis was carried out on a CIC, Gas Chromatograph model 2010 using a SE-52 packed column (length 2 m, 1/8'' OD) with a Flame Ionization Detector (FID), and nitrogen as carrier gas (30 mL/min).

2.3.11 HPLC analysis

HPLC analysis were performed using a Waters Tm 2487 dual k detector and assayed at fixed wavelengths using a C18, column (Nova-Pak C18, 3.9 x 150 mm, Waters).

2.3.12 Thermogravimetric analysis

Thermogravimetric analysis was done on SHIMADZU TGA-50 and Perkin-Elmer STA 6000 system using aluminum pan, at a heating rate of 10 ^{o}C/min under an atmosphere of nitrogen.

2.3.13 Melting point determination

Melting points were determined in open capillary tubes on a Büchi Melting Point B-540 apparatus and are uncorrected.

2.3.14 Magnetic susceptibility

Magnetic susceptibilities of the complexes were measured by the Gouy Method, using Hg [$Co(NCS)_4$] as the calibrant.

2.4 COMPUTATIONAL CALCULATION

Computational calculations were done by employing the density functional theory (DFT) method. DFT calculations were performed on the model complexes using the BLYP functional and DNP basis set as implemented in the program DMol^{3}.[9] The complex was first optimized at the BLYP/DNP level. The chemical softness value for the model complexes were calculated from the HOMO and LUMO energies.

REFERENCES

1. Djordjevic, C., et al. *Inorg. Chem.* **36**, 1798--1805, 1997.

2. Braun, D., Cherdron, H., Rehahn,M., Ritter, H. & Voit, B. *Polymer Synthesis: Theory and Practice: Fundamentals, Methods, Experiments*, 4th ed., Springer Berlin Heidelberg, New York, 2005, 176-177.

3. Jeffery, G.H., Basset, J., Mendham, J. & Denny R.C. *Vogel's Textbook of Quantitative Inorganic Analysis Including Elementary Instrumental Analysis*, 4th ed., Longman Group Limited, London, 1978, 472-473.

4. Vogel, A.I. *A Text Book of Quantitative Inorganic Analysis*, Longmans, Green and Co., New York, 1962, 295.

5. Vogel, A.I. *A Text Book of Quantitative Inorganic Analysis*, Longmans, Green and Co., New York, 1962, 363.

6. Vogel, A.I. *A Text Book of Quantitative Inorganic Analysis*, Longmans, Green and Co., New York, 1962, 325.

7. Brunauer, S., et al. *J. Am. Chem. Soc.* **60**, 309--319, 1938.

8. Barrett, E.P., et al. *J. Am. Chem. Soc.* **73**, 373--380, 1951.

9. Delly, B. *J. Chem. Phys.* **92**, 508--514, 1990.

CHAPTER 3

Synthesis and Characterization of Monoperoxo Molybdenum (VI) Complexes Immobilized on Polymer Supports

3.1 INTRODUCTION

The importance of polymer supported complexes of transition metals which rendered them the focus of one of the active areas of contemporary research, have been emphasized in the literature[1-7] and highlighted in the introductory Chapter. Polymer immobilized catalysts combine the specificity and selectivity of homogeneous catalysts and operational convenience of heterogeneous catalysts.[8-10] Our interest in attaching pMo species to insoluble polymer resin to obtain macrocomplexes has been stimulated mainly by the prospect of generating newer potential heterogeneous catalysts for organic oxidations since peroxo compounds of molybdenum have already been recognized as versatile reagents for organic oxidative transformations.[11-28] In contrast to the numerous reports dealing with synthesis of pMo compounds in various co-ligand environments, there are only a limited number of reported studies on the preparation of well-defined pMo containing macrocomplexes.

For the present investigation, since our goal was to prepare insoluble compounds with a plan to develop heterogeneous catalytic systems, we have selected two types of polymer matrices for immobilization of pMo species, viz., amino acid functionalized Merrifield resin (**MR**) and poly(acrylonitrile) (PAN). PAN was chosen for immobilization of the pMo species due to its being an insoluble, non-toxic, cheap and commercially available reagent.[29] Moreover, acrylonitrile polymers have attracted much

attention for their applications in diverse areas that include medicine,[29] antioxidants,[29] surface coatings,[30] catalysis,[31] textiles treatment,[29] binders[29] and as adsorbant for removal of heavy metal ions from water.[32,33] As far as we are aware, the compound **PANW** reported previously by us, is the only example where PAN has been used as polymeric support to obtain an immobilized peroxometal compound.[34]

Divinyl benzene cross-linked polystyrene, support that Merrifield first developed for solid-phase synthesis of peptides,[35] is still the most popular solid support due to its ready availability, low cost, mechanical and chemical robustness and its ability to undergo facile functionalization.[36,37] In order to obtain stable metal supported catalysts, formation of strong metal-polymer bond which can survive repeated catalytic cycles, preventing the metal species from leaching out of the polymer matrix, is an essential requirement.[24,38,39] Hence, functionalization of the resin with appropriate ligand groups is the most important step towards establishing stable metal-polymer linkage.[34,38,40] In this work, we have decided to use valine and alanine anchored **MR** as support mainly because molybdenum is known to form stable complexes with amino acids.[41] Although the first synthesis of metal complexes supported on cross-linked poly(styrene–divinylbenzene) resin through amino acid group was studied on copper(II) metal in the year 1977,[42] yet, we have come across only two reports on application of ruthenium(III) and palladium(II) complexes supported to L-valine functionalized **MR** as catalyst in olefin oxidation and hydrogenation, respectively.[43,44] No report seems to exist on anchoring of pMo species to amino acid functionalized Merrifield resin.

In **Chapter 3,** we report the synthesis and characterization of dioxomonoperoxo compounds of molybdenum(VI) immobilized on amino acid functionalized Merrifield resin of the type $\mathbf{[MoO_2(O_2)(L)_2]^{2-}}$**–MR** [L = valine (**MRVMo**) (**3.1**) or alanine

(**MRAMo**) (**3.2**) and **MR** = Merrifield resin] and on poly(acrylonitrile) of the type **$[MoO_2(O_2)(CN)_2]$-PAN** [PAN = poly(acrylonitrile)] (**PANMo**) (**3.3**).

3.2 EXPERIMENTAL SECTION

3.2.1 Anchoring of amino acids to Merrifield resin

The amino acid functionalized polymers were prepared by employing a reported procedure with some modification.[44] Pre-washed chloromethylated poly(styrene-divinylbenzene) copolymer beads (2 g, 5 mmol Cl) were allowed to swell in 6 mL methanol for 1 h. An aqueous solution of L-valine (0.73 g, 6.25 mmol) or DL-alanine (0.56 g, 6.25 mmol) in 20 mL distilled water was added to the swollen polymer in methanol. The molar ratio of Cl:amino acid:base on the basis of percent replaceable chlorine on resin was maintained approximately at 1:1.25:1.25. The resulting mixture was refluxed for 24 h in presence of pyridine (0.50 mL, 6.25 mmol). The contents were cooled and allowed to stand at room temperature for a week with occasional shaking. The pH of the reaction mixture was recorded to be *ca.* 7 at this stage. At the end of the period of 7 days, pH came down to *ca.* 5. The colour of the beads changed from off-white to pale yellow indicating the attachment of the amino acid. Subsequently, the L-valine (**MRV**) or DL-alanine (**MRA**) linked polymer beads were filtered, washed with hot water till no precipitate of AgCl was observed in the filtrate on treating with $AgNO_3$. This was followed by washing with ethanol and the product obtained was ultimately dried under vacuum at 90 °C for 8 h to yield 2.41 g and 2.23 g of **MRV** and **MRA**, respectively.

3.2.2 Synthesis of immobilized molybdenum dioxomonoperoxo compounds $[MoO_2(O_2)(L)_2]^{2-}$—MR, [L = valine (MRVMo) (3.1) or alanine (MRAMo) (3.2)]

In a typical reaction, H_2MoO_4 (0.40 g, 2.5 mmol) was dissolved in 30% H_2O_2 (2.55 mL, 22.5 mmol) by maintaining the temperature at 30-40 °C. The pH of the clear solution obtained was recorded to be *ca.* 1. Concentrated sodium hydroxide (*ca.* 8 M) was then added to the above solution dropwise with constant stirring to raise the pH of the reaction medium to 5.0. Keeping the temperature of the reaction mixture below 4 °C in an ice bath, 1.0 g of **MRV** or **MRA** was added to it which was pre-swelled in 5 mL ethanol for 1 h. The mixture was kept for 24 h under continuous stirring in an ice bath. The supernatant liquid was then decanted and the yellowish residue was repeatedly washed with pre-cooled acetone. The products were separated by centrifugation and dried in *vacuo* over concentrated sulfuric acid. The compounds were further dried by heating upto 70 °C under nitrogen atmosphere.

3.2.3 Synthesis of $[MoO_2(O_2)(CN)_2]$—PAN [PAN = poly(acrylonitrile)] (PANMo) (3.3)

Molybdic acid (3.01 g, 18.86 mmol) was dissolved in 30% H_2O_2 (20 mL, 176.40 mmol) by maintaining the temperature at 30-40 °C, to obtain a clear solution of pH *ca.* 1. Subsequently, pH of the reaction solution was raised to 5.0, by the addition of concentrated sodium hydroxide solution (*ca.* 8 M) dropwise with constant stirring. Keeping the temperature of the reaction mixture below 4 °C in an ice bath, 1.0 g of poly(acrylonitrile) was added to it. The reaction mixture was left for 24 h under constant stirring for swelling of the suspended polymer beads. The white residue obtained was separated by decanting off the supernatant liquid and was repeatedly washed with pre-cooled acetone. The product was dried in *vacuo* over concentrated sulfuric acid.

3.2.4 Elemental analysis

The methods described in Chapter 2 were used to obtain the quantitative determination of molybdenum, peroxide, carbon, hydrogen, nitrogen, chlorine and sodium. The analytical data of the compounds are summarized in Table 3.1.

3.2.5 Physical and spectroscopic measurements

According to the methods described in Chapter 2, the compounds were characterized with the help of spectroscopic measurements, TG analysis as well as scanning electron micrographs (SEM) and EDX analysis. Structurally significant IR bands and their assignments are summarized in Table 3.3. TGA data of the complexes are reported in Table 3.6. Table 3.4 and Table 3.5 describe the ^{13}C NMR chemical shift values for the complexes and their respective free polymers. ^{95}Mo NMR spectra for the complexes are presented in Fig. 3.13.

3.3 RESULTS AND DISCUSSION

3.3.1 Synthesis and Characterization

3.3.1.1 Synthesis

The polymer-supported compounds, **MRVMo (3.1)** and **MRAMo (3.2)** have been synthesized by adopting a two-step methodology. The functionalized polymer, **MRV** was obtained by reacting the polymer with the respective amino acid in methanol and using pyridine as a base, according to a previously established procedure.[44] The alanine functionalized polymer, **MRA** was isolated similarly by using alanine in lieu of valine.

We have used the chloromethylated polystyrene cross-linked with 2% DVB as support mainly owing to its superior flexibility, which is known to facilitate grafting of metallic atoms via polymer anchored ligands.[7,45] The amino acid containing polymer was subsequently allowed to react with peroxomolybdenum species, generated *in situ* by reacting H_2MoO_4 with 30% H_2O_2 at pH 5.0, to afford the immobilized peroxomolybdenum compounds, **3.1** and **3.2**. Since our earlier experience on synthesis of polymer-bound peroxometallates have shown that, formation and anchoring of pV[46] and pW[47] species to a polymer matrix with carboxylate ligands is most conducive at near neutral pH, in the present synthesis the pH was strategically maintained at *ca.* 5. Our effort to increase the loading by increasing the contact time to 7 days was however not successful.

The synthesis of the poly(acrylonitrile) anchored compound, **PANMo (3.3)** was achieved by allowing the polymer to swell in a reaction mixture consisting of peroxomolybdenum species, generated *in situ* by reacting H_2MoO_4 with 30% H_2O_2. In this case also the pH of *ca.* 5, maintained by adding alkali hydroxide, was found to be optimum for the formation of the peroxomolybdenum species and their subsequent anchoring to the pendant nitrile groups of the polymer. The factors such as maintenance of required contact time of 24 h and temperature at < 4 °C were also observed to be important for the desired synthesis. It is noteworthy that the compounds are non-hygroscopic, stable and can be stored for a prolonged period without any change in its catalytic efficiency.

3.3.1.2 Characterization and formulation

The elemental analysis data for the synthesized compounds are given in Table 3.1. From the data it is evident that nearly 70% of the Cl of -CH_2Cl groups have been replaced by valine to afford **MRV** whereas in **MRA**, alanine substituted *ca.* 58% of Cl. It is therefore estimated that about 70% of the ligand units are bound to pMo moieties in **MRV** (60% in **MRA**). In **PANMo**, about 4.51% of the nitrile units are observed to be anchored to the pMo moieties. Furthermore, the ratio of metal : repeat unit for the compounds **MRVMo** (**3.1**), **MRAMo** (**3.2**) and **PANMo** (**3.3**) was found to be 1 : 15, 1 : 19 and 1 : 21, respectively. The ratio of Mo:O_2^{2-} content for **3.1-3.3** was unity indicating that the attached pMo moieties are present in the compounds in their dioxomonoperoxo, [$MoO_2(O_2)$], form. The molybdenum loading on the compounds, **MRVMo** (**3.1**), **MRAMo** (**3.2**) and **PANMo** (**3.3**) correspond to 0.46, 0.38 and 0.77 mmol per gram of the polymeric support, respectively which was calculated on the basis of Mo content, obtained from gravimetric analysis and confirmed by EDX spectral analysis as well as with atomic absorption spectroscopy (AAS). The pMo compounds were diamagnetic in nature, as was evident from the magnetic susceptibility measurement in conformity with the presence of Mo centers in their +6 oxidation states.

3.3.1.2.1 SEM and Energy Dispersive X-ray (EDX) Analysis

Information regarding the morphological changes occurring on the surface of the polymer as a consequence of incorporation of the peroxomolybdates into the polymer matrix, was derived from scanning electron microscopic study. The micrographs revealed that the smooth and flat surface of the starting virgin resin, **MR** [Fig. 3.1(a)] undergoes considerable roughening upon incorporation of the amino acids [Fig. 3.1(b) and 3.1(d)]. Randomly oriented depositions on the external surface of the resin were seen on

attachment of the pMo units leading to further roughening of the polymeric surfaces in **MRVMo** (**3.1**) and **MRAMo** (**3.2**) [Fig. 3.1(c) and 3.1(e)]. The surface of compound **PANMo** (**3.3**), in contrast to the smooth and flat surface of the pristine polymer PAN, appeared to be coarse with the metal ions distributed across the surface [Fig. 3.1(f) and 3.1(g)].

Energy dispersive X-ray spectroscopic analysis, which provides *in situ* chemical analysis of the bulk, was carried out focusing multiple regions over the surface of the polymer. EDX spectra clearly showed Mo, Na, C, N and O as the constituents of the compounds **MRVMo** (**3.1**) and **MRAMo** (**3.2**). On the other hand, absence of sodium as counter ion in the compound **PANMo** (**3.3**) was confirmed from the EDX spectrum. The observation is in accord with the charge neutrality of the nitrile bound monoperoxomolybdenum(VI) species in **3.3**. The results presented in Table 3.1 for each of the compounds, **3.1-3.3** are the average of the data from these regions. The data obtained from energy dispersive X-ray spectroscopy on the composition of the compounds, **3.1-3.3** resemble those of the elemental analysis values (Table 3.1).

Table 3.1 Analytical data for the amino acid-anchored Merrifield resin and polymer-bound peroxomolybdates

Compound	% Found from elemental analysis (% obtained from EDX spectra)							Molybdenum loading [a] (mmol g^{-1} of polymer)
	C	H	N	Cl	Na	Mo	O_2^{2-}	
MRV	82.58	7.11	2.11	----	----	----	----	
	(82.01)	----	(2.05)	(2.24)	----	----	----	
MRA	82.04	7.29	1.78	----	----	----	----	
	(82.67)	----	(1.82)	(3.24)	----	----	----	
MRVMo	74.08	6.84	1.88	----	2.18[b]	4.52	1.60	0.46
	(74.54)	----	(1.86)	(2.36)	(2.03)	4.51[b]	----	
						(4.46)		
MRAMo	74.58	6.68	1.80	----	1.70[b]	3.66	1.29	0.38
	(74.14)	----	(1.77)	(2.89)	(1.73)	3.64[b]	----	
						(3.60)		
PANMo	59.76	4.58	23.86	----	----	7.38	2.44	0.77
	(59.52)	--	(23.17)	----	----	7.35[b]	----	
						(7.29)		

[a]Molybdenum loading $= \dfrac{\text{Observed metal \% X 10}}{\text{Atomic weight of metal}}$, [b] Determined by AAS.

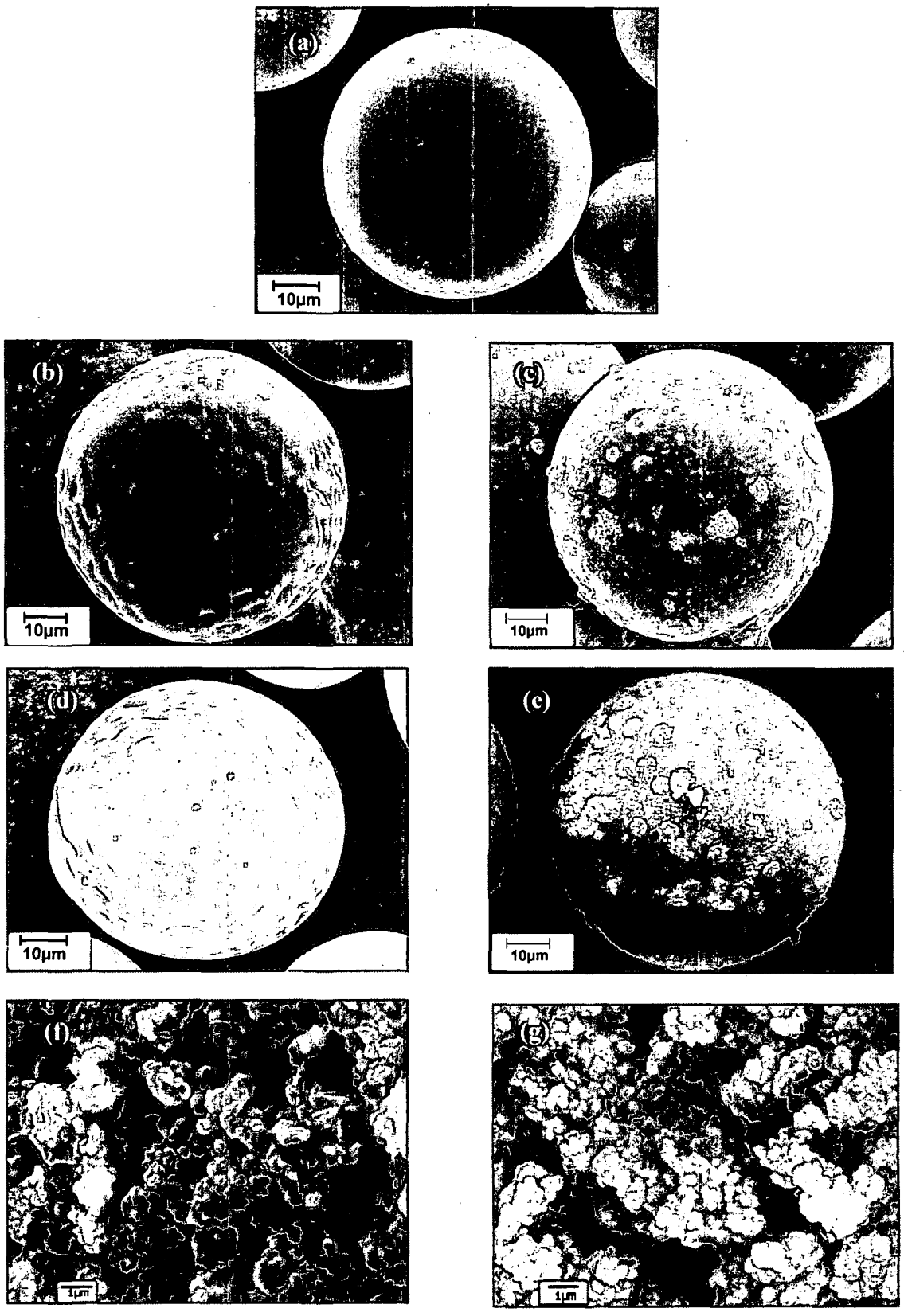

Fig. 3.1 Scanning electron micrographs of (a) **MR**, (b) **MRV**, (c) **MRVMo**, (d) **MRA**, (e) **MRAMo**, (f) **PAN** and (g) **PANMo**.

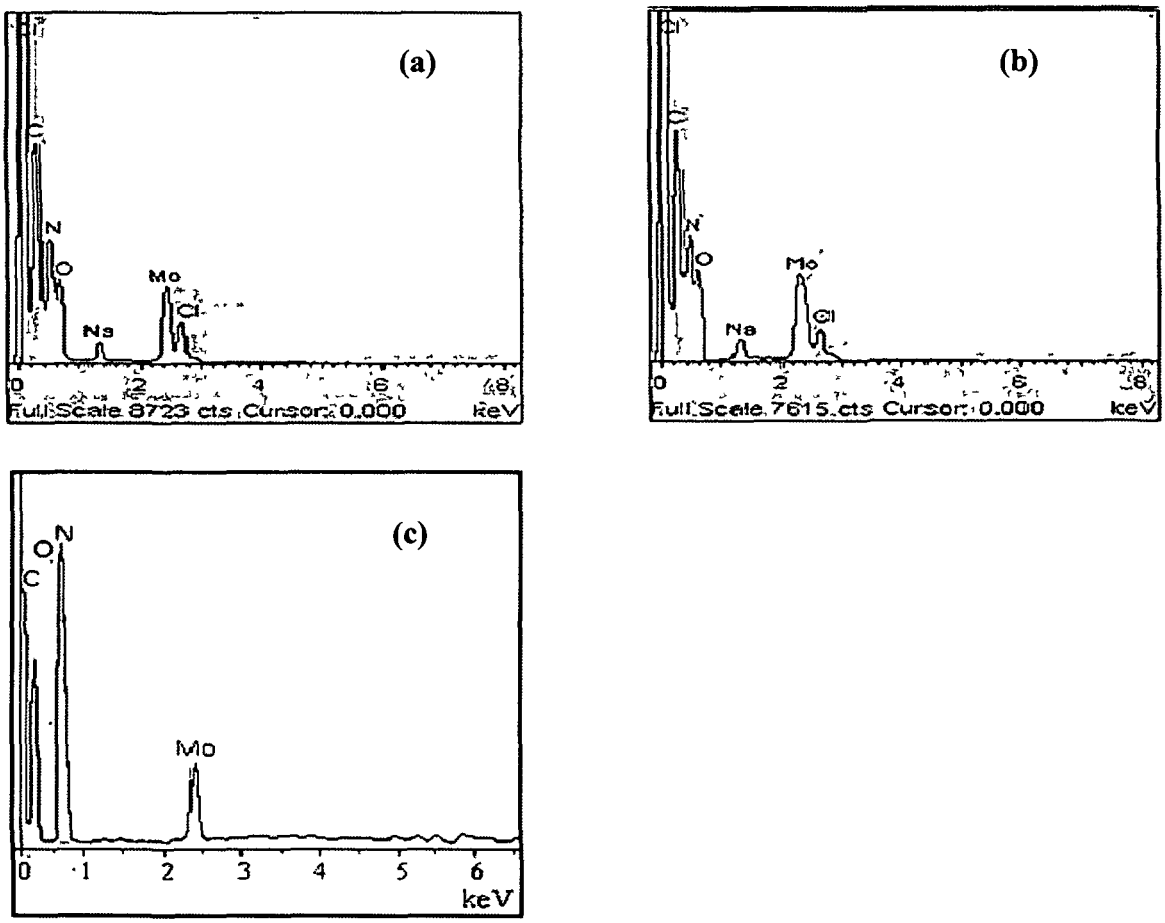

Fig. 3.2 EDX spectra of (a) **MRVMo**, (b) **MRAMo** and (c) **PANMo**.

3.3.1.2.2 BET analysis

The surface area of the polymeric samples viz., the pristine resin, functionalized resin and the metal incorporated polymers were measured by using BET analysis with the nitrogen adsorption method[48] and pore volume was determined by BJH model.[49] The N_2 adsorption/desorption isotherms for each of the samples (Fig. 3.3) showed typical TYPE II adsorption of an IUPAC standard[32] on particles which have macropores or nonpores, showing poor adsorption.[33] The textural properties of the neat polymer as well as the metal anchored polymeric samples are listed in Table 3.2. The results demonstrated that the surface area of **MR** (11.45 m^2/g) reduces after incorporation of amino acids to 8.57 m^2/g for **MRV** and 9.22 m^2/g for **MRA**. Further decrease in the surface area was noted on

complexation with pMo moieties to 3.92 m^2/g (for **MRVMo)** and 4.59 m^2/g (for **MRAMo)**. These reductions in surface area, total pore volume and pore radius are likely to be the result of blocking of pores by the attachment of amino acids and subsequent incorporation of pMo moieties with **MR**, as has been reported previously for metal bound **MR**.[50]

The surface area of poly(acrylonitrile) (PAN) was similarly found to be reduced from a value of 151.22 m^2/g to 101.35 m^2/g on metal loading to form **PANMo** (Table 3.2). Moreover, TYPE I isotherm is observed in case of PAN and **PANMo** indicating microporous nature of the adsorbent (Fig. 3.4).

Table 3.2 BET surface area, V_{tot} and pore radius of the pMo compounds **3.1-3.3** and base polymers

Compound	S_{BET} [a] (m^2/g)	V_{tot} [b] (cc/g)	Pore radius (Å)
MR	11.45	0.118	53.6673
MRV	8.57	0.073	36.5092
MRA	9.22	0.082	39.4426
MRVMo	3.92	0.014	24.0492
MRAMo	4.59	0.018	26.4517
PAN	151.22	0.158	8.2251
PANMo	101.35	0.127	6.1183

[a] BET surface area.

[b] Total pore volume.

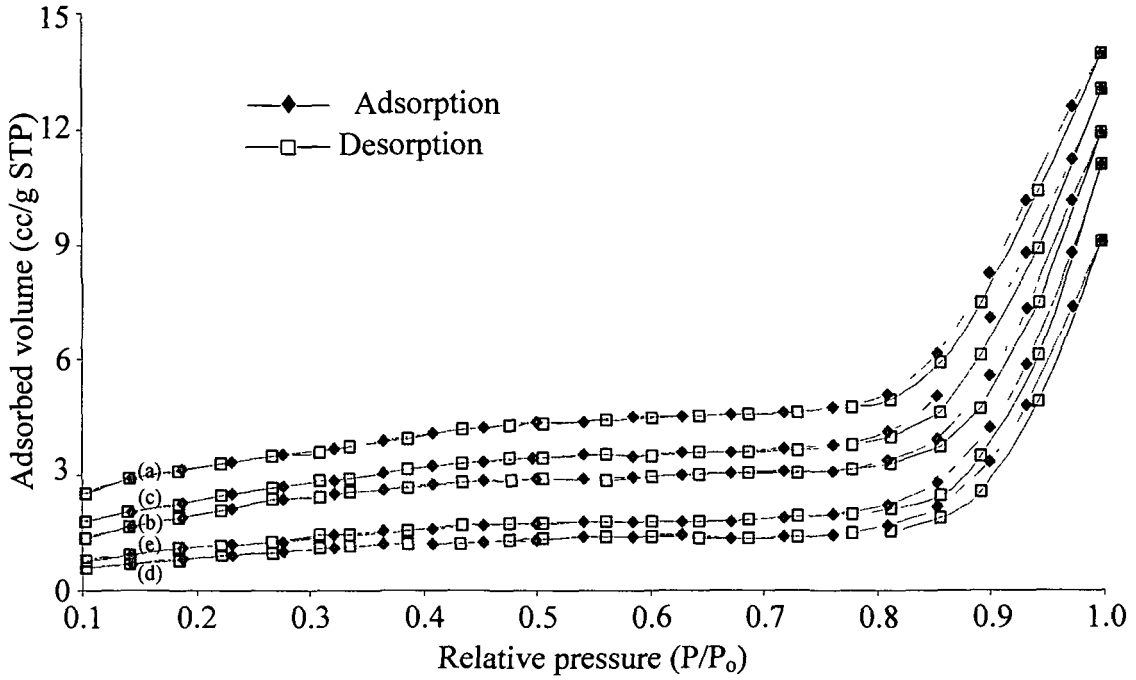

Fig. 3.3 The N_2 adsorption/desorption isotherm of (a) MR, (b) MRV, (c) MRA, (d) **MRVMo** and (e) **MRAMo**.

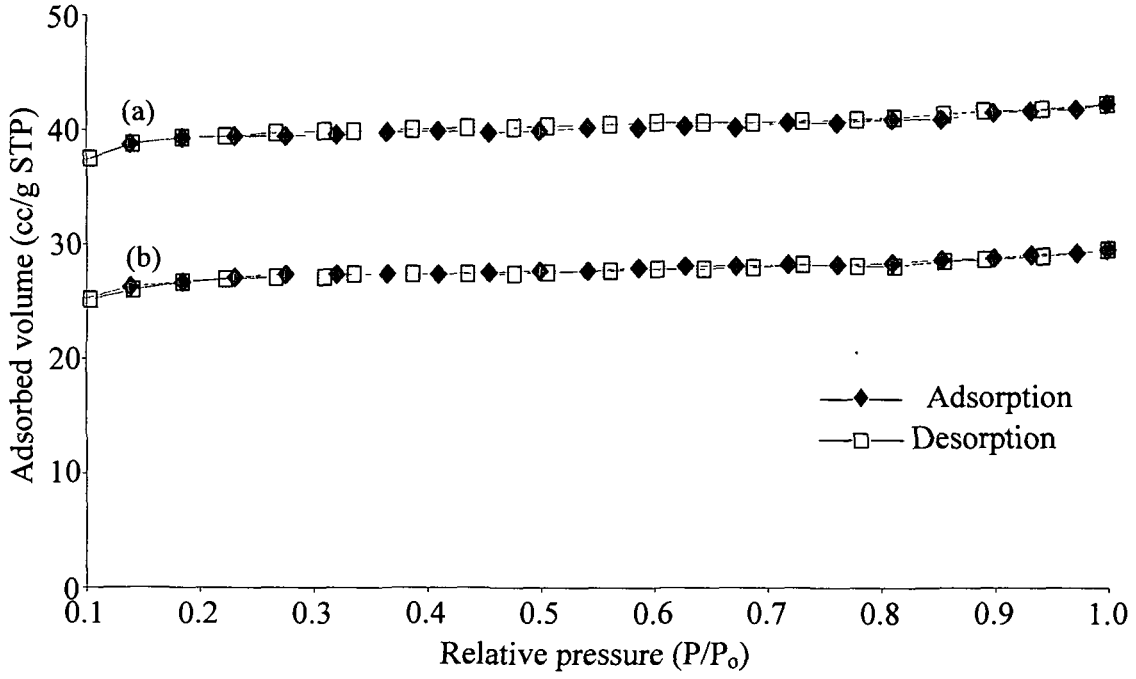

Fig. 3.4 The N_2 adsorption/desorption isotherm of (a) **PAN** and (b) **PANMo**.

3.3.1.2.3 IR spectral studies

The IR spectra for the polymer-anchored complexes **3.1-3.3** are presented in Fig. 3.5 – Fig. 3.7 and the significant features are summarized in Table 3.3. By comparison of IR spectra of the immobilized complexes to the spectra of pure polymers and available literature on metal compounds comprised of ligands relevant to the present study, assignments of the IR bands for the compounds, **3.1-3.3** were made. The three vibrational modes at *ca.* 850, *ca.* 625 and *ca.* 520 cm^{-1} assigned to ν(O-O), $\nu_{asym}(Mo\text{-}O_2)$ and $\nu_{sym}(Mo\text{-}O_2)$, respectively[51,52] confirmed the presence of side-on bound peroxo ligand in each of the title compounds. The intense absorption at *ca.* 960 cm^{-1} in the spectrum of each of the compounds, **3.1-3.3** was consistent with the presence of a terminally bonded Mo=O group.[51,52]

The IR spectra showed characteristic differences between the spectral pattern originating from the polymer-metal complexes, **3.1** and **3.2**, and the spectra of the amino acid functionalized polymer as well as the virgin **MR** (Fig. 3.5 and Fig. 3.6, Table 3.3). The intense band occurring at 1264 cm^{-1} in the virgin **MR** spectrum has been assigned to ν(C-Cl) mode of $-CH_2Cl$ moiety.[43,44] The intensity of the band was observed to be substantially reduced in the spectrum of the functionalized polymers **MRV** and **MRA** on anchoring of the amino acids, suggesting replacement of the Cl from the $-CH_2Cl$ group of the **MR** by the ligands.[43,44] Apart from the typical absorptions at *ca.* 3050, 2900, 1025 and 697 cm^{-1} due to $\nu_{aromatic}$(CH), $\nu_{aliphatic}$(CH), $\delta_{aromatic\ in\text{-}plane}$(CH) and $\delta_{aromatic\ out\text{-}of\text{-}plane}$(CH), in the spectra of **MRV** and **MRA,** new bands appear at *ca.* 1639, 1501, 1487, 1081 cm^{-1} (for **MRV**) and at *ca.* 1598, 1530, 1414, 1080 cm^{-1} (for **MRA**) attributable to ν_{asym}(COO), δ(NH) bending, ν_{sym}(COO) and ν(C-N), respectively, giving clear indication of the bonding of the amino acids to the polymeric matrix.[43,44,53]

Upon incorporation of the pMo moieties to the alanine or valine functionalized resins, spectra of both the compounds **MRVMo** (**3.1**) and **MRAMo** (**3.2**) exhibited a

distinct shift of ν_{asym}(COO) to a higher frequency and that of ν_{sym}(COO) to a lower frequency (Table 3.3) compared to the free polymeric ligand values along with some broadening. The corresponding ν_{sym}(COO) mode attributable to co-ordinated carboxylate group appeared at 1470 cm^{-1} for **MRVMo (3.1)** and at 1403 cm^{-1} for **MRAMo (3.2)**. The resulting $\Delta\nu$ [ν_{asym}(COO) - ν_{sym}(COO)] = 216 cm^{-1} for **MRVMo (3.1)** and 250 cm^{-1} for **MRAMo (3.2)** being much greater relative to the free **MRV** or **MRA** demonstrated the metal carboxylate co-ordination to be unidentate one.[54,55] Presence of free -COOH groups in each of the compounds, **MRVMo (3.1)** and **MRAMo (3.2)** was evident from an additional IR band appearing in the vicinity of 1710 cm^{-1}. The position of δ(NH) absorption in the polymeric complexes remained practically unaltered compared to its position in the spectrum of the corresponding free ligand. It is therefore inferred that the amine group was not participating in co-ordination.[44] Since the N-H stretching is occurred in the ν(OH) frequency region, the band could not be distinguished with certainty. The broad and strong band appears at 3500-3400 cm^{-1} indicated the presence of lattice water in the title complexes.

The IR spectrum of the neat poly(acrylonitrile), exhibits a strong ν(C≡N) absorption observed at 2247 cm^{-1}, in addition to the typical bands at 2938 and 2870 cm^{-1} due to $\nu_{asym}(CH_2)$ and $\nu_{sym}(CH_2)$, respectively (Fig. 3.7).[56-58] From the previous report it has been established that the ν(C≡N) stretching increases upon metal coordination through N atom of the nitrile group.[56,58,59] In the spectrum of **PANMo (3.3)**, apart from the band at 2247 cm^{-1} for the free nitrile groups, a new medium intensity band was observed at 2367 cm^{-1}. This latter band is attributable to a shift of ν(C≡N) to a higher frequency, resulting from co-ordination of the Mo(VI) ion with the nitrile groups of PAN.[56,59] The IR spectrum of **PANMo (3.3)** resembled closely the spectral pattern observed for the peroxotungsten(VI) anchored PAN analogue reported previously from our group.[39]

Table 3.3 Infrared spectral data for the pMo compounds **3.1-3.3** and base polymers

Compound	ν_{asym}(COO)	ν_{sym}(COO)	ν(C-Cl)	ν(C-N)	ν(C≡N)	ν(Mo=O)	ν(O-O)	ν_{asym}(Mo-O_2)	ν_{sym}(Mo-O_2)
MR	---	---	1264(m)	---	---	---	---	---	---
MRV	1639(vs)	1487(s)	1269(vw)	1081(w)	---	---	---	---	---
MRVMo	1686(vs)	1470(s)	1268(vw)	1081(w)	---	948(vs)	850(vs)	627(m)	519(m)
MRA	1598(vs)	1414(s)	1267(vw)	1080(w)	---	---	---	---	---
MRAMo	1653(vs)	1403(s)	1266(vw)	1080(w)	---	955(vs)	850(vs)	626(m)	514(m)
PAN	---	---	---	---	2247(vs)	---	---	---	---
PANMo	---	---	---	---	2247(vs) 2367(m)	950(m)	864(m)	639(m)	531(m)

vs, very strong; br, broad; s, strong; sh, shoulder; m, medium

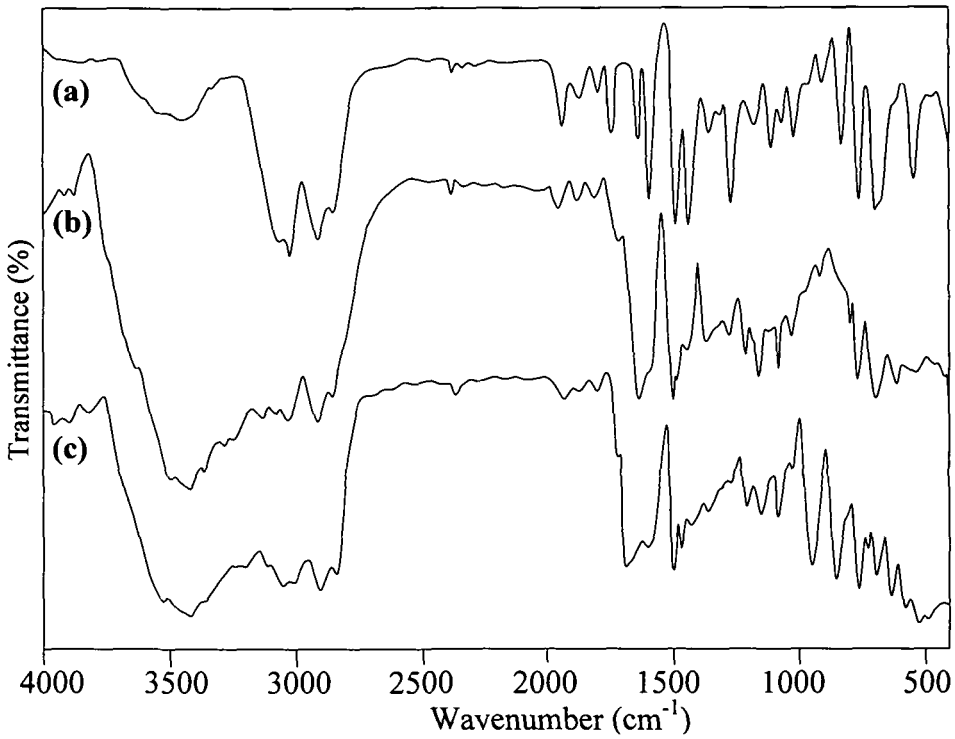

Fig. 3.5 IR spectra of (a) MR, (b) MRV and (c) **MRVMo**.

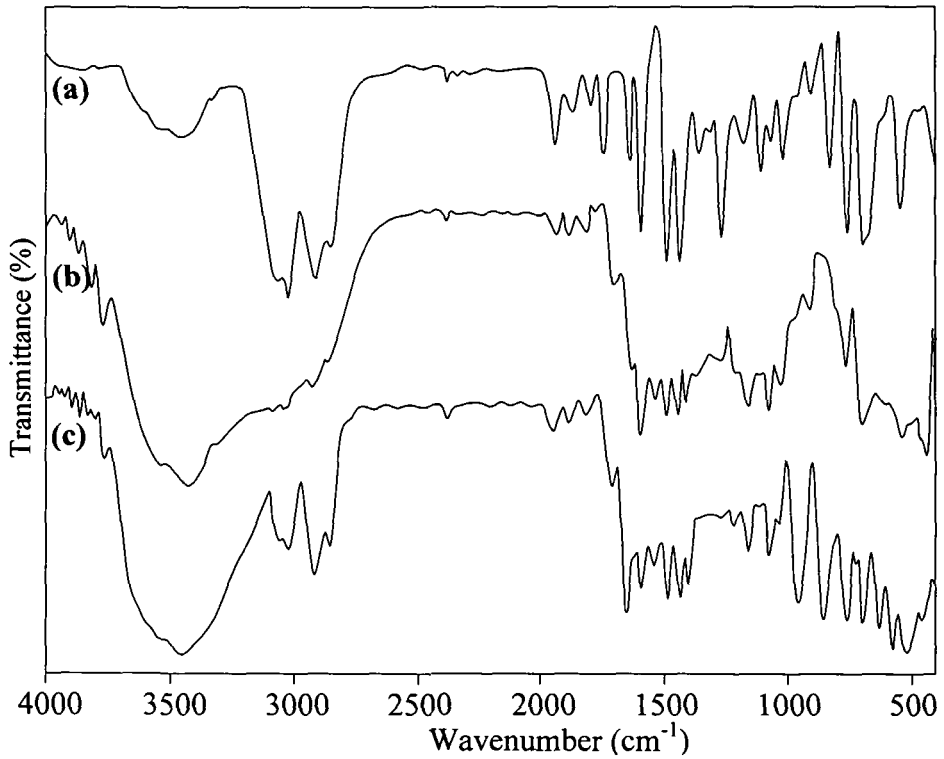

Fig. 3.6 IR spectra of (a) **MR**, (b) **MRA** and (c) **MRAMo**.

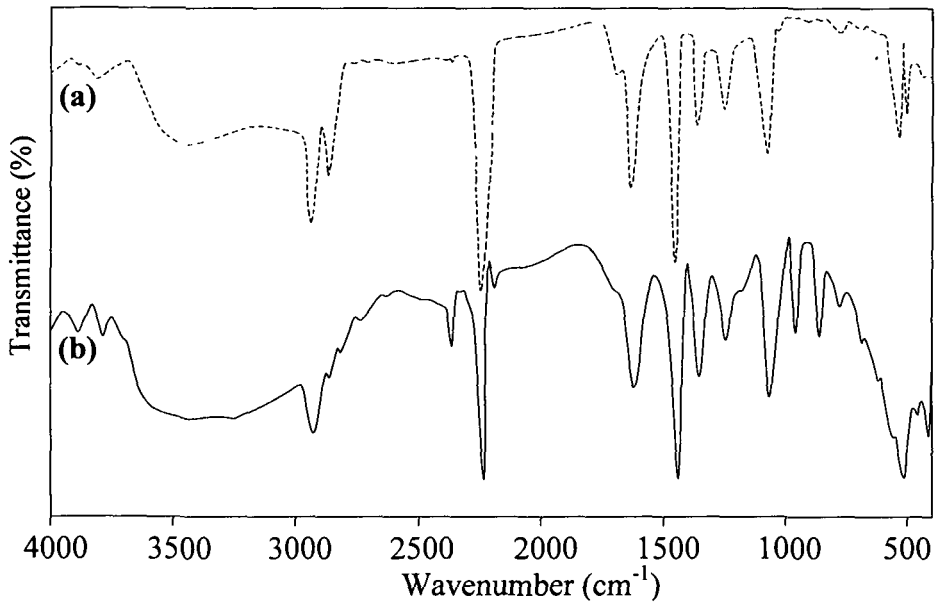

Fig. 3.7 IR spectra of (a) **PAN** and (b) **PANMo**.

3.3.1.2.4 Diffuse reflectance UV–visible analysis

The diffuse reflectance UV–visible spectra of **MRVMo (3.1)** and **MRAMo (3.2)** displayed two well resolved peaks in the region 270-380 nm (Fig. 3.8 and Fig. 3.9). The intense peak at *ca.* 271 nm may be ascribed to $\pi \rightarrow \pi^*$ transitions in the polymeric ligand.[60] The weak-intensity peak at *ca.* 368 nm occurs in the range characteristic of a monoperoxomolybdate(VI) species and has been assigned to a peroxo to metal (LMCT) transition.[61,62] For the compound **PANMo (3.3)**, such a LMCT band appeared at *ca.* 361 nm (Fig. 3.10).

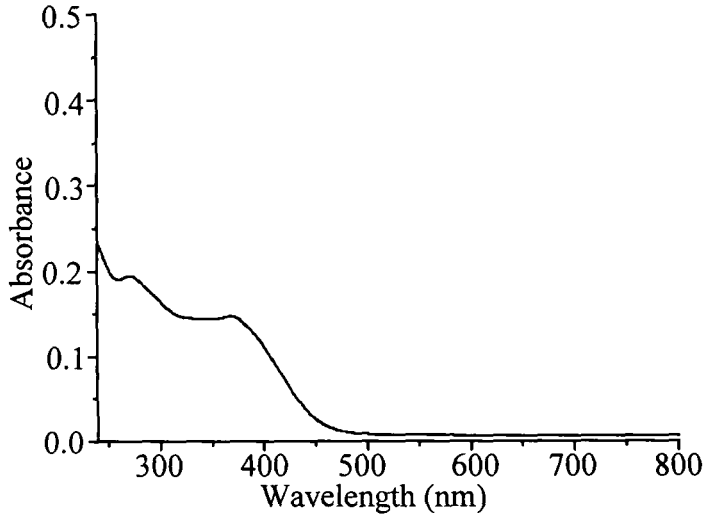

Fig. 3.8 Diffuse reflectance UV–vis spectrum of **MRVMo (3.1)**.

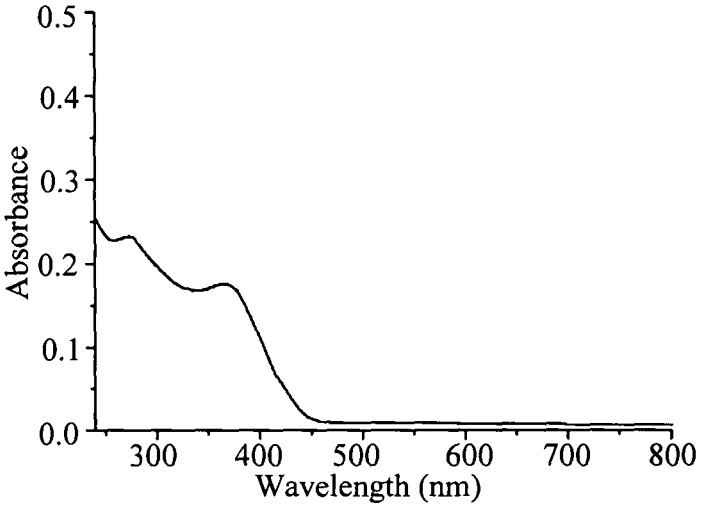

Fig. 3.9 Diffuse reflectance UV–vis spectrum of **MRAMo (3.2)**.

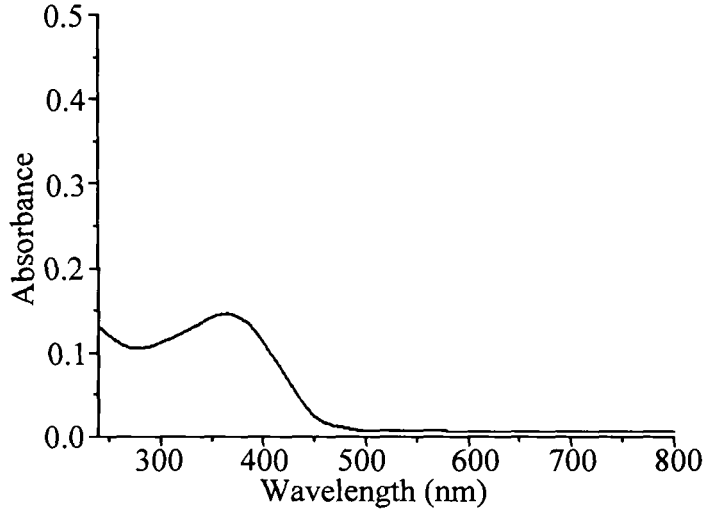

Fig. 3.10 Diffuse reflectance UV–vis spectrum of **PANMo (3.3)**.

3.3.1.2.5 ^{13}C NMR studies

The ^{13}C NMR chemical shift induced by co-ordination has been widely utilized as a convenient tool in understanding the mode of coordination of the co-ligands in metal compounds.[63-68] The ^{13}C NMR spectra and data for the polymer-anchored complexes **3.1-3.3** and the respective pristine and functionalized polymers are presented in Fig. 3.11 – Fig. 3.12 and Table 3.4 – Table 3.5, respectively. The interpretation of the major peaks were derived based on available reports.[69-72]

^{13}C NMR spectral studies provided evidence in support of the functionalization of the resin and subsequent metal binding to finally afford the macromolecular complexes, **MRVMo (3.1)** and **MRAMo (3.2)**. The spectra of the pristine **MR** and the resins after functionalization, **MRV** and **MRA** displayed typical peaks corresponding to quaternary aromatic, protonated aromatic and aliphatic methine carbons as well as the carbon atom of $-CH_2Cl$ group.[70] In addition to these resonances, several new peaks appeared in the spectra of **MRV** and **MRA**, including the peaks due to carboxylate carbon at 176.35 (**MRV**) and 176.02 ppm (**MRA**), testifying the presence of valine and alanine in the functionalized polymers.[71]The replacement of Cl from $-CH_2Cl$ group by the amino acids to form C-N bond, was evident in the spectra of both the amino acid containing polymers from a new signal at *ca.* 51 ppm which may be assigned to amine bound methylene carbon.[73,74]

After loading of the pMo species onto the **MRV** and **MRA**, a new additional peak appeared in the spectrum of both the polymers at considerably lower field of 206.11 (**MRVMo**) (**3.1**) and 205.16 ppm (**MRAMo**) (**3.2**), respectively attributable to the carbon atom of the complexed carboxylate group. Strong metal ligand interaction was indicated by the significant downfield shift, $\Delta\delta$ ($\delta_{complex} - \delta_{free\ carboxylate}$) $\approx$ 29.61 ppm in case of

MRVMo (3.1) and *ca.* 29.03 ppm in **MRAMo (3.2)** relative to the free carboxylate peak of amino acid.

The ^{13}C NMR spectrum of pure poly(acrylonitrile) displayed peaks at 120.21 ppm due to pendant nitrile groups in addition to the peak corresponding to chain carbon atoms at 33.35 (for CH_2) and 27.97 (for CH) ppm.[72] The spectrum of **PANMo (3.3)** on the other hand, apart from the signal at 120.28 ppm owing to free nitrile group of the polymer, showed a new signal at 129.02 ppm which may be ascribed to molybdenum bound nitrile group. The nitrile carbon resonance has been known to undergo a downfield shift on co-ordination to a metal.[75] The spectrum thus provided clear evidence for the existence of both coordinated as well as free nitrile groups in **PANMo (3.3)**. Presence of considerably strong metal-ligand interaction was evident from the value of $\Delta\delta$ ($\delta_{complexed\ nitrile}$ - $\delta_{free\ nitrile}$) $\approx$ 8 ppm.

Table 3.4 ^{13}C NMR chemical shift of **PANMo** and PAN

Compound	Chemical Shift (ppm)			
	Nitrile carbon		CH_2	CH
	Free	Complexed		
PAN	120.21		33.35	27.97
PANMo	120.28	129.02	33.36	27.97

Table 3.5 ^{13}C NMR chemical shift for polymer support, amino acid-anchored Merrifield resin and polymer-bound peroxomolybdates

Compound	Chemical Shift (ppm)								
	Merrifield Resin				Amino acid				
	Quaternary Aromatic Carbons	Protonated Aromatic Carbons	Aliphatic Methine Carbons	CH_2Cl	CH_3	CH_2/CH	C-NH	Carboxylate	
								Free	Complexed
MR	145.18	128.36	41.04	46.17	---	---	---	---	---
MRV	145.14	129.05	41.66	46.10	19.42	31.08	61.48	176.35	---
MRVMo	145.25	128.90	41.81	46.18	18.89	31.00	61.21	176.50	206.11
MRA	145.23	128.74	42.00	46.14	---	17.01	53.09	176.02	---
MRAMo	145.01	127.67	41.89	46.14	---	17.09	53.10	176.13	205.16

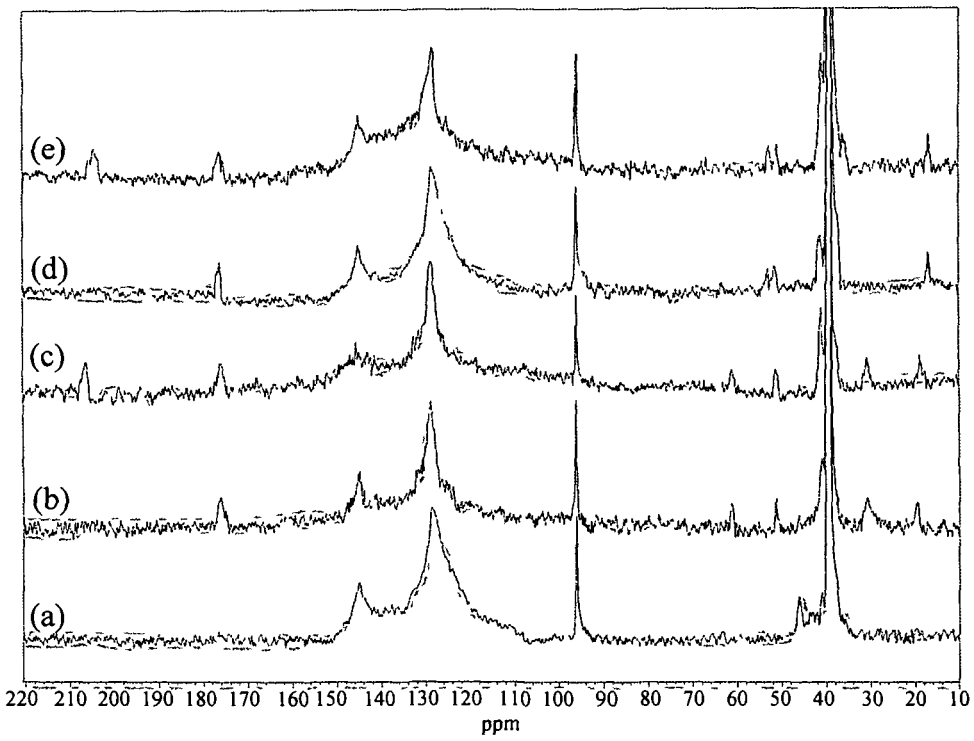

Fig. 3.11 ^{13}C NMR spectra of (a) **MR**, (b) **MRV**, (c) **MRVMo**, (d) **MRA** and (e) **MRAMo**.

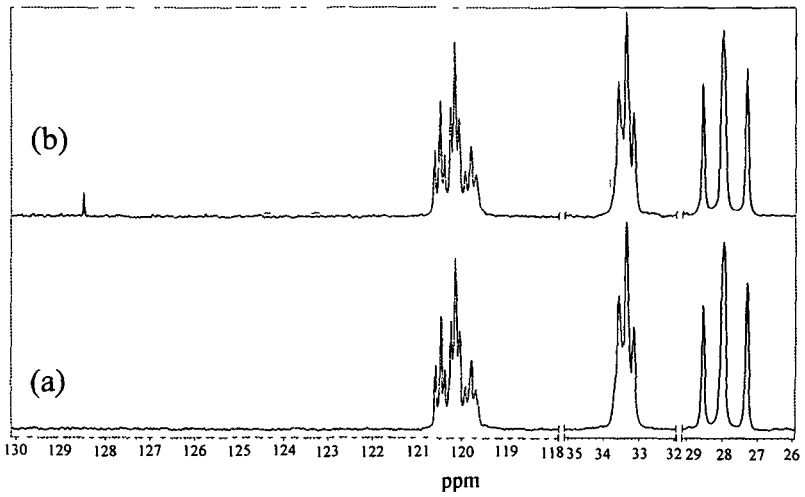

Fig. 3.12 ^{13}C NMR spectra of (a) **PAN** and (b) **PANMo**.

3.3.1.2.6 ^{95}Mo NMR studies

The ^{95}Mo NMR has been extensively used to identify the peroxomolybdate species present in a compound.[76] The ^{95}Mo NMR spectra for the polymer-anchored complexes **3.1-3.3** are presented in Fig. 3.13. The spectra were recorded by swelling the compounds in (CCl_4 + DMSO-d) for **3.1**and **3.2** and by dissolving in (DMF+DMSO-d) for **3.3**. The single resonance occurred at – 116 ppm , – 115 ppm and – 114 ppm, (relative to $[MoO_4]^{2-}$) for **MRVMo (3.1)**, **MRAMo (3.2)** and **PANMo (3.3)**, respectively which is in the region characteristic of monoperoxomolybdate species.[76] Moreover, appearance of single characteristic peak indicated the presence of single coordination environment of Mo(VI) in the compounds.

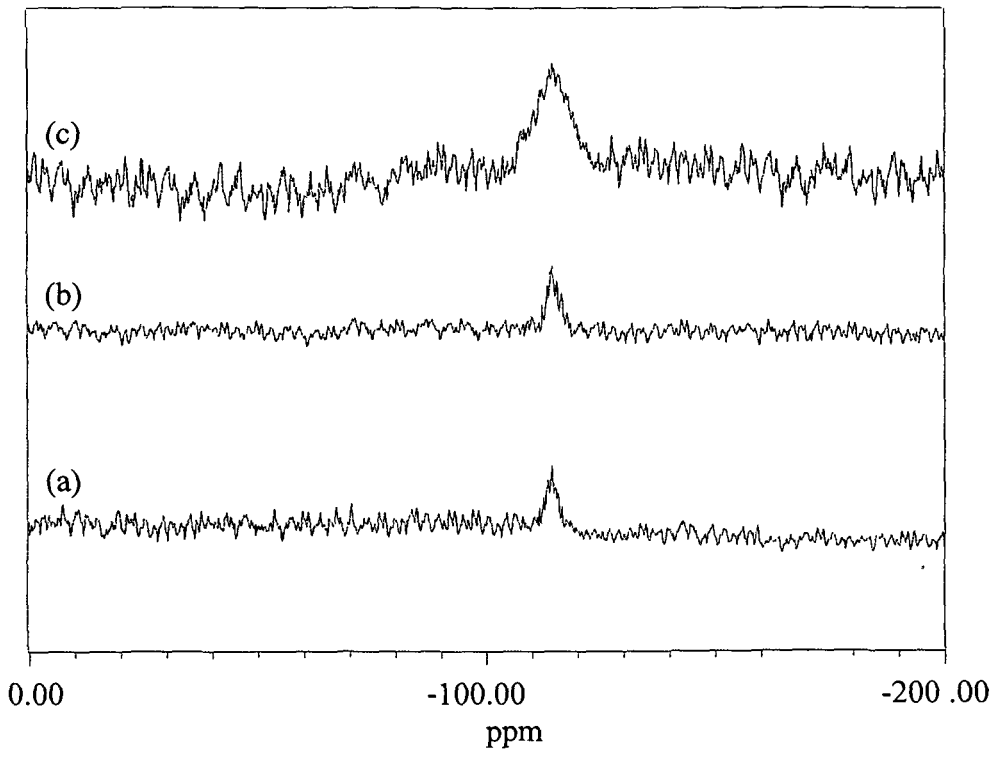

Fig. 3.13 ^{95}Mo NMR spectra of (a) **MRAMo** (b) **MRVMo** and (c) **PANMo**.

3.3.1.2.7 Thermal analysis

That the polymer-anchored compounds, **3.1-3.3** gradually undergo multistage decomposition on heating up to a final temperature of 750 °C, was evident from the corresponding thermogravimetric analysis data and the TG–DTG plots presented in Table 3.6 and Fig. 3.14 – Fig. 3.16, respectively.

A comparative evaluation of the thermogravimetric analysis data of **MR**, the functionalized resins, **MRV** and **MRA** and the corresponding pMo loaded polymers, **3.2** and **3.3** as shown in Table 3.6 and Fig. 3.14 and Fig. 3.15, respectively revealed that the two stage decomposition observed in the thermogram of the **MR** at the broad temperature range of 284-700 °C owing to the degradation of the base polymer occurs as a common feature in the thermogram of each of the polymeric species.[77] Apart from this, in case of **MRV** and the alanine functionalized analogue **MRA**, a decomposition step with weight loss of 17.61% and 12.08% occurs in the temperature range of 199-255 and 221-274 °C, respectively. By analogy with the thermal decomposition characteristics reported for valine, alanine and some other amino acids, we ascribe this decomposition to the release of amino acid ligands from the resin.[78] In these compounds, the first step of decomposition attributable to loss of water of crystallization occurred in the temperature range of 89-99 °C.

Close resemblance was observed in the thermal decomposition patterns in case of the compounds **MRVMo (3.1)** and **MRAMo (3.2)**. The initial step of dehydration occurring in the range of 69-100 °C is seen to be followed by weight loss of 1.59% and 1.19% in the temperature range of 103-181 and 103-177 °C, respectively for **MRVMo (3.1)** and **MRAMo (3.2)**, attributable to complete loss of co-ordinated peroxo group from the complexes. The IR spectral analysis of the decomposition product isolated at this stage confirms the absence of peroxide.

Weight loss of 15.89% and 11.89% in the temperature range of 205-259 and 216-271 °C, respectively from the complexes, **MRVMo (3.1)** and **MRAMo (3.2)** has been ascribed to the loss of the amino acid functional from the resin. Degradation of the amino acids from the compounds was further ascertained by recording the IR spectra of the degradation product obtained by heating the compounds separately to the respective temperatures, which showed the complete disappearance of the signature peaks originating from the amino acids. The black residue from the pMo compounds, after total loss of the components viz. lattice water, coordinated peroxide, amino acid and polymeric resin, was found to be a hydrated oxomolybdenum species. This was also identified from the IR spectra which displayed the characteristic ν(Mo=O) and ν(OH) absorptions and was devoid of bands attributable to peroxo and the polymeric ligands of the original compound.

In case of **PANMo (3.3)**, the first degradation has been observed in the temperature range of 112–157 °C, with the corresponding weight loss of 2.14%, consistent with the total loss of coordinated peroxo groups from the complexes. The next decomposition step appeared as a single peak in DTG, between 306-359 °C with a weight loss of 13.44%. It has been reported previously that the degradation of PAN below 400 °C is accompanied by elimination of HCN, NH_3 and H_2O and concomitant intramolecular polymerization of nitrile groups to form conjugated polyamine $(-C=N)_n$ and that the loss of nitrogen commences at 750 °C.[79] In the present study, the residue obtained at 359 °C was subjected to IR spectral analysis. The IR spectrum displayed bands at 1579 cm^{-1} and 1624 cm^{-1} typical of ν(C=C) and ν(C=N) stretching in addition to ν(Mo=O) at 950 cm^{-1}. The observations are in accord with the previous findings on thermal degradation pattern of PAN,[57] as well as **PANW**.[39] The degradation further continued up to 750 °C.

The total weight loss which occurred during the course of the overall decomposition process on heating the compound up to a final temperature of 750 °C was recorded to be 39.69%. The TGA–DTG analysis data for the polymer-anchored compounds were thus in complete agreement with their composition and formula assigned.

Table 3.6 Thermogravimetric data for **MRV**, **MRA**, **MRVMo**, **MRAMo** and **PANMo**

Compound	Temperature range (°C)	Observed weight loss (%)	Final residue (%)
MRV	89-99	0.72	2.56
	199-255	17.61	
	283-480	50.88	
	480-700	28.23	
MRA	91-99	0.67	1.23
	221-274	12.08	
	280-482	56.90	
	482-700	29.12	
MRVMo	70-100	1.04	9.06
	103-181	1.59	
	286-488	15.89	
	205-259	46.15	
	488-700	26.31	
MRAMo	69-100	1.14	6.58
	103-177	1.19	
	216-271	11.89	
	280-488	50.48	
	488-700	28.72	
PANMo	112-157	2.14	60.31
	306-359	13.44	
	359-750	24.11	

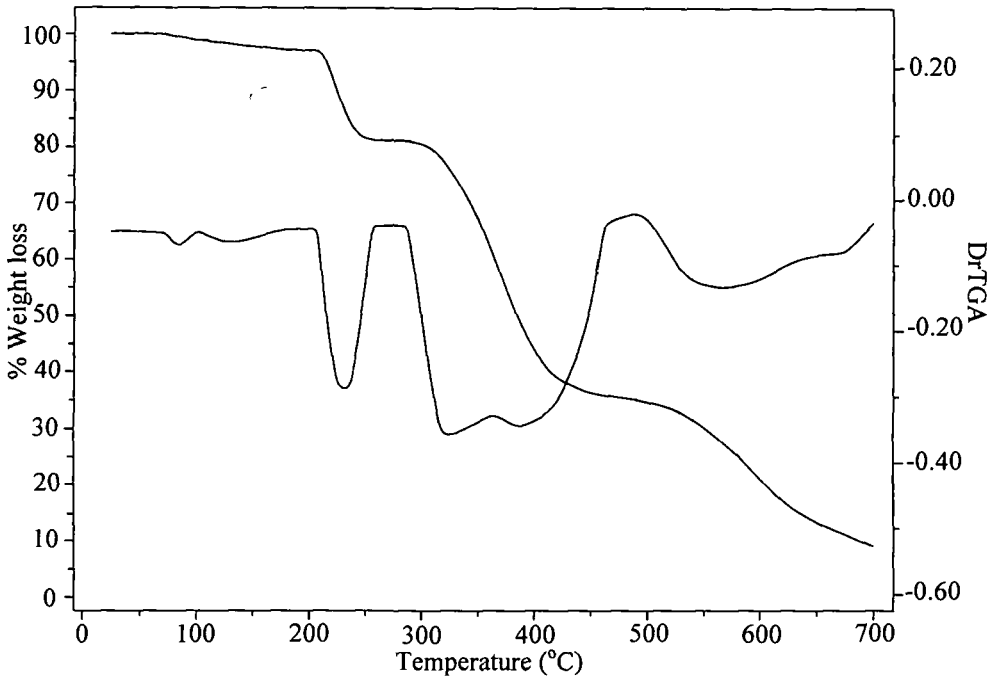

Fig. 3.14 TG-DTG plot of **MRVMo**.

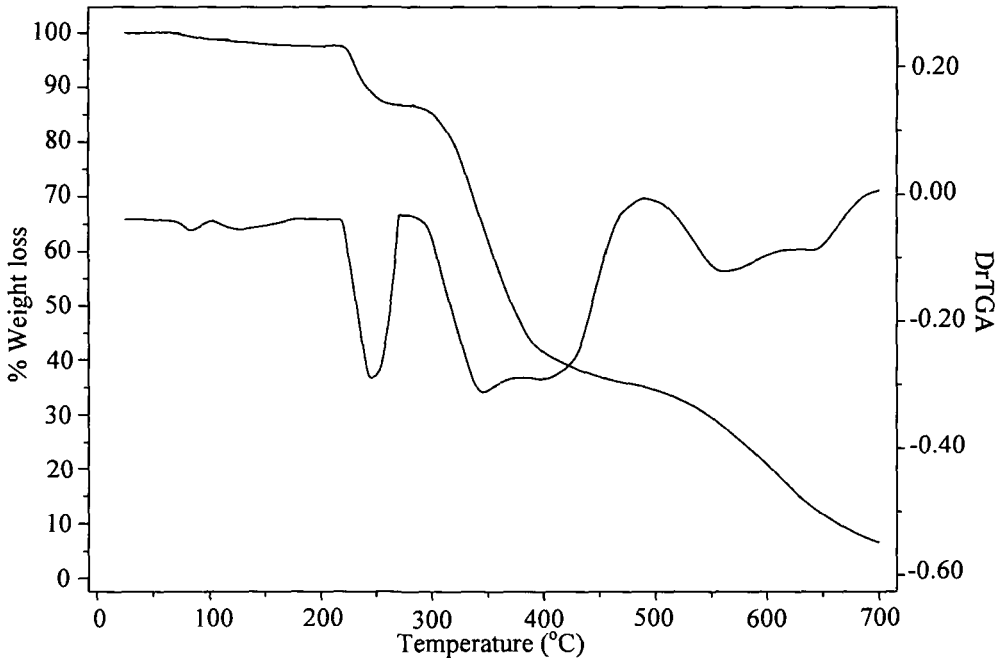

Fig. 3.15 TG-DTG plot of **MRAMo**.

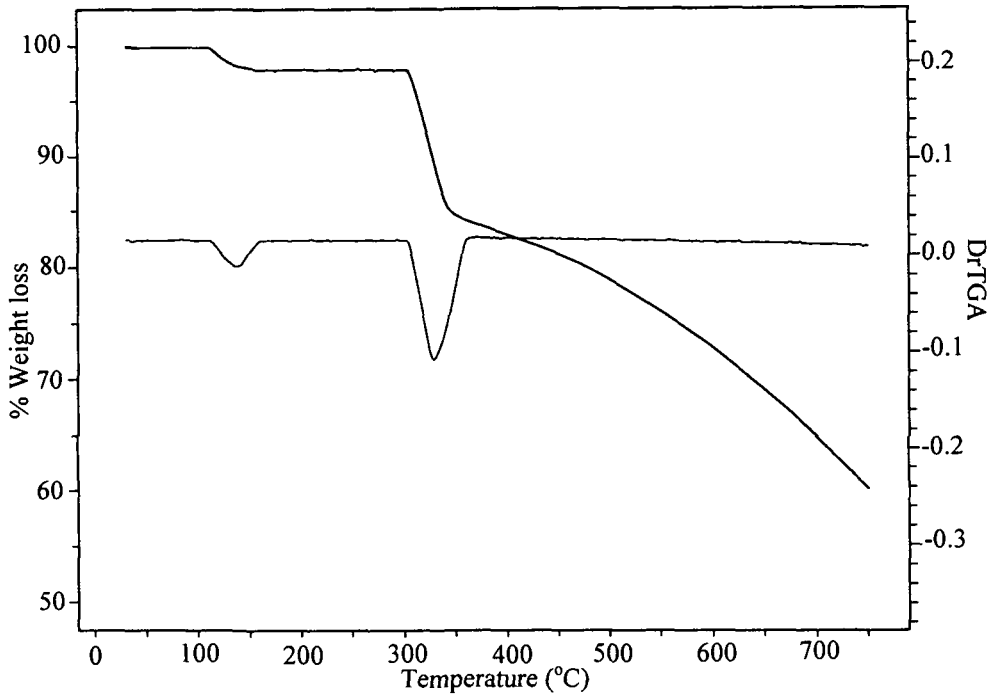

Fig. 3.16 TG-DTG plot of **PANMo**.

On the basis of the elemental analysis and above spectral data, structures of the type shown schematically in Fig. 3.17 have been envisaged for the macrocomplexes **MRVMo (3.1)**, **MRAMo (3.2)** and **PANMo (3.3)**. The structures incorporate carboxylate groups of the pendant amino acid of **MR** (in **MRAMo** or **MRVMo**), or the nitrile ligand of PAN (in **PANMo**) unidentately co-ordinated to dioxomonoperoxomolybdenum(VI) moiety, completing the hexa co-ordination around molybdenum atom.

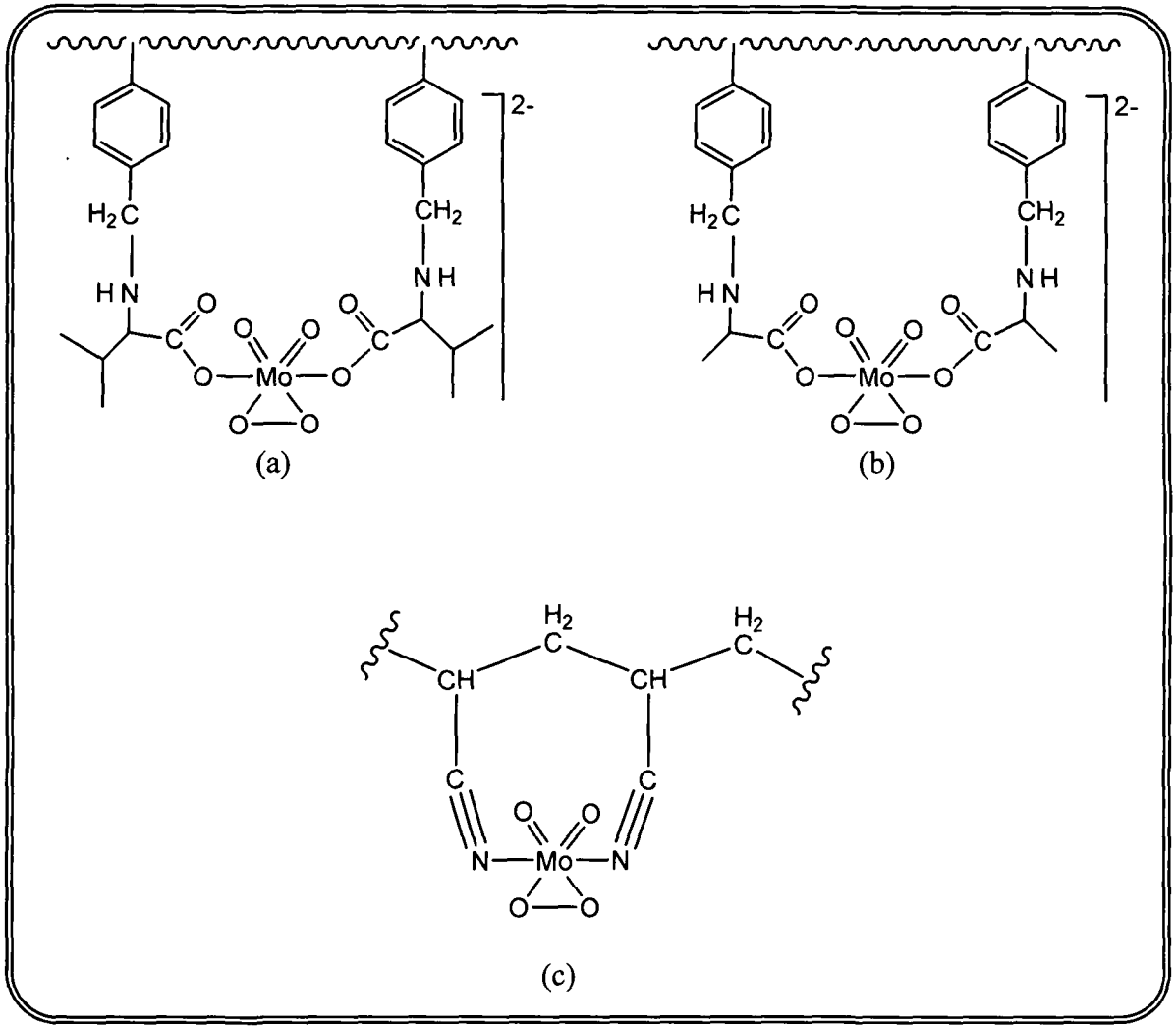

Fig. 3.17 Proposed structure of (a) **MRVMo**, (b) **MRAMo** and (c) **PANMo**. "〰" represents polymer chain.

3.4 CONCLUSIONS

In summary, immobilization of peroxomolybdenum(VI) species on amino acid functionalized Merrifield resin or poly(acrylonitrile) matrix, afforded a set of novel polymer supported monoperoxo complexes of molybdenum. All the compounds have been characterized spectroscopically as well as by other physico-chemical methods. One of the notable features of these insoluble compounds is the presence of molybdenum in its dioxomonoperoxo form. The synthetic methodology is simple involving easily available starting materials. It is significant to note that the **PANMo** remains stable up to a temperature of 112 °C whereas for the compounds **MRAMo** and **MRVMo**, after initial dehydration, decomposition starts only at 200 °C. Moreover, the compounds do not suffer from explosion upon heating unlike some monomeric peroxomolybdenum compound[80] or the neat polymer, PAN[57] and are non-hygroscopic and stable at room temperature and can be stored for a prolonged period. These remarkable features of the compounds, in addition to the reasonable simplicity in their method of preparation from commercially available starting materials enhance the potential prospect of being useful as catalysts in organic transformations. Results of investigation on the activity of the title compounds as catalysts in organic oxidations are presented in Chapters 5 and 6 of the thesis.

REFERENCES

1. Skorobogaty, A., & Smith, T.D. *Coord. Chem. Rev.* **53**, 55--226, 1984.

2. Sherrington, D.C. *Pure Appl. Chem.* **60**, 401--414, 1988.

3. Pomogalilo, A.D. *Catalysis by Polymer Immobilized Metal Complexes*, Gordon and Breach Science Publishers, Amsterdam, 1998.

4. Sherrington, D.C. *J. Poly. Sci. A: Polym. Chem.* **39**, 2364--2377, 2001.

5. Choplin, A., & Quignard, F. *Coord .Chem. Rev.* **178-180**, 1679--1702, 1998.

6. Sherrington, D.C. *Catal. Today* **57**, 87--104, 2000.

7. McNamara, C.A., et al. *Chem. Rev.* **102**, 3275--3300, 2002.

8. Bekturov, E.A. & Kudaibergenov, S.E. *Catalysis by Polymers*, WILEY-VCH Verlag GmbH & Co. KGaA, Weinheim, 2002.

9. Hodge, P. & Sherrington, P. (ed.), *Polymer Supported Reactions in Organic Synthesis*, J. Wiley and Sons, New York, 1980.

10. Lisichkin, G.V. & Yuffa, A. Ya. *"Geterogennye Metallokompleksnye Katalizatory" (Heterogeneous Metal Complex Catalysts)*, Nauka, Moscow, 1981.

11. Herbert, M., et al. *J. Mol. Catal. A: Chem.* **338**, 111--120, 2011.

12. Romanelli, G.P., et al. *Catal. Commun.* **12**, 726--730, 2011.

13. Tundo, P., et al. *Catal. Commun.* **11**, 1181--1184, 2010.

14. Gharah, N., et al. *Inorg. Chim. Acta* **362**, 1089--1100, 2009.

15. Gamelas, C.A., et al. *Tetrahedron Lett.* **49**, 4708--4712, 2008.

16. Cross, W.B., et al. *Inorg. Chem.* **45**, 4556--4561, 2006.

17. Maiti, S.K., et al. *New J. Chem.* **29**, 554--563, 2005.

18. Wang, G., et al. *Inorg. Chim. Acta* **358**, 933--940, 2005.

19. Fuerte, A., et al. *J. Mol. Catal. A: Chem.* **211**, 227--235, 2004.

20. Fronczek, F.R., et al. *Inorg. Chem. Commun.* **5**, 384--387, 2002.

21. Choudary, B.M., et al. *J. Chem. Soc., Perkin Trans. 1* 2069--2074, 2002.

22. Batigalhia F., et al. *Tetrahedron* **57**, 9669--9676, 2001.

23. Gresley, N.M., et al. *J. Mol. Catal. A.: Chem.* **117**, 185--198, 1997.

24. Tamami, B., & Yeganeh, H. *Eur. Polym. J.* **35**, 1445--1450, 1999.

25. Dickman, M.H., & Pope, M.T. *Chem. Rev.* **94**, 569--584, 1994.

26. Ghiron, A.F., & Thompson, R.C. *Inorg. Chem.* **28**, 3647--3650, 1989.

27. Bortolini, O., et al. *J. Org. Chem.* **50**, 2688--2690, 1985.

28. Cross, R.J., et al. *J. Mol. Catal. A: Chem.* **144**, 273--284, 1999.

29. Peng, F.M. in *Encyclopedia of Polymer Science and Engineering,* H.F. Mark et al., eds., John Wiley and Sons, New York, 1985, **1**, 426-470.

30. Petropoulos, J.C., et al. *Ind. Eng. Chem.* **49**, 379--381, 1957.

31. Michalska, Z.M., et al. *React. Polym.* **16**, 213--221, 1992.

32. Maria, L.C.S. *React. Funct. Polym.* **49**, 133--143, 2001.

33. Rayford, W.E., et al. *J. Appl. Polym. Sci.* **24**, 105--113, 1979.

34. Das, S.P., et al. *J. Mol. Catal. A: Chem.* **356**, 36--45, 2012.

35. Merrifield, R.B. *J. Am. Chem. Soc.* **85**, 2149--2154, 1963.

36. Clark, J.H. *Green Chem.* **1**, 1--8, 1999.

37. Roscoe, S.B., et al. *J. Polym. Sci.: Part A: Polym. Chem.* **38**, 2979--2992, 2000.

38. Pomogalilo, A.D. *Catalysis by Polymer Immobilized Metal Complexes*, Gordon and Breach Science Publishers, Amsterdam, 1998.

39. Tamami, B., & Yeganeh, H. *React. Funct. Polym.* **50**, 101--106, 2002.

40. Skoróbogaty, A., & Smith, T.D. *Coord. Chem. Rev.* **53**, 55--226, 1984.

41. Djordjevic, C., et al. *Inorg. Chem.* **36**, 1798--1805, 1997.

42. Petit, M.A., & Jozefonvicz, J. *J. Appl. Polym. Sci.* **21**, 2589--2596, 1977.

43. Valodkar, V.B., et al. *React. Funct. Polym.* **56**, 1--15, 2003.

44. Valodkar, V.B., et al. *J. Mol. Catal. A: Chem.* **202**, 47--64, 2003.

45. Gil, S., et al. *React. Funct. Polym.* **42**, 65--72, 1999.

46. Kalita, D., et al. *React. Funct. Polym.* **68**, 876--890, 2008.

47. Das, S.P., et al. *RSC Adv.* **2**, 7248--7261, 2012.

48. Brunauer, S., et al. *J. Am. Chem. Soc.* **60**, 309--319, 1938.

49. Barrett, E.P., et al. *J. Am. Chem. Soc.* **73**, 373--380, 1951.

50. Gokak, D.T., & Ram, R.N. *J. Mol. Catal.* **49**, 285--298, 1989.

51. Campbell, N.J. et al. *Polyhedron* **8**, 1379--1386, 1989.

52. Lever, A.B.P., & Gray, H.B. *Acc. Chem. Res.* **11**, 348--355, 1978.

53. Nakamoto, K. *Infrared and Raman Spectra of Inorganic and Co-ordination Compounds, Part B,* 5th ed., Wiley and Sons, New York, 1997, 62-67.

54. Nakamoto, K. *Infrared and Raman Spectra of Inorganic and Co-ordination Compounds, Part B,* 5th ed., Wiley and Sons, New York, 1997, 60.

55. Deacon, G.B., & Phillips, R.J. *Coord. Chem. Rev.* **33**, 227--250, 1980.

56. Michalska, Z.M., et al. *React. Polym.* **16**, 213--221, 1992.

57. Badawy, S.M., & Dessouki, A.M. *J. Phys. Chem. B* **107**, 11273--11279, 2003.

58. Nakamoto, K. *Infrared and Raman Spectra of Inorganic and Co-ordination Compounds, Part B,* 5th ed., Wiley and Sons, New York, 1997, 113–115.

59. Rach, S.F., & Kühn, F.E. *Chem. Rev.* **109**, 2061--2080, 2009.

60. Silverstein, R.M., Bassler, G.C. & Morrill, T.C. *Spectrometric identification of Organic Compounds*, 5th ed., John Wiley and Sons, New York, 1991, 294.

61. Djordjevic, C., et al. *Inorg. Chem.* **27**, 2926--2932, 1988.

62. Maurya, M.R., & Bharti, N. *Transition Met. Chem.* **24**, 389--393, 1999.

63. Dengel, A.C., et al. *J. Chem. Soc., Dalton Trans.* 991--995, 1987.

64. Bayot, D., et al. *Inorg. Chim. Acta* **357**, 809--816, 2004.

65. Justino, L.L.G., et al. *Inorg. Chim. Acta* **356**, 179--186, 2003.

66. Pettersson, L., et al. *Coord. Chem. Rev.* **237**, 77--87, 2003.

67. Conte, V., et al. *J. Mol. Catal.* **94**, 323--333, 1994.

68. Jacobson, S.E., et al. *Inorg. Chem.* **17**, 3055--3063, 1978.

69. Lorge, F., et al. *J. Comb. Chem.* **1**, 25--27, 1999.

70. Mohanraj, S., & Ford, W.T. *Macromolecules* **18**, 351--356, 1985.

71. Kawamoto, K., & Tsujimoto, Y. *J. Endod.* **30**, 45--50, 2004.

72. Schaefer, J. *Macromolecules* **4**, 105--107, 1971.

73. Kassaee, M.Z., et al. *Molecules* **9**, 825--829, 2004.

74. LeTiran, A., et al. *Bioorg. Med. Chem.* **9**, 2693--2708, 2001.

75. Kim, J.H., et al. *J. Am. Chem. Soc.* **115**, 3618--3622, 1993.

76. Nardello, V., et al. *Inorg. Chem.* **34**, 4950--4957, 1995.

77. Mukherjee, A., & Biswas, M. *J. Appl. Polym. Sci.* **50**, 1485--1492, 1993.

78. Rodante, F., et al. *Thermochim. Acta* **194**, 197--213, 1992.

79. Xue, T.J., et al. *Polym. Degrad. Stabil.* **58**, 193--202, 1997.

80. Bhengu, T.T., & Sanyal, D.K. *Thermochim. Acta* **397**, 181--197, 2003.

CHAPTER 4

A Family of Diperoxomolybdate(VI) Compounds Anchored to Water Soluble Polymers: Synthesis and Characterization

4.1 INTRODUCTION

Development of water soluble macromolecular metal complexes is one of the promising new trends in the area of metal containing polymers.[1,2] One of the significant features of a soluble polymer supported reagent is the facility of product synthesis and characterization afforded by the soluble support due to the advantages of homogeneity offered by it.[3,4] Polymers are usually devoid of some of the unfavorable properties of monomeric species, such as lability, volatility, toxicity and odour.[5] Binding of active drug molecules to water-soluble polymeric drug carriers offer various advantages including improved drug pharmacokinetics, lower toxicity to healthy organs, possible facilitation of preferential uptake by targeted cells and programmed drug release profile.[6-10]

A polymeric support is known to impart stability to the anchored support. Recent work in our laboratory have shown that soluble macrocomplexes of peroxovanadium (pV) and peroxotungsten (pW), the first known examples of peroxometal derivatives supported on water soluble polymer (WSP),[11,12] exhibited unique oxidant activity as well as biochemical properties including antibacterial[12] and enzyme inhibitory activities.[11] Moreover, polyacrylate bound pV (**PAV**) exerted vasomodulatory effect on rat aortic rings.[13] These interesting findings clearly show that a lot remains to be unraveled on other possible chemical and biochemical applications of these compounds. Synthesis of newer

members of this class of new materials appears to be an important pre-requisite from which other aspects can be developed.

In the present work we have endeavored to synthesize pMo containing macrocomplexes by anchoring the peroxomolybdate species to appropriate water soluble macroligands. The task of constructing metal containing macromolecules that are stable, active as well as selective with respect to a specific property obviously requires adequate consideration particularly with respect to choice of the macroligand. We have selected for the present investigation a set of WSP with pendant functional groups such as carboxylate, amide or sulfonate anticipating facile attachment of active metal complexes which would also reduce the requirement of pre-functionalization step. These macroligands are known to serve as effective chelatogen giving rise to stable metal ligand linkage.[14] Most importantly, each of the selected polymers are chemically stable, commercially available or can be prepared easily and are relatively cheaper.[12] The additional attractive attributes of the polymers are their biocompatibility as evident from their use in different biomedical applications such as in bioadhesive products, drug delivery and anti-microbial activity.[15]

The present chapter deals with the synthesis and characterization of a series of new water soluble polymer bound diperoxomolybdate complexes of the type **$[Mo_2O_2(O_2)_4$(carboxylate)]–PA** [PA = poly(sodium acrylate)] **(PAMo) (4.1)**, **$[MoO(O_2)_2$(carboxylate)]–PMA** [PMA = poly(sodium methacrylate)] **(PMAMo) (4.2)**, **$[MoO(O_2)_2$(amide)]–PAm** [PAm = poly(acrylamide)] **(PAmMo) (4.3)**, and **$[MoO(O_2)_2$(sulfonate)]–PS** [PS = poly(sodium vinyl sulfonate)] **(PSMo) (4.4)**.

4.2 EXPERIMENTAL SECTION

4.2.1 Synthesis of $[Mo_2O_2(O_2)_4(carboxylate)]$–PA [PA = poly (sodium acrylate)] (PAMo) (4.1), $[MoO(O_2)_2(carboxylate)]$–PMA [PMA = poly (sodium methacrylate)] (PMAMo) (4.2), $[MoO(O_2)_2(amide)]$–PAm [PAm = poly(acrylamide)] (PAmMo) (4.3) and $[MoO(O_2)_2(sulfonate)]$–PS [PS = poly(sodium vinyl sulfonate)] (PSMo) (4.4)

In a representative procedure, molybdic acid (0.64 g, 4.0 mmol for compounds **PAMo** and **PMAMo**; 3.4 g, 21.12 mmol for **PAmMo**; 1.84 g, 11.50 mmol for **PSMo**) was dissolved in 30% H_2O_2 (12 mL, 105.84 mmol for **PAMo** and **PMAMo**; 22 mL, 194.11 mmol for **PAmMo**; 15 mL, 132.30 mmol for **PSMo**) with constant stirring and by maintaining the temperature at 30-40 °C. To the clear solution obtained, 1.5 g of respective polymer was added in portions with continuous stirring. The mixture was stirred for *ca.* 60 min in an ice bath until all solids dissolved. At this stage the pH of the reaction medium was recorded to be *ca.* 2. The pH of the solution was raised to *ca.* 5 by dropwise addition of concentrated NaOH solution (*ca.* 8 M) with constant stirring. A red colored pasty mass separated out on adding pre-cooled acetone (*ca.* 50 mL) to this mixture under vigorous stirring. The reaction mixture was allowed to stand for about 30 min and the residue obtained after decanting the supernatant liquid was washed repeatedly with pre-cooled acetone under scratching. The microcrystalline product, separated by centrifugation, was washed with cold acetone and dried in *vacuo* over concentrated sulfuric acid. The compounds were finally dried by heating upto 70 °C under nitrogen atmosphere.

4.2.2 Elemental analysis and physical measurements

The molybdenum, peroxide, carbon, hydrogen, nitrogen and sodium content in the synthesized compounds were quantitatively determined by procedures described in Chapter 2. The analytical data of the compounds are summarized in Table 4.1. The methods employed for thermogravimetric analysis, scanning electron micrographs (SEM) and EDX analysis, as well as spectroscopic measurements have been outlined in Chapter 2. Structurally significant IR bands and their assignments are listed in Table 4.2. Presented in Table 4.3, are the ^{13}C NMR chemical shift values for the complexes and their respective free polymers. TGA data of the complexes are reported in Table 4.4.

4.3 RESULTS AND DISCUSSION

4.3.1 Synthesis and characterization

4.3.1.1 Synthesis

Use of a soluble polymeric ligand for the synthesis of macromolecular metal complexes often offers the convenience of adopting synthetic methodologies used for preparing their low molecular weight analogues.[1] In the present study, the compounds, **4.1-4.4** supported on water soluble macromolecules containing pendant functional groups such as carboxylate, amide and sulfonate were obtained by the reaction of molybdic acid, H_2MoO_4, with 30% H_2O_2 and the respective polymer in aqueous medium at ice-bath temperature. The degree of dissociation as well as mode and extent of chelation of the water soluble polyelectrolytes used as support in the present study, are known to be strongly dependent on pH.[16-18] The pH of *ca.* 5 was found to be favorable for the desired

synthesis of each of the compound. The alkali used to maintain the pH of the reaction solution also provided the required counter cations for the complex anions. It was important to limit the amount of water to that contributed by the alkali hydroxide solution and hydrogen peroxide used. The compounds were obtained as solids by solvent induced precipitation which is a common and effective means for isolating soluble polymeric compounds.[3,4] Whereas a metal : ligand ratio of (1 : 4) was obtained for the compounds **PAMo**, the same was found to be rather low for the rest of the compounds, **PMAMo** (1 : 7), **PAmMo** (1 : 12) and **PSMo** (1 : 6). Our attempts to improve the molybdenum loading in the synthesized compounds, have not been successful so far. In the solid state, the compounds were found to be stable for several weeks stored dry in closed containers at ambient temperature. All the synthesized pMo compounds are soluble in water.

4.3.1.2 Characterization and formulation

The results of elemental analysis listed in Table 4.1, indicated the presence of two peroxide groups per Mo centre in each of the compounds **4.1-4.4** consistent with the formulation of pMo species as $[MoO(O_2)_2]$. The compounds were diamagnetic in nature as was evident from the magnetic susceptibility measurement in conformity with the presence of Mo in +6 oxidation states. The molybdenum loading on the compounds, **4.1-4.4** estimated on the basis of EDX, atomic absorption spectroscopy (AAS) and elemental analysis data are presented in Table 4.1.

4.3.1.2.1 SEM and Energy Dispersive X-ray (EDX) Analysis

The scanning electron micrographs of the polymer anchored complexes showed significant alteration of their surfaces in contrast to the smooth surfaces of the pure polymers

(Fig. 4.1 and 4.2) and revealed that the metal ions are distributed across the surface of the polymers.

Energy dispersive X-ray spectroscopic analysis was carried out focusing multiple regions over the surface of the polymer. The results presented in Table 4.1 are the averaging out of the data from these regions and the data obtained were consistent with that of the elemental analysis values (Table 4.1).

Table 4.1 Analytical data for the polymer-bound peroxometallates

Compound	% Found from elemental analysis (% obtained from EDX spectra)						Molybdenum loading[a] (mmol g^{-1} of polymer)
	C	H	N	Na	Mo	O_2^{2-}	
PAMo	30.52 (30.76)	2.34	----	19.26[b] (19.19)	13.92 13.90[b] (13.88)	9.31	1.45
PMAMo	39.74 (40.07)	4.53	----	19.96[b] (19.89)	6.50 6.49[b] (6.39)	4.30	0.68
PAmMo	46.72 (46.89)	6.96	17.79 (17.13)	----	5.82 5.80[b] (5.79)	3.71	0.61
PSMo	15.26 (15.85)	1.87 ---	----	14.90[b] (14.97)	9.82 9.78[b] (10.01)	6.47	1.02

[a]Molybdenum loading = $\frac{\text{Observed metal \% X 10}}{\text{Atomic weight of metal}}$,

[b] Determined by AAS.

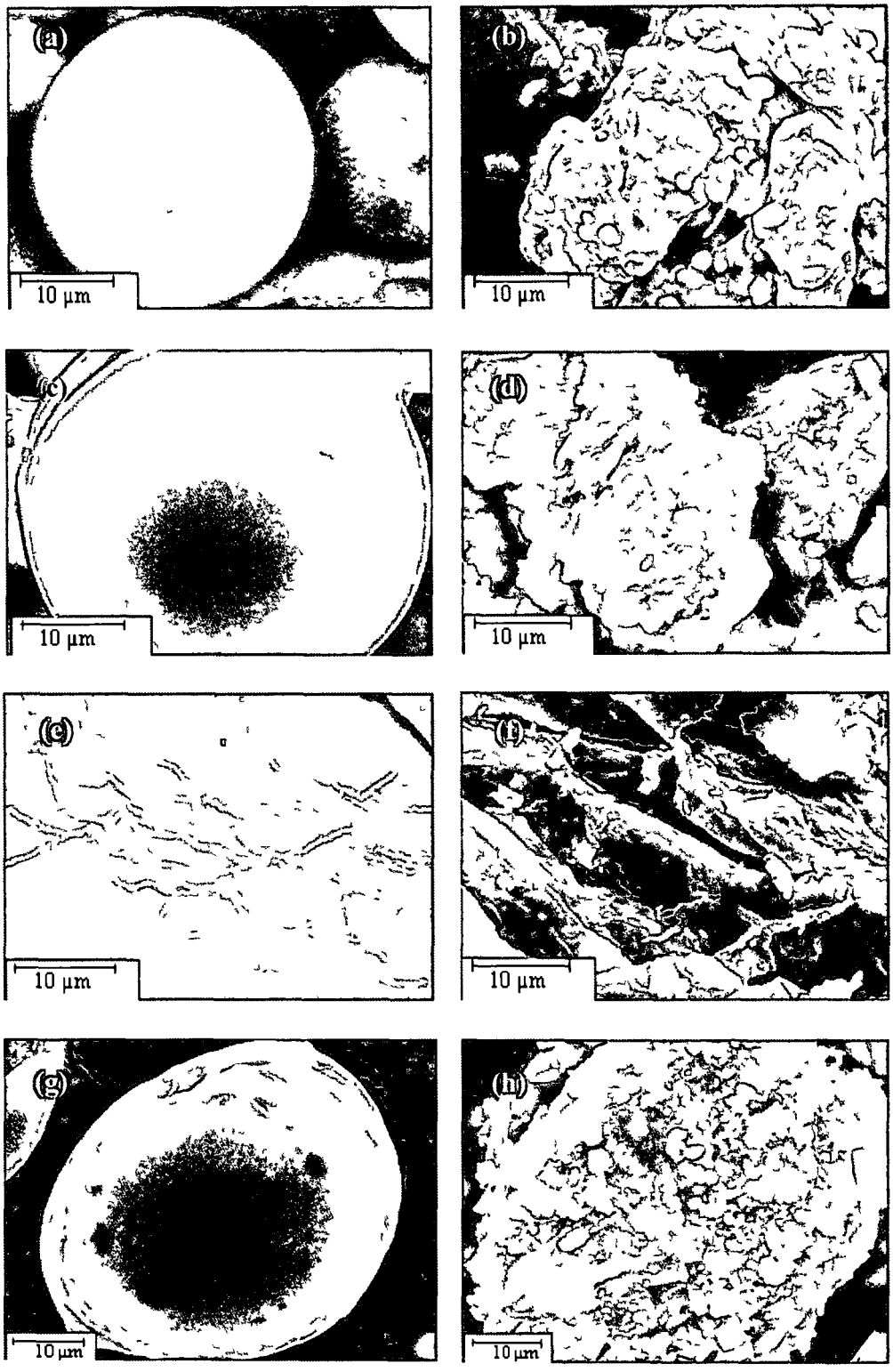

Fig. 4.1 Scanning electron micrographs of (a) PA, (b) **PAMo**, (c) PMA, (d) **PMAMo**, (e) PAm, (f) **PAmMo**, (g) PS and (h) **PSMo**.

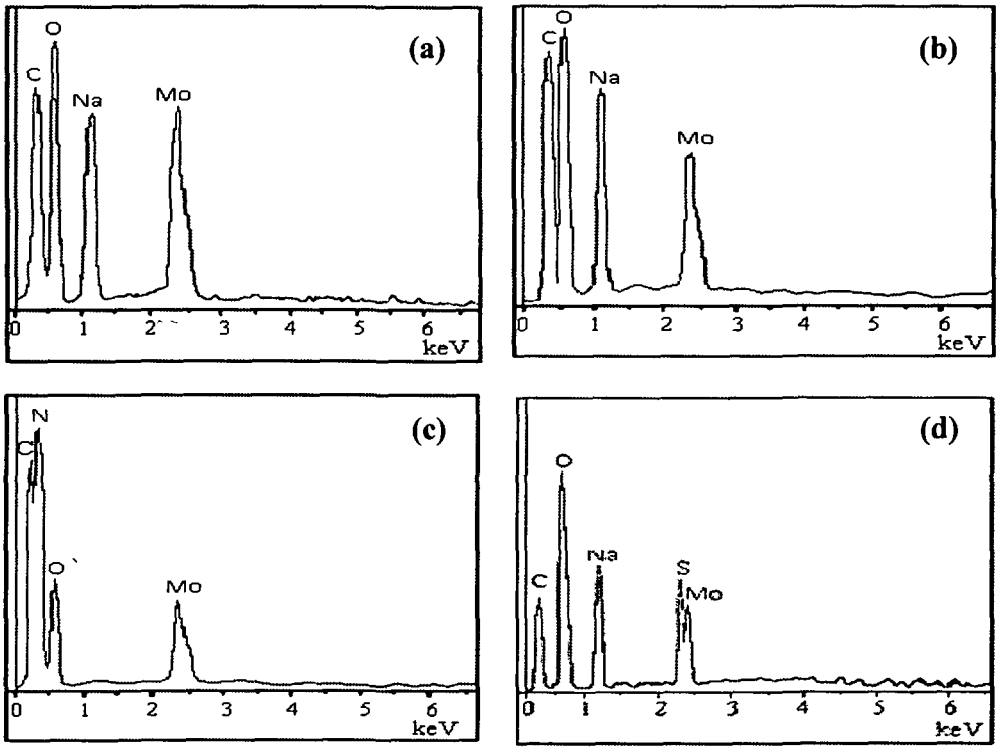

Fig. 4.2 EDX spectra of (a) **PAMo**, (b) **PMAMo**, (c) **PAmMo** and (d) **PSMo**.

4.3.1.2.2 IR spectral studies

Each of the title compounds, **4.1-4.4,** displayed typical spectral patterns in the infra-red region involving absorptions due to co-ordinated peroxo and polymer bound ligands (Fig. 4.3 - Fig. 4.6). The significant IR spectral data are summarized in Table 4.2.

The IR spectral investigation on the nature of metal-carboxylate co-ordination has been the subject of numerous reports.[19-24] Depending on the nature of the metal, ligand or pH of the reaction medium, a carboxylate group may bind to a metal in a unidentate, bridged bidentate or bidentate chelating fashion.[19,20] These modes can be easily distinguished in the complexes by comparing the values of $\Delta\nu$ [ν_{asym} (COO) – ν_{sym}(COO)] and this relationship is also valid for polycarboxylates[21,22] as well as for polyacrylates.[23,24]

In the spectrum of pristine poly(acrylate), the ν_{asym}(COO) and ν_{sym}(COO) modes are observed at 1565 and 1409 cm^{-1}, respectively resulting $\Delta\nu$= 156 cm^{-1}. In **PAMo**, after

pMo incorporation, the corresponding peaks for ν_{asym}(COO) and ν_{sym}(COO) were shifted to 1574 and 1406 cm^{-1}, respectively giving $\Delta\nu$ = 168 cm^{-1} which is close to that observed for free PA suggesting a bidentate bridging coordination of carboxylate group.[19,20,23,24] Moreover, the ν_{asym}(COO) band was broadened after metal incorporation which is ascribed to the presence of uncoordinated carboxylate groups.

The spectrum of pure poly(methacrylate) displays ν_{asym}(COO) and ν_{sym}(COO) absorptions at 1540 and 1415 cm^{-1}, respectively. In case of **PMAMo**, ν_{asym}(COO) was observed as a strong broad band at 1659 cm^{-1}. The corresponding ν_{sym}(COO) mode attributable to co-ordinated carboxylate group appeared at 1407 cm^{-1} with a shoulder at 1414 cm^{-1} probably owing to the presence of free carboxylate. The resulting $\Delta\nu$ = 252 cm^{-1} being much greater relative to the free PMA ($\Delta\nu$ = 125 cm^{-1}) gave clear indication of the presence of unidentately coordinated carboxylate groups in the compound.[19,20] Presence of free COOH groups in each of the compounds **PAMo** and **PMAMo** was evident from an additional IR band appearing in the vicinity of 1710 cm^{-1}.

In the pendant amide groups of poly(acrylamide), amide nitrogen and the carbonyl oxygen are the two possible alternative metal binding sites.[25-30] The carbonyl absorption is known to shift to lower value in case of co-ordination via carbonyl oxygen whereas, ν(C=O) (amide-I) band frequency increases upon binding of the metal through the lone pair of nitrogen.[25-27] The pure PAm spectrum has a strong carbonyl stretching absorption at 1643 cm^{-1}, whereas the spectrum of the complex displayed, in addition to the band at 1643 cm^{-1}, a new typical absorption in the carbonyl region at 1658 cm^{-1}. This latter band at higher wave number has been ascribed to a shift of the amide I absorption to a higher frequency as a consequence of N(amide) co-ordination to Mo(VI) ion. The medium intensity band at 1425 cm^{-1} with a shoulder at 1445 cm^{-1} was assigned for ν(C-N).

Table 4.2 Infrared spectral data for the pMo compounds **4.1-4.4** and base polymers

Compound	ν_{asym}(COO)	ν_{sym}(COO)	ν(C=O)	ν(S-O)	ν(Mo=O)	ν(O-O)	ν_{asym}(Mo-O_2)	ν_{sym}(Mo-O_2)
PA	1565(s)	1409(s)	---	---	---	---	---	---
PAMo	1710(s) 1574(br, s)	1406(s)	---	---	963(vs)	864(vs)	626(m)	525(m)
PMA	1540(s)	1415(s)	---	---	---	---	---	---
PMAMo	1708(s) 1659(br, s)	1407(s)	---	---	963(vs)	853(vs)	610(m)	527(m)
PAm	---	---	1643(s)	---	---	---	---	---
PAmMo	---	---	1643(sh) 1658(br, s)	---	961(vs)	861(vs)	600(m)	509(m)
PS	---	---	---	1210(sh) 1127(vs) 1040(s)	---	---	---	---
PSMo	---	---	---	1220(vs) 1210(sh) 1189(vs) 1127(vs) 1042(s)	965(vs)	857(vs)	629(m)	533(m)

vs, very strong; br, broad; s,strong; sh, shoulder; m, medium.

Definite assignment of the band due to N-H frequency was not possible as it occurred in O-H frequency region.

IR spectrum of pure poly(vinyl sulfonate) displayed, apart from the symmetric stretching of sulfonate anion at ca. 1040 cm^{-1}, two bands representing S-O stretching of the sulfonate group in the region at ca. 1210 and ca. 1130 cm^{-1}.[25,30] The **PSMo** spectrum on the other hand, exhibits distinct splitting pattern with new absorptions at 1219 and 1189 cm^{-1} in addition to the ν_{asym}(S-O) at 1127cm^{-1} attributable to complexed sulfonate group.[25,30-32] The presence of uncoordinated sulfonate group in the compound **4.4** was confirmed from the appearance of bands at *ca.* 1127 and *ca.* 1210 cm^{-1}.

The presence of terminally bound oxo and peroxo groups in each of the compounds was ascertained from the occurrence of a strong ν(Mo=O) band at ca. 960 cm^{-1}, and the typical ν(O-O), ν_{asym}(Mo-O_2) and ν_{sym}(Mo-O_2) modes at ca. 860, 610 and 530 cm^{-1}, respectively.[33,34]

The weak intensity bands appearing in the range between 500-400 cm^{-1} in the compounds, **4.1-4.4** are attributable to metal oxygen vibrations. The spectra also revealed the presence of lattice water in the water soluble complexes by showing a broad ν(OH) absorption centered in the 3500–3400 cm^{-1} region.

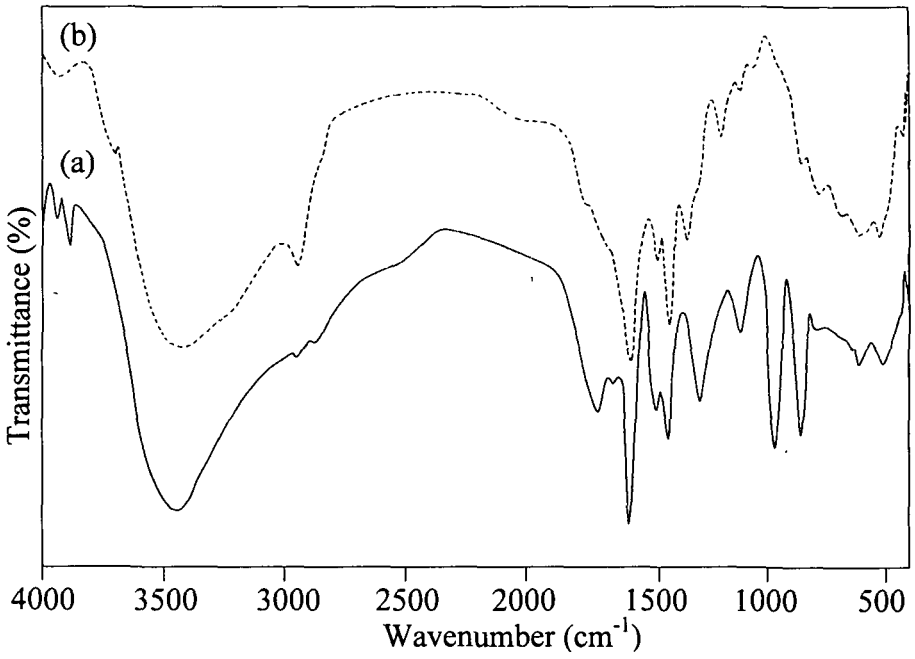

Fig. 4.3 IR spectra of (a) **PAMo** (solid line) and (b) PA (broken line).

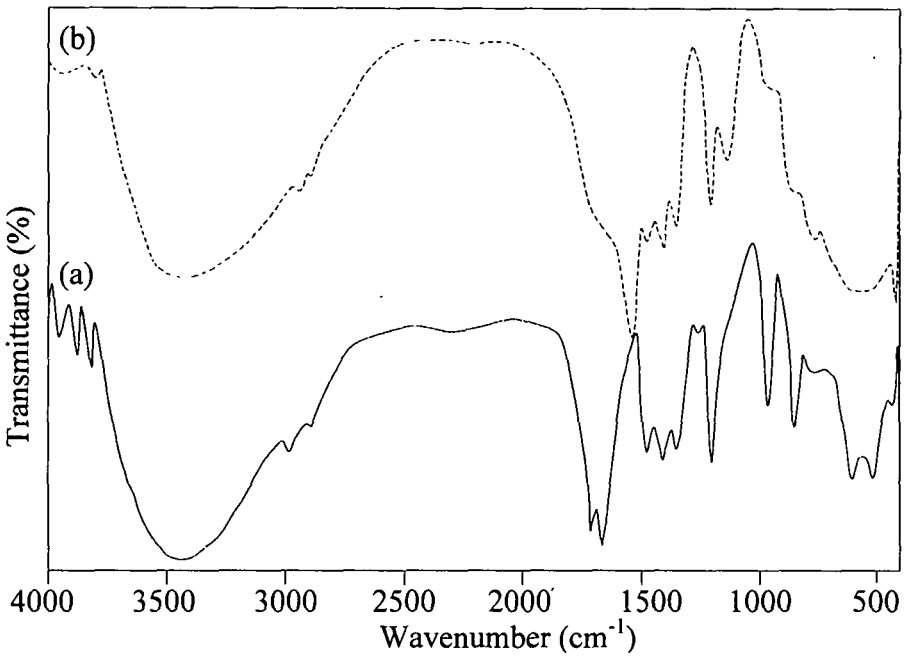

Fig. 4.4 IR spectra of (a) **PMAMo** (solid line) and (b) PMA (broken line).

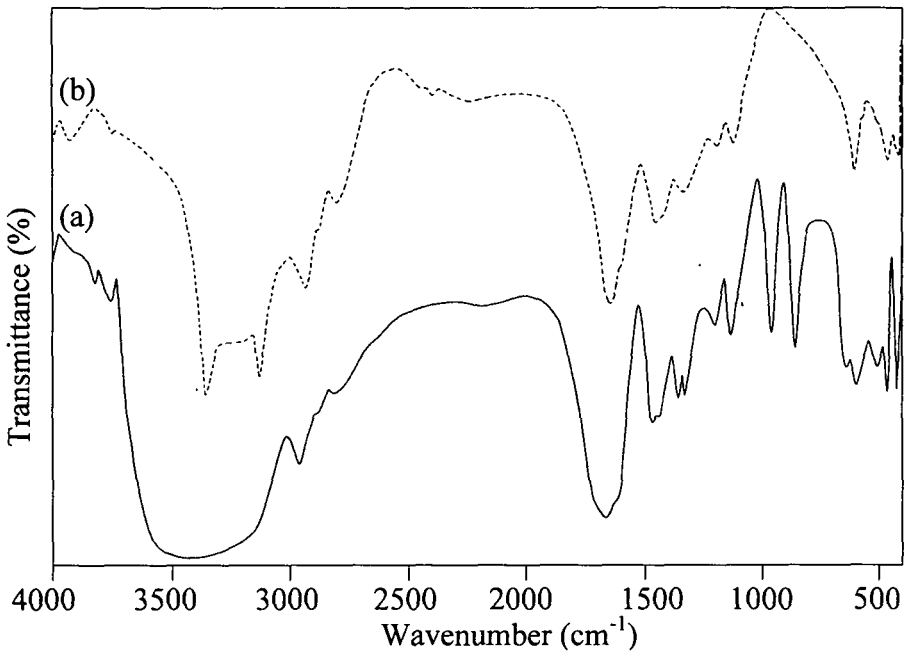

Fig. 4.5 IR spectra of (a) **PAmMo** (solid line) and (b) PAm (broken line).

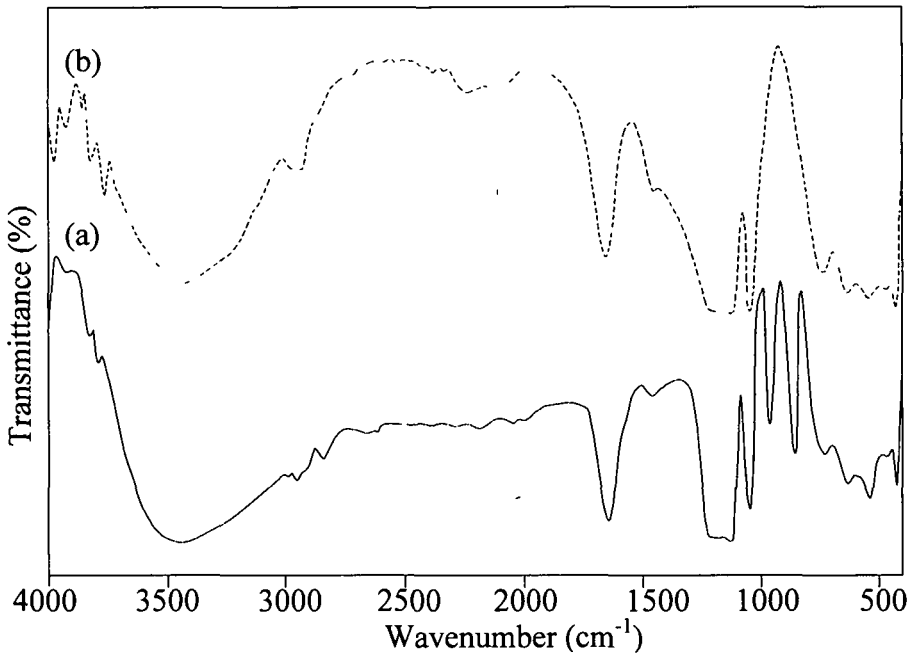

Fig.4.6 IR spectra of (a) **PSMo** (solid line) and (b) PS (broken line).

4.3.1.2.3 Electronic spectra

The electronic spectra of all the compounds were recorded in aqueous solution (Fig. 4.7 - Fig. 4.10). The weak intensity broad band observed at 310-330 nm in each of the pMo compounds, **4.1-4.4** are typical of peroxo to metal (LMCT) transition of a diperoxomolybdate species.[35,36]

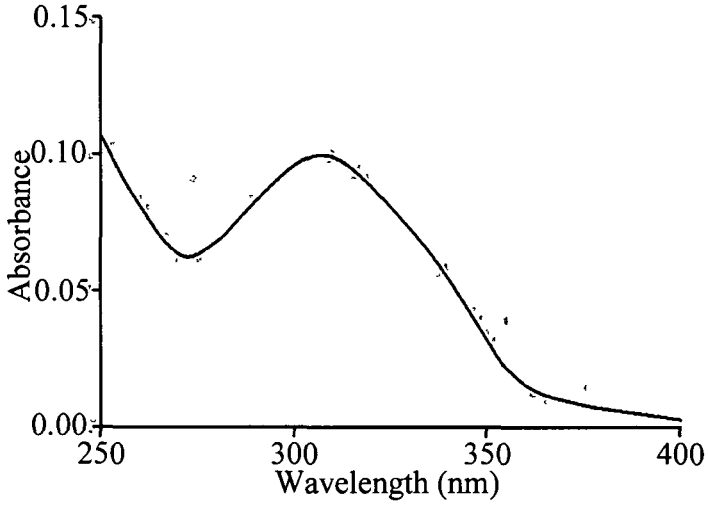

Fig. 4.7 UV spectrum of **PAMo**.

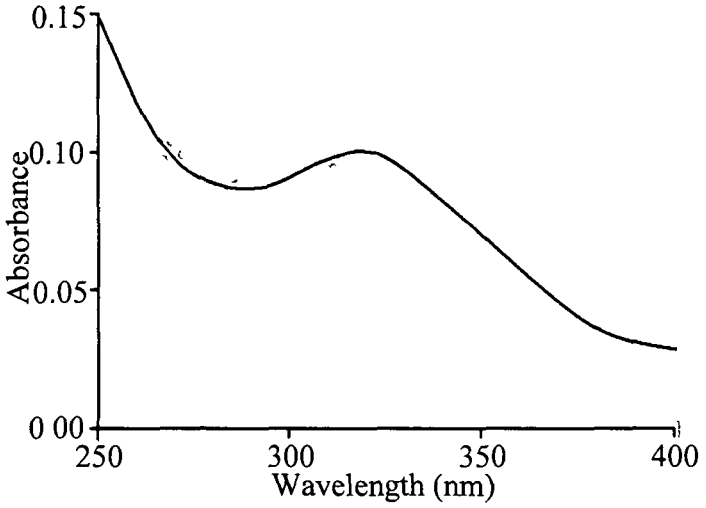

Fig. 4.8 UV spectrum of **PMAMo**.

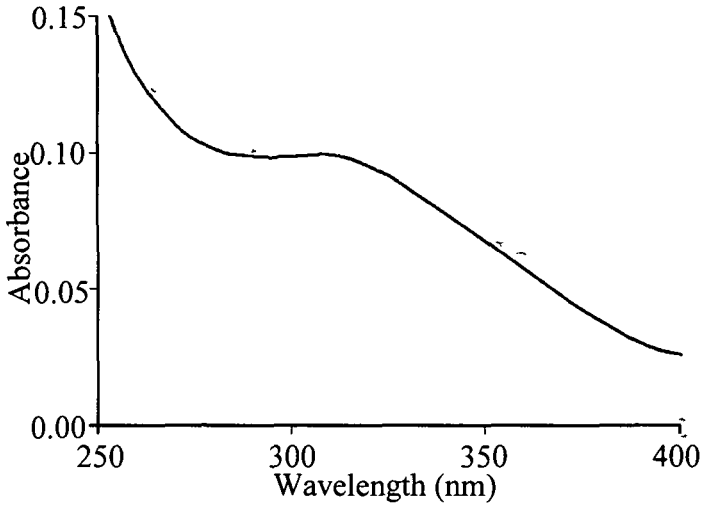

Fig. 4.9 UV spectrum of **PAmMo**.

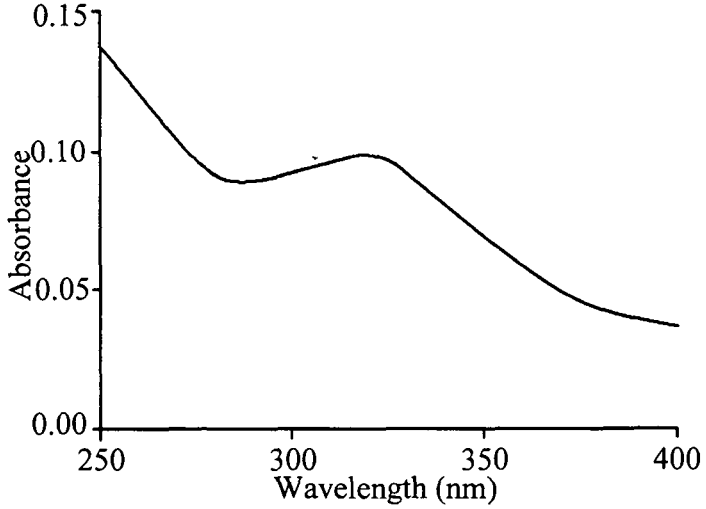

Fig. 4.10 UV spectrum of **PSMo**.

4.3.1.2.4 ^{13}C NMR studies

^{13}C NMR spectral studies provided evidence in support of the bonding pattern of the macromolecular ligands to the metal centres in the compounds and their stability in solution. ^{13}C NMR data pertaining to the polymer bound compounds, **4.1-4.4** as well as the pure polymers are shown in Table 4.3 and presented in Fig. 4.11 – Fig. 4.13. The major peaks were assigned on the basis of available literature data.[37-46]

The ^{13}C NMR spectra of pristine polymers PA and PMA display, in addition to the characteristic signals corresponding to chain carbon atoms, resonances due to the C (carboxylate) atoms centered at 184 and 187 ppm, respectively[43-46] (Fig. 4.11 and Fig. 4.12, Table 4.3). Two closely spaced peaks observed in this region are possibly due to the presence of carboxylate as well as –COOH groups of the polymers in solution. A striking common feature observed in the spectra of each of the polymeric compounds after metal anchoring via carboxylate group (**PAMo** and **PMAMo**), is the appearance of a new peak at considerably lower field of *ca.* 215 ppm attributable to carbon atom of complexed carboxylate group. The substantial downfield shift, $\Delta\delta$ ($\delta_{complex}$ - $\delta_{free\ carboxylate}$) $\approx$ 31 ppm in case of **PAMo**, and *ca.* 27 ppm in **PMAMo** relative to the free carboxylate peak of the pristine polymer suggests strong metal ligand interaction. It is notable that for the compound **PAMo**, with the bridging carboxylate co-ordination, the observed downfield shift of the peak due to complexed carboxylate is higher ($\Delta\delta \approx 31$ ppm) than the one with, monodentate carboxylate co-ordination ($\Delta\delta \approx 27$ ppm), **PMAMo**. Similar observation was made earlier in case of a polyacrylate bound vanadium containing analogue with bridging carboxylate group.[12,47]

The ^{13}C NMR spectrum of PAm in solution has been thoroughly investigated by others under varying pH conditions.[48] The spectrum of the pMo incorporated poly(acrylamide) compound, **PAmMo** provides evidence for the presence of complexed

as well as free amide groups by displaying a new peak at 200.13 ppm, in addition to the characteristic amide resonance at 179.48 ppm corresponding to the free amide groups as observed in the pure polymer (Table 4.3).

In **PSMo**, the peaks attributable to CH and CH_2 groups of the poly(vinyl sulfonate) remained practically unaffected by complexation as compared to the pure polymer. This is not unexpected keeping in view that Mo(VI) atoms are bound to the polymer through the sulfonate groups and hence are well separated from the chain carbon atoms of the polymer support.

Table 4.3 ^{13}C NMR chemical shift data for polymer-anchored peroxomplybdate compounds **4.1-4.4** and base polymers

Compound	Chemical Shift (ppm)				
	Carboxylate/amide carbon		CH_2	CH	CH_3
	Free	Complexed			
PA	184.50		36.10	45.52	
PAMo	184.51	215.51	36.04	45.81	
PMA	187.41		17.36		56.54
PMAMo	187.53	215.47	17.32		56.42
PAm	179.49		34.88	41.66	
PAmMo	179.48	200.13	34.91	41.66	
PS	--	--	30.97	54.51	
PSMo	--	--	30.98	54.53	

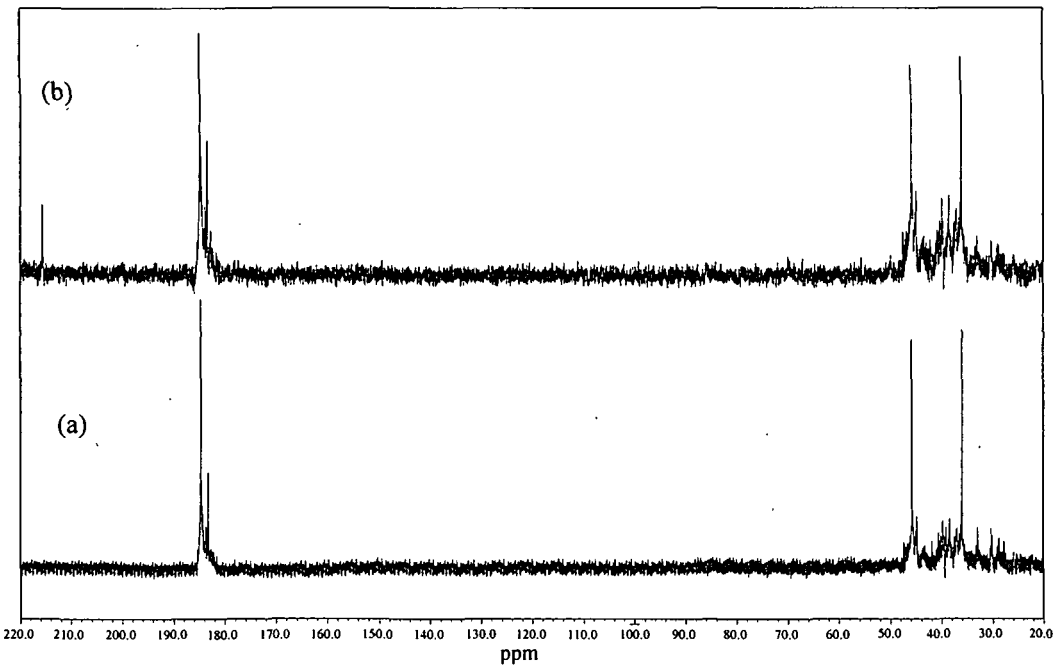

Fig. 4.11 ^{13}C NMR of (a) PA and (b) **PAMo**.

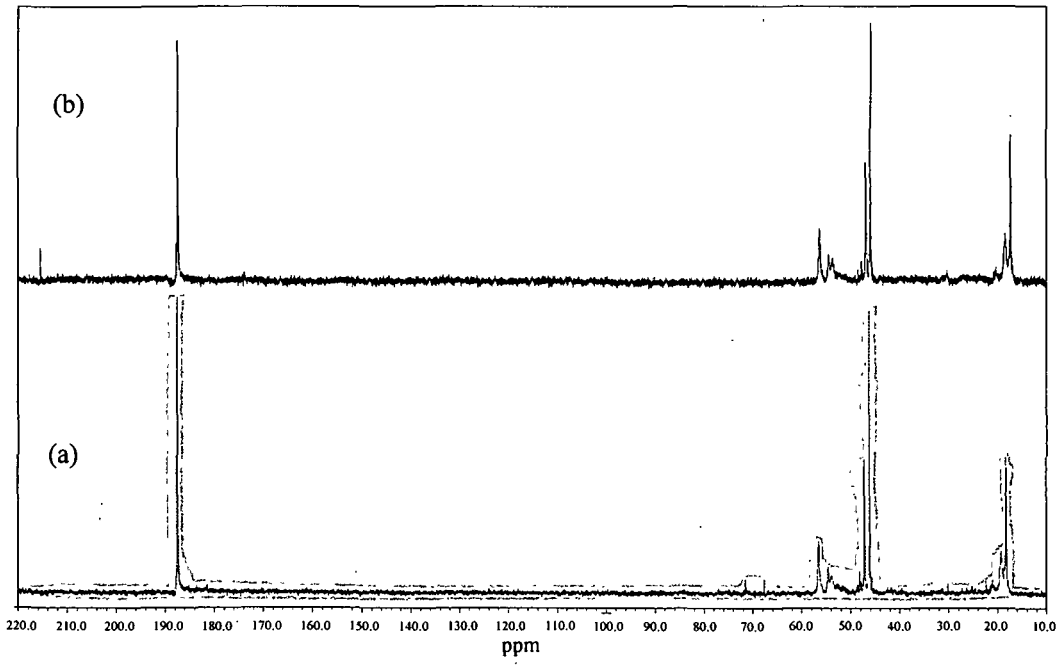

Fig. 4.12 ^{13}C NMR of (a) PMA and (b) **PMAMo**.

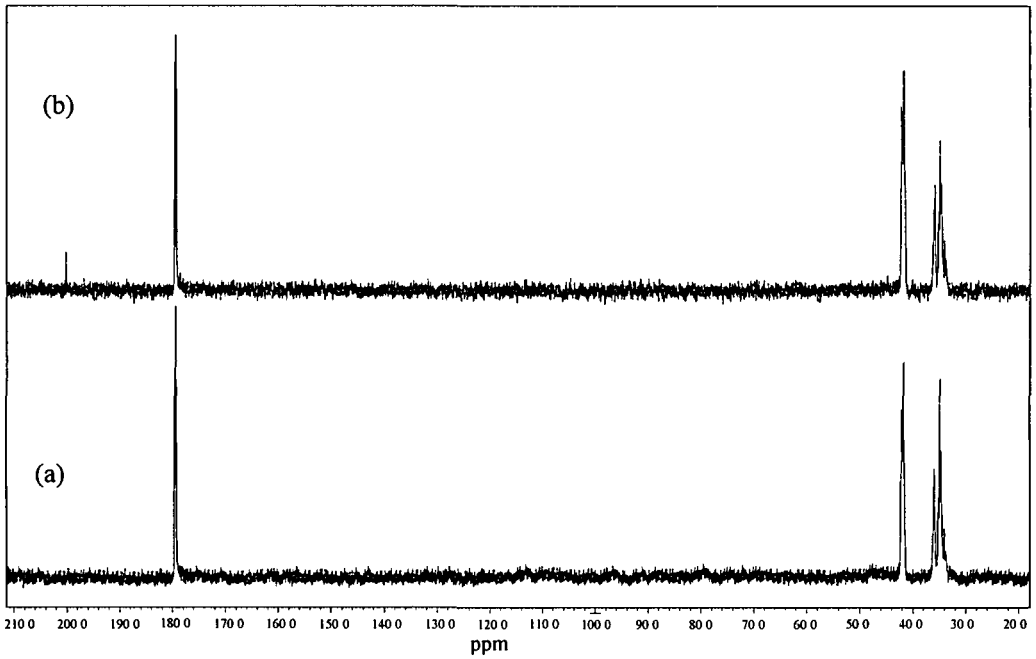

Fig. 4.13 ^{13}C NMR of (a) PAm and (b) **PAmMo**.

4.3.1.2.5 ^{95}Mo NMR studies

The ^{95}Mo NMR technique has been used as a sensitive and useful tool for study of the structure of molybdenum peroxo complexes in aqueous solution.[49] The ^{95}Mo NMR spectrum of **PAMo** (Fig. 4.14) displayed a single resonance at -225 ppm (relative to $[MoO_4]^{2-}$) indicating the presence of peroxomolybdenum species.[37,49] For the complexes, **PMAMo**, **PAmMo** and **PSMo** similarly only one peak was observed in each of the spectra at δ –217, –220 and –230 ppm, respectively (Fig. 4.14). The appearance of a lone characteristic peak in the ^{95}Mo NMR spectra of the compounds under investigation confirmed the presence of a single co-ordination environment for the peroxomolybdenum species present in solution.

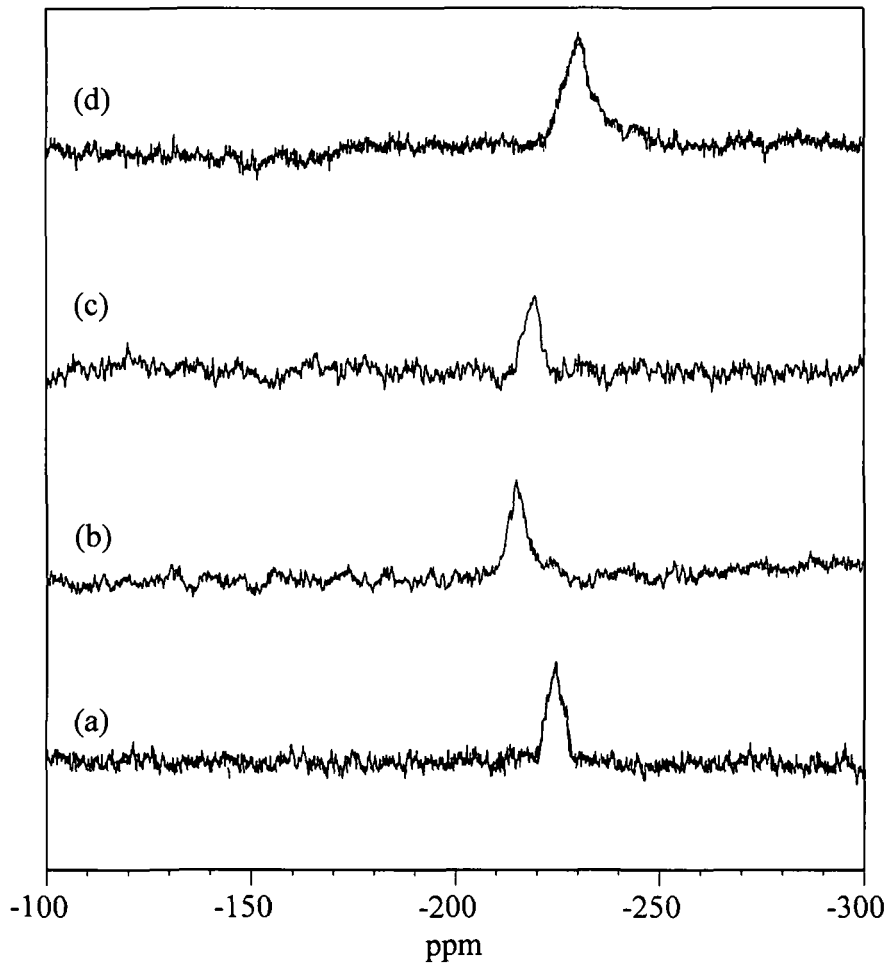

Fig. 4.14 ^{95}Mo NMR spectra of the pMo compounds (a) **PAMo**, (b) **PMAMo**, (c) **PAmMo** and (d) **PSMo**.

4.3.1.2.6 Thermal analysis

The thermogravimetric analysis data revealed that the polymer anchored peroxo compounds undergo multistage decomposition after initial dehydration (Table 4.4). It is notable that the complexes, unlike some monomeric peroxomolybdenum compounds,[38] do not explode on heating. The TG-DTG plots for the compounds **4.1-4.4** are presented in Fig. 4.15 – Fig. 4.18. The first stage of decomposition occurring in the temperature range of *ca.* 70-110 °C, for each of the pMo compounds correspond to liberation of molecules of water of crystallization from the complexes. The second decomposition

stage is in the temperature range of 108-250 °C attributable to the complete loss of co-ordinated peroxo groups from the complexes. Absence of peroxide in the decomposition product, isolated at this stage, was confirmed from the IR spectral analysis.

The loss of peroxide is seen to be followed by the decomposition stage associated with decarboxylation and breakdown of the polymer in the temperature ranges of 312-591 °C (**PAMo**) and 313-553 °C (**PMAMo**), respectively. Further evidence regarding decarboxylation of the polymers was obtained from the IR spectra recorded after heating the compounds separately up to the final decomposition temperature which showed complete disappearance of the strong peaks originating from ν_{asym}(COO) of the spectra of the original compounds. The compound **PAmMo** on heating up to a temperature of 750 °C, after the loss of peroxo groups, undergo final decomposition consisting of two weight loss processes in the temperature range of *ca.* 211-447 °C, due to breakdown of the polymer ligand (Fig. 4.17). By analogy with the thermal decomposition characteristics reported for some polyacrylamides,[50] we attribute the first stage of decomposition (211–333 °C) to the release of water, ammonia and small amount of carbon dioxide, from the pendant amide groups where the polymer chains remain intact.[50] In the second stage of decomposition (333–447 °C) main chain breakdown occurs accompanied by majority of weight loss (50.27%).

In case of **PSMo**, after the loss of peroxide (110-199 °C), a two stage decomposition occurred in the temperature range of 379–750 °C may be attributed to loss of sulfonate group and rupturing of the polymers. On comparing the available literature data for thermal degradation pattern of poly(vinyl sulfonate) sodium salt,[51] the first step of degradation in the temperature range of 379-443 °C corresponds to the loss of sulfonate groups and the second step of degradation occurred in the temperature range of 443-750 °C is

attributable to the rupturing of the polymer accompanied by evolution of ethylene, water and SO_2 and CS_2.

The sticky residue from the pMo compounds, after the complete loss of the components viz. lattice water, coordinated peroxide and polymeric functionals was found to be a hydrated oxomolybdenum species. This was evident from the IR spectra which displayed the characteristic ν(Mo=O) and ν(OH) absorptions and was devoid of bands attributable to peroxo and the polymeric ligands of the original compound. Thermogravimetric analysis data of the compounds thus provided further evidence in support of their composition and formula assigned.

Table 4.4 Thermogravimetric data of polymer-anchored peroxomolybdenum complexes **4.1-4.4**

Compound	Temperature range (^{O}C)	Observed weight loss (%)	Final residue (%)
PAMo	68-90	3.36	46.01
	90-227	9.34	
	312-591	41.29	
PMAMo	63-101	2.12	50.34
	107-188	4.10	
	313-553	43.44	
PAmMo	69-105	1.07	26.83
	145-184	3.45	
	211-333	18.38	
	333-447	50.27	
PSMo	74-101	1.04	49.29
	110-199	6.04	
	379-443	16.46	
	443-750	27.17	

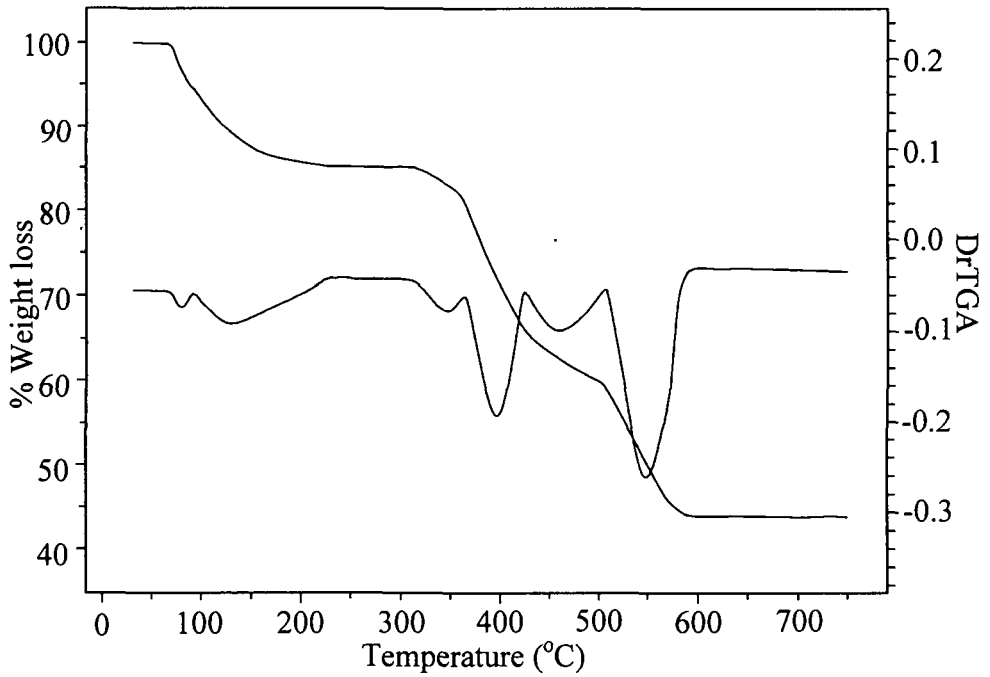

Fig. 4.15 TG-DTG thermogram of **PAMo**.

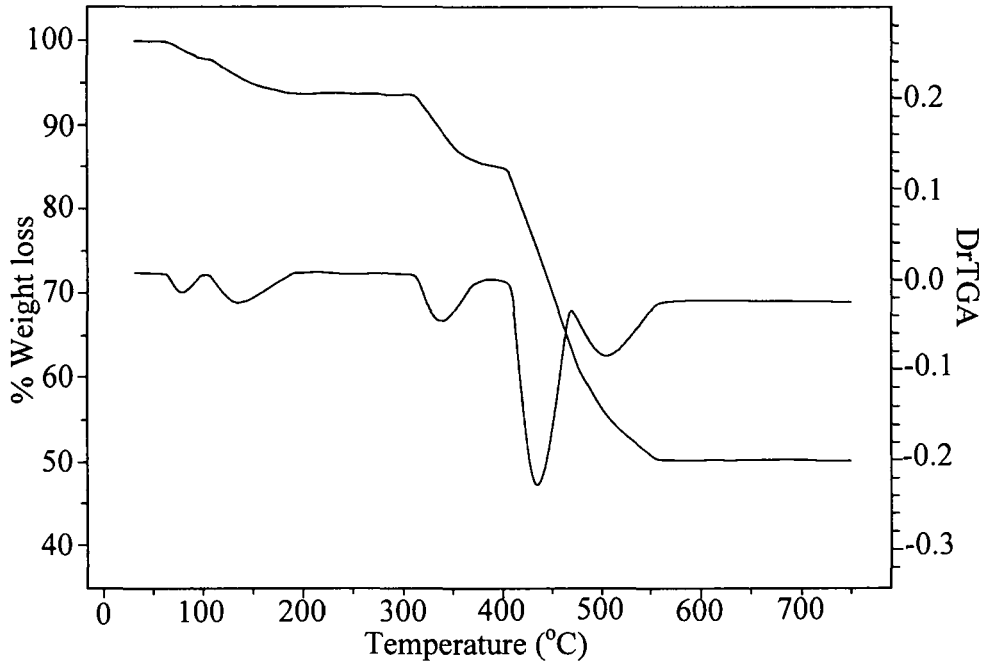

Fig. 4.16 TG-DTG thermogram of **PMAMo**.

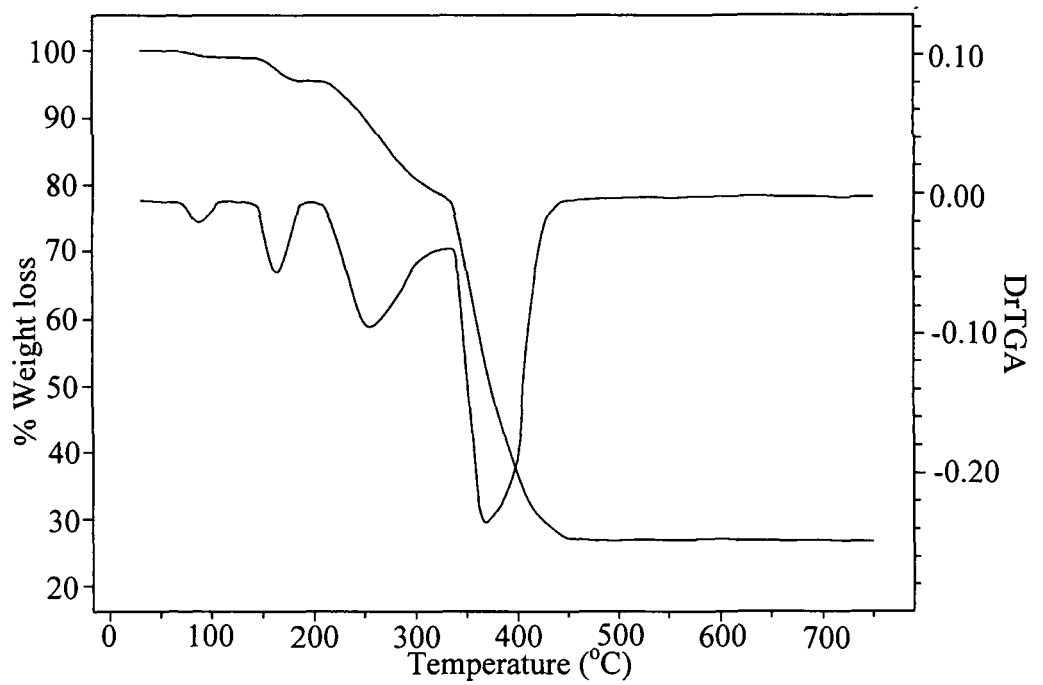

Fig. 4.17 TG-DTG thermogram of **PAmMo**.

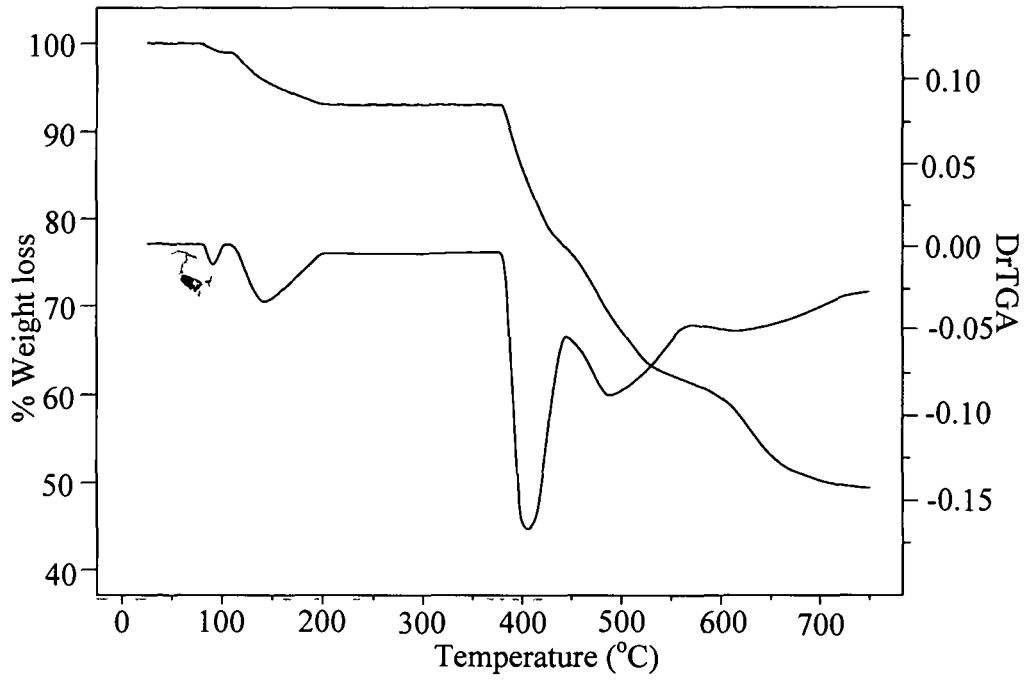

Fig. 4.18 TG-DTG thermogram of **PSMo**.

Based on the above data, a structure of the type shown in Fig. 4.19(a), has been proposed for the compound **PAMo** (**4.1**) that contains two Mo atoms co-ordinated to the polymer chain via a bidentate bridged carboxylate group, side-on bound peroxo ligands and terminal Mo=O. The results are also consistent with the proposed structures of the complexes **PMAMo** (**4.2**), **PAmMo** (**4.3**) and **PSMo** (**4.4**) presented in Fig. 4.19(b) – Fig. 4.19(d).

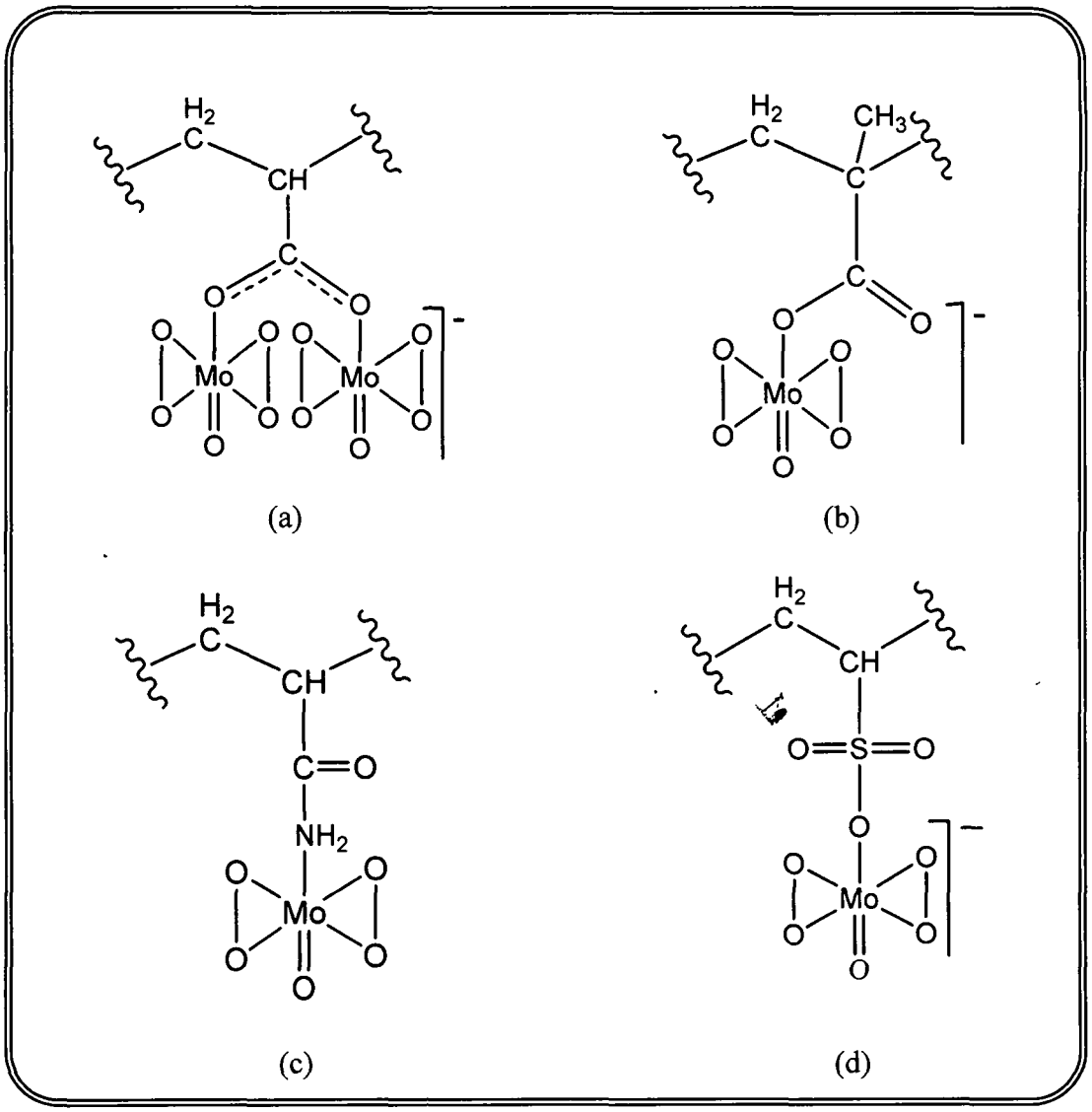

Fig. 4.19 Proposed structures of polymer anchored pMo compounds, (a) **PAMo**, (b) **PMAMo**, (c) **PAmMo** and (d) **PSMo**. "∿∿" represents polymer chain.

4.3.1.2.7 Density Functional studies

It is interesting to note that the carboxylate functional group present in the two closely related polymer matrices, poly(acrylate) and poly(methacrylate), binds the pMo moiety in two different coordination modes leading to formation of two structural forms viz. a dimeric tetraperoxomolybdate (**PAMo**) and monomeric diperoxomolybdate (**PMAMo**). Such variation in mode of coordination of carboxylate groups present in poly(acrylate) based polymers is not unprecedented.[23,24] Similar observation was made earlier with respect to peroxovanadium compounds bound to PA and PMA chains.[12] We proposed that the difference in coordination pattern in the compounds is likely to be a consequence of the presence of CH_3 groups attached to the polymer backbone in PMA which being relatively bulkier probably prevent formation of a dinuclear pV species through a carboxylate bridge.[12,47] Results of density functional studies performed on the pV complexes were in agreement with this hypothesis.[47] Therefore, in order to derive further information in support of the proposed structures of **PAMo** and **PMAMo**, reported herein, we have carried out theoretical studies on structural and electronic properties of pMo complexes using the DFT method.

A model complex has been generated based on available experimental data which correspond to a section of the pMo-anchored complex **PAMo**, containing three repeating units of the polymer with one dinuclear pMo moiety bound through a bridging carboxylate group (Fig. 4.20). DFT calculations were performed on this model complex using the BLYP functional and DNP basis set as implemented in the program DMol^3.[52] The complex was optimized at the BLYP/DNP level to conform to the stability of the

complex. The selected geometrical parameters obtained for the model complex are in good agreement with the available experimental data.[35,53] We have calculated the chemical softness value for the model complex from the HOMO and LUMO energies and found to be 27.780 au^{-1}. Calculations were performed similarly on a complex generated by replacing the α - hydrogen of the repeating unit with a methyl group so as to model the compound attached to a PMA chain. The chemical softness value calculated for this model compound was found to be 45.032 au^{-1}. The higher softness value obtained for the later model complex indicated lower stability of the complex compared to the α - hydrogen containing one. Similar experiments were performed on model complexes containing monomeric pMo moieties. It is notable that the presence of monomeric pMo units, bonded through a monodentate carboxylate, in the model complex corresponding to **PMAMo** (Fig. 4.21), afforded a stable structure (chemical softness value is 22.510 au^{-1}). In case of PA supported complex, model complexes with monomeric pMo units provided a structure of comparable stability with the one containing dimeric pMo unit. The results are consistent with the proposed structures for the complexes **PAMo** and **PMAMo** [Fig. 4.19(a,b)].

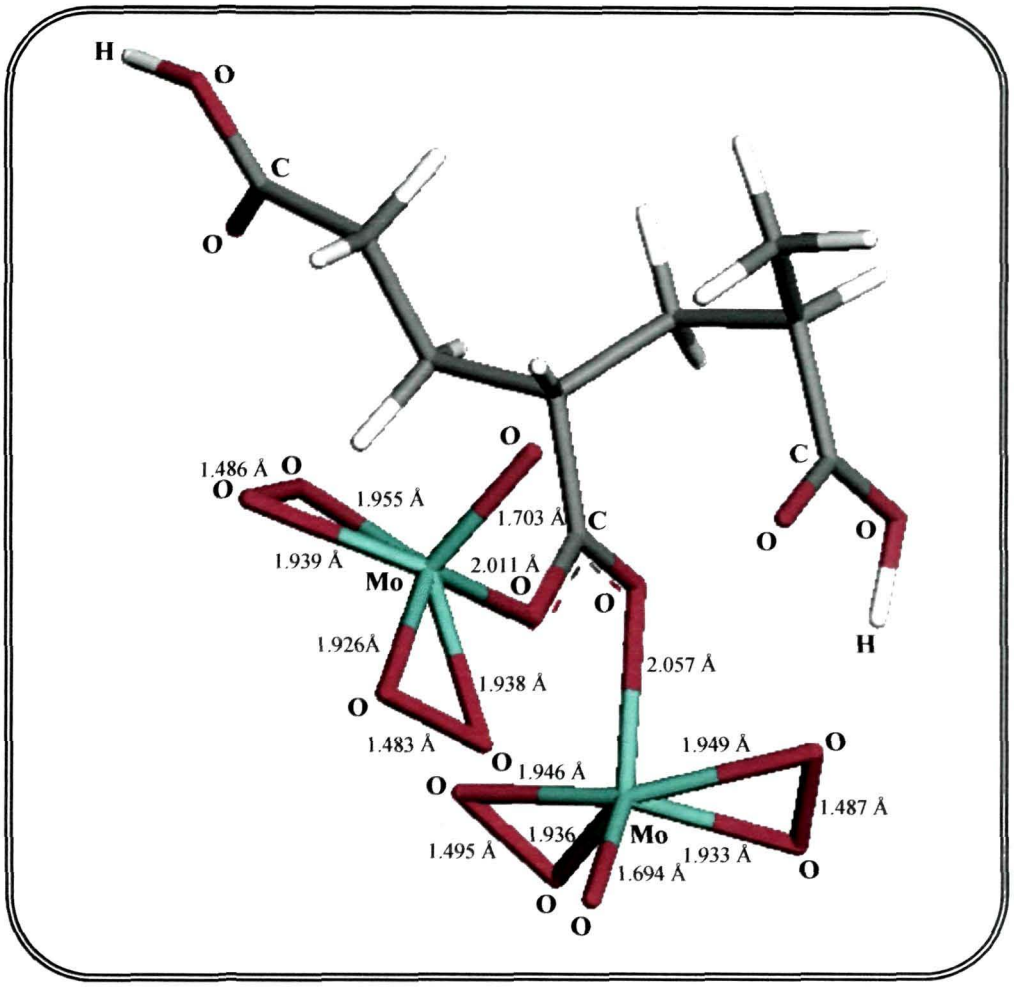

Fig. 4.20 Optimized structure of **PAMo** model complex obtained by using BLYP functional and DNP basis set. Selected geometric parameters are also shown in Figure.

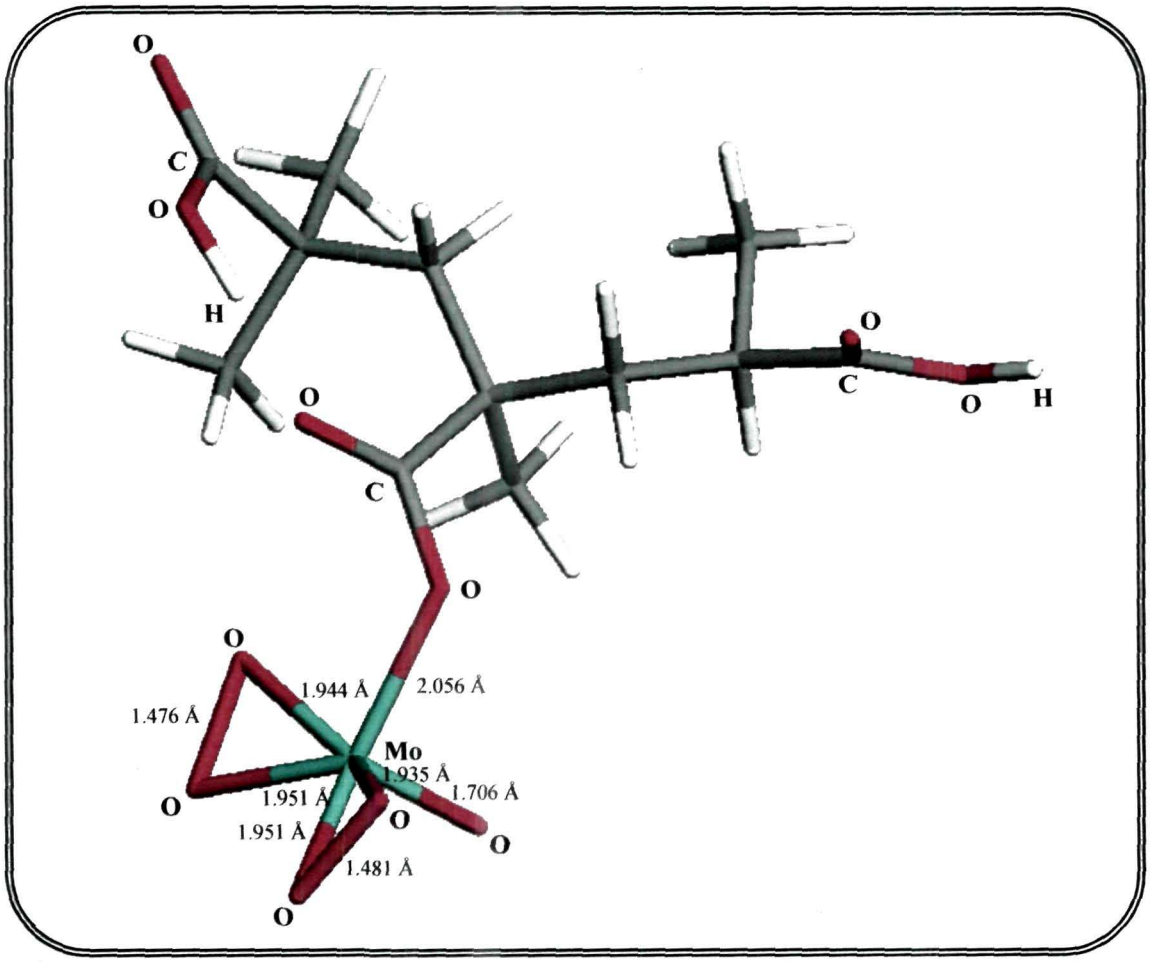

Fig. 4.21 Optimized structure of **PMAMo** model complex obtained by using BLYP functional and DNP basis set. Selected geometric parameters are also shown in Figure.

4.4 CONCLUSIONS

In this work we have introduced an efficient, straightforward synthetic pathway to obtain a set of novel and structurally defined macrocomplexes by anchoring diperoxomolybdenum(VI) species to water soluble polymer matrices. The compounds were characterized by spectroscopic and other conventional methods, including ^{95}Mo-NMR and SEM-EDX analysis. As far as we are aware these are the first known example of peroxomolybate complexes where water soluble polymers are used as supports. It is notable that in each of the water soluble macrocomplexes, **4.1-4.4**, the pMo species are present in its oxodiperoxo form, whereas in case of the insoluble complexes, **3.1-3.3** reported in chapter 3, pMo occurs as monoperoxomolybdate(VI) species.

The work presented in Chapter 7 demonstrates that the compounds **4.1-4.4** are stable in solution and possess novel biochemically relevant properties. The findings of our investigation on oxidant activity of the compounds are presented in Chapters 5 and 6.

REFERENCES

1. Bekturov, E.A. & Kudaibergenov, S.E. *Catalysis by Polymers*, WILEY-VCH Verlag GmbH & Co. KGaA, Weinheim, 2002.
2. Rivas, B.L., et al. *Prog. Polym. Sci.* **28**, 173--208, 2003.
3. Bergbreiter, D.E. *Chem. Rev.* **102**, 3345--3384, 2002.
4. Dickerson, T.J., et al. *Chem. Rev.* **102**, 3325--3344, 2002.
5. Skorobogaty, A., & Smith, T. D. *Coord. Chem. Rev.* **53**, 55--226, 1984.
6. Minko, T. *Drug Discov Today Technol.* **2**, 15--20, 2005.
7. Schechter, B., et al. *React. Polym.* **25**, 167--175, 1995.
8. Jagur-Grodzinski, J. *React. Funct. Polym.* **39**, 99--138, 1999.
9. Avichezer, D., et al. *React. Polym.* **36**, 59--69, 1998.
10. Ohya, Y., et al. *Macromol. Sci. Pure Appl. Chem. A* **33**, 1005--1016, 1996.
11. Das, S.P., et al. *RSC Adv.* **2**, 7248--7261, 2012.
12. Kalita, D., et al. *React. Funct. Polym.* **68**, 876--890, 2008.
13. Khanna, V., et al. *Pharmacol. Res.* **64**, 274--282, 2011.
14. Rivas, B.L., et al. *Prog. Polym. Sci.* **36**, 294--322, 2011.
15. Kadajji, V.G., & Betageri, G.V. *Polymers* **3**, 1972--2009, 2011.
16. Rivas, B.L., & Moreno-Villoslada, I. *J. Appl. Polym. Sci.* **70**, 219--225, 1998.
17. Rivas, B.L., & Moreno-Villoslada, I. *J. Phys. Chem. B* **102**, 6994--6999, 1998.
18. Rivas, B.L., & Moreno-Villoslada, I. *Chem Lett.* **29**, 166--167, 2000.
19. Nakamoto, K. *Infrared and Raman Spectra of Inorganic and Co-ordination Compounds, Part B*, 5th ed., Wiley and Sons, New York, 1997, 60.
20. Deacon, G.B., & Phillips, R.J. *Coord. Chem. Rev.* **33**, 227--250, 1980.
21. Djordjevic, C., et al. *Inorg. Chem.* **28**, 719--723, 1989.

22. Schwendt, P., et al. *Polyhedron* **17**, 2161--2166, 1998.

23. Li, H., & Tripp,C.P. *Langmuir* **20**, 10526--10533, 2004.

24. Jones, F., et al. *Langmuir* **14**, 6512--6517, 1998.

25. Feng, Y., et al. *Macromolecules* **29**, 3909--3917, 1996.

26. Penland, R.B., et al. *J. Am. Chem. Soc.* **79**, 1575--1578, 1957.

27. Bull, W.E., et al. *Inorg. Chem.* **2**, 303--306, 1963.

28. Murugan, R., et al. *J. Korean Phys. Soc.* **31**, 505--512, 1998.

29. Silverstein, R.M., Bassler, G.C. & Morrill, T.C. *Spectrometric identification of Organic Compounds*, 5th ed., John Wiley and Sons, 1991, 122.

30. Silverstein, R.M., Bassler, G.C. & Morrill, T.C. *Spectrometric identification of Organic Compounds*, 5th ed., John Wiley and Sons, 1991, 129.

31. Rivas, B.L., et al. *J. Appl. Polym. Sci.* **85**, 2546--2551, 2002.

32. Sun, Z.M., et al. *Inorg. Chem.* **43**, 336--341, 2004.

33. Campbell, N.J., et al. *Polyhedron* **8**, 1379--1386, 1989.

34. Lever, A.B.P., & Gray, H.B. *Acc. Chem. Res.* **11**,.348--355, 1978.

35. Djordjevic, C., et al. *Inorg. Chem.* **36**, 1798--1805, 1997.

36. Djordjevic, C., et al. *Mol. Cell. Biochem.* **153**, 25--29, 1995.

37. Dengel, A.C., et al. *J. Chem. Soc., Dalton Trans.* 991--995, 1987.

38. Bayot, D., et al. *Inorg. Chim. Acta* **357**, 809--816, 2004.

39. Justino, L.L.G., et al. *Inorg. Chim. Acta* **356**, 179--186, 2003.

40. Pettersson, L., et al. *Coord. Chem. Rev.* **237**, 77--87, 2003.

41. Conte, V., et al. *J. Mol. Catal.* **94**, 323--333, 1994.

42. Jacobson, S.E., et al. *Inorg. Chem.* **17**, 3055--3063, 1978.

43. Bodor, A., et al. *Coord. Chem. Rev.* **228**, 175--186, 2002.

44. Zhou, Z.H., et al. *Inorg. Chem.* **44**, 6912--6914, 2005.

45. Justino, L.L.G., et al. *Inorg. Chim. Acta* **311**, 119--125, 2000.

46. Matzapetakis, M., et al. *Inorg. Chem.* **38**, 618--619, 1999.

47. Boruah, J.J., et al. *Inorg. Chem.* **50**, 8046--8062, 2011.

48. Garces, F.O., et al. *Macromolecules* **27**, 272--278, 1994.

49. Nardello, V., et al. *Inorg. Chem.* **34**, 4950--4957, 1995.

50. Van Dyke, J.D., & Kasperski, K.L. *J. Polymer Sci.: Polymer Chem.* **31**, 1807--1823, 1993.

51. Jiang, D.D., et al. *Polym. Degrad. Stabil.* **63**, 423--434, 1999.

52. Delly, B. *J. Chem. Phys.* **92**, 508--514, 1990.

53. Sergienko, V.S. *Crystallogr. Rep.* **53**, 18--46, 2008.

CHAPTER 5

Polymer Supported Peroxomolybdenum(VI) Compounds: New Efficient Catalysts for Selective and Mild Oxidation of Sulfides with Hydrogen Peroxide

5.1 INTRODUCTION

With an ever increasing level of ecological consciousness in recent times, research efforts towards developing viable and environmentally benign synthetic methodologies for oxidation of organic sulfides to sulfoxides and sulfones appear to have intensified.[1-3] As has been mentioned in Chapter 1, importance of sulfoxides and sulfones as commodity chemicals, their utility as versatile building blocks for construction of chemically and biologically useful molecules including therapeutic agents, are well-documented in the literature.[4-12]The selective oxidation of sulfides is also gaining importance in the context of oxidative desulfurization, which is emerging as a sustainable route to obtain ultra low sulfur fuel.[13-18]

Although a multitude of oxidants are now available for sulfide oxidation, aqueous H_2O_2 remains the most attractive, clean and ideal green oxidant with effective oxygen content as high as 47%.[19-21] Furthermore, it is cost effective, readily available and ecologically acceptable as it produces only water as the by-product.[22-26] Hydrogen peroxide induced oxidations are however rather slow due to its being a relatively weaker oxidant and commonly needs to be activated by an appropriate catalyst.[27-29] As a result, a vast number of useful transition metal based catalysts have emerged over the years for oxidation of sulfides by H_2O_2[8,20,22,27,29-47] including molybdenum containing ones such as, MoO_3,[48] dioxo-molybdenum(VI) complex,[49] tetra-(tetraalkylammonium)octamolybdate,[50]

immobilized molybdenum heteropolyacid[51] and MoO_2Cl_2.[52] However, only a few of these are able to stop at the sulfoxide stage averting over oxidation to sulfone. Apart from this, majority of the available protocols still suffer from one or more limitations viz., difficulty in recovery of the catalyst, high cost, and requirement of a promoter or a co-catalyst, high temperature, long reaction time, chlorohydrocarbon solvents and excessive H_2O_2 and low TON. Selective oxidation of DBT, a refractory sulfide, still remains a difficult task.[22,24,53] These disadvantages are becoming more conspicuous in view of the growing environmental concerns in recent times.[24,54,55] Therefore the quest for newer alternative catalysts and methodologies that adhere to green chemistry specifications continues.

Heterogenization of homogeneous catalysts by immobilization of active soluble catalysts on insoluble polymeric resins provides an elegant solution to the separation and recovery of catalysts.[56-58] Furthermore, enhanced catalyst stability within the polymer support, increased selectivity, simplicity in handling toxic and odorous materials and easy work up of reaction mixture are other important benefits gained as a consequence of immobilization.[56-58]

In continuation of our work on peroxomolybdates as described in the preceding Chapters, one of the objectives of the present study was to verify the possibility of generating newer heterogeneous catalysts and procedures for oxidation of sulfides based on pMo containing macrocomplexes **3.1-3.3**, under mild conditions. Although peroxo compounds of molybdenum have been finding extensive applications as catalysts or oxidants in a variety of organic oxidations[31,32,36,59-70] including several industrial processes, such as epoxidation of olefins,[31,64,71,72] olefin metathesis[65,66] and isomerization of allylic alcohol,[67-69] however, there is still a dearth of information on use of pMo compounds as catalyst in sulfide oxidation. Moreover, over the past decades, numerous transition metal catalysts supported on **MR** were prepared and their activity in various

catalytic organic transformations have been reported which has been reviewed recently.[56-58,73,74] It is therefore intriguing to note that only few groups have so far investigated the potential of polymer-immobilized peroxometallates as catalysts in organic oxidations.[61,75-78]

Apart from insoluble polymeric resins used as support, application of water-soluble polymeric materials to attach catalytically active transition metal complexes, although a relatively newer strategy, has received considerable contemporary interest.[79,80] This is mainly because the soluble supports have ensured phase homogeneity to catalysts and reactants, which is a significant advantage over insoluble supports.[81,82] The recycling of such catalysts can be achieved by reducing the solubility, with poor solvent or by temperature variation.[81,82] Having gained an access to the WSP bound complexes **4.1-4.4** we considered it imperative to explore the activity of this set of compounds as homogeneous catalysts or reagents in mediating oxidation of sulfides.

Attention may be drawn to the fact that besides the difference in the solubility profile of the two sets of compounds, **3.1-3.3** and **4.1-4.4**, the compounds also differ with respect to the type of the anchored pMo species. The pMo moieties are present in the insoluble polymers in its monoperoxo form whereas in the soluble macrocomplexes, **4.1-4.4** peroxomolybdates bind to the polymer matrix as oxo-diperoxo units. Previous reports including work carried out in our laboratory have shown that the monoperoxo and diperoxo compounds of tungsten[83-86] and molybdenum[31,32,36,62,87,88] differ considerably in their oxidant activity both in terms of efficiency as well as mechanism of action. The two classes of compounds synthesized in the present study thus enabled us to draw comparison on their catalytic efficiency for the chosen reactions.

The present chapter comprises of two sections. In **Section A**, we report our findings on the activity of the pMo compounds immobilized on functionalized **MR** as well as PAN, as efficient heterogeneous catalysts in selective oxidation of a variety of

thioethers and dibenzothiophene with H_2O_2 as terminal oxidant. The results incorporated in **Section B** demonstrate that the water-soluble complexes, **4.1-4.4** are capable of serving as homogeneous catalysts in sulfide oxidation. Also, these compounds are active as stoichiometric oxidants of sulfides. Conclusions drawn from our investigation on the two families of the compounds are enumerated at the end of **Section B** of the Chapter. The results presented herein illustrate the features which make the developed procedures synthetically valuable.

5.2 Section A:

Immobilized Monoperoxomolybdenum (VI) Compounds as Heterogeneous Catalysts in Selective Oxidation of Sulfides

5.2.1 EXPERIMENTAL SECTION

5.2.1.1 General procedure for catalytic oxidation of sulfides to sulfoxides

In a representative procedure, organic substrate (5 mmol) was added to a mixture of catalysts (containing 0.005 mmol of Mo) [**MRVMo** (10.86 mg) or **MRAMo** (13.15 mg) or **PANMo** (6.49 mg)] and 30% H_2O_2 (1.13 mL, 10 mmol) in methanol (5 mL), maintaining molar ratio of Mo:substrate at 1:1000 and substrate:H_2O_2 at 1:2, in a 50 mL two-necked round-bottomed flask. The reaction was conducted at room temperature (RT) under continuous stirring. The progress of the reaction was monitored by thin layer chromatography (TLC) and GC. After completion of the reaction, the catalyst was separated by filtration and washed with acetone. The product as well as unreacted organic substrates were extracted with diethyl ether from the filtrate and dried over anhydrous Na_2SO_4 and distilled under reduced pressure to remove excess diethyl ether. The corresponding sulfoxide obtained was purified by column chromatography on silica gel using ethyl acetate and n-hexane (1:9).

The products obtained were characterized by IR, ^1H NMR, ^{13}C NMR spectroscopy and in case of solid sulfoxide products, in addition to the above spectral analysis, we have also carried out melting point determination (see **Appendix 5A**).

5.2.1.2 General procedure for oxidation of sulfides to sulfones

To a stirred solution of sulfide (5 mmol) in acetonitrile (5 mL), 50% H_2O_2 (1.36 mL, 20 mmol) and the catalysts (containing 0.005 mmol of Mo) [**MRVMo** (10.86 mg) or **MRAMo** (13.15 mg) or **PANMo** (6.49 mg)] were added successively maintaining molar ratio of Mo:substrate at 1:1000 and substrate:H_2O_2 at 1:4. The resulting reaction mixture was stirred at room temperature. After completion of the reaction, the sulfone obtained

was isolated, purified and characterized by methods similar to those mentioned under procedure for oxidation of sulfide to sulfoxide (Section 5.2.1.1).

5.2.1.3 Regeneration of the catalyst

The reusability of the catalysts for subsequent catalytic cycles was examined by using methyl phenyl sulfide (MPS) as substrate. In the sulfoxidation reaction, mentioned under section 5.2.1.1, after completion of the reaction, the solid catalyst was separated from the reaction mixture by filtration, washed with acetone and dried *in vacuo* over concentrated sulfuric acid. The solid dried catalyst was then added to a fresh reaction mixture of 30% H_2O_2 (1.13 mL, 10 mmol), substrate (5 mmol) and methanol (5 mL). The progress of the reaction was monitored by thin layer chromatography (TLC) and GC.

In case of the reaction of oxidation of MPS to sulfone, the catalyst was similarly recovered after completion of the reaction by separating it from the reaction mixture and charging it with fresh lot of 50% H_2O_2 (1.36 mL, 20 mmol), MPS (5 mmol) and acetonitrile (5 mL), as mentioned under section 5.2.1.2.

In an alternative procedure, regeneration of the spent catalysts could also be achieved simply by charging the spent reaction mixture, remaining in the reaction vessel after separating the organic reaction product, with fresh H_2O_2 and substrate and then repeating the experiment. Each of the procedures was repeated for six reaction cycles.

5.2.2 RESULTS AND DISCUSSION

A variety of aromatic and aliphatic sulfides as well as DBT have been selectively oxidized to sulfoxide or sulfone by using H_2O_2 as terminal oxidant in presence of catalytic amounts of the compounds **MRVMo (3.1)** or **MRAMo (3.2)** or **PANMo (3.3)** in

excellent yields. Each of the polymer bound pMo compounds, **3.1-3.3** are insoluble in the reaction mixture and heterogeneously catalyzed the oxidation reactions. These monoperoxomolybdenum compounds are however, inactive in the oxidation of sulfide on their own, in absence of hydrogen peroxide.

5.2.2.1 Oxidation of sulfides to sulfoxides – Optimization of reaction condition

The effect of various reaction parameters such as type of solvent, reaction temperature, substrate:H_2O_2 stoichiometry, catalyst concentration, etc., were evaluated by using MPS as model substrate and **MRAMo** as the catalyst, in order to optimize the reaction conditions as shown in Table 5.1.

5.2.2.1.1 The influence of oxidant and catalyst amount on the catalytic efficiency

The reactions were performed at ambient temperature under magnetic stirring. From the results presented in Table 5.1, it is evident that the reaction conducted at the molar ratio of MPS:H_2O_2 at 1:1 and Mo:MPS at 1:1000 in methanol proceed smoothly to selectively yield sulfoxide as the exclusive product. However, the reaction remained incomplete with maximum of 74% conversion (Table 5.1, entry 1). We could achieve complete conversion of MPS to sulfoxide as exclusive product, with nearly a 12-fold increase in TOF by increasing the amount of 30% H_2O_2 to 2 equivalents with respect to substrate, under otherwise identical reaction conditions (Table 5.1, entry 2). Significantly, even after a prolonged reaction time, no overoxidation to sulfone was noted (Table 5.1, entry 1).

Table 5.1 Optimization of reaction conditions for **MRAMo** catalyzed selective oxidation of methyl phenyl sulfide (MPS) by 30% H_2O_2[a]

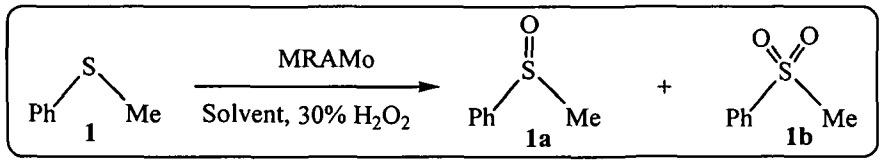

Entry	Molar ratio Mo:MPS	H_2O_2 (equiv.)	Solvent	Temperature	Time (min)	Isolated Yield (%)	**1a : 1b**	TOF (h^{-1})
1	1:1000	1	MeOH	RT	360	74	100 : 0	123
2	**1:1000**	**2**	**MeOH**	**RT**	**40**	**98**	**100 : 0**	**1470**
3	1:500	2	MeOH	RT	30	97	100 : 0	970
4	1:100	2	MeOH	RT	15	98	100 : 0	292
5	1:1000	2	EtOH	RT	40	95	100 : 0	1425
6	1:1000	2	$CHCl_3$	RT	120	11	91 : 9	55
7	1:1000	2	CH_2Cl_2	RT	120	13	88 :12	65
8	1:1000	2	MeCN	RT	120	94	59 : 41	470
9	1:1000	2	MeOH	50 °C	25	97	100 : 0	2328
10	1:1000	2	MeOH	65 °C	15	99	100 : 0	3960
11[b]	1:1000	2	MeOH	RT	180	99	76 : 24	330
12[c]	---	2	MeOH	RT	360	7	86 : 14	---

[a]All reactions were carried out with 5 mmol of substrate in 5 mL of solvent.

The amount of catalyst had a substantial influence on the rate of reaction as evident from the data presented (Table 5.1, entries 3 and 4). Increasing the catalyst amount enhanced the reaction rate and reduced the reaction time from 40 min (with 0.1 mol% catalyst) to 15 min (with 1.0 mol% catalyst) without compromising the selectivity. However, the TOF was found to decrease abruptly from 1470 h^{-1} to 292 h^{-1}. Thus in order to attain high conversion without affecting the selectivity, oxidant:substrate molar ratio of 2:1 and catalyst:substrate ratio of 1:1000 have been found to be optimal. Subsequent reactions were therefore carried out under these concentration ratios.

That the catalyst plays a vital role in leading to the formation of the desired product was confirmed by conducting a blank experiment without the catalyst. In absence of the catalyst the reaction was sluggish and non-selective affording a mixture of **1a** and **1b** in very low yield (Table 5.1, entry 12). We have further compared the heterogeneous phase reaction with the homogeneous one by conducting the oxidation reaction in presence of soluble unsupported peroxomolybdenum species in lieu of the heterogeneous catalyst **MRAMo** or **MRVMo**, under otherwise identical reaction conditions. Since the reaction of molybdate is known to form pMo species in presence of excess H_2O_2, the neat pMo species were generated *in situ* by adding Na_2MoO_4 to the standard reaction mixture containing H_2O_2.[59] As seen from the data in Table 5.1, entry 11, facile oxidation of MPS could also be achieved in presence of neat pMo catalyst under optimized reaction conditions. However, the reaction was non-selective leading to a mixture of sulfoxide and sulfone in the ratio of 76:24. Moreover, the TOF of the conversion was nearly 5-fold lower compared to that obtained in presence of the heterogeneous catalysts.

5.2.2.1.2 Effect of solvent

Our emphasis in the present work has been to conduct the oxidation reactions using environmentally safe organic solvents including water and to preclude the use of chlorinated solvents. Nevertheless, apart from water, methanol, ethanol, acetonitrile, we have screened the sulfoxidation reaction in chloroform and dichloromethane as well. The nature of solvent was observed to have a profound effect on the activity of the catalyst and the product selectivity of the reactions. From our results it is apparent that best performance in terms of TOF and product selectivity of the reaction was achieved by using methanol or ethanol as solvents (Table 5.1, entries 2 and 5), which is likely to be the consequence of complete miscibility of the organic substrate and H_2O_2 in these solvents, in addition to the conducive effect of the protic solvents. Moreover, according to available literature, the formation of sulfoxide with high chemoselectivity are favoured in presence of solvents of high hydrogen bonding ability.[36,89,90] However, very little conversion was noted when water was used as solvent (< 2%). This may be expected keeping in view the insolubility of the catalyst as well as the substrate in water. The reactions in solvents such as chloroform or dichloromethane were found to be very slow (Table 5.1, entries 6 and 7), presumably due to similar reasons. In acetonitrile, although the reaction proceeded rapidly, simultaneous formation of sulfone was also observed along with sulfoxide yielding a mixture of **1a** and **1b** (Table 5.1, entry 8).

5.2.2.1.3 Effect of reaction temperature

In order to assess the effect of temperature on the reaction rate, we have carried out the reactions at three different temperatures viz., room temperature (RT), 50 and 65 ^{o}C under otherwise analogous conditions (Table 5.1, entries 2, 9 and 10). A remarkable

increase in rate was observed accompanied by 2 to 3-fold enhancement in TOF on increasing temperature from RT to 65 °C without any over oxidation to sulfone.

5.2.2.1.4 Selective sulfoxidation catalyzed by MRVMo, MRAMo or PANMo

In an effort to establish the scope of the protocol, we have assessed the catalytic activity of **MRVMo**, **MRAMo** and **PANMo** under the optimized conditions (see Scheme 5.1), using a series of various types of aliphatic and aromatic sulfides as well as DBT and findings are summarized in Table 5.2. Each of the substrate underwent complete conversion to the corresponding sulfoxide exhibiting excellent TOFs. Most importantly, the reaction was observed to stop completely at sulfoxide stage even on increasing the reaction time. On this aspect, the present catalyst displayed superior activity compared to some heterogeneous pW catalysts reported previously by us[84] and others,[19,20,23,24,28,32,33,38,91] where the oxidation was required to be terminated at < 75% conversion to sulfoxide in order to avert overoxidation to sulfone.[84]

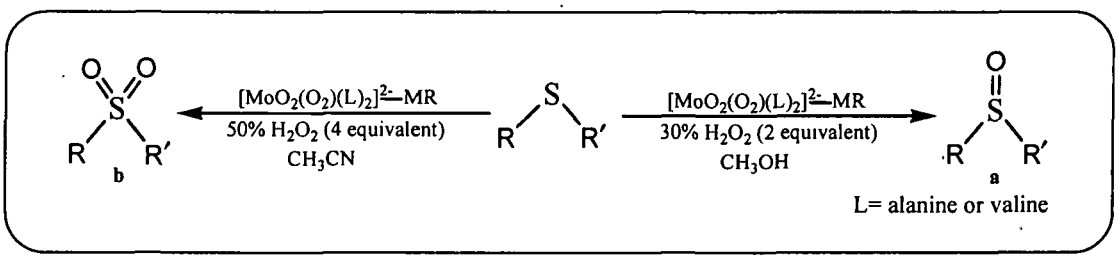

Scheme 5.1

Although each of the title compounds was found to be effective catalyst in the oxidation reactions, the amino acid functionalized Merrifield resin supported catalysts, **MRVMo** and **MRAMo** displayed slightly superior activity over poly(acrylonitrile)

supported catalyst, **PANMo** in terms of TOF (Table 5.2). The rates of oxidation however, varied depending upon the nature of the substrate which is not unusual, as it has been known that rate of oxidation of sulfides by H_2O_2 increases with the increased nucleophilicity of the sulfide.[20,24] Aliphatic sulfides are oxidized at faster rate than the aromatic sulfides and allylic and vinylic sulfides (Table 5.2, entries 8 and 9) were less readily oxidized by H_2O_2 than the dialkyl sulfides. Conjugation of lone pair of electrons over sulfur atom obviously influences the rates of the reaction for these substrates. Most importantly, a much less nucleophillic sulfide, such as DBT (Table 5.2, entry 12) could also be effectively oxidized to sulfoxide in presence of the newly developed catalysts. In the present work although the reaction was rather sluggish at room temperature, reasonably good TOF was attained by raising the reaction temperature to 65 ^{o}C and using a higher amount of catalyst (Table 5.2, entry 12). Another important feature of synthetic value of the protocol could be seen in the chemoselective oxidation of substituted sulfides with co-existing functional groups susceptible to oxidation. Allylic and vinylic sulfides afforded exclusively sulfoxide without epoxidation of the double bonds (Table 5.2, entries 8 and 9) and the benzylic and alcoholic sulfides could be oxidized to the corresponding sulfoxides without affecting the benzylic C–H bond and –OH group (Table 5.2, entries 7 and 11). The suitability of the protocol for relatively larger scale synthetic applications was also ascertained by carrying out the oxidation at a ten-fold scale under standard condition (Table 5.2, entry 1[f]).

Table 5.2 Selective oxidation of sulfides to sulfoxides with 30% H_2O_2 catalyzed by **PANMo, MRVMo** and **MRAMo**[a]

Entry	Substrate	Product	MRAMo			MRVMo			PANMo		
			Time (min)	Isolated Yield (%)	TOF[b] (h^{-1})	Time (min)	Isolated Yield (%)	TOF[b] (h^{-1})	Time (min)	Isolated Yield (%)	TOF[b] (h^{-1})
1	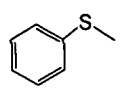	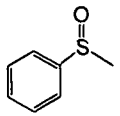	40	98	1470	45	97	1293	60	98	980
			15[c]	99	3960	17[c]	99	3494	20[c]	97	2910
			40	96[d]	1440	45	95[d]	1266	60	97[d]	970
			15[c]	97[d]	3880	17[c]	97[d]	3423	20[c]	96[d]	2880
			40	98[e]	1470	45	97[e]	1293	60	96[e]	960
			15[c]	97[e]	3920	17[c]	98[e]	3458	20[c]	98[e]	2940
2	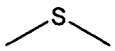	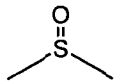	35	98	1680	40	97	1455	55	98	1069
3	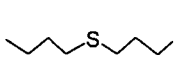	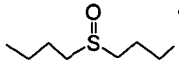	40	98	1485	45	96	1280	60	97	970
			15[c]	97	3880	17[c]	99	3494	20[c]	98	2940
4	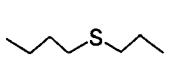	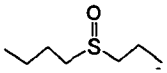	40	96	1455	45	97	1293	60	95	950
			15[c]	99	3960	15[c]	98	3920	20[c]	97	2910
5	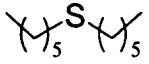	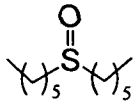	40	97	1455	45	98	1306	60	96	960
			15[c]	98	3920	17[c]	97	3423	20[c]	98	2940
6	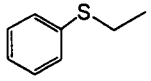	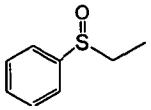	50	98	1176	55	99	1080	65	97	895
			20[c]	96	2880	20[c]	98	2940	22[c]	98	2672

Continued...

Entry	Substrate	Product	MRAMo			MRVMo			PANMo		
			Time (min)	Isolated Yield (%)	TOF[b] (h^{-1})	Time (min)	Isolated Yield (%)	TOF[b] (h^{-1})	Time (min)	Isolated Yield (%)	TOF[b] (h^{-1})
7	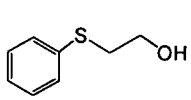	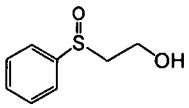	100	96	576	110	96	523	150	97	388
			30[c]	95	1900	40[c]	98	1470	60[c]	95	950
8	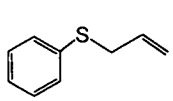	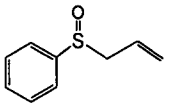	80	98	735	90	97	646	120	96	480
			20[c]	96	2880	25[c]	95	2280	40[c]	98	1470
9	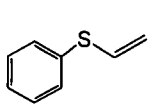	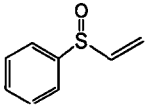	210	97	277	240	96	240	270	98	217
			80[c]	95	712	85[c]	98	691	90[c]	97	646
10	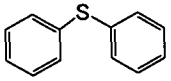	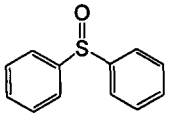	240	97	242	250	98	235	290	97	200
			90[c]	96	640	95[c]	97	612	130[c]	96	443
11	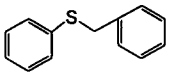	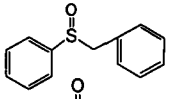	90	98	653	110	96	523	140	98	420
			30[c]	95	1900	35[c]	98	1680	50[c]	99	1188
12[f]	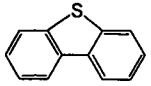	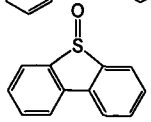	10 h[c]	96	9.6	10 h[c]	94	9.4	10 h[c]	87	8.7

[a]All reactions were carried out with 5 mmol substrate, 10 mmol 30% H_2O_2 and catalyst (0.005 mmol of Mo) in 5 mL methanol at RT, unless otherwise indicated.
[b]TOF (Turnover frequency) = mmol of product per mmol of catalyst per hour.
[c]Reaction at 65 °C in refluxing methanol.
[d]Yield of 6th reaction cycle.
[e]Yield at 5 g scale.
[f]Substrate (5 mmol), catalyst (0.05 mmol of Mo), methanol (5 mL).

5.2.2.2 Oxidation of sulfides to sulfones

Having achieved the excellent results with respect to chemoselective oxidation of sulfides to sulfoxides, we have endeavored to attain selective oxidation of sulfides to sulfones by using the same catalysts. Taking cues from our earlier experience with sulfide oxidation by a polymer supported pW catalyst,[84] as well as observation in the present study that showed the concomitant formation of sulfone along with sulfoxide in acetonitrile (Table 5.1, entry 8), we have carried out the reactions in acetonitrile. The reaction conditions were optimized by using MPS and **MRAMo** as catalyst (Table 5.3). We have ultimately achieved the selective oxidation of MPS to pure sulfone by using 4 equivalents of 50% H_2O_2, under the conditions mentioned in Table 5.3, entry 4. The desired selectivity with respect to sulfone could not be obtained even by using 5-fold excess of 30% H_2O_2 over the substrate. The results presented in Table 5.4 show that the methodology is also highly effective for a variety of structurally diverse sulfides. It is noteworthy that on conducting the reaction under reflux at 78 °C, there was a considerable enhancement in the rate of the reaction with a 3-fold increase in TOF. The excellent chemoselectivity of the catalysts, **3.1-3.3** toward sulfide group was evident in case of selective oxidation to sulfone as well, despite the reasonable excess of 50% H_2O_2 used in these reactions. The reaction could also be conveniently conducted on a larger scale as shown in the Table 5.4, entry 1[f].

Table 5.3 Optimization of reaction conditions for **MRAMo** catalyzed selective oxidation of methyl phenyl sulfide (MPS) to sulfone by 50% H_2O_2[a]

Entry	Molar ratio Mo:MPS	H_2O_2 (equiv.)	Solvent	Temperature	Time (min)	Isolated Yield (%)	**1a : 1b**	TOF (h^{-1})
1	1:1000	1	MeCN	RT	300	73	55 : 46	146
2	1:1000	2	MeCN	RT	210	99	29 : 71	282
3	1:1000	3	MeCN	RT	150	98	11 : 89	392
4	**1:1000**	**4**	**MeCN**	**RT**	**120**	**99**	**0 : 100**	**495**
5	1:500	4	MeCN	RT	80	97	0 : 100	363
6	1:100	4	MeCN	RT	50	98	0 : 100	117
7	1:1000	4	MeCN	78 °C	40	98	0 : 100	1476

[a]All reactions were carried out with 5 mmol of substrate in 5 mL of solvent.

Table 5.4 Selective oxidation of sulfides to sulfones with 50% H_2O_2 catalyzed by **PANMo, MRVMo** and **MRAMo**[a]

Entry	Substrate	Product	MRAMo			MRVMo			PANMo		
			Time (min)	Isolated Yield (%)	TOF[b] (h^{-1})	Time (min)	Isolated Yield (%)	TOF[b] (h^{-1})	Time (min)	Isolated Yield (%)	TOF[b] (h^{-1})
1	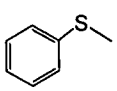	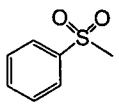	120	99	495	130	98	452	160	97	363
			40[c]	98	1470	40[c]	97	1455	50[c]	98	1176
			120	96[d]	480	130	97[d]	447	160	96[d]	360
			40[c]	97[d]	1455	40[c]	98[d]	1470	50[c]	97[d]	1164
			120	98[e]	490	130	99[e]	456	160	95[e]	356
			40[c]	96[e]	1440	40[c]	96[e]	1440	50[c]	96[e]	1152
2	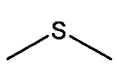	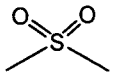	100	97	582	110	98	534	140	96	411
3	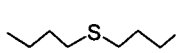	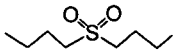	110	99	540	115	99	516	160	98	367
			35[c]	96	1645	40[c]	97	1455	50[c]	96	1152
4	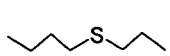	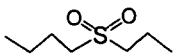	110	97	529	115	96	500	160	97	363
			35[c]	98	1680	40[c]	97	1455	50[c]	99	1188
5	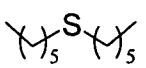	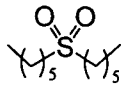	110	97	529	115	99	516	160	99	371
			40[c]	96	1440	40[c]	97	1455	50[c]	98	1176
6	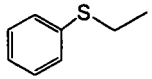	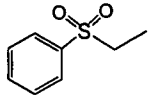	130	98	452	140	98	420	180	96	320
			45[c]	97	1293	50[c]	97	1164	60[c]	97	363

Continued...

Entry	Substrate	Product	MRAMo			MRVMo			PANMo		
			Time (min)	Isolated Yield (%)	TOF[b] (h^{-1})	Time (min)	Isolated Yield (%)	TOF[b] (h^{-1})	Time (min)	Isolated Yield (%)	TOF[b] (h^{-1})
7	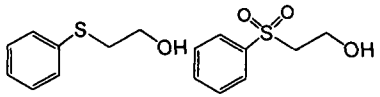		260	97	223	270	96	213	310	97	187
			90[c]	95	633	100[c]	98	588	120[c]	98	490
8	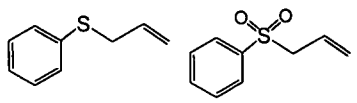		180	98	326	190	98	309	210	97	277
			50[c]	99	1188	60[c]	97	970	80[c]	98	735
9	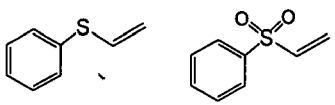		370	96	155	380	97	153	420	98	140
			150[c]	97	388	160[c]	96	360	180[c]	98	326
10	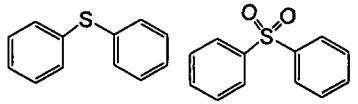		400	98	147	410	96	140	440	99	135
			160[c]	97	363	170[c]	98	345	190[c]	96	303
11	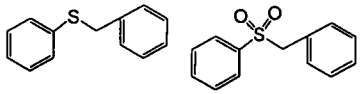		190	99	312	200	97	291	230	97	253
			60[c]	96	960	70[c]	98	840	90[c]	98	653
12[f]	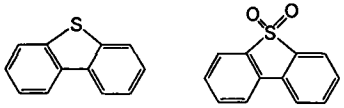		13 h[c]	94	7.2	13 h[c]	90	6.9	13 h[c]	88	6.7

[a]All reactions were carried out with 5 mmol substrate, 20 mmol 50% H_2O_2 and catalyst (containing 0.005 mmol of Mo) in 5 mL acetonitrile at RT, unless otherwise indicated.
[b]TOF (Turnover frequency) = mmol of product per mmol of catalyst per hour.
[c]Reaction at 78 °C in refluxing acetonitrile.
[d]Yield of 6th reaction cycle.
[e]Yield at 5 g scale.
[f]Substrate (5 mmol), catalyst (0.05 mmol of Mo), acetonitrile (5 mL).

5.2.2.3 Recyclability of the catalysts

The catalysts could be easily separated from the spent reaction mixture simply by filtration due to their heterogeneous characteristics. The recyclability was examined for six cycles by charging the spent catalyst with H_2O_2, MPS and MeOH (acetonitrile for sulfone) after each cycle of reaction, using MPS as the substrate. It is evident from Fig. 5.1 and the data presented in Table 5.2 (entry 1[e]) and Table 5.4 (entry 1[e]) that the activity and the selectivity of the catalysts remain undiminished even after six reaction cycles. This also demonstrates that the catalysts retain their structural integrity after its use in a number of reaction cycles. It is notable that for **MRAMo** the total TOF after 6th reaction cycles was estimated to be 8745 h^{-1} (7717 h^{-1} for **MRVMo**, 5870 h^{-1} for **PANMo**) in case of sulfoxidation and 2925 h^{-1} (2693 h^{-1} for **MRVMo**, 2174 h^{-1} for **PANMo**) for sulfone formation at room temperature, which could be increased to 23440 and 8760 h^{-1} (20644 and 8790 h^{-1} for **MRVMo**, 17430 h^{-1} and 7008 h^{-1} for **PANMo**). These values appear to be higher than that attained by most of the reported tungsten[19,20,23,24,27,28,32,33,36,38,70,91-93] or molybdenum[21,27,31,32,34,35,36,49,52,59-61,94-96] containing catalysts and demonstrate the synthetic value of the protocols.

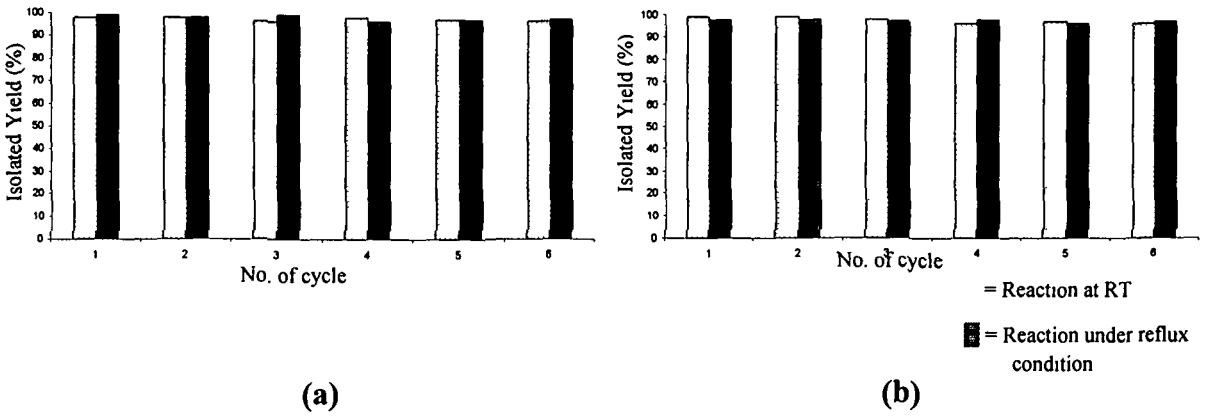

Fig. 5.1 Recyclability of **MRAMo** (used as representative) for the selective oxidation of MPS to (a) sulfoxide or (b) sulfone.

5.2.2.4 Heterogeneity of the catalytic process

With an aim to confirm that the oxidation reactions occur via a heterogeneous catalytic process, and to examine whether any leaching of the metal complex from the polymer-bound catalysts viz. **MRVMo**, **MRAMo** and **PANMo** into the reaction medium occurs during the oxidation reactions, separate experiments were conducted using MPS as the substrate under standard conditions. The filtrate obtained by separating the solid catalyst after completion of the reaction, was subsequently treated with a fresh batch of MPS and H_2O_2 mixture in a reaction vessel and the reactions were allowed to continue for another 4 h. The conversion of MPS was recorded to be only about 6% after removal of the catalyst, in line with the value obtained in the absence of any catalyst in the control experiment. This suggests that the reaction does not proceed after removal of the catalyst. Moreover, the presence of molybdenum could not be detected when the filtrate obtained after isolating the solid catalysts by filtration was subjected to AAS analysis. Possibility of pMo species leaching out of the catalyst can thus be ruled out on the basis of the evidences gathered which also prove *inter-alia*, the heterogeneous nature of the catalytic process.

5.2.2.5 Nature of the spent catalyst

The spent catalysts, **3.1-3.3** isolated after the oxidation reactions, were characterized by elemental, EDX and IR spectral analysis. The IR spectra of each of the spent catalysts were found to be identical with the respective original catalyst which showed the characteristic bands for metal-peroxo and metal bound amino acid or nitrile groups as well as the polymer support. Furthermore, no significant lowering of peroxide content and metal loading value of the recovered catalyst was indicated by the elemental analysis and EDX spectral data compared to the respective original complex. All the

information gathered from these studies thus demonstrate that the catalysts retain their structural integrity even after their use in a number of cycles of oxidation.

5.2.2.6 The proposed mechanism

A plausible mechanism for the selective oxidation of sulfides to sulfoxides or sulfones in presence of the heterogeneous catalysts **3.1-3.3** is shown in Fig. 5.2. In presence of excess H_2O_2, the monoperoxomolybdate species **I**, is likely to be converted into diperoxomolybdate species **II** (reaction a). The active diperoxomolybdate species **II** would then transfer its electrophilic oxygen to the substrate **V** to yield sulfoxide **VI** (reaction b). This facile oxygen transfer may indeed be expected since the electrophilicity of the peroxomolybdate is much higher than that of H_2O_2.[19] The sulfide formation reaction is accompanied by simultaneous regeneration of the original monoperoxomolybdate species **I** thus completing the catalytic cycle. The sulfoxide formed may undergo further oxidation by a diperoxomolybdate species **II**, formed in a separate cycle, to form sulfone (reaction c) making the sulfone formation a two–step process. The oxidation of nucleophilic sulfide to sulfoxide seems to be relatively more facile than the second oxidation of the resulting less nucleophilic sulfoxide to sulfone.[19,20]

The mechanism of action of pMo complexes, particularly the Mimoun type of complexes[97] with an oxodiperoxo Mo(VI) core in oxygen transfer reactions[59,98] with respect to alkene epoxidation[31,64,71,72,97,99-102] as well as in bromide oxidation[87,88] has been well studied.[103] The nature of the active catalytic species involved in the proposed reaction pathway is therefore fairly simple to understand. The reactive diperoxo species are known to perform substrate oxidation converting itself into more stable monoperoxo species which has been proven to be less reactive in oxidation.[31,36,87,88,103-108] In fact it has been emphasized that for a peroxomolybdenum(VI) or peroxotungsten(VI) species to be

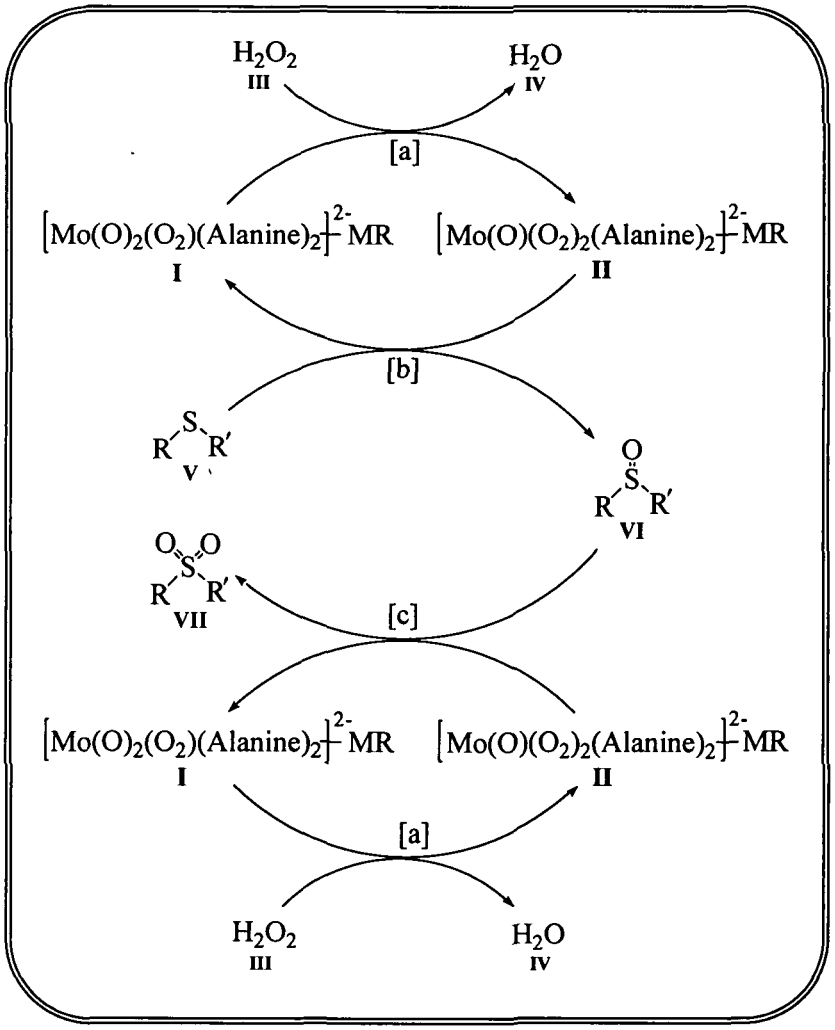

Fig. 5.2 Schematic representation of reactions occurring with heterogeneous catalysts **MRAMo (3.2)** as representative. [a] The polymer-bound monoperoxomolybdenum species **I** reacts with H_2O_2 to yield the reactive diperoxomolybdenum intermediate **II**. [b] Transfer of electrophilic oxygen from **II** to the substrate **V** takes place to yield sulfoxide **VI** with concomitant regeneration of the original catalyst **I**. [c] The sulfoxide **VI** may further react with active diperoxomolybdenum species **II** leading to the formation of sulfone **VII** and simultaneous regeneration of the original catalyst **I**. No attempt is made to show the exact stoichiometry of the reaction.

catalytically active in oxidation, formation of an oxo-diperoxo configuration may be a pre-requisite.[63,85,87] It is therefore significant to note that even a relatively inactive monoperoxo species of Mo when attached to **MR** served as an efficient heterogeneous catalyst for sulfide oxidation by H_2O_2 as a consequence of its immobilization. The results are consistent with our previous findings[84,86] which demonstrated that poly(acrylonitrile) supported catalyst **PANW** containing monoperoxo-tungstate[84] was active in selective oxidation of sulfides[84] as well as organic bromides[86] by H_2O_2.

5.3 Section B:

The Water Soluble Mo-Macrocomplexes as Homogeneous Catalysts / Oxidants in Selective Oxidation of Sulfides

5.3.1 EXPERIMENTAL SECTION

5.3.1.1 Typical procedure for the selective oxidation of sulfides to sulfoxides

A 50 mL two-necked round-bottomed flask equipped with a magnetic stirring bar was charged with organic substrate (5 mmol), 30% H_2O_2 and 5 mL of methanol. Under magnetic stirring the catalysts (containing 0.005 mmol of Mo) [**PAMo** (3.44 mg) or **PMAMo** (7.35 mg) or **PAmMo** (8.19 mg) or **PSMo** (4.90 mg)] was added to the mixture. A clear homogeneous solution was obtained at this stage. This maintains molar ratio of Mo:substrate at 1:1000 and substrate:H_2O_2 at 1:2. The reactions were performed at room temperature (RT) and progress was monitored by thin layer chromatography (TLC) and GC. At the end of the reaction, the product and unreacted substrate were isolated by extraction with diethyl ether and dried over anhydrous Na_2SO_4. Further the sulfoxides were purified and characterized by methods similar to those mentioned under procedure for oxidation of sulfide to sulfoxide (Section 5.2.1.1).

5.3.1.2 Typical procedure for the selective oxidation of sulfides to sulfones

The reaction mixture containing sulfide (5 mmol), 50% H_2O_2 (1.36 mL, 20 mmol), acetonitrile (5 mL) and the catalysts (containing 0.005 mmol of Mo) [**PAMo** (3.44 mg) or **PMAMo** (7.35 mg) or **PAmMo** (8.19 mg) or **PSMo** (4.90 mg)] were charged into a 50 mL two-necked round-bottomed flask maintaining Mo:substrate at 1:1000 and substrate:H_2O_2 at 1:4. The resulting homogeneous mixture was stirred magnetically at room temperature till the completion of the reaction (as monitored by TLC and GC). At the end of the reaction, the product sulfone was isolated followed by purification and analyzed by using similar procedure as mentioned for oxidation of sulfide to sulfoxide (Section 5.2.1.1).

5.3.1.3 Recycling of catalysts

Each of the homogeneous catalysts, **4.1-4.4** were regenerated and recycled by carrying out the reaction using MPS as substrate. For selective sulfoxidation, after completion of the reaction (Section 5.3.1.1), the product and unreacted substrate were isolated by extraction with diethyl ether and to the aqueous portion containing the spent catalyst was treated with a fresh batch of 30% H_2O_2 (1.13 mL, 10 mmol), followed by employing MPS (5 mmol) and methanol (5 mL). The progress of the reaction was monitored by thin layer chromatography (TLC) and GC. The process is repeated for a total of three reaction cycles.

Similar procedure has been adopted in case of oxidation of sulfide to sulfone. In the typical experiment, after completion of the reaction mentioned under Section 5.3.1.2, the product and unreacted substrate were extracted from the reaction mixture by ether extraction. The aqueous portion of the reaction mixture containing the spent catalyst was charged with a fresh lot of 50% H_2O_2 (1.36 mL, 20 mmol) followed by addition of MPS (5 mmol) and acetonitrile (5 mL). The reaction was followed by TLC and GC and the process was repeated for a total of three reaction cycles.

5.3.2 RESULTS AND DISCUSSION

The catalytic performance of the water soluble polymer bound pMo compounds, **PAMo**, **PMAMo**, **PAmMo** and **PSMo** in the oxidation of organic sulfides as well as DBT were examined. In order to optimize the reaction conditions several reaction runs were performed using MPS as substrate and **PAMo** as the catalyst in presence of a variety of solvents including water as described under section 5.3.1.1. It is notable that the catalysts are insoluble in the pure organic solvents including methanol and acetonitrile.

Interestingly however, in presence of H_2O_2 used as oxidant in the reaction, each of the catalysts dissolves completely in water miscible solvents such as methanol, ethanol and acetonitrile giving rise to homogeneous reaction condition. It is apparent that the presence of water contributed by the aqueous H_2O_2 is responsible for the solubility of the water soluble catalysts in the reaction mixture leading to the homogeneity of the catalytic process. On the other hand the catalysts remain insoluble in water immiscible solvents such as dichloromethane and chloroform even in the presence of H_2O_2, obviously due to the immiscibility of these solvents with H_2O_2 and water.

The data presented in Table 5.5 (entry 2) demonstrate that the reaction conducted using MeOH as solvent maintaining the oxidant:substrate molar ratio of 2:1 and catalyst:substrate ratio of 1:1000 at room temperature proceeded smoothly to selectively afford sulfoxide with reasonably good TOF. No overoxidation to sulfoxide was noted even on prolonging the reaction time. Interestingly, these optimized reaction conditions are not very different from the conditions established for the heterogeneously catalyzed reactions described under section 5.2.2.1. Considerable enhancement of the rate of the reaction, without effecting the product selectivity, was observed on increasing the reaction temperature from room temperature to 65 ^{o}C (Table 5.5, entry 10).

Apart from MPS, various types of structurally diverse sulfides as well as DBT underwent clean and selective oxidation to the corresponding sulfoxide under the optimum condition in presence of each of the complexes (Table 5.6). The reagents exhibited excellent chemoselectivity toward sulfur group of substituted sulfides containing other oxidation prone functional groups such as –C=C–, benzylic C-H and –OH (Table 5.6, entries 7 – 9 and 11). The present protocol is also effective for much less nucleophillic sulfide, such as DBT (Table 5.6, entry 12). The homogeneously catalyzed reactions also shared other common features with the reactions catalyzed by the

heterogeneous counterparts, **3.1-3.3**, such as faster rate of oxidation of aliphatic sulfides compared to the aromatic substrates (Table 5.6, entries 2-5), enhancement of rate of reaction on increasing the reaction temperature (Table 5.6, entries 1^c-12^c) without affecting the product selectivity and the prospect for larger scale applications (Table 5.6, entry1^e). However, on comparing the TOF, it is observed that heterogeneous catalysts, **3.1-3.3** display superior activity compared to the homogeneous analogues, **4.1-4.4**. On the basis of TOF values, **PMAMo** is found to exhibit higher catalytic activity in comparison to **PAMo**, **PAmMo** and **PSMo**.

Table 5.5 Optimization of reaction conditions for **PAMo** catalyzed selective oxidation of methyl phenyl sulfide (MPS) by 30% H_2O_2[a]

Entry	Molar ratio Mo:MPS	H_2O_2 (equiv.)	Solvent	Temperature	Time (min)	Isolated Yield (%)	**1a : 1b**	TOF (h^{-1})
1	1:1000	1	MeOH	RT	390	68	100 : 0	104
2	**1:1000**	**2**	**MeOH**	**RT**	**120**	**97**	**100 : 0**	**485**
3	1:500	2	MeOH	RT	70	96	100 : 0	411
4	1:100	2	MeOH	RT	45	98	100 : 0	130
5	1:1000	2	EtOH	RT	100	97	100 : 0	582
6	1:1000	2	$CHCl_3$	RT	120	8	87 : 13	40
7	1:1000	2	CH_2Cl_2	RT	120	13	84 : 16	65
8	1:1000	2	MeCN	RT	150	98	61 : 39	392
9	1:1000	2	MeOH	50 °C	50	97	100 : 0	1164
10	1:1000	2	MeOH	65 °C	45	98	100 : 0	1306

[a]All reactions were carried out with 5 mmol of substrate in 5 mL of solvent.

Table 5.6 Selective oxidation of sulfides to sulfoxides with 30% H_2O_2 catalyzed by **PAMo, PMAMo, PAmMo** and **PSMo**[a]

Entry	Substrate	Product	PAMo			PMAMo			PAmMo			PSMo		
			Time (min)	Isolated Yield (%)	TOF[b] (h^{-1})	Time (min)	Isolated Yield (%)	TOF[b] (h^{-1})	Time (min)	Isolated Yield (%)	TOF[b] (h^{-1})	Time (min)	Isolated Yield (%)	TOF[b] (h^{-1})
1	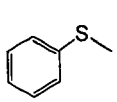	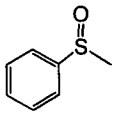	120	97	485	90	98	653	100	98	594	110	98	534
			45[c]	98	1306	30[c]	97	1940	35[c]	99	1680	40[c]	99	1485
			120	47[d]	235	90	49[d]	326	100	46[d]	276	110	44[d]	240
			45[c]	43[d]	573	30[c]	47[d]	940	35[c]	45[d]	771	40[c]	45[d]	675
			120	96[e]	480	90	97[e]	646	100	96[e]	576	110	97[e]	529
			45[c]	98[e]	1306	30[c]	99[e]	1980	35[c]	97[e]	1662	40[c]	96[e]	1440
2	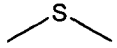	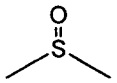	100	96	576	80	98	735	90	97	646	95	98	618
3	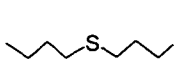	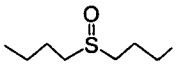	120	98	496	90	97	646	100	96	576	110	99	540
			45[c]	97	1293	25[c]	98	2352	35[c]	98	1680	40[c]	97	1455
4	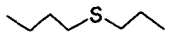	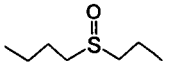	110	96	523	90	95	633	100	97	582	105	96	548
			45[c]	98	1306	25[c]	96	2305	35[c]	98	1680	40[c]	98	1470
5	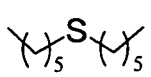	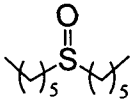	120	94	470	90	95	633	100	94	564	110	93	507
			45[c]	95	1266	30[c]	96	1920	35[c]	93	1594	40[c]	95	1425
6	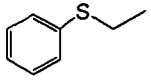	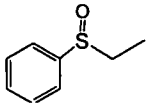	130	95	438	100	96	576	110	95	518	120	94	470
			55[c]	93	1014	40[c]	95	1425	45[c]	94	1253	50[c]	96	1152

Continued...

Entry	Substrate	Product	PAMo			PMAMo			PAmMo			PSMo		
			Time (min)	Isolated Yield (%)	TOF[b] (h^{-1})	Time (min)	Isolated Yield (%)	TOF[b] (h^{-1})	Time (min)	Isolated Yield (%)	TOF[b] (h^{-1})	Time (min)	Isolated Yield (%)	TOF[b] (h^{-1})
7	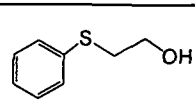	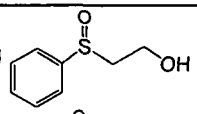	170	98	345	150	97	388	160	96	360	165	98	356
			70[c]	96	822	50[c]	94	1128	60[c]	98	980	65[c]	96	886
8	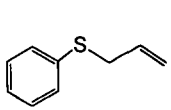	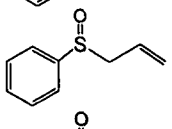	150	98	392	120	96	480	130	97	447	140	97	415
			60[c]	97	970	45[c]	98	1306	50[c]	96	1152	55[c]	98	1069
9	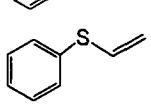	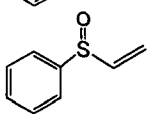	350	96	164	300	94	188	330	94	170	340	94	165
			120[c]	98	490	100[c]	95	570	110[c]	97	529	115[c]	96	500
10	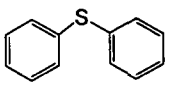	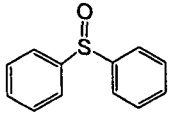	370	96	155	330	97	176	340	98	350	350	96	164
			140[c]	98	420	110[c]	98	534	120[c]	97	130	130[c]	97	447
11	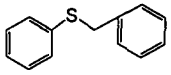	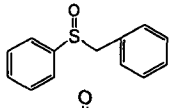	160	97	363	130	98	452	140	98	150	150	98	392
			65[c]	98	904	50[c]	96	1152	55[c]	97	60	60[c]	97	970
12[f]	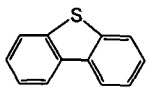	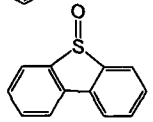	11 h[c]	89	8.0	11 h[c]	94	8.5	11 h[c]	92	8.3	11 h[c]	90	8.1

[a]All reactions were carried out with 5 mmol substrate, 10 mmol 30% H_2O_2 and catalyst (0.005 mmol of Mo) in 5 mL methanol at RT, unless otherwise indicated.

[b]TOF (Turnover frequency) = mmol of product per mmol of catalyst per hour.

[c]Reaction at 65 °C in refluxing methanol.

[d]Yield of 3rd reaction cycle.

[e]Yield at 7.5 g scale.

[f]Substrate (5 mmol), catalyst (0.05 mmol of Mo), methanol (5 mL).

5.3.2.1 Oxidation of sulfides to sulfones

Selective oxidation of sulfide to the corresponding sulfone could also be accomplished in presence of the homogeneous catalysts, **4.1-4.4** under identical reaction conditions optimized for the heterogeneous catalysts (**3.1-3.3**). In order to attain clean conversion to sulfone, it was necessary to use acetonitrile as solvent instead of methanol and 4 equivalents of 50% H_2O_2 in lieu of 30% H_2O_2 (Table 5.7). The results presented in Table 5.8 shows that the protocol is also useful for various types of sulfides including DBT. Moreover, reaction time could be considerably reduced by conducting the reactions under reflux condition at 78 °C. As seen from the data presented in Table 5.8 (entries 7-9 and 11), the oxidation of sulfides to the corresponding sulfones has been achieved with complete chemoselectivity. The procedure also provides scope for using it for relatively larger scale synthesis (Table 5.8, entry1[c]).

Table 5.7 Optimization of reaction conditions for **PAMo** catalyzed selective oxidation of methyl phenyl sulfide (MPS) to sulfone by 50% H_2O_2[a]

Entry	Molar ratio Mo:MPS	H_2O_2 (equiv.)	Solvent	Temperature	Time (min)	Isolated Yield (%)	**1a : 1b**	TOF (h^{-1})
1	1:1000	1	MeCN	RT	420	64	88 : 12	91
2	1:1000	2	MeCN	RT	300	96	29 : 71	192
3	1:1000	3	MeCN	RT	250	97	16 : 84	232
4	**1:1000**	**4**	**MeCN**	**RT**	**240**	**99**	**0 : 100**	**247**
5	1:500	4	MeCN	RT	120	95	0 : 100	237
6	1:100	4	MeCN	RT	90	96	0 : 100	64
7	1:1000	4	MeCN	78 °C	100	98	0 : 100	588

[a]All reactions were carried out with 5 mmol of substrate in 5 mL of solvent.

Table 5.8 Selective oxidation of sulfides to sulfones with 50% H_2O_2 catalyzed by **PAMo, PMAMo, PAmMo** and **PSMo**[a]

Entry	Substrate	Product	PAMo			PMAMo			PAmMo			PSMo		
			Time (min)	Isolated Yield (%)	TOF[b] (h^{-1})	Time (min)	Isolated Yield (%)	TOF[b] (h^{-1})	Time (min)	Isolated Yield (%)	TOF[b] (h^{-1})	Time (min)	Isolated Yield (%)	TOF[b] (h^{-1})
1	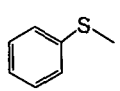	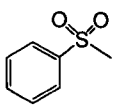	240	99	247	200	97	291	220	99	270	230	97	253
			100[c]	98	588	80[c]	99	742	90[c]	98	653	95[c]	98	618
			240	51[d]	127	200	56[d]	195	220	56[d]	152	230	54	140
			100[c]	54[d]	324	80[c]	52[d]	390	90[c]	53[d]	353	95[c]	57	360
			240	98[e]	245	200	98[e]	294	220	98[e]	267	230	98	255
			100[c]	97[e]	582	80[c]	97[e]	727	90[c]	99[e]	660	95[c]	97	612
2	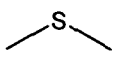	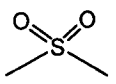	210	98	280	180	97	323	200	97	291	200	98	294
3	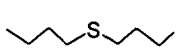	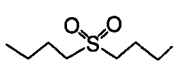	230	96	250	190	96	303	210	98	280	220	99	270
			90[c]	98	653	80[c]	98	735	90[c]	96	640	90	98	653
4	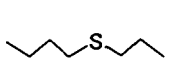	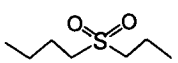	220	98	267	190	97	306	210	98	280	230	97	253
			90[c]	96	640	75[c]	98	784	80[c]	97	727	95	98	618
5	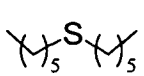	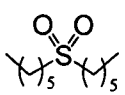	240	94	235	200	96	288	220	95	259	230	93	242
			100[c]	93	558	80[c]	95	712	90[c]	94	626	95	94	593
6	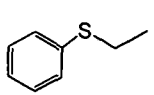	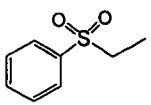	250	97	232	210	96	274	230	97	253	240	96	240
			110[c]	96	523	90[c]	98	653	100[c]	96	576	110	98	534

Continued...

Entry	Substrate	Product	PAMo			PMAMo			PAmMo			PSMo		
			Time (min)	Isolated Yield (%)	TOF[b] (h^{-1})	Time (min)	Isolated Yield (%)	TOF[b] (h^{-1})	Time (min)	Isolated Yield (%)	TOF[b] (h^{-1})	Time (min)	Isolated Yield (%)	TOF[b] (h^{-1})
7	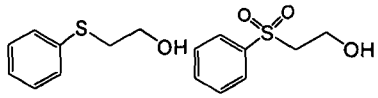		380	95	150	360	98	163	370	96	155	370	97	157
			160[c]	97	363	140[c]	97	415	150[c]	98	392	155[c]	98	379
8	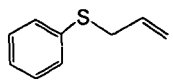	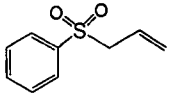	270	96	213	240	96	240	250	98	235	260	96	221
			120[c]	97	485	100[c]	98	588	110[c]	97	529	115[c]	98	511
9	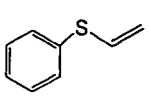	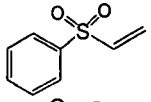	510	98	115	480	96	120	490	98	120	500	98	117
			210[c]	97	277	190[c]	97	306	200[c]	96	288	200[c]	97	291
10	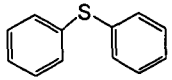	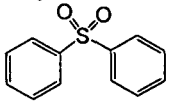	540	97	107	500	96	115	520	95	109	530	98	110
			250[c]	98	235	220[c]	97	264	230[c]	98	255	240[c]	96	240
11	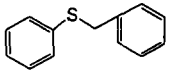	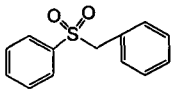	280	98	210	250	99	237	260	97	223	270	97	215
			130[c]	96	443	110[c]	96	523	120[c]	98	490	130[c]	99	456
12[f]	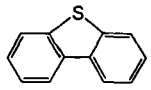	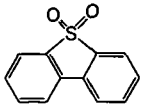	15 h[c]	85	5.6	15 h[c]	93	6.2	15 h[c]	88	5.9	15 h[c]	86	5.7

[a]All reactions were carried out with 5 mmol substrate, 20 mmol 50% H_2O_2 and catalyst (containing 0.005 mmol of Mo) in 5 mL acetonitrile at RT, unless otherwise indicated.
[b]TOF (Turnover frequency) = mmol of product per mmol of catalyst per hour.
[c]Reaction at 78 °C in refluxing acetonitrile.
[d]Yield of 3rd reaction cycle.
[e]Yield at 7.5 g scale.
[f]Substrate (5 mmol), catalyst (0.05 mmol of Mo), acetonitrile (5 mL).

5.3.2.2 Recyclability of the catalysts

A homogeneous catalytic process often suffers from the drawback of difficulty in regeneration of the catalyst. In the present work, however, the water soluble catalysts could be regenerated *in situ* after separating the oxidized product and unreacted sulfide from the reaction mixture by extraction with ether, without much difficulty. After completion of each cycle of reaction, the spent reaction mixture containing the soluble catalyst was treated with H_2O_2, a fresh lot of substrate and the respective solvent. A decrease in TOF was however noted with every increasing number of reaction cycles (Fig. 5.3 and Tables 5.6 and 5.8, entry1[d]) in contrast to the heterogeneous analogues which showed consistent activity even after several reaction cycles (Tables 5.2 and 5.4, entry1[d]). The observed loss of activity of the catalysts may be attributed to the possibility of leaching of the active pMo species from the polymer matrices.

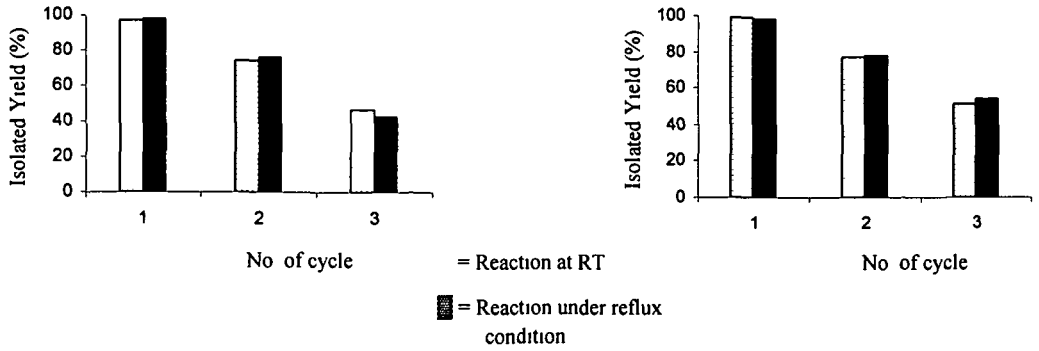

(a) (b)

Fig. 5.3 Recyclability of **PAMo** (used as representative) for the selective oxidation of MPS to (a) sulfoxide or (b) sulfone.

5.3.2.3 Nature of the spent catalyst

After completion of the reaction, the spent catalysts, **4.1-4.4** were isolated from the reaction mixture by treatment with acetone, dried and subsequently characterized by elemental, EDX and IR spectral analysis. The IR spectrum of each of the recovered catalysts resembled closely the spectrum of the corresponding original starting compound displaying the typical bands for metal-peroxo and metal bound carboxylate, amide or sulfonate groups. However, the elemental analysis data for the spent catalysts showed decrease in peroxide and molybdenum content indicating the gradual leaching of pMo species from the catalyst. The finding is also consistent with the observed loss of activity on reuse of the recovered catalyst.

5.3.2.4 Peroxomolybdate complexes, 4.1-4.4 as stoichiometric oxidants of sulfides

It has been our anticipation that since the compounds, **4.1-4.4** contains pMo species in its active diperoxo form, these compounds would be effective as stoichiometric oxidants of sulfides. We have accordingly evaluated the oxidant activity of the compounds using MPS as a model substrate. From the findings of our investigation presented in Table 5.9 it is evident that the reaction of **PAMo** with MPS in the molar ratio of Mo:MPS at 1:1 in methanol/water (1:1) as solvent, proceeded smoothly at room temperature to afford a mixture of sulfoxide and sulfone in the ratio of 87:13 with 86% yield (Table 5.9, entry 2). Our attempts to attain selective sulfoxidation by lowering the molar ratio of Mo:MPS to 0.5:1 (Table 5.9, entry 1), or by changing the solvent system (Table 5.9, entries 2-4), were unsuccessful.

Besides methanol/water solvent system, we have also run the reactions in different solvents such as ethanol/water, acetonitrile/water and also in the pure solvents like methanol, ethanol, acetonitrile, dichloromethane and chloroform. Interestingly, the

reaction did not take place when pure organic solvents were used (Table 5.9, entries 8-12). On the other hand, the oxidation of MPS proceeded smoothly on including water in the water miscible solvent system. The lack of reactivity in pure organic solvents may be ascribed to the insolubility of the oxidant in these solvents. In case of the reaction procedure where the compounds **4.1-4.4** serve as catalysts (Section 5.2), no additional water was apparently needed for the activity of the complexes as the aqueous component has been contributed by the dilute H_2O_2 used as oxidant.

It is notable that selective oxidation of MPS to sulfone could be achieved in excellent yield by conducting the reaction in acetonitrile/water and increasing the Mo:oxidant ratio to 3:1 (Table 5.9, entry 6). Under the optimized reaction condition, oxidation of a number of different sulfides to sulfones was carried out with the pMo complexes **4.1-4.4**. The results summarized in Table 5.10 also demonstrate that the oxidations proceed with complete chemoselectivity towards sulfur groups in presence of other oxidation prone functional groups in the substituted sulfides.

Table 5.9 Optimization of reaction conditions for the selective oxidation of methyl phenyl sulfide (MPS) to sulfoxide (**1a**) and sulfone (**1b**) by **PAMo**[a]

Entry	Mo:MPS	Solvent	Time (min)	**1a:1b**	Isolated Yield (%)
1	0.5:1	$MeOH/H_2O$ (1:1)	180	88:12	42
2	1:1	$MeOH/H_2O$ (1:1)	120	87:13	86
3	1:1	$EtOH/H_2O$ (1:1)	130	85:15	84
4	1:1	CH_3CN/H_2O (1:1)	100	80:20	80
5	2:1	CH_3CN/H_2O (1:1)	150	10:90	98
6	3:1	CH_3CN/H_2O (1:1)	130	0:100	99
7[b]	3:1	CH_3CN/H_2O (1:1)	70	0:100	98
8	1:1	MeOH	360	No reaction	
9	1:1	CH_3CN	360	No reaction	
10	1:1	EtOH	360	No reaction	
11	1:1	DCM	360	No reaction	
12	1:1	$CHCl_3$	360	No reaction	

[a]All reactions were carried out using MPS (1 mmol) as substrate at room temperature, unless otherwise indicated.

[b]Reaction at 78 °C in refluxing acetonitrile.

Table 5.10 Selective oxidation of sulfides to sulfones by soluble polymer bound pMo complexes, **4.1-4.4**[a]

Substrate	Product	**PAMo**		**PMAMo**		**PAmMo**		**PSMo**	
		Time (min)	Yield (%)	Time (min)	Yield (%)	Time (min)	Yield (%)	Time (min)	Yield (%)
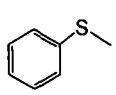	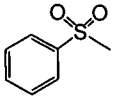	130	99	100	97	110	98	120	96
		70[b]	98	50[b]	99	55[b]	96	60[b]	98
		130	98[c]	100	98[c]	110	97[c]	120	97[c]
		70[b]	96[c]	50[b]	98[c]	55[b]	98[c]	60[b]	96[c]
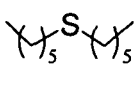	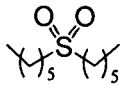	140	96	100	98	110	99	120	98
		70[b]	98	50[b]	97	55[b]	98	60[b]	99
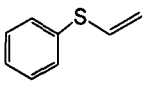	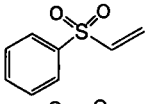	360	96	300	97	320	96	330	98
		150[b]	97	120[b]	96	130[b]	98	140[b]	97
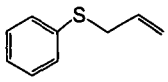	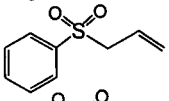	180	97	120	99	130	99	160	95
		90[b]	98	60[b]	98	70[b]	96	80[b]	98
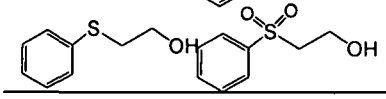		250	95	180	97	200	98	220	98
		120[b]	98	100[b]	98	110[b]	97	110[b]	97

[a]All reactions were carried out with 1.00 mmol of substrate in 10 mL of CH_3CN/H_2O (1:1) at room temperature by maintaining molar ratio of Mo:substrate at 3:1, unless otherwise indicated.

[b]Reaction at 78 °C in refluxing acetonitrile.

[c]Yield of 6th reaction cycle.

5.3.2.5 The proposed mechanism

The scheme of reactions proposed for the homogeneously catalyzed selective oxidation of sulfides is shown in Fig. 5.4 using **PMAMo** as representative. Since the homogeneous catalysts consist of reactive diperoxomolybdate (VI) species, transfer of electrophilic oxygen from species **I** is likely to occur as a first step to yield sulfoxide **IV** with concomitant formation of intermediate monoperoxomolybdate (VI) **II** [reaction (a)]. The intermediate species **II** further reacts with H_2O_2, and regenerate the original reactive species **I** [reaction (b)]. The sulfoxide **IV** thus formed may subsequently react with another molecule of diperoxomolybdate (VI) species, **I** to yield sulfone [reaction (c)]. The proposed reaction pathway is in accord with our previous observations mentioned under section 5.2.2.6.

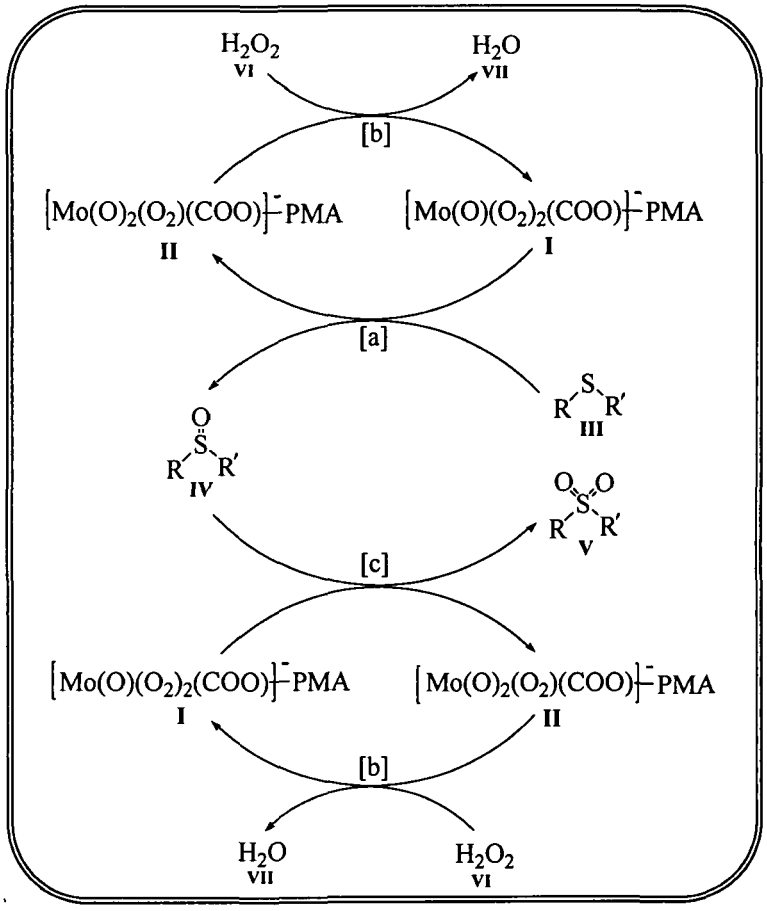

Fig. 5.4 Schematic representation of reactions occurring with homogeneous catalysts shown with **PMAMo (3.2)** as representative.

5.4 CONCLUSIONS

Immobilization of peroxomolybdate in its monoperoxo form on amino acid functionalized Merrifield resin as well as poly(acrylonitrile) led to the development of a set of heterogeneous catalysts, highly effective in mediating selective oxidation of sulfides by H_2O_2. It is worth noting that clean conversion to high purity sulfoxide as well as sulfone could be obtained from the corresponding sulfides and DBT in impressive yields and TOF in presence of the catalysts by establishing appropriate reaction conditions. Water soluble macrocomplexes containing diperoxomolybdate(VI) species **4.1-4.4** on the other hand served as homogeneous catalysts for the same reactions under identical reaction conditions. The heterogeneous catalysts however exhibited superior activity over its homogeneous counterparts. Significantly, the pMo compounds anchored to WSP were also capable of serving as stoichiometric oxidants of sulfides, in absence of H_2O_2. In contrast, the insoluble pMo compounds were totally inactive in sulfide oxidation on their own, under analogous reaction conditions.

The catalytic protocols developed are straightforward, safe and environmentally clean being free from halogenated solvent or any other additives such as a co-catalyst or acid. In addition, the oxidation is chemoselective for sulfide or sulfoxide leaving an alcoholic, benzylic C-H or olefinic linkage unaffected. Easy recovery and reusability for several catalytic cycles with unaltered activity and selectivity are other significant and attractive features of the heterogeneous catalysts. The developed methodologies thus conform to several guiding principles of "green" chemistry.[109]

REFERENCES

1. Kulkarni, P.S., & Afonso, C.A.M. *Green Chem.* **12**, 1139--1149, 2010.

2. Imada, Y., et al. *Tetrahedron Lett.* **54**, 621--624, 2013.

3. Palermo, V., et al. *J. Mol. Catal. A: Chem.* **373**, 142--150, 2013.

4. Carreno, M.C. Chem. *Rev.* **95**, 1717--1760, 1995.

5. Holland, H.L. *Chem. Rev.* **88**, 473--485, 1988.

6. Fernandez, I., & Khiar, N. *Chem. Rev.* **103**, 3651--3706, 2003.

7. Legros, J., et al. *Adv. Synth. Catal.* **347**, 19--31, 2005.

8. Srour, H., et al. *Coord. Chem. Rev.* **In Press**, 2013.

9. Romanowski, G., & Kira, J. *Polyhedron* **53**, 172--178, 2013.

10. Srour, H., et al. *J. Mol. Catal. A: Chem.* **370**, 75--79, 2013.

11. Palermo, V., et al. *J. Mol. Catal. A: Chem.* **373**, 142--150, 2013.

12. Patai, S. & Rappoport, Z. *Synthesis of Sulfones, Sulfoxides and Cyclic Sulfides*, John Wiley, Chichester, 1994.

13. Yu, G., et al. *Energy Fuels* **19**, 447--452, 2005.

14. Gonzalez, L.A., et al. *Energy Fuels* **26**, 5164--5176, 2012.

15. Nie, Y., et al. *Fuel* **103**, 997--1002, 2013.

16. Maurya, M.R., et al. *Inorg. Chem.* **49**, 6586--6600, 2010.

17. Liang, W., et al. *Fuel Process. Technol.* **109**, 27--31, 2013.

18. Lü, H., et al. *Appl. Catal. A* **453**, 376--382, 2013.

19. Sato, K., et al. *Tetrahedron* **57**, 2469--2476, 2001, and references therein.

20. Choudary, B.M., et al. *J. Chem. Soc., Perkin Trans. 1* 2069--2074, 2002.

21. Jeyakumar, K., et al. *Catal. Commun.* **10**, 1948--1951, 2009.

22. Noyori, R., et al. *Chem. Commun.* 1977--1986, 2003.

23. Sato, K., et al. *Science* **281**, 1646--1647, 1998.

24. Hulea, V., et al. *Appl. Catal. A* **313**, 200--207, 2006.

25. Lane, B.S., & Burgess, K. *Chem. Rev.* **103**, 2457--2474, 2003.

26. Jones, C.W. *Applications of Hydrogen Peroxide and Derivatives*, Royal Society of Chemistry, Cambridge, 1999.

27. Kaczorowska, K., et al. *Tetrahedron* **61**, 8315--8327, 2005.

28. Karimi, B., et al. *Org. Lett.* **7**, 625--628, 2005.

29. Sheldon, R.A. & Kochi, J.K. *Metal Catalyzed Oxidations of Organic Compounds*, Academic Press, London, 1981.

30. Contreras-Valdez, Z., et al. *Fuel* **106**, 519--527, 2013.

31. Gharah, N., et al. *Inorg. Chim. Acta* **362**, 1089--1100, 2009.

32. Gresley, N.M., et al. *J. Mol. Catal. A.: Chem.* **117**, 185--198, 1997.

33. Shi, X.-Y., & Wei, J.-F. *J. Mol. Catal. A: Chem.* **280**, 142--147, 2008.

34. Romanelli, G.P., et al. *Catal. Commun.* **12**, 726--730, 2011.

35. Tundo, P., et al. *Catal. Commun.* **11**, 1181--1184, 2010.

36. Maiti, S.K., et al. *New J. Chem.* **29**, 554--563, 2005.

37. Jahier, C., et al. *Polyhedron* **57**, 57--63, 2013.

38. Koo, D.H., et al. *Org. Lett.* **7**, 5015--5018, 2005.

39. Romanowski, G., *J. Mol. Catal. A: Chem.* **368–369**, 137--144, 2013.

40. Yamaura, T., et al. *Catal. Today* **203**, 76--80, 2013.

41. Lazar, A., et al. *Microporous Mesoporous Mater.* **170**, 331--339, 2013.

42. Hussain, S., et al. *Tetrahedron Lett.* **53**, 6512--6515, 2012.

43. Conte, V., et al. *Pure Appl. Chem.* **81**, 1265--1277, 2009.

44. Gregori, F., et al. *J. Mol. Catal. A: Chem.* **286**, 124--127, 2008.

45. Stanger, K.J., et al. *J. Mol. Catal. A: Chem.* **243**, 158--169, 2006.

46. Egami, H., & Katsuki, T. *J. Am. Chem. Soc.* **129**, 8940--8941, 2007.

47. Xie, F., et al. *J. Mol. Catal. A: Chem.* **307**, 93--97, 2009.

48. Khodaei, M.M., et al. *Can. J. Chem.* **85**, 7--11, 2007.

49. Sheikhshoaie, I., et al. *Polyhedron* **28**, 733--738, 2009.

50. Yang, C., et al. *Green Chem.* **11**, 1401--1405, 2009.

51. Palermo, V., et al. *Phosphorus, Sulfur Silicon Relat. Elem.* **184**, 3258--3268, 2009.

52. Jeyakumar, K., & Chand, D.K. *Tetrahedron Lett.* **47**, 4573--4576, 2006.

53. Hussain, S., et al. *Eur. J. Org. Chem.* **20**, 3319--3322, 2009.

54. Clark, J.H. *Green Chem.* **1**, 1--8, 1999.

55. Arends, I., Sheldon, R. & Hanefeld, U. *Green Chemistry and Catalysis*, Wiley-VCH Verlag GmbH & Co. KGaA, Weinheim, 2007.

56. Gupta, K.C., et al. *Coord. Chem. Rev.* **253**, 1926--1946, 2009.

57. McNamara, C.A., et al. *Chem. Rev.* **102**, 3275--3300, 2002.

58. Barbaro, P., & Liguori, F. *Chem. Rev.* **109**, 515--529, 2009.

59. Dickman, M.H., & Pope, M.T. *Chem. Rev.* **94**, 569--584, 1994.

60. Fuerte, A., et al. *J. Mol. Catal. A: Chem.* **211**, 227--235, 2004.

61. Tamami, B., & Yeganeh, H. *Eur. Polym. J.* **35**, 1445--1450, 1999.

62. Batigalhia, F., et al. *Tetrahedron* **57**, 9669--9676, 2001.

63. Ghiron, A.F., & Thompson, R.C. *Inorg. Chem.* **28**, 3647--3650, 1989.

64. Herbert, M., et al. *J. Mol. Catal. A: Chem.* **338**, 111--120, 2011.

65. Cross, R.J., et al. *J. Mol. Catal. A: Chem.* **144**, 273--284, 1999.

66. Cross, W.B., et al. *Inorg. Chem.* **45**, 4556--4561, 2006.

67. Ivin, K.J., & Mol, J.C. *Olefin Metathesis and Metathesis Polymerisation*, Academic Press, London, 1997.

68. Wang, G., et al. *Inorg. Chim. Acta* **358**, 933--940, 2005.

69. Fronczek, F.R., et al. *Inorg. Chem. Commun.* **5**, 384--387, 2002.

70. Bortolini, O., et al. *J. Org. Chem.* **50**, 2688--2690, 1985.

71. Kirshenbaum, K.S., & Sharpless, K.B. *J. Org. Chem.* **50**, 1979--1982, 1985.

72. Mimoun, H. *Catal. Today* **1**, 281--295, 1987.

73. Maurya, M.R. *Curr. Org. Chem.* **16**, 73--88, 2012.

74. da Silva, J.A.L., et al. *Coord. Chem. Rev.* **255**, 2232--2248, 2011.

75. Tamami, B., & Yeganeh, H. *React. Funct. Polym.* **50**, 101--106, 2002.

76. Hinner, M.J., et al. *Z. Anorg. Allg. Chem.* **629**, 2251--2257, 2003.

77. Maurya, M.R., et al. *React. Funct. Polym.* **66**, 808--818, 2006.

78. Vassilev, K., et al. *React. Funct. Polym.* **46**, 165--173, 2000.

79. Okhapkin, I.M., et al. *Adv. Polym. Sci.* **195**, 177--210, 2006.

80. Bekturov, E.A. & Kudaibergenov, S.E. *Catalysis by Polymers*, WILEY-VCH Verlag GmbH & Co. KGaA, Weinheim, 2002.

81. Bergbreiter, D.E. *Chem. Rev.* **102**, 3345--3384, 2002.

82. Dickerson, T.J., et al. *Chem. Rev.* **102**, 3325--3344, 2002.

83. Das, S.P., et al. *Tetrahedron Lett.* **53**, 1163--1168, 2012.

84. Das, S.P., et al. *J. Mol. Catal. A: Chem.* **356**, 36--45, 2012.

85. Hazarika, P., et al. *Polyhedron* **25**, 3501--3508, 2006.

86. Boruah, J.J., et al. *Polyhedron* **52**, 246--254, 2013.

87. Reynolds, M.S., et al. *Inorg. Chem.* **33**, 4977--4984, 1994.

88. Meister, G.E., & Butler, A. *Inorg. Chem.* **33**, 3269--3275, 1994.

89. Baciocchi, E., et al. *J. Org. Chem.* **69**, 3586--3589, 2004.

90. Patonay, T., et al. *J. Org. Chem.* **66**, 2275--2280, 2001.

91. Yamada, Y.M.A., et al. *Tetrahedron* **60**, 4087--4096, 2004.

92. Zhu, W., et al. *J. Mol. Catal. A: Chem.* **347**, 8--14, 2011.

93. Schultz, H.S., et al. *J. Org. Chem.* **28**, 1140--1142, 1963.

94. Gamelas, C.A., et al. *Tetrahedron Lett.* **49**, 4708--4712, 2008.

95. Basak, A., et al. *Tetrahedron: Asymmetry* **17**, 508--511, 2006.

96. Bagherzadeh, M., et al. *Inorg. Chim. Acta* **361**, 2019--2024, 2008.

97. Mimoun, H., et al. *Bull. Soc. Chim. Fr.* **5**, 1481--1492, 1969.

98. Joergensen, K.A., *Chem. Rev.* **89**, 431--458, 1989.

99. Gharah, N., et al. *Chem. Commun.* 2630--2632, 2004 and references cited therein.

100. Thiel, W.R., & Eppinger, J. *Chem. Eur. J.* **3**, 696--705, 1997.

101. Maiti, S.K., et al. *Inorg. Chem.* **45**, 9843--9857, 2006.

102. Maiti, S.K., et al. *New J. Chem.* **30**, 479--489, 2006.

103. Sensato, F.R., et al. *J. Org. Chem.* **68**, 5870--5874, 2003.

104. Hazarika, P., et al. *Mol. Cell. Biochem.* **284**, 39--47, 2006.

105. Hazarika, P., et al. *J. Enz. Inhib. Med. Chem.* **23**, 504--513, 2008.

106. Kalita, D., et al. *Biol. Trace Elem. Res.* **128**, 200--219, 2009.

107. Djordjevic, C., et al. *Inorg. Chim. Acta* **104**, L7-L9, 1985

108. Djordjevic, C., et al. *Inorg. Chem.* **27**, 2926--2932, 1988.

109. Anastas, P.T., & Warner, J.C. *Green Chemistry: Theory and Practice*, Oxford University Press, New York, 1998.

Appendix: 4A Characterization of Sulfoxides and Sulfones

(a) Methylphenylsulfoxide: Isolated as light yellow solid; mp 28-29°C; ν (KBr)/cm^{-1} 1046;

^{1}H NMR (400MHz; $CDCl_3$, δ): 2.73(s, 3H); 7.30-7.36(m, 1H); 7.41-7.50(m, 2H); 7.62-7.69(m, 2H)

^{13}C NMR (100.5MHz; $CDCl_3$, δ): 43.93; 123.54; 128.63; 130.95; 145.42

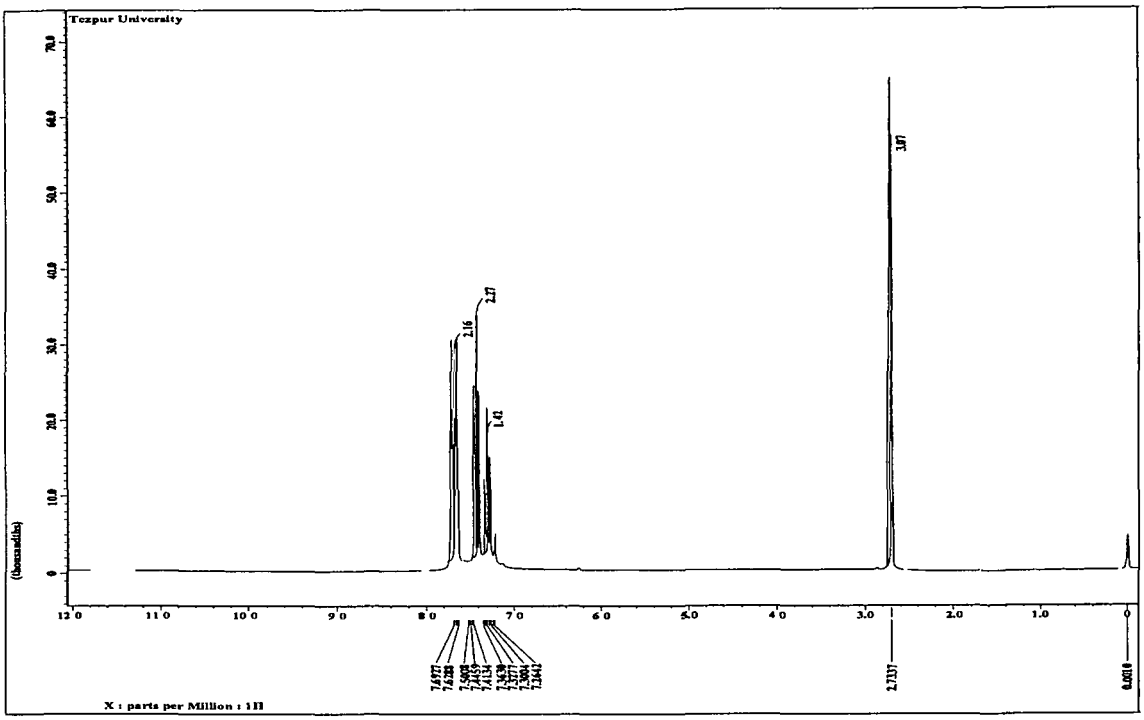

Fig. 4A.1 ^{1}H NMR spectra of methyl phenyl sulfoxide.

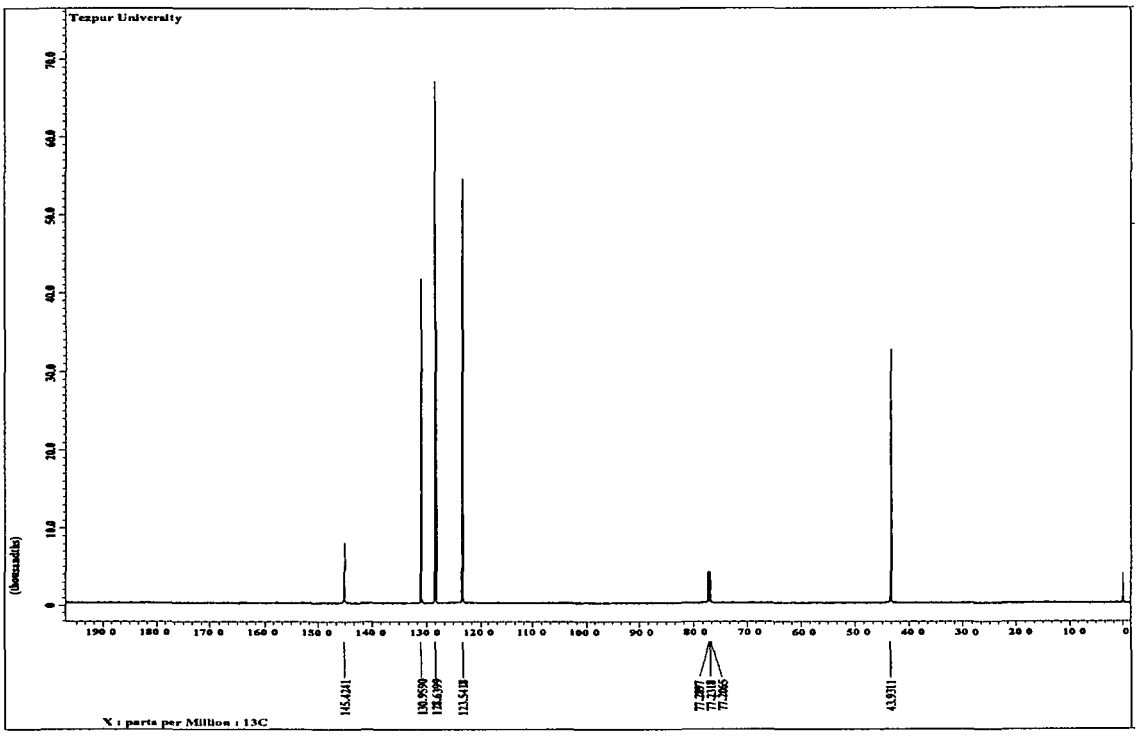

Fig. 4A.2 ^{13}C NMR spectra of methyl phenyl sulfoxide.

(b) Methylphenylsulfone: Isolated as white solid; mp 85-86°C; ν (KBr)/cm^{-1} 1321, 1165;

^{1}H NMR (400MHz; $CDCl_3$, δ): 3.02(s, 3H); 7.52-7.59(m, 1H); 7.61-7.71(m, 2H); 7.89-7.95(m, 2H)

^{13}C NMR (100.5MHz; $CDCl_3$, δ): 44.83; 126.23; 128.54; 133.21; 137.44

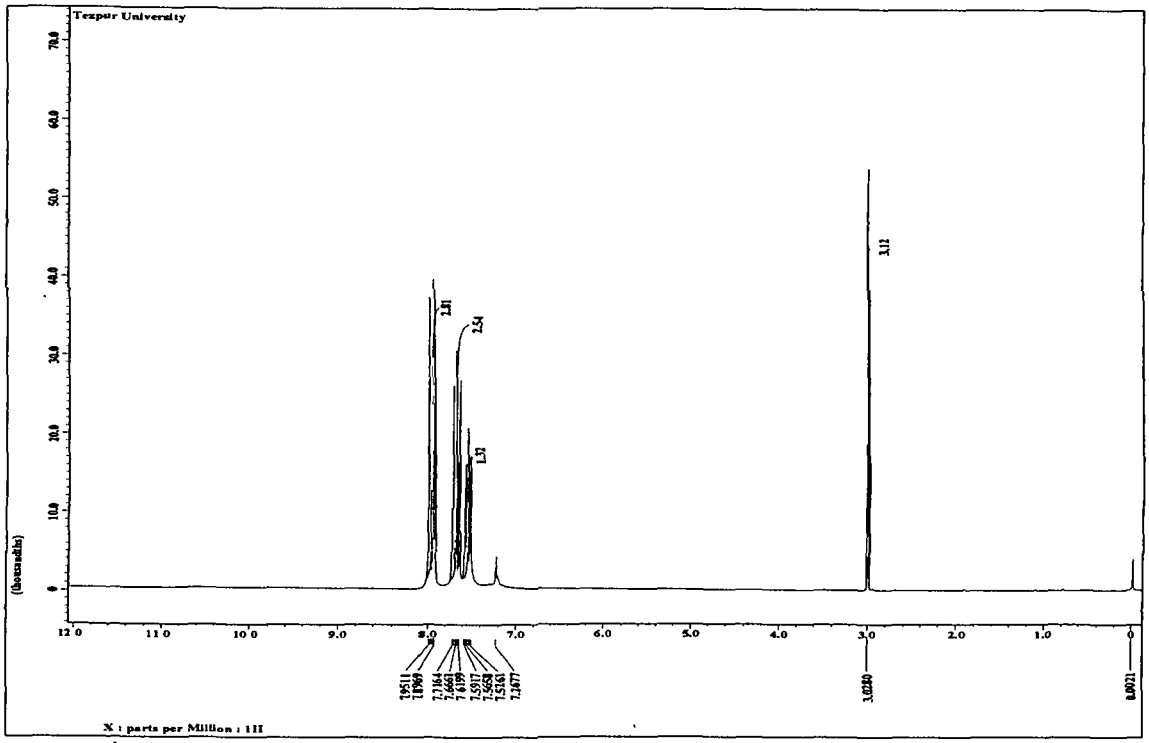

Fig. 4A.3 ^{1}H NMR spectra of methyl phenyl sulfone.

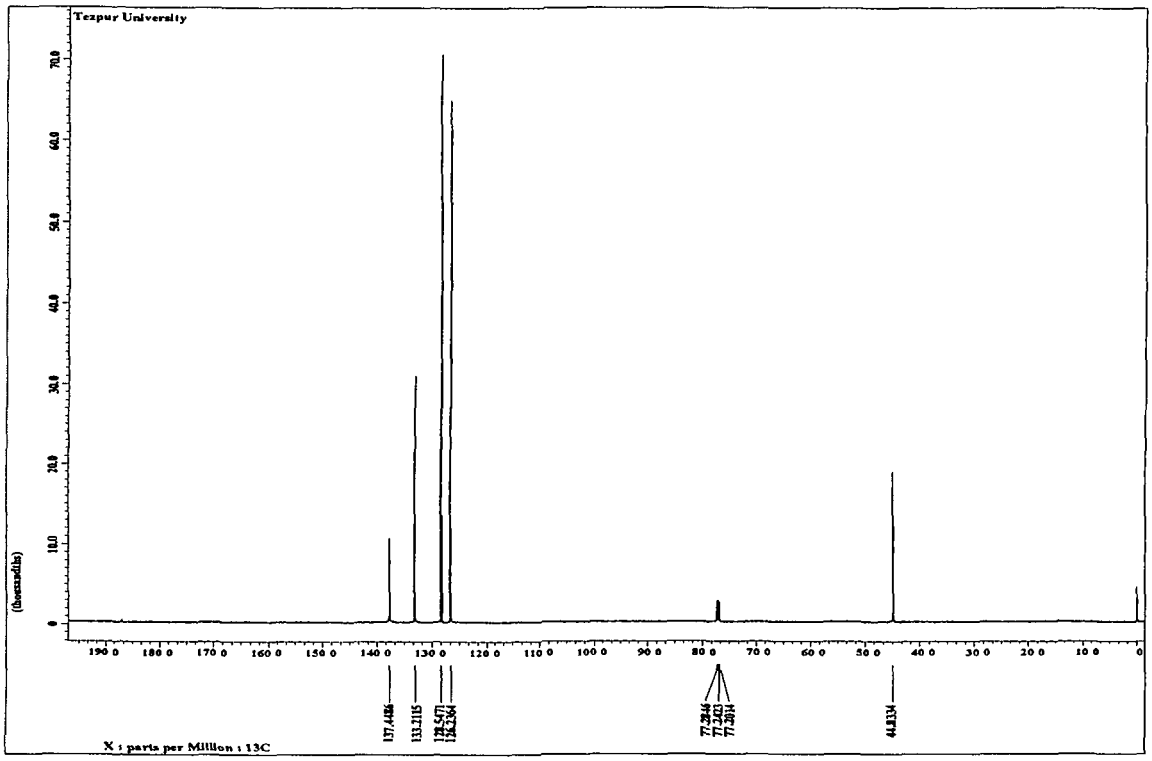

Fig. 4A.4 ^{13}C NMR spectra of methyl phenyl sulfone.

(c) Dimethylsulfoxide: Isolated as liquid; ν (KBr)/cm^{-1} 1053;

^{1}H NMR (400MHz; $CDCl_3$, δ): 2.63(s, 6H)

^{13}C NMR (100.5MHz; $CDCl_3$, δ): 40.53

(d) Dimethylsulfone: Isolated as white solid; mp 236-237°C; ν (KBr)/cm^{-1} 1314, 1136;

^{1}H NMR (400MHz; $CDCl_3$, δ): 3.27(s, 6H)

^{13}C NMR (100.5MHz; $CDCl_3$, δ): 44.63

(e) Dibutylsulfoxide: Isolated as white solid; mp 32-33°C; ν (KBr)/cm^{-1} 1063;

^{1}H NMR (400MHz; $CDCl_3$, δ): 0.96(t, 6H, J=7.41Hz); 1.37-1.49(m, 4H); 1.68-1.78(m, 4H); 2.61-2.69(m, 4H)

^{13}C NMR (100.5MHz; $CDCl_3$, δ): 13.74; 22.13; 24.52; 51.91

(f) Dibutylsulfone: Isolated as white solid; mp 42-43°C; ν (KBr)/cm^{-1} 1342, 1135;

^{1}H NMR (400MHz; $CDCl_3$, δ): 0.96 (t, 6H, J=7.41Hz); 1.39-1.51(m, 4H); 1.79-1.88(m, 4H); 2.87-2.94(m, 4H)

^{13}C NMR (100.5MHz; $CDCl_3$, δ): 13.54; 21.72; 23.98; 52.53

(g) Butylpropylsulfoxide: Isolated as liquid; ν (KBr)/cm^{-1} 1057;

^{1}H NMR (400MHz; $CDCl_3$, δ): 0.92-0.99(m, 6H); 1.28-1.39(m, 2H); 1.71-1.79(m, 4H); 2.54-2.62 (m, 4H)

^{13}C NMR (100.5MHz; $CDCl_3$, δ): 13.76; 22.14; 24.51; 51.97

(h) Butylpropylsulfone: Isolated as white solid; mp 81-82°C; ν (KBr)/cm^{-1} 1342, 1132;

^{1}H NMR (400MHz; $CDCl_3$, δ): 0.94-0.99(m, 6H); 1.29-1.39(m, 2H); 1.82-1.89(m, 4H); 2.85-2.95(m, 4H)

^{13}C NMR (100.5MHz; $CDCl_3$, δ): 13.51; 21.75; 23.99; 52.53

(i) Dibenzothiophene sulfoxide: Isolated as white solid; mp 188-189°C; ν (KBr)/cm^{-1} 1043;

^{1}H NMR (400MHz; $CDCl_3$, δ): 7.52-7.59(m, 2H); 7.71-7.75(m, 2H); 7.91-7.98(m, 4H)

^{13}C NMR (100.5MHz; $CDCl_3$, δ): 123.45; 124.16; 126.37; 129.83; 132.67; 143.33

(j) Dibenzothiophene sulfone: Isolated as white solid; mp 231-232°C; ν (KBr)/cm^{-1} 1363, 1165;

^{1}H NMR (400MHz; $CDCl_3$, δ): 7.51-7.55(m, 2H); 7.61-7.66(m, 2H); 7.77-7.85(m, 4H)

^{13}C NMR (100.5MHz; $CDCl_3$, δ): 121.54; 121.97; 130.16; 131.53; 133.77; 137.62

(k) Phenylvinylsulfoxide: Isolated as pale yellow liquid; ν (KBr)/cm^{-1} 1054;

^{1}H NMR (400MHz; $CDCl_3$, δ): 5.94(d, 1H, J=10.13Hz); 6.26(d, 1H, J=15.89Hz); 6.55-6.69(m, 1H); 7.27-7.37(m, 1H); 7.44-7.53(m, 2H); 7.62-7.68(m, 2H)

^{13}C NMR (100.5MHz; $CDCl_3$, δ): 120.55; 124.52; 129.38; 131.13; 142.95; 143.41

(l) Phenylvinylsulfone: Isolated as white solid; mp 63-64°C; ν (KBr)/cm^{-1} 1364, 1161;

^{1}H NMR (400MHz; $CDCl_3$, δ): 6.11(d, 1H, J=9.60Hz); 6.43(d, 1H, J=16.42Hz); 6.64-6.78(m, 1H); 7.44-7.51(m, 1H); 7.56-7.68(m, 2H); 7.87-7.93(m, 2H)

^{13}C NMR (100.5MHz; $CDCl_3$, δ): 127.85; 129.33; 133.77; 138.51; 139.70

(m) 2-(Phenylsulfinyl)ethanol: Isolated as light brown solid; mp 42-43°C; ν (KBr)/cm^{-1} 1040;

^{1}H NMR (400MHz; $CDCl_3$, δ): 2.43(s, 1H); 3.12(t, 2H, J=5.31Hz); 3.87(t, 2H, J=5.26Hz); 7.26-7.39(m, 1H); 7.48-7.57(m, 2H); 7.61-7.68(m, 2H)

^{13}C NMR (100.5MHz; $CDCl_3$, δ): 56.15; 60.91; 125.47; 129.98; 131.23; 144.55

(n) Dihexylsulfoxide: Isolated as pale yellow liquid; ν (KBr)/cm^{-1} 1042;

^{1}H NMR (400MHz; $CDCl_3$, δ): 0.95 (t, 6H, J= 7.65 Hz), 1.21-1.37 (m, 12H), 1.68 (m, 4H), 2.71 (t, 4H, J=6.71Hz)

^{13}C NMR (100.5MHz; $CDCl_3$, δ): 13.54, 21.91, 32.85, 27.64, 28.53, 52.64

(o) Dihexylsulfone: Isolated as pale yellow liquid; ν (KBr)/cm^{-1} 1323, 1161;

^{1}H NMR (400MHz; $CDCl_3$, δ): 0.95 (t, 6H, J= 7.66 Hz), 1.21-1.38 (m, 12H), 1.91 (m, 4H), 3.36 (t, 4H, J=6.71Hz)

^{13}C NMR (100.5MHz; $CDCl_3$, δ): 13.48, 21.78, 32.64, 27.91, 26.45, 53.72

(p) Allylphenylsulfone: Isolated as pale yellow liquid; ν (KBr)/cm^{-1} 1318, 1144;

^{1}H NMR (400MHz; $CDCl_3$, δ): 3.91(dt, 2H, J= 7.19, 1.22Hz); 5.02(dq, 1H, J= 1.48, 17.21Hz); 5.18(dq,1H, J= 1.22, 10.31Hz); 5.63(ddt, 1H, J= 7.19, 10.31, 17.21Hz); 7.37-7.44(m, 1H); 7.62-7.69(m, 2H); 7.91-7.95(m, 2H)

^{13}C NMR (100.5MHz; $CDCl_3$, δ): 60.67; 117.51; 124.63; 128.88; 129.02; 133.74; 138.27

(q) Ethylphenylsulfoxide: Isolated as pale yellow liquid; ν (KBr)/cm^{-1} 1054;

^{1}H NMR (400MHz; $CDCl_3$, δ): 1.23(t, 3H, J=6.61Hz); 2.69-2.78(q, 1H, J=6.61Hz); 2.91(q, 1H, J=6.61Hz) 7.13-7.48(m, 3H); 7.49-7.84(m, 2H)

^{13}C NMR (100.5MHz; $CDCl_3$, δ): 10.39, 47.19, 125.42, 129.85, 131.47, 145.69

(r) Ethylphenylsulfone: Isolated as white solid; mp > 261 °C; ν (KBr)/cm^{-1} 1322, 1153;

^{1}H NMR (400MHz; $CDCl_3$, δ): 1.30(t, 3H, J=7.11Hz); 3.09(q, 2H, J=7.11Hz); 7.59(m, 3H); 7.99(m, 2H)

^{13}C NMR (100.5MHz; $CDCl_3$, δ): 7.34, 50.28, 127.86, 128.92, 133.47, 138.31

(s) Diphenyl sulfoxide: Isolated as white solid; mp 70 °C; ν (KBr)/cm^{-1} 1043;

^{1}H NMR(400MHz; $CDCl_3$, δ): 7.63-7.68(m, 4H), 7.43-7.51(m, 6H)

^{13}C NMR (100.5MHz; $CDCl_3$, δ): 144.71, 129.87, 128.23, 123.71

(t) Diphenyl sulfone: Isolated as pale yellow solid; mp 127°C; ν (KBr)/cm^{-1} 1322, 1155;

^{1}H NMR(400MHz; $CDCl_3$, δ): 7.91-7.99(m, 4H),7.44-7.53(m, 6H)

^{13}C NMR (100.5MHz; $CDCl_3$, δ): 141.77, 133.20, 129.32, 127.69

(u) Benzylphenylsulfoxide: Isolated as white solid; mp 120 °C; ν (KBr)/cm^{-1} 1033;

^{1}H NMR (400MHz; $CDCl_3$, δ): 3.98(s, 2H), 6.93-7.11(m, 5H), 7.17-7.36(m, 3H), 7.42-7.55(m, 2H)

^{13}C NMR (100.5MHz; $CDCl_3$, δ): 63.44, 124.21, 128.15, 128.24, 128.57, 128.87, 130.26, 130.83, 142.59

(v) Benzylphenylsulfone: Isolated as white solid; mp 143 °C; ν (KBr)/cm^{-1} 1328, 1159;

^{1}H NMR (400MHz; $CDCl_3$, δ): 4.41(s, 2H), 7.06-7.14(m, 5H), 7.32-7.41(m, 3H), 7.65-7.74(m, 2H)

^{13}C NMR (100.5MHz; $CDCl_3$, δ): 62.53, 128.31, 128.39, 128.47, 128.61, 130.53, 133.44, 137.49

(w) 2-(Phenylsulfonyl)ethanol: Isolated as white solid; mp 96-97°C; ν (KBr)/cm^{-1} 1334, 1152;

^{1}H NMR (400MHz; $CDCl_3$, δ): 2.47(s, 1H); 3.33(t, 2H, J=5.46Hz); 3.95(t, 2H, J=5.26Hz); 7.44-7.53(m, 1H); 7.57-7.68(m, 2H); 7.89-7.97(m, 2H)

^{13}C NMR (100.5MHz; $CDCl_3$, δ): 57.35; 61.56; 128.92; 129.58; 134.06; 140.71

(x) Allylphenylsulfoxide: Isolated as pale yellow liquid; ν (KBr)/cm^{-1} 1043;

^{1}H NMR (400MHz; $CDCl_3$, δ): 3.43(dt, 2H, J=7.11, 1.12Hz); 5.01(dq, 1H, J=1.42, 17.10Hz); 5.16(dq, 1H, J=1.12, 10.22Hz); 5.44(ddt, 1H, J=7.11, 10.22, 17.10 Hz); 7.26-7.31(m, 1H); 7.36-7.39(m, 2H); 7.60-7.64(m, 2H)

^{13}C NMR (100.5MHz; $CDCl_3$, δ): 60.36; 117.93; 124.71; 125.09; 129.06; 131.24; 142.13

Splitting patterns are designated as s (singlet), d (dublet), t (triplet), dt (double triplet), ddt (double-double triplet), q (quartet), dq (double quartet), m (multiplet).

CHAPTER 6

Polymer Bound Peroxomolybdate as Catalysts or Reagents for Environmentally Safe Organic Bromination

6.1 INTRODUCTION

Bromination of organic compounds has been an area of tremendous contemporary interest mainly due to the commercial importance of bromo-organics.[1-10] Numerous industrially valuable products such as pesticides, insecticides, herbicides, fire retardants, and other new materials carry bromo functionality.[11,12] The halogenated organic compounds are in fact, being recognized as designer molecules for material science.[13] They are regarded as important precursors to a number of species useful in the synthesis of natural products and pharmaceutically important compounds.[14] In addition, the bromo-organics may undergo C-C coupling reactions via Stille and Suzuki transmetallation processes,[15-21] Heck[22-26] and Sonogashira[27-30] or carbon-heteroatom bond formation.[31-34]

The conventional synthesis of bromoorganics require the use of elemental bromine which is toxic, corrosive and difficult to handle due to its high reactivity, leading to highly exothermic and nonselective reactions giving only 50% of bromine atom efficiency.[34-36] Additional problems arise from using chlorinated solvents and the release of corrosive HBr as a by-product which are environmentally hazardous and toxic.[3,13,34-41] Alternative safer stoichiometric brominating agents such as, N-bromosuccinimide (NBS),[42,43] N-bromoacetamide (NBA),[44] or bromodimethylsulfonium bromide are although useful,[45] however, high cost and organic waste generation associated with these reagents limit their synthetic utility. A few polymeric reagents were reported to be

effective as halogenating agents under relatively milder conditions, nevertheless, their preparation require specific polymer backbone and direct contact with bromine.[46,47] Therefore, there remains a pressing need for alternative environmentally benign bromination protocols,[48-54] which can mimic the biological bromoperoxidation for the synthesis of brominated organics.[2,50]

Vanadium Bromoperoxidases (V-BPO), the enzymes, present in several marine organisms, involved in the biosynthesis of a variety of naturally occurring brominated products, catalyze bromination by using H_2O_2 and bromide salts instead of Br_2.[41,55] The enzymes function explicitly in catalyzing rate determining bromide oxidation to generate an oxidized bromine species capable of transferring bromine atoms to acceptor molecules with electron rich π bonds.[48]

Aqueous H_2O_2 is capable of oxidizing bromide on its own in highly acidic medium (pH < 3), but is ineffective in solution at pH > 5.0 and often require to be activated by homogeneous or heterogeneous catalysts. This feature has provided impetus to attempt to create synthetic V-BPO mimics leading to the development of plethora of useful catalyst based mainly on d^0 complexes such as vanadium,[5,39,56-64] molybdenum,[65-70] tungsten[2,3,65,71,72] or rhenium.[73] Sakurai and Tsuchia,[74] for the first time reported a vanadium based biomimetic functional model of bromoperoxidase using vanadyl sulfate, H_2O_2 and KBr in a phosphate buffer medium of pH 6.0. In the late 90s, Conte et al.[52,75-78] reported an interesting catalytic method of bromination of aromatic compounds by KBr, H_2O_2 and Na_2MoO_4 envisaged in a manner similar to the bio-halogenation performed by haloperoxidase enzymes. Interestingly, it has been observed that molybdate exhibits superior bromoperoxidase activity than the vanadate.[11,79] In the subsequent years, a large number of vanadium, molybdenum and tungsten based functional models have been

synthesized.[51,53,54,62] Nevertheless, scope for improvement still remains owing to some of the disadvantages associated with the available protocols. For instance, in contrast to natural V-BPO which is most efficient at pH 5.5–7 most of the model complexes reported, were found to be catalytically active only in presence of acid.[48-54,74,76,80] These acids, although readily available and cheap, are difficult to separate from organic products and lead to production of large volumes of hazardous wastes.[41,81-83]

Our group has a long standing interest in developing functional mimics of haloperoxidases with an ability to mediate organic oxidations under mild condition.[84-91] A number of monomeric and dimeric peroxovanadium (pV) and peroxotungsten (pW) complexes,[84-91] and a polymer-anchored peroxovanadium (pV) compound,[92] has been generated which proved to be effective oxidants of bromide with good activity at ambient temperature and neutral pH, an essential requirement of a biomimetic model.[84,89-91] However, much remains yet to be explored on activity of pMo complexes supported or free, in oxidative bromination.

Inspired by the above findings, in the present work we have directed our efforts to explore the synthetic scope of pMo complexes immobilized on **MR** or PAN, **3.1 – 3.3** as heterogeneous catalysts in oxidative bromination of organic substrates under ecologically suitable reaction conditions.

An additional concern was to explore the activity of the water soluble compounds with diperoxomolybdenum moieties in bromide oxidation in aqueous medium with an aim to pursue biomimetic chemistry of bromoperoxidase. With the increase in different environmental safety regulations, the water based reactions are gaining importance in different catalytic reactions.[93,94] Catalytic properties of water soluble synthetic polymers have long been a subject of considerable interest, which was inspired by the investigation

of enzyme action mechanism.[95] Normally, organic solvents are conventional media for catalytic reactions. A number of studies based on biomimetic approaches for construction of synthetic macromolecular enzyme models used water, the natural medium of enzymes.[93,96-98]

The results of our investigation incorporated in **Chapter 6**, have been distributed over two sections. The activity of the insoluble polymer supported complexes **$[MoO_2(O_2)(valine)_2]^{2-}$–MR** (**3.1**), **$[MoO_2(O_2)(alanine)_2]^{2-}$–MR** (**3.2**) and **$[MoO_2(O_2)(CN)_2]$-PAN** (**3.3**) as heterogeneous catalysts in the oxidative bromination of several activated aromatics to afford the corresponding bromoorganics constitute the subject matter of **Section A**. The main focus of **Section B** is the efficient stoichiometric oxidative bromination of the organic substrate by water soluble polymer bound pMo compounds, **$[Mo_2O_2(O_2)_4$(carboxylate)]-PA** (**4.1**), **$[MoO(O_2)_2$(carboxylate)]-PMA** (**4.2**), **$[MoO(O_2)_2$(amide)]-PAm** (**4.3**) and **$[MoO(O_2)_2$(sulfonate)]-PS** (**4.4**) at physiological pH, in absence of H_2O_2.

6.2 Section A:

Insoluble pMo Complexes, 3.1-3.3 as Heterogeneous Catalysts in Oxidative Bromination by H_2O_2

6.2.1 EXPERIMENTAL SECTION

6.2.1.1 Bromination of organic substrates with H_2O_2 catalyzed by PANMo, MRAMo and MRVMo and product analysis

Organic substrate (1.0 mmol) was added to a solution of acetonitrile:water (1:1, 5 mL) containing KBr (4.0 mmol) and 30% H_2O_2 (16.0 mmol) in a 50 mL two necked round-bottomed flask. A weighed amount of the solid compound viz. **PANMo** (0.129 g, 0.1 mmol Mo) or **MRAMo** (0.263 g, 0.1 mmol Mo) or **MRVMo** (0.217 g, 0.1 mmol Mo) maintaining metal:substrate, substrate:Br^- and Br^-:H_2O_2 at 1:10, 1:4 and 1:4, respectively was then added to the reaction mixture at room temperature under continuous stirring. The progress of the reaction was monitored by TLC. After completion of the reaction the products as well as unreacted organic substrate were then extracted with diethyl ether and dried over anhydrous Na_2SO_4. Products were then separated by TLC and HPLC. ^1H NMR spectroscopy and melting point determinations were made to interpret the products [see **Appendix 6A**].

6.2.1.2 Regeneration and reuse of the catalysts

Regeneration of the insoluble compounds, **PANMo**, **MRAMo** and **MRVMo** was achieved by separating the spent catalyst, after completion of the reaction, by centrifugation followed by washing with acetone and drying *in vacuo* over concentrated sulfuric acid. The catalyst was then placed into a fresh reaction mixture containing the substrate (1.0 mmol), KBr (4.0 mmol) and 30% H_2O_2 (16.0 mmol) in acetonitrile:water (1:1, 5 mL). The process was repeated up to 6^{th} reaction cycle.

In an alternative, yet equally effective, procedure adopted for regeneration of the catalysts, the spent reaction mixture remaining in the reaction vessel after separating the

organic reaction product, was charged with fresh substrate, KBr, H_2O_2 and acetonitrile and then the experiment was repeated.

6.2.2 RESULTS AND DISCUSSION

Catalytic performances of the immobilized complexes **PANMo (3.3)**, **MRVMo (3.1)** and **MRAMo (3.2)** in oxidative bromination of a series of aromatic compounds have been explored. Based on the results of trial runs, the reaction conditions were initially optimized.

6.2.2.1 Optimization of reaction conditions

For optimization of reaction condition, aniline has been used as the model substrate, potassium bromide as bromide source and **PANMo** as catalyst (Table 6.1). The reactions were conducted at room temperature (RT) under magnetic stirring.

6.2.2.1.1 The influence of the amount of KBr and H_2O_2

The reaction of the substrate with potassium bromide (2 equivalents), in presence of the terminal oxidant H_2O_2 (2 equivalents) and Mo:substrate molar ratio maintained at 1:10, was observed to proceed smoothly in CH_3CN:H_2O (1:1) with 100% conversion of the substrate [Table 6.1, entry 1] to afford a mixture of ortho- and para-bromo aniline, with the p–substituted aniline as the predominant product.

Enhancement of the rate of conversion was observed on increasing the substrate:bromide ratio to 1:4 leading to an increase of TOF to 16.28 h^{-1} [Table 6.1, entry 2]. The TOF could further be improved by increasing the amount of H_2O_2 to 4 equivalents with respect to bromide [Table 6.1, entry 4]. However, it was observed that increase in

molar ratio of Br:H_2O_2 beyond 1:4 had no observable effect on rate of reaction. We have therefore carried out the subsequent reactions by maintaining the Br:oxidant ratio at 1:4. It is also notable that rate of the reaction was found to be reduced substantially when Et_4NBr was used as source of bromide instead of KBr [Table 6.1, entry 8].

6.2.2.1.2 Effect of catalyst amount

The effect of catalyst amount has also been evaluated. A two fold increase in the amount of the catalyst although slightly speeded up the reaction, the corresponding TOF was observed to decrease [Table 6.1, entry 5]. On the other hand, decreasing the amount of catalyst reduced the rate, as well as TOF of reaction [Table 6.1, entry 6]. A catalyst:substrate ratio of 1:10 was thus found to be most conducive for the synthesis.

That the catalyst **PANMo** plays a crucial role in facilitating the desired reactions was apparent from a control experiment conducted in absence of the catalyst. Very little conversion of aniline was recorded (< 5%) under the optimized condition in absence of the catalyst [Table 6.1, entry 10].

It is notable that a nearly two fold increase in TOF of the reaction was observed when conducted in presence of perchloric acid at a highly acidic pH [Table 6.1, entry 9]. In the present study, however, we have strategically maintained a mild reaction condition by avoiding addition of acid or other additives, as far as possible.

6.2.2.1.3 Effect of temperature

We have carried out the reactions at two different temperatures, viz. room temperature (RT) and 78 °C in refluxing acetonitrile. A significant increase in TOF was noted when the reaction was carried out at 78 °C [Table 6.1, entry 7].

6.2.2.1.4 Bromination of organic substrates catalyzed by 3.1-3.3

In order to explore the prospect of using the developed methodology for bromination of other substrates, a series of structurally diverse activated aromatics were subjected to the oxidative bromination by H_2O_2-Br^- system under the optimized reaction conditions. The data presented in Table 6.2 show that each of the compounds, **PANMo, MRAMo** as well as **MRVMo**, efficiently catalyzed the bromoperoxidation of the chosen substrates to the corresponding bromo-organics in impressive yield with good TOF. From the findings (Table 6.2) it is evident that the immobilized compounds exhibit comparable catalytic activity, although the catalyst **MRAMo** appears to show slightly superior activity in comparison to **PANMo** and **MRVMo**.

Table 6.1 Optimization of reaction conditions for **PANMo**[a] catalyzed oxidation of bromide by H_2O_2

Entry	Molar ratio			Temperature	Time (min)	Isolated Yield (%)	TOF (h^{-1})
	Mo:S	S:Br	Br:H_2O_2				
1	1:10	1:2	1:1	RT	40	96	14.40
2	1:10	1:4	1:1	RT	35	95	16.28
3	1:10	1:4	1:2	RT	30	96	19.20
4	**1:10**	**1:4**	**1:4**	**RT**	**25**	**97**	**23.27**
5	1:5	1:4	1:4	RT	20	95	14.24
6	1:20	1:4	1:4	RT	60	96	18.60
7	1:10	1:4	1:4	78 °C	20	98	29.40
8	1:10	1:4[b]	1:4	RT	55	95	10.36
9	1:10	1:4[c]	1:4	RT	15	96	38.40
10	---	1:4[d]	1:4	RT	30	< 5	

[a] All the reactions were carried out using 0.129 g catalyst (1.0 mmol Mo), aniline as substrate, KBr as bromide source and CH_3CN/H_2O (1:1, 5 mL) as solvent unless otherwise stated.

[b] Et_4NBr used as bromide source.

[c] Using $HClO_4$ (4 equivalents of substrate).

[d] Control reaction: aniline (1.0 mmol), KBr (4.0 mmol), H_2O_2(16.0 mmol) and CH_3CN/H_2O (1:1, 5 mL).

Table 6.2 Bromination of organic substrates with H_2O_2 **catalyzed by MRAMo, MRVMo and PANMo**[a]

Entry	Substrate	Product	MRAMo			MRVMo			PANMo		
			Time (min)	Yield (%)	TOF[b] (h^{-1})	Time (min)	Yield (%)	TOF[b] (h^{-1})	Time (min)	Yield (%)	TOF[b] (h^{-1})
1	Aniline	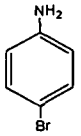	15	82	38.4	20	84	29.1	25	83	23.27
		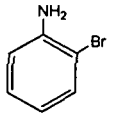		14			13			14	
2	p-aminophenol	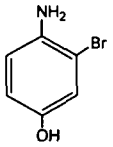	35	94	16.1	40	96	14.4	45	95	12.66
3	m-aminophenol	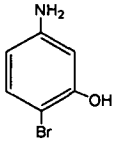	30	81	19.6	35	81	15.9	40	75	14.39
		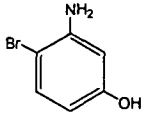		17			12			20	
4	o-aminophenol	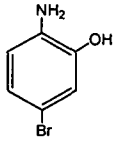	35	96	16.4	40	95	14.2	45	97	12.93

Continued...

Entry	Substrate	Product	MRAMo			MRVMo			PANMo		
			Time (min)	Yield (%)	TOF[b] (h^{-1})	Time (min)	Yield (%)	TOF[b] (h^{-1})	Time (min)	Yield (%)	TOF[b] (h^{-1})
5	p-nitroaniline	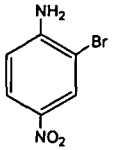	55	83	10.1	60	85	9.8	60	84	9.70
		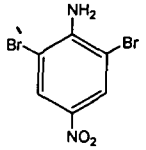		10			13			13	
6	m-nitroaniline	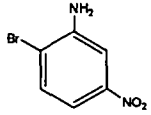	45	82	12.5	50	82	11.6	50	83	11.80
		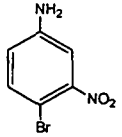		12			15			15	
7	o-nitroaniline	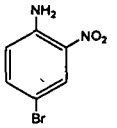	55	86	10.5	60	83	9.6	60	85	9.60
		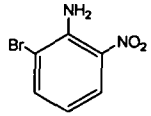		11			13			11	
8	Quinol	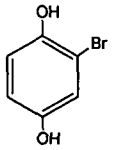	100	95	5.7	110	97	5.3	120	97	4.85

Continued...

Entry	Substrate	Product	MRAMo			MRVMo			PANMo		
			Time (min)	Yield (%)	TOF[b] (h^{-1})	Time (min)	Yield (%)	TOF[b] (h^{-1})	Time (min)	Yield (%)	TOF[b] (h^{-1})
9	Pyrogallol	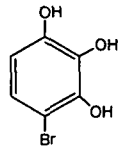	70 (70)	97 (96)	8.3 (8.2)	75 (75)	96 (93)	7.6 (7.4)	80 (80)	97 (96)	7.29 (7.21)
10	Resorcinol	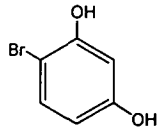	190 (190)	96 (97)	3.0 (3.1)	200 (200)	98 (96)	2.9 (2.8)	210 (210)	95 (94)	2.71 (2.68)
11	Acetanilide	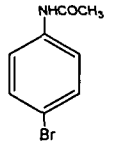	85	94	6.6	90	95	6.3	90	97	6.46
12	Salicylaldehyde	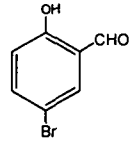	130 (130)	95 (96)	4.3 (4.4)	140 (140)	98 (97)	4.2 (4.1)	150 (150)	97 (95)	3.88 (3.80)
13	o-methoxytoluene	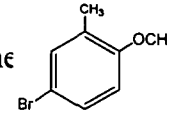	60	93	9.3	65	96	8.8	70	95	8.18
14	Catechol	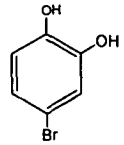	110	96	5.2	120	95	4.7	120	94	4.70

[a]All reactions were carried out with 1.0 mmol substrate, 4.0 mmol KBr, 16.0 mmol 30 % H_2O_2 and compound (containing 0.1 mmol Mo) in CH_3CN/H_2O (1:1, 5 mL) at RT.

[b]TOF (Turnover frequency) = mmol of product per mmol of catalyst per hour.

[c]Yield of 6th reaction cycle (values within the parenthesis).

6.2.2.2 Evidence for electrophilic bromination

The observation that the bromination occurred preferentially at either ortho or para position of the aromatic ring giving mono substituted product in each case (Table 6.2) suggested an electrophilic bromination mechanism. Further evidence in support of the involvement of an oxidized bromine species as the brominating agent instead of a $Br^{\bullet}$ radical was apparent from the ring substituted product, bromo-methoxy toluene[53] (Table 6.2, entry 13) obtained from the substrate 2-methoxytoluene. Bromination through radical reaction would have produced benzyl bromide instead of bromo-methoxy toluene[53] (Fig. 6.1).

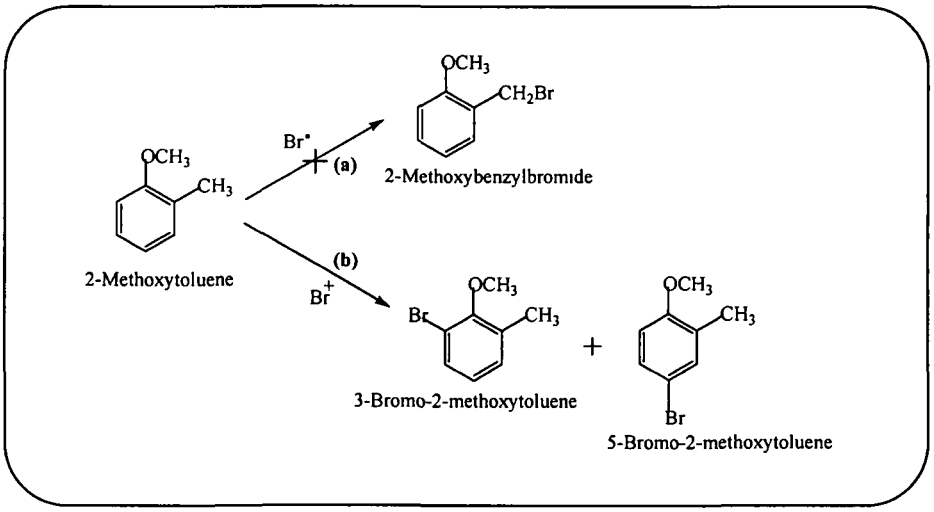

Fig. 6.1 Bromination reaction of 2-methoxytoluene. (a) Possible product of bromination through radical reaction, (b) electrophilic bromination involving 'Br^{+}' forms exclusively ring substituted products. Bromination reaction using pMo compounds produces exclusively bromomethoxytoluene.

6.2.2.3 Test for heterogeneity of the reaction

It was necessary to ascertain the heterogeneous nature of the insoluble catalysts, **3.1-3.3** and to test the leaching of the metal complexes from the polymer-bound catalysts into the reaction medium during the oxidation reactions. We have therefore carried our

experiments using salicylaldehyde as the substrate with the catalysts under optimized reaction condition. The filtrate obtained by separating the solid catalyst after completion of the reaction was transferred to a reaction vessel and the reaction was allowed to continue for another 5 h, by adding fresh salicylaldehyde, KBr and H_2O_2. The reaction afforded product yield of < 5%, which is comparable to the conversion obtained in absence of any catalyst. The results are in accord with the occurrence of a purely heterogeneous catalytic process.[99,100]

6.2.2.4 Regeneration and reuse of the catalysts

Each of the heterogeneous catalysts, **PANMo, MRAMo** and **MRVMo** could be recovered and recycled without further conditioning, after separating it from the spent reaction mixture after completion of each cycle of bromination, by charging it with H_2O_2, a fresh lot of substrate and bromide. It has been found that the catalyst remains effective upto a minimum of six reaction cycles without further treatment with any reagent [Table 6.2, entries 9^c, 10^c and 12^c]. However, in case of highly basic substrates like aniline and nitroaniline, it was observed that catalytic activity of **PANMo** gradually decreases. This observation may not be unusual, since nitrile group of PAN is known to be oxidation prone in presence of H_2O_2 to form amide in alkaline medium at pH > 7.5.[101,102] This change in the nature of polymer anchored ligand group of the catalyst is likely to lead to leaching of the pMo moieties from the polymer matrix resulting in the loss of its catalytic activity. The fact that no such decrease in activity towards bromination of basic substrates occur in case of **MRAMo** and **MRVMo**, lend credence to our hypothesis.

6.2.2.5 Nature of the spent catalyst

After completion of the reaction, the spent catalysts, **3.1-3.3** were isolated and subjected to elemental, EDX and IR spectral analysis. The peroxide and molybdenum content in the spent catalysts remained unchanged in comparison to those of the fresh catalysts. IR spectra of the spent catalysts displayed no change in characteristic bands for metal-peroxo and complexed carboxylate or nitrile groups with those observed in the original catalysts. This provides the evidence that the molybdenum centres are intact and the coordination environments were not altered during the catalytic reaction. Additionally, the catalysts are found to be stable even after several cycles of reaction.

6.2.2.6 The proposed mechanism mediated by complexes 3.1-3.3

A scheme of reactions, shown in Fig. 6.2 using **PANMo** as a representative, is proposed which is based on our results and work of some other laboratories.[65,70,84,85,103-105] In case of the oxidative bromination, heterogeneously catalyzed by monoperoxomolybdate complexes, **3.1-3.3** with H_2O_2 as terminal oxidant, the first step is possibly the formation of (Fig. 6.2) bromination competent diperoxomolybdate species **II** from the reaction of species **I** with H_2O_2. Species **I** is inactive as stoichiometric oxidant of bromide on its own. The reactive diperoxo intermediate then oxidizes bromine leading to subsequent bromine transfer to form bromo-organics (reaction c). The reaction is accompanied by the regeneration of the starting monoperoxomolybdenum complex (reaction b).

The proposed reaction pattern is in agreement with our previous findings[84,85] on pW complex as well as observations of others that for a peroxomolybdate or peroxotungsten complex to be active in oxidation an oxo-diperoxo configuration may be a principal requirement.[70,84,103,104] Involvement of monoperoxo Mo(VI) or W(VI) as

intermediate has been previously proposed by Reynolds et al.[70] as well as by Butler and co-workers[65] in the Mo(VI) and W(VI) catalyzed bromide oxidations. The aforementioned considerations lend further support to the proposed scheme. It is reasonable to expect that bromide would attack an edge-bound peroxo group in preference to a hepta co-ordinated molybdenum or tungsten centre as observed in some other redox processes involving peroxo compounds of W(VI) and Mo(VI).[70,104,105]

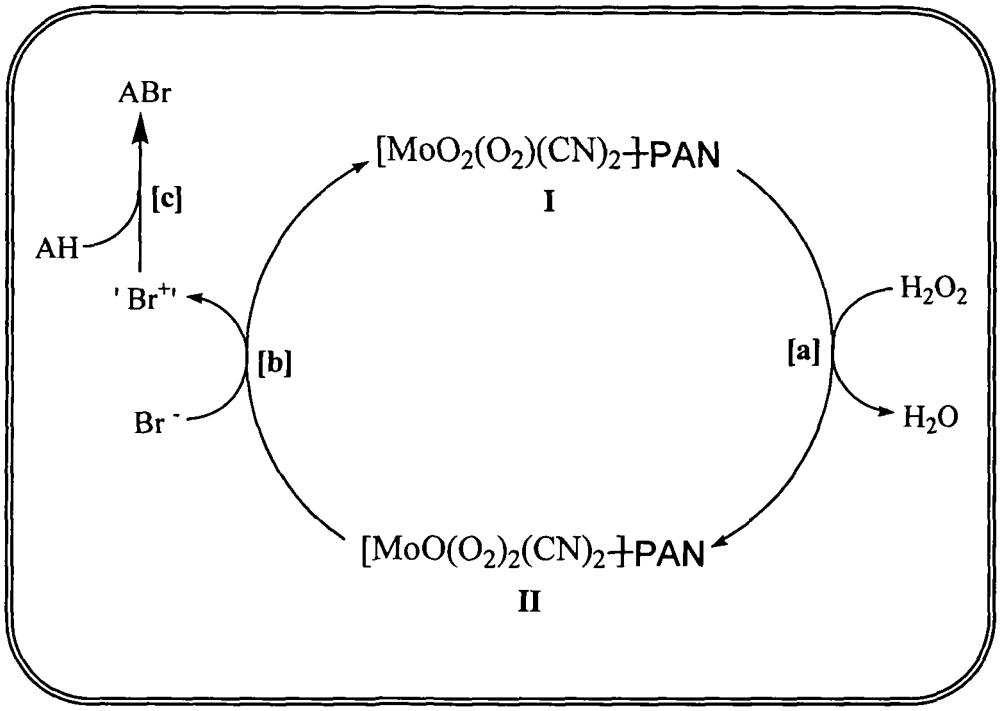

Fig. 6.2 The proposed mechanism shown with **PANMo** as a representative. (a) In presence of excess H_2O_2 the polymer-bound monoperoxo species **I** combines with peroxide to form the reactive diperoxomolybdate intermediate **II**; (b) reaction of the diperoxo intermediate **II** with bromide to yield oxidized bromine with concomitant regeneration of the original catalyst; (c) transfer of bromine from the active species to acceptor AH. The monoperoxo species **I** formed combines with H_2O_2 to regenerate the active diperoxomolybdate intermediate **II** giving rise to a catalytic cycle. No attempt is made to show the exact stoichiometry of the reaction.

6.3 Section B:

Water Soluble pMo Compounds, 4.1-4.4 as Stoichiometric Reagents for Oxidative Bromination

6.3.1 EXPERIMENTAL SECTION

6.3.1.1 Measurement of bromination activity in water

The method of de Boer et al.[106] of introducing four bromine atoms into the molecule of phenol red (ε^{433} mM=19.7) to form a bromophenol blue (ε^{592} mM = 67.4) was used to measure bromination activity. In case of water soluble polymeric compounds, viz. **PAMo (4.1)**, **PMAMo (4.2)**, **PAmMo (4.3)** or **PSMo (4.4)** the reaction mixture contained phosphate buffer (50 mM, pH 5.5), KBr (1 M) and phenol red (20 μM). The redox activity was tested by adding a measured amount of aliquot from complex solution and by monitoring the possible change in the absorbance at 592 nm at 30 °C. The volume of the reaction mixture was kept at 25 mL. Aliquots were transferred to the spectrophotometer immediately after mixing.

6.3.1.2 Bromination activity of PAMo, PMAMo, PAmMo and PSMo in aqueous - organic medium and product analysis

In a representative procedure, substrate (0.5 mmol) was added to a solution of acetonitrile:water (1:1, 5 mL) containing Et_4NBr (1 mmol) in a 50 mL two necked round-bottomed flask. A weighed amount of solid polymeric compounds, **4.1-4.4** maintaining substrate:pMo at 1:1 was then added to the reaction mixture at room temperature under continuous stirring. The progress of the reaction was monitored by TLC. After completion of the reaction the products as well as unreacted organic substrates were then extracted with diethyl ether and dried over anhydrous Na_2SO_4. Products were then separated by TLC and HPLC. ^1H NMR spectroscopy and melting point determinations were made to interpret the products [See **Appendix: 6A**].

6.3.1.3 Regeneration of the reagents

The regeneration and reusability of the water soluble reagents viz., **PAMo (4.1)**, **PMAMo (4.2)**, **PAmMo (4.3)** and **PSMo (4.4)** were tested by using p-nitroaniline as model substrate. In the typical procedure, the reaction mixture contained the same recipe mentioned above with a 4-fold increase in the amounts of the components. In order to regenerate the compounds, **4.1-4.4** after completion of the reaction, the following method has been adopted. After extraction of the organic reaction product, the aqueous part of the reaction mixture was transferred to a 250 mL beaker. Keeping the solution in an ice bath, 2 mL H_2O_2 was added to it maintaining the Mo:peroxide at 1:4 followed by addition of excess DMF with constant stirring until a white pasty mass separated out. After allowing it to stand for 10 min in the ice bath, the supernatant liquid was decanted off and the residue was treated repeatedly with DMF and distilled acetone until it became white microcrystalline solid. The product was separated by centrifugation, washed with cold acetone and dried *in vacuo* over concentrated sulfuric acid.

6.3.2 RESULTS AND DISCUSSION

6.3.2.1 Bromination in aqueous solution

Having gained an access to the water soluble macrocomplexes with pMo species and water being the prospective environment friendly solvent for 'green' chemistry perspective,[94] we have evaluated the activity of the complexes in oxidative bromination of a variety of activated aromatics in aqueous-organic medium. Work from several laboratories has shown earlier that peroxomolybdenum compounds with oxodiperoxo configuration could serve as effective oxidants in various organic transformations.[65,70,104,107-113] Since the compounds **4.1-4.4** contain

oxodiperoxomolybdate moieties, we were particularly interested to evaluate the oxidant activity of this class of complexes in bromination of organic substrate in absence of H_2O_2 or any other exogeneous oxidant. In the present study the method of de Boer et al.[106] was used to assess the bromination activity of the compounds in water, in line with our earlier work on peroxovanadium and peroxotungsten mediated bromination reactions.[84,89,90,92,114] Phenol red undergoes facile stoichiometric bromination to form its tetra brominated product bromophenol blue, which can be monitored conveniently using electronic spectroscopy (Fig. 6.3 and Fig. 6.4). The yellow colour of the standard reaction solution containing phenol red and bromide in phosphate buffer gradually changed to blue on addition of the freshly prepared aqueous solution of each of the compounds, **4.1-4.4** at concentrations indicated in Table 6.3. The spectrum recorded showed a decrease in absorbance of the peak at A_{433} and a new peak at A_{592} characteristic of the product bromophenol blue (Fig. 6.3). From the results summarized in Table 6.4, it is evident that each of the soluble pMo complexes, **4.1-4.4** possess bromination activity. Significantly, no additional H_2O_2 or any other oxidant is required for the bromination activity of the pMo complexes.

It is noteworthy that, a reaction conducted under identical condition without the substrate phenol red, displayed a peak at 262 nm with a shoulder at 237 nm on addition of solution of each of the compounds **4.1-4.4** (Fig. 6.5). Addition of phenol red to this solution led to the formation of bromophenol blue, as indicated by the appearance of peak at 592 nm and concomitant decrease in A_{262} nm. The 262 nm peak may therefore be ascribed to an oxidized species of bromide, active as brominating agent, likely to be an mixture of BrOH, Br_2 and Br_3^- equilibrium as proposed earlier.[48,53,65,70,115]

Interestingly, for each of the pMo complexes, the bromination activity was found to be only half of that expected on the basis of the total number of peroxo groups present

in the complexes. This implies that *ca.* 50% of the co-ordinated peroxide has been effective in bromination (Table 6.3). Moreover, this feature could not be altered by decrease or increase in concentrations of the compounds, substrate or KBr in the reaction solution. It is pertinent to mention that diperoxotungsten compounds were earlier found to behave similarly with respect to their activity in oxidative bromination as well as sulfide oxidation.[84,116] Most importantly, the immobilized compounds **3.1-3.3**, with monoperoxmolybdenum species, although highly efficient as catalyst in oxidative bromination, were found to be totally inactive as stoichiometric bromination agents as such, as has been anticipated.

Table 6.3 Bromination of phenol red with peroxomolybdate complexes **PAMo**, **PMAMo**, **PAmMo** and **PSMo** [a]

Compound	Concentration (mM Mo)	Rate of bromine transfer		Total bromine transfer (Extrapolated to 1mM compound)
		ΔA_{592}/min	μM Br/min	mM Br / mM Mo
PAMo	0.05	0.114	6.76	0.98
PMAMo	0.05	0.136	8.07	1.00
PAmMo	0.05	0.126	7.47	0.99
PSMo	0.05	0.120	7.12	0.98

[a] Reaction conditions: phosphate buffer (0.05 M, pH=5.5), phenol red (20μM), KBr (1 M), and compound (0.05 mM of Mo).

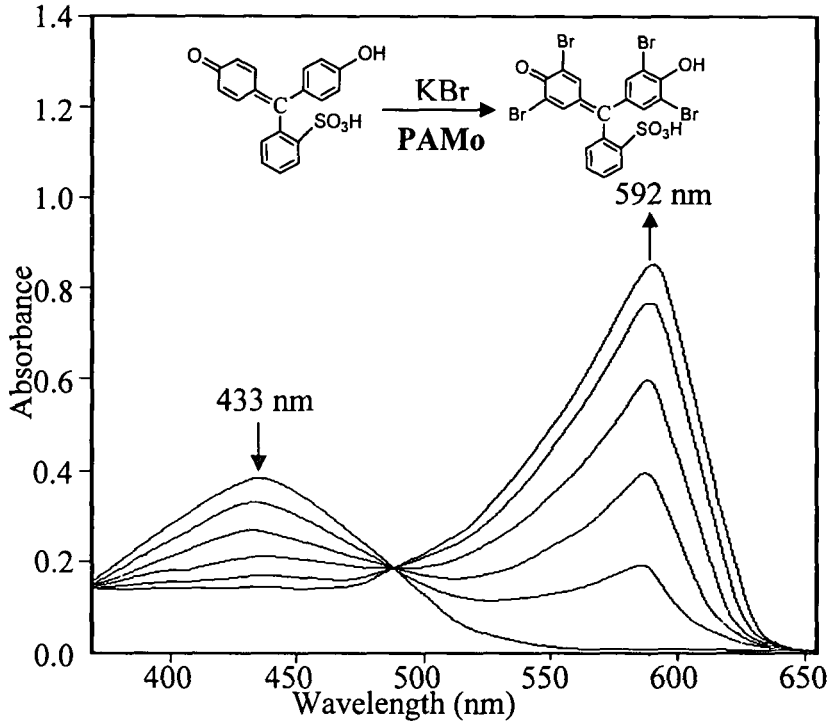

Fig. 6.3 Bromination activity with **PAMo**. Spectral changes at 2 min interval following bromination of phenol red to bromophenol blue on addition of compound solution to the reaction mixture containing phosphate buffer (0.05 M, pH 5.5), KBr (1 M) and phenol red (20 μM) and **PAMo** (0.05 mM of pMo).

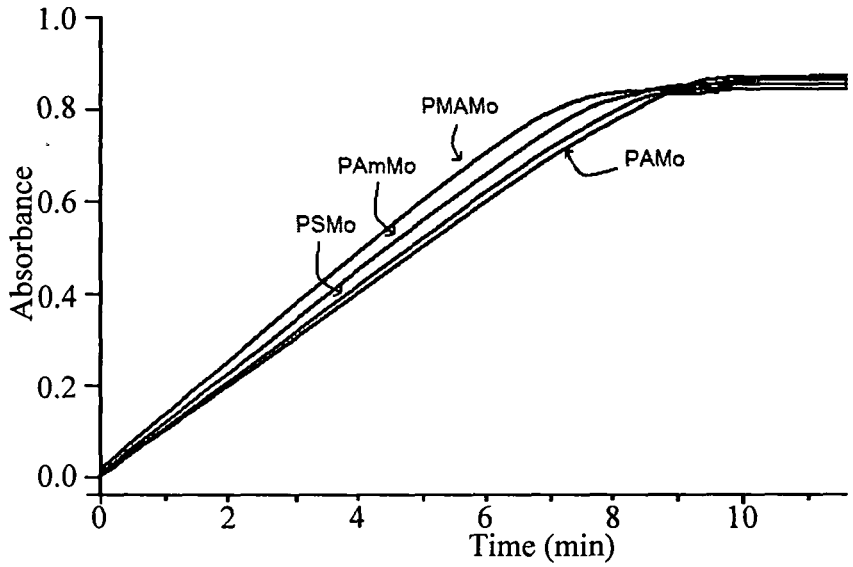

Fig. 6.4 Bromination activity with **PAMo**, **PMAMo**, **PAmMo** and **PSMo**. The reaction mixture contained phosphate buffer (0.05 M, pH=5.5), phenol red (20 μM), KBr (1 M), and compound (0.05 mM of pMo). Absorbance were measured at 592 nm.

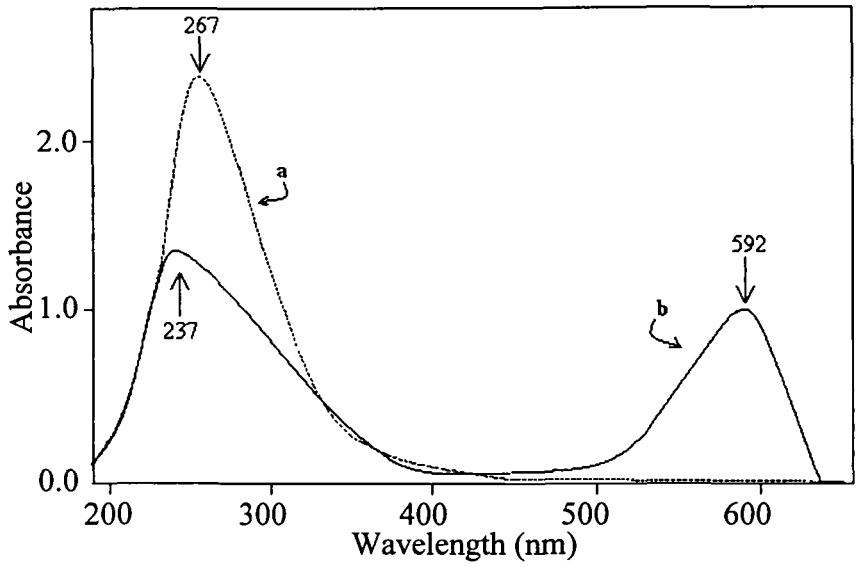

Fig. 6.5 Spectral changes following bromination of phenol red to bromophenol blue on addition of **PAMo** (**4.1**). The reaction mixture contained phosphate buffer (0.05 M, pH 5.5), KBr (1 M) and phenol red (20 μM) **PAMo** (0.05 mM of pMo). (a) KBr + compound in absence of phenol red (b) KBr + compound + phenol red.

6.3.2.1.1 Effect of pH

The effect of pH on bromination activity was assessed by conducting the reactions at pH 7.0, the physiological pH at which the bromoperoxidases function,[117] in addition to pH 5.5 as well as in absence of buffer at pH *ca.* 5.8, the natural pH of the reaction medium. The data presented in Table 6.3 were obtained by conducting the reactions at pH 5.5 because the employed procedure requires the pH to be maintained near 5.0 in order to achieve conversion from phenol red (pKa 7.9) to bromophenol blue (pKa 4.0). However, it was found that the presence of phosphate buffer was not essential for such activity of the peroxomolybdenum compounds as was evident from the reactions conducted separately by removing phosphate buffer from the reaction medium which

showed no change in the bromination activity of the complexes. The maximum activity of the compounds was observed at pH 7.0 (Fig. 6.6), a remarkable feature, which is in contrast to pV mediated oxidative bromination where the rate was reported to increase steadily with increasing acidity of the reaction medium.[118] A similar trend was observed earlier in case of bromination activity of pW complexes.[84]

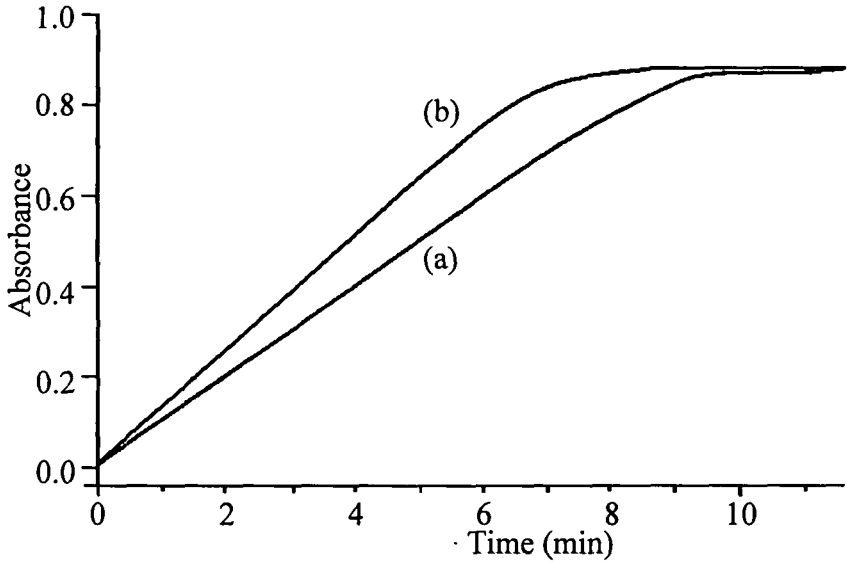

Fig. 6.6 Effect of pH on bromination activity of **PAMo**. The reaction mixture contained KBr (1 M), phenol red (20 μM) and compound PAMo (0.05 mM of pMo) in phosphate buffer (0.05 M) of pH 5.5 (a) and 7.0 (b). The absorbances were recorded at 592 nm.

6.3.2.1.2 Catalytic cycle in presence of H_2O_2

It is notable that each of the soluble pMo complexes, **4.1-4.4** act as stoichiometric oxidant of bromide and does not require additional H_2O_2 for their activity as evident from Table 6.3. Initial addition of H_2O_2 (0.5 mM) to the reaction solution had no significant effect on the initial rate of bromination (Table 6.3). On the other hand, addition of H_2O_2 (0.5 mM) to the reaction solution after completion of the reaction leads to a revival of bromination activity (Fig 6.7) giving rise to catalytic cycle. It may therefore be inferred

that an inactive molybdenum intermediate formed after completion of the stoichiometric bromination process, would combine with peroxide in presence of exogenous H_2O_2 to regenerate the respective diperoxomolybdenum species, active in bromination.

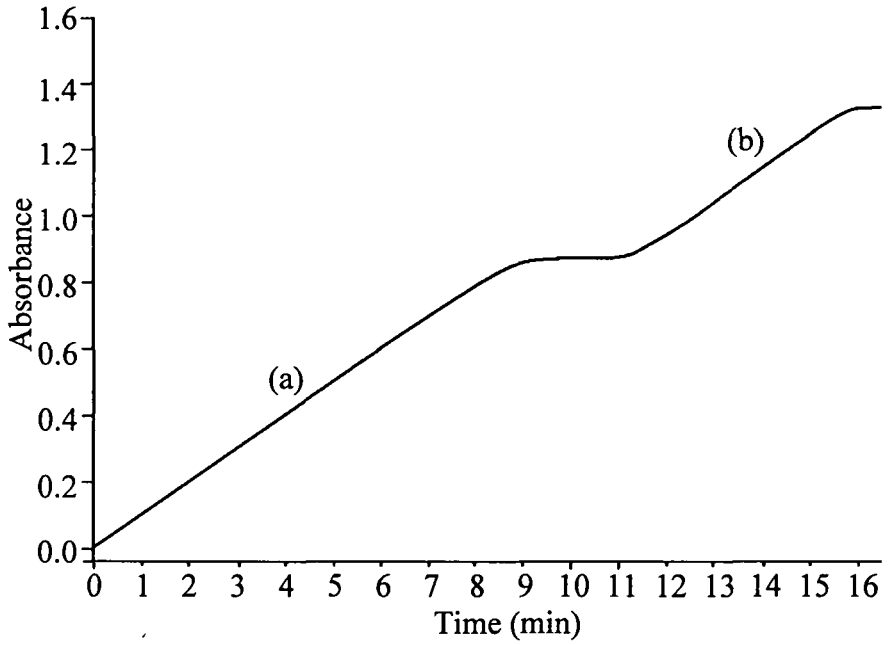

Fig 6.7 Revival of bromination activity of **PAMo** on addition of H_2O_2. (a) The reaction mixture contained phosphate buffer (0.05 M, pH=5.5), phenol red (20 μM), KBr (1 M), and compound (0.05 mM of pMo). (b) After addition of H_2O_2 (0.5 mM) to the spent reaction solution of (a). Absorbance was measured at 592 nm.

6.3.2.2 Peroxomolybdate induced substrate bromination in aqueous-organic media

The above interesting observations on bromination activity of the compounds **4.1-4.4** in aqueous medium prompted us to explore their efficacy in bromination of a variety of organic substrates under mild reaction condition. The results summarized in Table 6.5 show that each of the compounds, **4.1-4.4** efficiently mediated oxidative bromination of several activated aromatics into their corresponding bromo-organics. The reaction conditions were optimized by using aniline as model substrate, Et_4NBr as source of

bromide and **PAMo** as representative (Table 6.4). The reaction carried out at room temperature under mechanical stirring, maintaining a metal:substrate molar ratio of 1:1 using CH_3CN:H_2O (1:1) as solvent afforded the product in reasonably good yield, within 7-8 h. The rate of the reaction could further be enhanced by increasing the reaction temperature upto 78 °C (Table 6.4, entry 4). The bromination reactions induced by the compounds **4.1-4.4** follow the electrophilic bromination leading to the formation of ortho or para substituted product as was observed in case of heterogeneous pMo compounds, **3.1-3.3**. Furthermore, it is significant to note that in this case also only one of the peroxo group of the diperoxomolybdenum moiety was found to be active in bromination.

We have also attempted the catalytic oxidative bromination reaction with each of the reagents, **4.1-4.4** in presence of exogenous H_2O_2 by maintaining identical reaction conditions as mentioned under Section 6.2.1.1. However, the water soluble complexes **4.1-4.4**, in contrast to the heterogeneous analogues **3.1-3.3**, were catalytically incompetent in H_2O_2 induced oxidative bromination under the analogous reaction conditions.

Table 6.4 Optimization of reaction condition of **PAMo**[a] mediate oxidative bromination of aniline

Entry	Molar ratio		Temperature	Time (h)	Yield (%)
	Mo:S	S:Br			
1	0.5:1	1:2	RT	15.0	46
2	1:1	1:2	RT	7.0	94
3	1:1	1:4	RT	6.7	96
4	1:1	1:2	78 °C	3.0	91

[a] All reactions were carried out using aniline (0.5 mmol) as substrate in CH_3CN/H_2O (1:1) as solvent using Et_4NBr as source of bromide.

Table 6.5 Bromination of organic substrates mediated by **PAMo**, **PMAMo**, **PAmMo** and **PSMo** [a]

Entry	Substrate	Product	PAMo		PMAMo		PAmMo		PSMo	
			Time (h)	Yield (%)	Time (h)	Yield (%)	Time (h)	Yield (%)	Time (h)	Yield (%)
1	Aniline	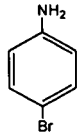	7.0	75	6.0	81	6.5	73	7.0	76`
		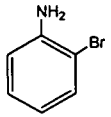		19		12		17		16
2	p-aminophenol	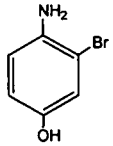	8.0	93	6.5	90	7.0	91	7.5	89
3	m-aminophenol	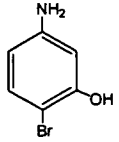	7.0	76	6.0	77	6.5	79	7.0	80
		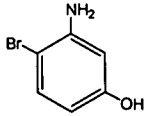		16		13		10		13
4	o-aminophenol	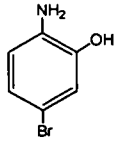	8.0	90	6.5	89	7.0	87	7.5	86

Continued...

Entry	Substrate	Product	PAMo		PMAMo		PAmMo		PSMo	
			Time (h)	Yield (%)	Time (h)	Yield (%)	Time (h)	Yield (%)	Time (h)	Yield (%)
5	p-nitroaniline	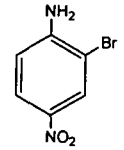	8.0	69	8.0	71	7.5	86	7.5	79
		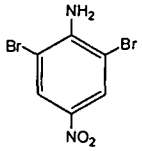		13		11		5		7
6	m-nitroaniline	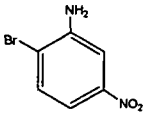	7.5	75	7.0	72	6.5	76	7.0	77
		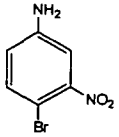		16		19		17		15
7	o-nitroaniline	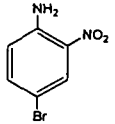	8.0	79	7.5	82	7.5	83	7.5	85
		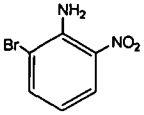		13		11		9		8
8	Quinol	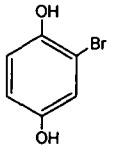	7.0	87	7.0	89	6.5	86	6.5	86

Continued...

Entry	Substrate	Product	PAMo		PMAMo		PAmMo		PSMo	
			Time (h)	Yield (%)	Time (h)	Yield (%)	Time (h)	Yield (%)	Time (h)	Yield (%)
9	Pyrogallol	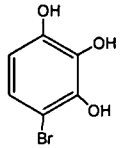	7.5	87	6.5	89	7.0	91	7.0	90
10	Resorcinol	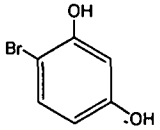	8.0	89	7.0	91	7.5	87	7.5	93
11	Acetanilide	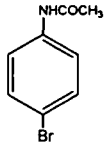	7.5	93	7.0	90	7.0	89	7.5	88
12	Salicylaldehyde	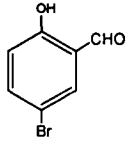	7.5	85	7.0	86	7.0	88	7.0	84
13	o-methoxytoluene	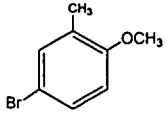	7.0	89	7.0	92	6.5	91	7.0	89
14	Catechol	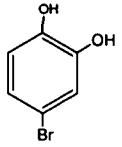	7.5	84	7.0	87	7.0	81	7.5	80

[a]All reactions were carried out with 0.5 mmol substrate, 1.0 mmol TEAB and compound (containing 0.5 mmol Mo) in CH_3CN/H_2O (1:1, 5 mL) at RT.

6.3.2.3 Regeneration of the reagents

Solvent induced precipitation followed by filtration are the most frequently used techniques for recovery of soluble supported catalysts from reaction mixtures.[119,120] Proper choice of the solvent which would serve as non-solvent to facilitate precipitation of the reagent, and temperature are crucial for satisfactory recovery of the soluble polymer.

The regeneration of the reagents, **4.1-4.4** was achieved by treating the aqueous extract of the spent reaction mixture with H_2O_2 maintaining the Mo:peroxide ratio at 1:4 and subsequent addition of DMF to this solution at ambient temperature. Each of the polymeric complexes are insoluble in DMF, whereas Et_4NBr used as a bromide source is soluble. Thus addition of excess DMF causes complete precipitation of the polymeric compound leaving behind Et_4NBr in the solution phase. Pertinent here is to mention that we have chosen Et_4NBr as bromide source due to this advantageous feature, although KBr was also equally effective as source of bromide. A fresh cycle of reaction conducted by using the recovered complex afforded the corresponding bromination product, demonstrating that the metal complex remains intact and active as oxidant after the first reaction cycle. However, with subsequent recycling, a slight decrease of product yield was observed which may be ascribed to leaching of molybdenum centers from the polymeric matrix. The addition of H_2O_2 was required in order to compensate for the peroxide consumed during the bromination reaction.

6.3.2.4 Identification of the molybdenum intermediate

In order to rationalize the reaction pathway involved in the stoichiometric bromination mediated by the supported diperoxomolybdenum compounds, **4.1-4.4** it was important to confirm the identity of the inactive molybdenum intermediate formed during the course of the reaction. The product obtained from the aqueous extract of the spent

reaction mixture, from experiments conducted separately using each of the complexes, **4.1-4.4** was studied by IR, ^{95}Mo NMR, EDX and elemental analysis. IR spectrum of each of the isolated compounds resembled the spectrum of the corresponding original compound indicating the presence of peroxo, oxo and coordinated polymeric ligands. However, the elemental analysis and EDX results proved that there was only one peroxo group per Mo centre in each case. Interestingly, ^{95}Mo NMR spectra of each of the isolated compound displayed a single resonance at *ca.* -120 ppm (relative to $[MoO_4]^{2-}$) which was absent in the spectra of the fresh compound. The disappearance of peak at *ca.* -220 ppm from the spectra of the original complex and formation of new peak at *ca.* -120 ppm indicates that the initial diperoxomolybdate compound undergoes transformation into monoperoxomolybdate species during the bromination reaction.[121] An analogous monoperoxomolybdate species was isolated from a separate experiment conducted with the complex **4.1** (0.5 mmol Mo) and KBr (2.0 mM) under standard assay condition by removing phenol red from the reaction medium.

6.3.2.5 The proposed mechanism mediated by the complexes 4.1-4.4

The findings from our study reveal the clear difference between the immobilized monoperoxomolybdenum compounds and the diperoxomolybdenum compounds anchored to water soluble polymers with respect to their activity in oxidative bromination reaction. A reaction pathway has been envisaged in order to account for the stoichiometric bromination activity of the diperoxomolybdenum compounds as shown in Fig. 6.8.

In Fig 6.8 shown with **PMAMo** as a representative, the supported active diperoxomolybdate species **I** first reacts with bromide to yield the oxidized bromine species, with the simultaneous formation of monoperoxomolybdate intermediate **II**

(reaction a). The oxidized bromine species transfers its bromine atom to the substrate AH to yield brominated product (reaction b). In presence of added H_2O_2, the inactive intermediate **II** accepts peroxide to regenerate the original active diperoxomolybdate species **I** giving rise to a catalytic cycle (reaction c).

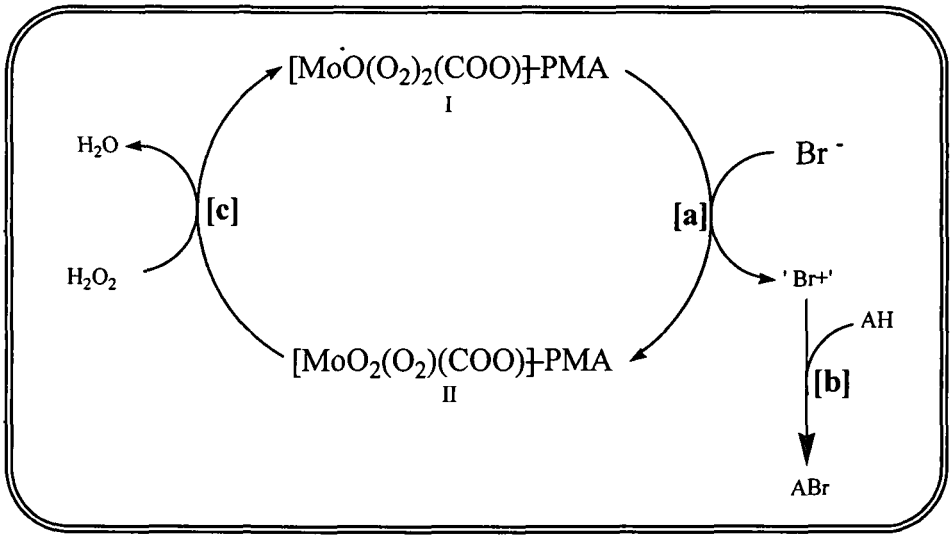

Fig. 6.8 The proposed mechanism shown with **PMAMo (4.2)** as a representative. a) Reaction of the diperoxomolybdate species **I** with bromide to yield oxidized bromine with concomitant formation of monoperoxomolybdate intermediate **II**; b) transfer of bromine from the active species to acceptor AH; c) in presence of excess H_2O_2 the monoperoxomolybdate intermediate **II** combines with peroxide to form the original diperoxo species **I**. The monoperoxo species **II** formed combines with H_2O_2 to regenerate the active diperoxomolybdate intermediate **I** giving rise to a catalytic cycle. No attempt is made to show the exact stoichiometry of the reaction.

6.4 CONCLUSIONS

In summary, the notable aspects emerging out of the present investigation demonstrate that the newly synthesized monoperoxomolybdenum(VI) complexes anchored to insoluble polymeric matrices, **3.1-3.3** heterogeneously catalyzed the oxidative bromination of a variety of aromatic substrates in aqueous-organic medium in presence of H_2O_2 in high yields under environmentally acceptable reaction conditions. On the other hand, the diperoxomolybdenum(VI) complexes anchored to water soluble polymer matrices, **4.1-4.4** stoichiometrically oxidized bromides at near neutral pH. The attractive features associated with the developed procedures are: (i) use of harmless bromide salt instead of bromine as source of bromide; (ii) avoidance of acid, halogenated solvent or any other additive; (iii) easy regeneration and reusability of the catalyst, and (iv) the reactions occur at ambient temperature. It is therefore reasonable to expect that the synthesized supported pMo complexes may be useful additions to range of bioinspired catalysts or reagents for organic oxidations. Moreover, the compounds may be considered as potential functional models of the enzyme bromoperoxidase.

REFERENCES

1. Ghorbani-Vaghei, R. et al. *Tetrahedron Lett.* **53**, 2325--2327, 2012.

2. Sels, B.F., et al. *J. Catal.* **216**, 288--297, 2003.

3. Sels, B.F., et al. *J. Am. Chem. Soc.* **123**, 8350--8359, 2001.

4. Butler, A., & Walker, J.V. *Chem. Rev.* **93**, 1937--1944, 1993.

5. Dinesh, C.U., et al. *J. Chem. Soc., Chem. Commun.* 611--612, 1995.

6. Muathen, H.A. *J. Org. Chem.* **57**, 2740--2741, 1992.

7. Conte, V., et al. *Tetrahedron Lett.* **35**, 7429--7432, 1994.

8. Smith, K., & Bahzad, D. *Chem. Commun.* 467--468, 1996.

9. Clark, J.H., et al. *Chem. Commun.* 1203--1204, 1997.

10. Chaudhuri, M.K., et al. *Tetrahedron Lett.* **39**, 8163--8166, 1998.

11. Lévêque, J.-M., et al. *Ultrason. Sonochem.* **18**, 753--756, 2011.

12. Cabanal-Duvillard, I., et al. *Tetrahedron Lett.* **39**, 5181--5184, 1998.

13. Podgorsek, A., et al. *Angew. Chem. Int. Ed.* **48**, 8424--8450, 2009.

14. Krishna Mohan, K.V.V., et al. *Synth. Commun.* **34**, 2143--2152, 2004.

15. Stille, J.K. *Pure Appl. Chem.* **57**, 1771--1780, 1985.

16. Miyaura, N., & Suzuki, A. *Chem. Rev.* **95**, 2457--2483, 1995.

17. Herrmann, W.A., Reisinger, C.-P., Haerter, P. *Aqueous-Phase Organometallic Catalysis*, B. Cornils, & W. A. Herrmann, eds., Wiley-VCH Verlag GmbH & Co. KGaA, Weinheim, Germany, 2004, 511-523.

18. Zhao, D., et al. *J. Am. Chem. Soc.* **126**, 15876--15882, 2004.

19. Spivey, A.C., et al. *Curr. Org. Synth.* **1**, 211--226, 2004.

20. Bedford, R.B., et al. *Chem. Eur. J.* **9**, 3216--3227, 2003.

21. Choudary, B.M., et al. *J. Am. Chem. Soc.* **124**, 14127--14136, 2002.

22. Beletskaya, I.P., & Cheprakov, A.V. *Chem. Rev.* **100**, 3009--3066, 2000.

23. Oestreich, M., et al. *Angew. Chem. Int. Ed.* **44**, 149--152, 2005.

24. Kressierer, C.J., & Muller, T.J.J. *Angew. Chem. Int. Ed.* **43**, 5997--6000, 2004.

25. Yao, Q., et al. *Org. Lett.* **6**, 2997--2999, 2004.

26. Arnold, L.A., et al. *Org. Lett.* **6**, 3005--3007, 2004.

27. Sonogashira, K. *Metal-Catalyzed Cross-Coupling Reactions*, F. Diede-rich, & P.J. Stang, eds., Wiley-VCH Verlag GmbH & Co. KGaA, Weinheim, Germany, 1998, 203.

28. Garcia, D., et al. *Org. Lett.* **6**, 4175--4178, 2004.

29. DeVasher, R.B., et al. *J. Org. Chem.* **69**, 7919--7927, 2004.

30. Cheng, J., et al. *J. Org. Chem.* **69**, 5428--5432, 2004.

31. Hartwig, J.F. *Angew. Chem. Int. Ed.* **37**, 2046--2067, 1998.

32. Wolfe, J.P., et al. *Acc. Chem. Res.* **31**, 805--818, 1998.

33. Hartwig, J.F. *Acc. Chem. Res.* **31**, 852--860, 1998.

34. Kavala, V., et al. *J. Org. Chem.* **70**, 4267--4271, 2005.

35. Kikushima, K., et al. *Tetrahedron* **66**, 6906--6911, 2010.

36. Adimurthy, S., et al. *Green Chem.* **8**, 916--922, 2006.

37. Vyas, P.V., et al. *Tetrahedron Lett.* **44**, 4085--4088, 2003.

38. Roy, S.C., et al. *Tetrahedron Lett.* **42**, 6941--6942, 2001.

39. Rothenberg, G., & Clark, J.H. *Org. Process Res. Dev.* **4**, 270--274, 2000.

40. Clark, J.H. *Green Chem.* **1**, 1--8, 1999.

41. Clark, J.H. (ed.), *Chemistry of Waste Minimisation*, Chapman and Hall, London, 1995.

42. Carreno, M.C., et al. *J. Org. Chem.* **60**, 5328--5331, 1995.

43. Tenaglia, A., et al. *J. Org. Chem.* **61**, 1129--1132, 1996.

44. Buckles, R.E., et al. *J.Org. Chem.* **22**, 55--59, 1957.

45. Majetich, G., et al. *J. Org. Chem.* **62**, 4321--4326, 1997.

46. Cacchi, S., et al. *Synthesis* **1979**, 64--66, 1979.

47. Bongini, A., et al. *Synthesis* **1980**, 143--146, 1980.

48. de Boer, E., & Wever, R. *J. Biol. Chem.* **263**, 12326--12332, 1988.

49. Butler, A., et al. *Chem. Rev.* **94**, 625--638, 1994.

50. Sels, B.F., et al. *Nature* **400**, 855--857, 1999.

51. Rehder, D., Bashirpoor, M., Jantzen, S., Schmidt, H., Farahbakhsh, M., & Nekola, H. in *Vanadium Compounds. Chemistry, Biochemistry and Therapeutic Applications*, Tracey, A. S., & Crans, D.C. eds., Oxford University Press, New York, 1998, 60-70.

52. Butler, A. *Coord. Chem. Rev.* **187**, 17--35, 1999.

53. Clague, M.J., & Butler, A. *J. Am. Chem. Soc.* **117**, 3475--3484, 1995.

54. Bhattacharjee, M. *Polyhedron* **11**, 2817--2818, 1992.

55. de Boer, E., et al. *Biochem. Biophys. Acta* **869**, 48--53, 1986.

56. Conte, V., & Floris, B. *Inorg. Chim. Acta* **363**, 1935--1946, 2010.

57. Michibata, H. (ed.), *Vanadium: Biochemical and Molecular Biological Approaches*, Springer, 2012, 127-142.

58. Chen, C., et al. *J. Coord. Chem.* **66**, 671--688, 2013.

59. Galloni, P., et al. *Dalton Trans.*, **in press**, 2013.

60. Natalio, F., et al. *Nat. Nanotechnol.***7**, 530--535, 2012.

61. Conte, V., et al. *Pure Appl. Chem.* **77**, 1575--1581, 2005.

62. Clague, M.J., et al. *Inorg. Chem.* **32**, 4754--4761, 1993.

63. Moriuchi, T., et al. *Tetrahedron Lett.* **48**, 2667--2670, 2007.

64. Bora, U., et al. *Org. Lett.* **2**, 247--249, 2000.

65. Meister, G.E., & Butler, A. *Inorg. Chem.* **33**, 3269--3275, 1994.

66. Zhang, Q., et al. *Process Saf. Environ. Prot.* **91**, 86--91, 2013.

67. Bora, U., et al. *Pure Appl. Chem.* **73**, 93--102, 2001.

68. Sinha, J., et al. *Chem. Commun.* 1916--1917, 2001.

69. Choudary, B.M., et al. *Catal. Commun.* **5**, 215--219, 2004.

70. Reynolds, M.S., et al. *Inorg. Chem.* **33**, 4977--4984, 1994.

71. Rana, S., et al. *Catal. Today* **198**, 52--58, 2012.

72. Reynolds, M.S., et al. *Inorg. Chim. Acta* **263**, 225--230, 1997.

73. Espenson, J.H., et al. *J. Am. Chem. Soc.* **116**, 2869--2877, 1994.

74. Sakurai, H., & Tsuchiya, K. *FEBS Lett.* **260**, 109--112, 1990.

75. Conte, V., et al. *Tetrahedron Lett.* **37**, 8609--8612, 1996.

76. Colpas, G.J., et al. *J. Am. Chem. Soc.* **118**, 3469--3478, 1996.

77. Bhattacharjee, M., & Patra, B. *J. Chem. Sci.* **118**, 583--591, 2006.

78. Das, S., et al. *Tetrahedron Lett.* **44**, 4915--4917, 2003.

79. Conte, V., & Floris, B. *Dalton Trans.* **40**, 1419--1436, 2011.

80. Pecoraro, V.L., Slebodnick, C. & Hamstra, B. *Vanadium Compounds. Chemistry, Biochemistry and Therapeutic Applications*, A.S. Tracey, & D.C. Crans, eds., Oxford University Press, New York, 1998, 157.

81. Okuhara, T. *Chem. Rev.* **102**, 3641--3666, 2002.

82. Wilson, K., & Clark, J.H. *Pure Appl. Chem.* **72**, 1313--1319, 2000.

83. Ji, J., et al. *Chem. Sci.* **2**, 484--487, 2011.

84. Hazarika, P., et al. *Polyhedron* **25**, 3501--3508, 2006.

85. Hazarika, P., et al. *Mol. Cell. Biochem.* **284**, 39--47, 2006.

86. Hazarika, P., et al. *J. Enzym. Inhib. Med. Chem.* **23**, 504--513, 2008.

87. Kalita, D., et al. *Biol. Trace Elem. Res.* **128**, 200--219, 2009.

88. Kalita, D., et al. *Inorg. Chem. Commun.* **10**, 45--48, 2007.

89. Sarmah, S., et al. *Polyhedron* **23**, 1097--1107, 2004.

90. Sarmah, S., et al. *Mol. Cell. Biochem.* **236**, 95--105, 2002.

91. Sarmah, S., et al. *Polyhedron* **21**, 389--394, 2002.

92. Kalita, D., et al. *React. Funct. Polym.* **68**, 876--890, 2008.

93. Okhapkin, I.M., et al. *Adv. Polym. Sci.* **195**, 177--210, 2006.

94. Anastas, P.T. & Warner, J.C. *Green Chemistry: Theory and Practice*, Oxford University Press, Oxford, 1998.

95. Bekturov, E.A. & Kudaibergenov, S.E. *Catalysis by Polymers*, WILEY-VCH Verlag GmbH & Co. KGaA, Weinheim, 2002.

96. Haupt, K., & Mosbach, K. *Chem. Rev.* **100**, 2495--2504, 2000.

97. Wulff, G. *Chem. Rev.* **102**, 1--28, 2002.

98. Okhapkin, I.M., et al. *Macromolecules* **37**, 7879--7883, 2004.

99. Hulea, V., et al. *Appl. Catal. A* **313**, 200--207, 2006.

100. Maurya, M.R., et al. *React. Funct. Polym.* **66**, 808--818, 2006.

101. Payne, G.B. *J. Org. Chem.* **26**, 668--670, 1961.

102. Payne, G.B., & Williams, P.H. *J. Org. Chem.* **26**, 651--659, 1961.

103. Das, S.P., et al. *J. Mol. Catal. A: Chem.* **356**, 36--45, 2012.

104. Ghiron, A.F., & Thompson, R.C. *Inorg. Chem.* **28**, 3647--3650, 1989.

105. Jacobson, S.E., et al. *J. Org. Chem.* **44**, 921--924, 1979.

106. de Boer, E., et al. *Biotech. Bioeng.* **30**, 607--610, 1987.

107. Dickman, M.H., & Pope, M.T. *Chem. Rev.* **94**, 569--584, 1994.

108. Herbert, M. et al. *J. Mol. Catal. A: Chem.* **338**, 111--120, 2011.

109.Gharah, N., et al. *Inorg. Chim. Acta* **362**, 1089--1100, 2009.

110. Wang, G., et al. *Inorg. Chim. Acta* **358**, 933--940, 2005.

111. Cross, R.J., et al. *J. Mol. Catal. A: Chem.* **144**, 273--284, 1999.

112. Batigalhia, F., et al. *Tetrahedron* **57**, 9669--9676, 2001.

113. Tamami, B., & Yeganeh, H. *Eur. Polym. J.* **35**, 1445--1450, 1999.

114. Sarmah, S., & Islam, N.S. *J. Chem. Research (S)* 172--174, 2001.

115. Rao, A.V.S., et al. *Arch. Biochem. Biophys.* **342**, 1289–297, 1997.

116. Das, S.P., et al. *Tetrahedron Lett.* **53**, 1163–1168, 2012.

117. Butler, A., & Carter-Franklin, J.N. *Nat. Prod. Rep.* **21**, 180--188, 2004.

118. Rao, A.V.S., et al. *Arch .Biochem. Biophys.* **334**, 121--134, 1996.

119. Bergbreiter, D.E. *Chem. Rev.* **102**, 3345--3384, 2002.

120. Dickerson, T.J., et al. *Chem. Rev.* **102**, 3325--3344, 2002.

121. Nardello, V., et al. *Inorg. Chem.* **34**, 4950--4957, 1995.

Appendix: 6A Characterization of Brominated products

(a) 4-Bromoaniline :

Isolated as light yellow solid.
mp: 63 °C
^{1}H NMR (400MHz; $CDCl_3$): 7.16(d, 2H, J=7Hz), 6.5(d, 2H, J=7Hz), 3.5 (s, 2H, $-NH_2$)

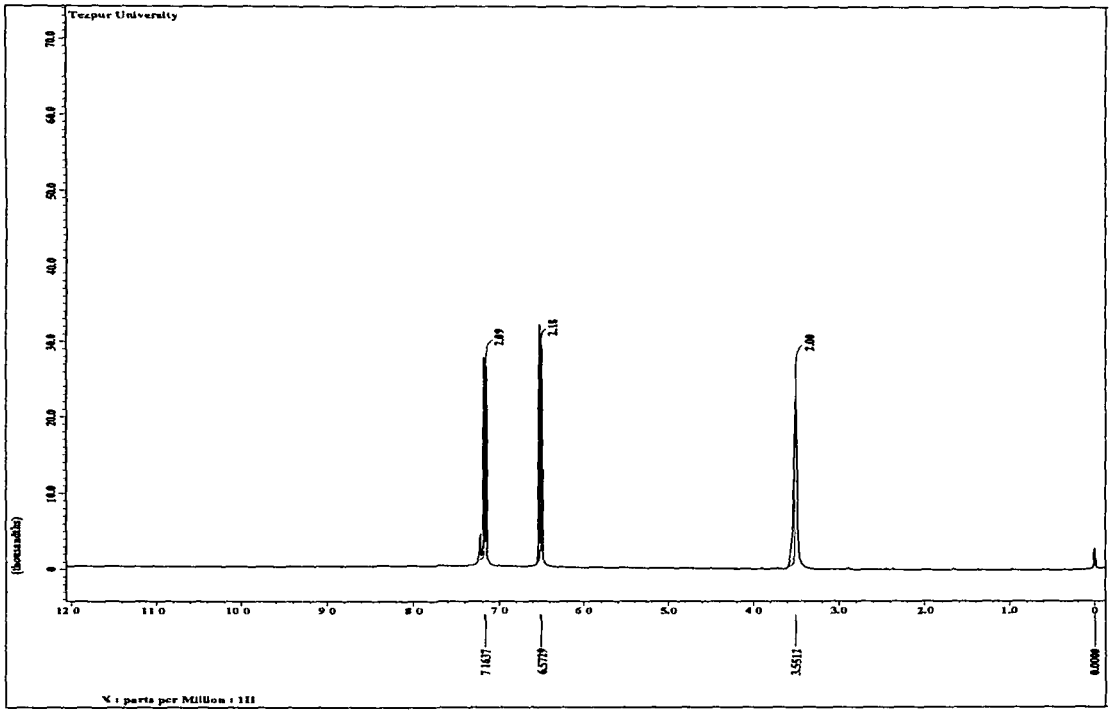

Fig. 6A. 1 ^{1}H NMR spectra of 4-bromoaniline.

(b) 2-Bromoaniline :

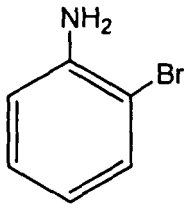

Isolated as light yellow solid.
mp: 31 °C
^{1}H NMR (400MHz; $CDCl_3$): 7.5-6.36 (m, 4H), 4.0 (s, 2H, $-NH_2$)

(c) 4-Amino-3-bromophenol :

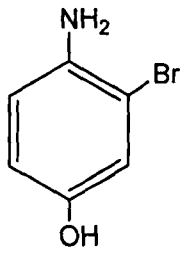

Isolated as yellow solid.
mp: 151 °C
^{1}H NMR (400MHz; $CDCl_3$): 8.3(s,1H), 7.4(d, 1H, J=6Hz), 6.9 (d, 1H, J=6Hz), 6.2-5.9(s, 2H, $-NH_2$)

(d) 5-Amino-2-bromophenol

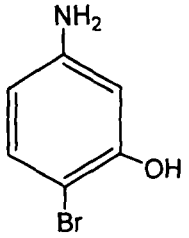

Isolated as light yellow solid.
mp: 139 °C
^{1}H NMR (400MHz; $CDCl_3$): 7.8-7.25(m, 3H), 5.3-5.0(s, 2H, -NH_2)

(e) 3-Amino-4 -bromophenol

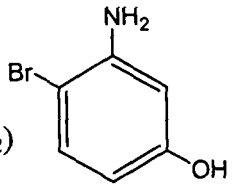

Isolated as yellow solid.
mp: 168 °C
^{1}H NMR (400MHz; $CDCl_3$): 8.1-7.5(m,3H), 5.6-5.3(br, 2H, -NH_2)

(f) 2-Amino-5- bromophenol :

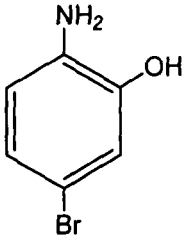

Isolated as light yellow solid.
mp: 137 °C
^{1}H NMR (400MHz; $CDCl_3$): 8.3(s,1H), 7.8(d, 1H, J=6Hz), 7.1 (d, 1H, J=6Hz), 6.5-6.2(s, 2H, -NH_2)

(g) 2-Bromo-4-nitroaniline

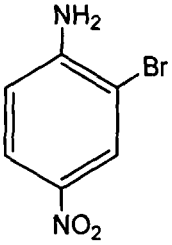

Isolated as brown powder.
mp: 104°C
^{1}H NMR (400MHz; $CDCl_3$): 8.25(s,1H), 7.9(d,1H, J=6Hz), 6.64 (d,1H, J=6Hz), 4.8-4.6 (br, 2H, -NH_2)

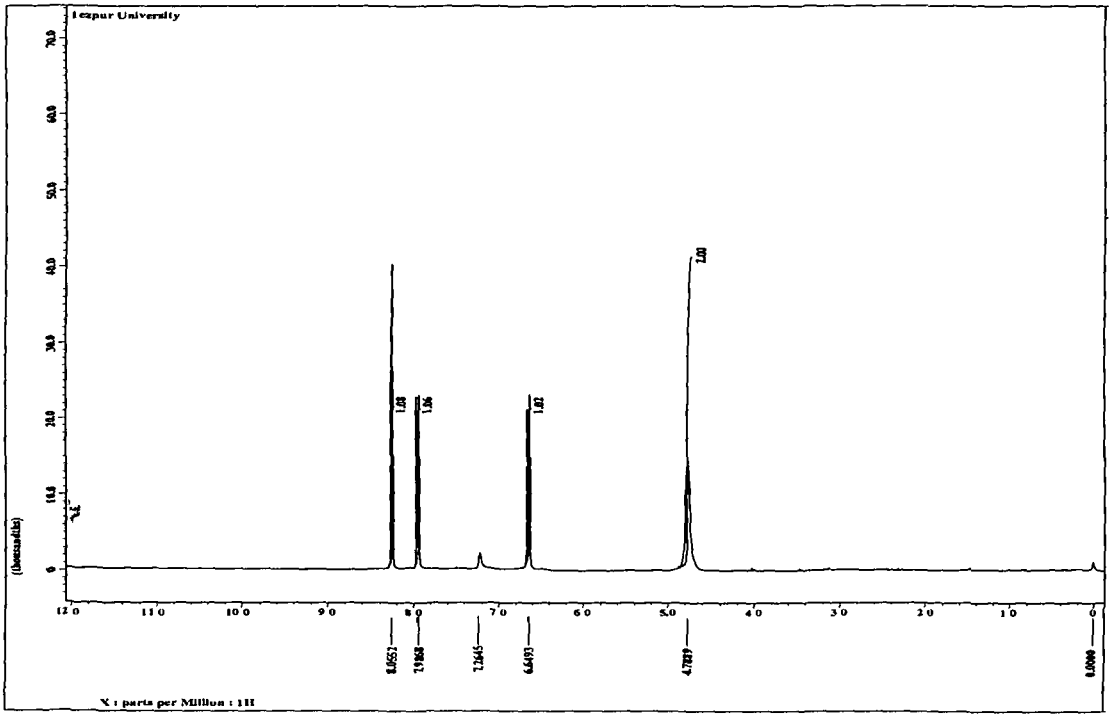

Fig. 6A. 2 ^{1}H NMR spectra of 2-bromo-4-nitroaniline.

(h) 2,6-Bibromo-4-nitroaniline

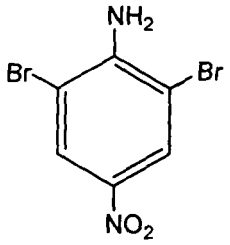

Isolated as yellow powder.
mp: 208 °C
^{1}H NMR (400MHz; $CDCl_3$): 8.05(s, 2H), 4.9-4.6 (br, 2H, -NH_2)

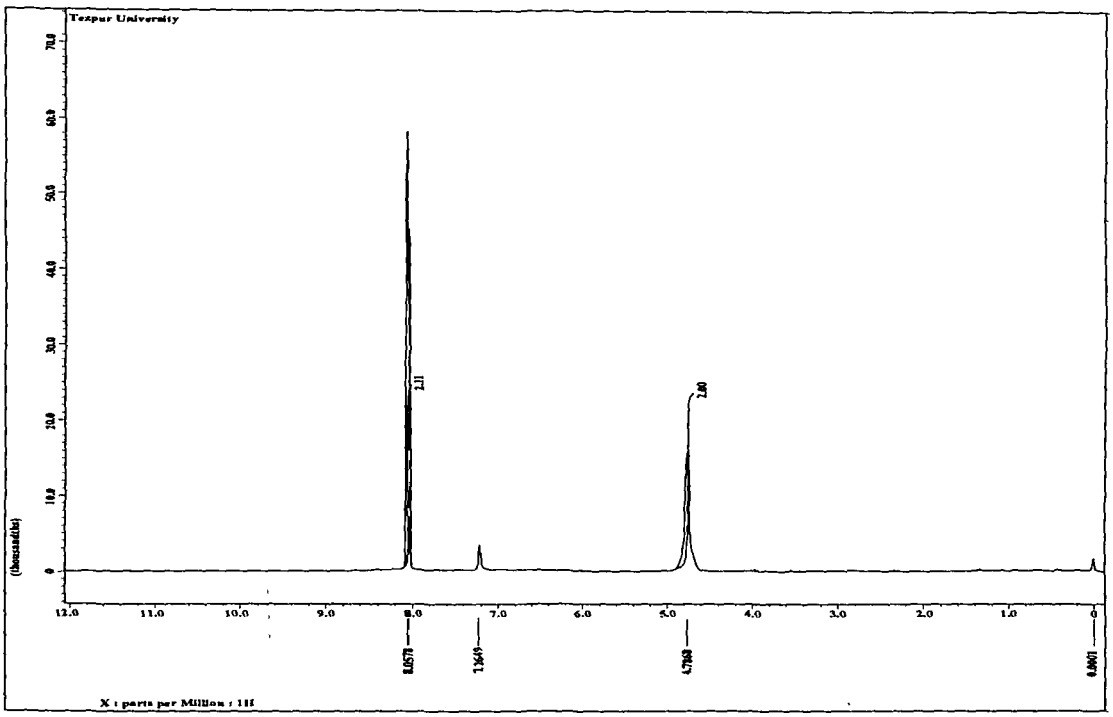

Fig. 6A. 3 ^{1}H NMR spectra of 2,6-Dibromo-4-nitroaniline.

(i) 2-Bromo-5-nitrobenzenamine

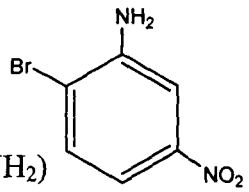

Isolated as dark yellow fine crystalline needles.
mp: 140 °C
^{1}H NMR (400MHz; $CDCl_3$): 7.7-7.25(m, 3H), 4.6-5.0(br, 2H, -NH_2)

(j) 4-Bromo-3-nitroaniline

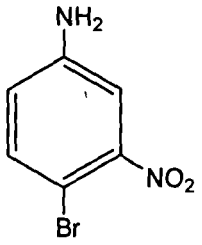

Isolated as orange crystalline powder.
129 °C
^{1}H NMR (400MHz; $CDCl_3$): 7.5-6.7(m, 3H), 4.5-4.8(br, 2H, -NH_2)

(k) 4-Bromo-2-nitroaniline

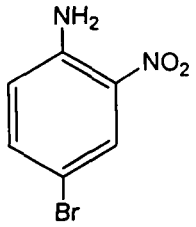

Isolated as solid orange powder.
mp: 110 °C
^{1}H NMR (400MHz; $CDCl_3$): 8.3(s, 1H), 7.45(d, 1H, J=7Hz), 6.75(d,1H, J=7Hz), 6.35-6.05(br, 2H, $-NH_2$)

(l) 2-Bromo-6-nitroaniline

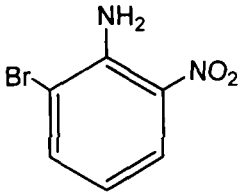

Isolated as orange solid.
mp: 72-74 °C
^{1}H NMR (400MHz; $CDCl_3$): 7.3-7.05(m, 3H), 6.5(s,2H, $-NH_2$)

(m) 2-Bromobenzene-1,4-diol

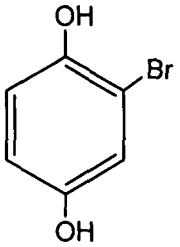

Isolated as brown fine crystalline powder.
mp: 114 °C
^{1}H NMR (400MHz; $CDCl_3$): 8.5(s, 1H), 8.2-7.5(m, 2H)

(n) 4-Bromobenzene-1,2,3-triol

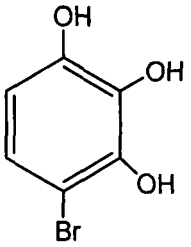

Isolated as brown solid.
mp: 280 °C
^{1}H NMR (400MHz; $CDCl_3$): 6.7 (d, 1H, J=6Hz), 6.4(d, 1H, J=6Hz), 5.3-5.0 (br, 3H, -OH)

(o) 4-Bromobenzene-1,3-diol

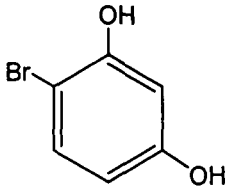

Isolated as pink crystalline powder.
mp: 100 °C
^{1}H NMR (400MHz; $CDCl_3$): 6.9(d, 1H, J=7Hz), 6.3(d, 1H, J=7Hz), 6.1(s, 1H), 5.6-5.2(br, 2H, -OH)

(p) N-(4-bromophenyl)acetamide

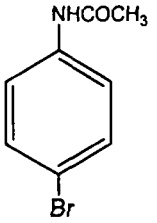

Isolated as off-white powder.
mp: 166 °C.
^{1}H NMR (400MHz; $CDCl_3$): 7.7-7.3(m, 5H), 1.9(s, 3H)

(q) 5-Bromo-2-hydroxybenzaldehyde

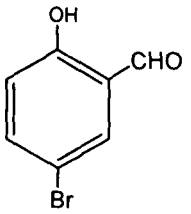

Isolated as slightly yellow powder.
mp: 105 °C
^{1}H NMR (400MHz; $CDCl_3$): 10.0(s, -CHO), 7.9(s, 1H), 7.5(d, 1H, J=6Hz), 6.9(d, 1H, J=6Hz), 5.0(s, 1H, -OH)

(r) 1-Methoxy-2-methyl-4-bromobenzene

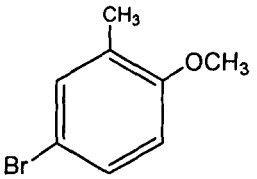

Isolated as light yellow solid.
mp: 69 °C
^{1}H NMR (400MHz; $CDCl_3$): 7.9(s, 1H), 7.4(d, 1H, J=6Hz), 6.85(d, 1H, J=6Hz), 3.6(s, 3H, $-OCH_3$), 1.2 (s, 3H, $-CH_3$)

(s) 4-Bromo-1,2-dihydroxybenzene

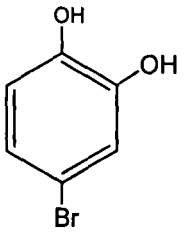

Isolated as white crystals.
mp: 87 °C
^{1}H NMR (400MHz; $CDCl_3$): 6.9(d, 1H, J=7Hz), 6.7(s, 1H), 6.3(d, 1H, J=7Hz), 5.3-4.9(br, 2H, -OH)

CHAPTER 7

Studies of Bio-relevant Properties of Water Soluble Peroxomolybdenum Macrocomplexes: Hydrolytic Stability and their Interaction with Biomolecules

7.1 INTRODUCTION

Phosphate ester bond functions as an extremely important linkage within the living cell.[1] It participates in storage and transfer of the genetic information, carries chemical energy and regulates the activity of enzymes and signaling molecules in the cell.[1,2] Enzymes capable of acting on ester bonds and catalyzing the cleavage of phosphate esters constitute the subclass of phosphohydrolases, or phosphatases.[1] Alkaline phosphatase (ALP) is a ubiquitous enzyme that can be isolated from bone, kidney, intestine, plasma, liver, spleen, plants and microorganisms.[3,4] It is a membrane bound zinc metalloenzyme with broad substrate specificity and optimal activity at higher pH (>7.5).[5,6] The enzyme has been used extensively in immunoassays as increase or decrease in the level of ALP in human body is useful in the diagnosis of bone and liver pathology, hypethyroidism and primary or metastatic bone cancer.[5,7,8]

Acid phosphatases (ACP) are widespread in nature, and can be found in many animal and plant species.[9] The enzyme catalyzes the hydrolysis of phosphate ester bond at an optimum pH of 4.9-6.0.[6] Acid phosphatases from human prostate, wheat germ, and other sources have been isolated as phosphohistidyl enzymes containing an active site histidine.[10] The mammalian enzyme acid phosphatase possesses dinuclear iron active sites[6,11] and highly conserved amino acid sequences.[12-15] Human acid phosphatases are normally found at low concentrations.[9] However, pronounced changes in their synthesis

occur in particular diseases, where unusually high or low enzyme expression is seen as part of the pathophysiological process.[9] Thus ACP has been reported to be diagnostically useful as serological and histological markers of diseases such as prostatic cancer and bone metastasis.[9]

Phosphatases are, in general inhibited by oxyanions such as vanadate,[10,16-18] molybdate and tungstates.[19,20] Enzyme inhibition studies by metals and metal complexes is important as it has been recognized as one of the mechanisms of action for inorganic drugs.[21,22] For instance, a correlation has been found to exist between the abilities of the oxyanions of V, Mo and W as well as their corresponding peroxo complexes to inhibit protein phosphatases and their *in vivo* insulin mimetic activities.[16,17,23] It has been reported by Goto et al.,[24] in 1992, and subsequently, by Shechter and co-workers[25] that molybdate and peroxomolybdate (pMo) as well as tungstate and peroxotungstate (pW) exhibit insulin-like action, similar to vanadate and peroxovanadate (pV). It has also been found that the peroxo derivatives offer many fold (80-180 fold) higher activity than their respective oxyanions.[25] These remarkable findings led to a revival of interest on synthetic peroxo compounds of Mo and W. The exact mechanism involved in the metabolic actions of these metal ions is yet to be fully understood and hence are still under active investigation. The phosphatase inhibitory effect of vanadate and pV compounds however, has been extensively investigated which has been the topic of several reviews.[16,26-40] It is noteworthy that out of numerous synthetic pV compounds tested for possible therapeutic activities in recent years, to our knowledge only three compounds have been clinically tested on human.[27,41,42] One possible factor responsible for limiting the therapeutic potential of pV compounds is their hydrolytic instability and toxicity.[17,27,43-46] An intense search for biologically relevant pV compounds spurred by the pressing need for stable, better absorbed, more efficacious vanadium compounds with therapeutic potential still

continues. In this context it is somewhat intriguing that notwithstanding the superior bio-relevant characteristics exhibited by pMo compounds viz., stability, bioavailability and low toxicity,[22,25] the pMo compounds have received very little attention as biologically active agents. For instance we have not come across any previous report on effect of discreet pMo compounds on acid or alkaline phosphatases.

In view of the above background and as a direct sequel to our work on peroxo-metal incorporated water soluble polymers, in the present study one of our objectives has been to study the effect of these macrocomplexes on the function of phosphohydrolases vis-à-vis neat pMo complexes. Two types of membrane associated enzymes viz., wheat thylakoid membrane ACP and rabbit intestine ALP were chosen for our investigation because in addition to being excellent models to investigate toxic metal inhibitory effect in membrane proteins, these enzymes, as has already been mentioned, play key roles in a variety of biological phenomena.[6,11,47]

Besides phosphohydrolases we considered it imperative to assess the interaction of the macrocomplexes with catalase, the ubiquitous enzyme responsible for the breakdown of H_2O_2 to H_2O and O_2 in the intercellular peroxisomes. Hydrogen peroxide, a reactive oxygen species (ROS) produced as a by-product of aerobic respiration,[48] has long been treated as a major contributor to DNA damage, protein oxidation and lipid peroxidation, which can ultimately result in cell death and/or tumourigenesis.[49] On the other hand, during the last two decades hydrogen peroxide has assumed importance as a key signal transducing agent regulating a variety of cellular processes.[49] Studies on the cellular effects of H_2O_2 are however constrained by the need for high concentrations and long duration of treatment because cells are abundantly equipped with catalase and glutathione peroxidase that rapidly deplete intracellular H_2O_2.[50] These findings have lead

to a search for catalase resistant peroxide derivatives which can substitute for H_2O_2 at far lower concentration.

It has been documented previously that diperoxovanadate (DPV) compound can be used as a tool in the study of the signaling actions of H_2O_2 owing to its relative resistance to catalase action.[51,52] In this context, it is also notable that several heteroligand pV and pW complexes previously synthesized in our laboratory exhibited reasonable resistance to catalase action.[45,46,53-57] However, no report seems to be available on the interaction of catalase with discrete pMo compounds in solution. We were therefore interested to undertake *in vitro* studies in order to understand the fate of the peroxomolybdenum compounds in presence of catalase vis-à-vis H_2O_2, the natural substrate of the enzyme.

Presented in this chapter are the results of our studies on the effect of catalase on the synthesized macrocomplexes **$[Mo_2O_2(O_2)_4$(carboxylate)]-PA (4.1)**, **$[MoO(O_2)_2$(carboxylate)]-PMA (4.2)**, **$[MoO(O_2)_2$(amide)]-PAm (4.3)** and **$[MoO(O_2)_2$(sulfonate)]–PS (4.4)** as well as a set of previously reported free monomeric pMo complexes **$[MoO(O_2)_2$(glycine)$(H_2O)]$ (DMo_1) (7.1)** and **$[MoO(O_2)_2$(asparagine)$(H_2O)]$ (DMo_2) (7.2)**. Also reported herein are our findings on kinetics of inhibition of rabbit intestine alkaline phosphatase (ALP) and wheat thylakoid membrane acid phosphatase (ACP) by the macrocomplexes and monomeric compounds. We endeavored to draw comparison between the two types of pMo compounds, macro as well as neat, with respect to their tested properties. We have also examined the stability of the macrocomplexes towards degradation in solutions of a wide range of pH values.

7.2 EXPERIMENTAL SECTION

7.2.1 Hydrolytic stability of the macrocomplexes 4.1 - 4.4 and neat monomeric compounds DMo_1(7.1) and DMo_2(7.2)

The hydrolytic stability of the compounds, **4.1-4.4** in aqueous medium, at their natural pH, was examined by estimating the peroxide content in aliquots drawn at different time intervals from the respective solution of the compound, with initial concentration of peroxide maintained at 0.4 mM in each case. The test solution was prepared by adding **PAMo** (0.137 mg/mL), **PMAMo** (0.294 mg/mL), **PAmMo** (0.327 mg/mL), **PSMo** (0.196 mg/mL), **DMo_1** (0.054 mg/mL), or **DMo_2** (0.065 mg/mL). The stability of the compounds in solution at different pH values such as pH 1.2 and 2.1 (50 mM KCl/HCl buffer), 3.1 (50 mM citrate buffer), and 4.4, 7.0 or 8.0 (50 mM phosphate buffer) was measured in a similar way. The stability of the compounds were further ascertained by recording their electronic spectra at ambient temperature over a period of 12 h at an interval of 30 min and examining the band at *ca.* 320 nm for any change in absorbance.

In addition, the ^{13}C and ^{95}Mo NMR spectra of the pMo compounds were monitored over a period of 12 h for any change in the spectral pattern.

7.2.2 Interaction of the peroxomolybdenum compounds with catalase

The effect of catalase on complexes was studied by determining the peroxide content of the compounds in a solution containing catalase at specified time intervals. The test solution contained phosphate buffer (50 mM, pH 7.0) and catalase (40 μg/mL). The volume of the reaction solution was kept at 70 mL. The solution was incubated at 30 °C. The polymeric compound was then added to the test solution and aliquots of 5 mL were

drawn and titrated for peroxide content after stopping the reaction by adding it to cold sulfuric acid (0.7 M, 100 mL) at an interval of 5 min from the starting of reaction. Since the free mononuclear compounds **DMo_1** or **DMo_2** degraded at a faster rate, in order to obtain a measurable rate the amount of catalase used was 10 μg/mL. Degradation of the compounds with respect to their loss of peroxide was also followed by monitoring the band at *ca.* 320 nm with time. For the polymer bound compounds concentrations were on the basis of actual peroxometal loading (mmol g^{-1}).

7.2.3 Enzyme Inhibition

7.2.3.1 Assay of Alkaline phosphatase activity

Phosphatase activity was assayed spectrophotometrically by using p-nitrophenyl phosphate (p-NPP) as a substrate. The continuous production of p-nitrophenol (p-NP) was determined at 30 °C by measuring absorbance at 405 nm in a reaction mixture containing ALP from rabbit intestine (3.3 μg protein/mL), p-NPP (2 mM) in incubation buffer (25 mM glycine + 2 mM $MgCl_2$, pH 10.0). The initial reaction rates were obtained by starting the reaction by adding ALP to the reaction solution, which was pre-incubated for 5 min. The initial reaction rate of p-NPP hydrolysis in the absence of the inhibitors, V_o was determined which was used as control. The effect of pMo and bare ligands were assessed by adding different concentrations of each species in the ALP assay. For the polymer bound compounds concentrations were on the basis of actual peroxometal loading (mmol g^{-1}). The IC_{50} values were graphically determined as the half-maximal inhibitory concentration of the inhibitor species giving 50% inhibition. All the assays were performed in triplicate. The data in figures are presented as the means ± SE from three separate experiments.

7.2.3.2 Assay of Acid phosphatase activity

The activity of acid phosphatase was monitored by assay of the p-nitrophenol (p-NP) released from p-nitrophenyl phosphate (p-NPP) at the pH optimum, 4.6 at 30 °C by measuring absorbance at 405 nm. In the standard assay, the reaction mixture contained acetate buffer (0.1 M, pH=4.6), acid phosphatase (18.38 μg protein/mL) and compound solution (concentration varies between 0.1-80 μM) was first pre-incubated at 30 °C for 5 min. Subsequently, the substrate, p-NPP (2 mM) was added and the mixture was incubated for 30 min at 30 °C and finally the reaction was stopped by adding NaOH solution (0.5 M). The molar extinction coefficient of *p*-nitrophenolate ion, at 405 nm, in alkaline medium is 18000 M^{-1} cm^{-1}.[58] The activity in the absence of inhibitor was considered as control (100%). For the polymer bound compounds concentrations were on the basis of actual peroxometal loading (mmol g^{-1}). All the assays were performed in triplicate. The data in figures are presented as the means ± SE from three separate experiments.

7.2.3.3 Kinetic measurements

The kinetic parameters V_{max} and K_m of an enzyme catalyzed reaction were determined using Lineweaver – Burk (LB) plot following rearrangement of the Michaelis Menten equation. The Lineweaver Burk plot (also called *double-reciprocal diagram*) is based on the reciprocal form of the Michaelis-Menten equation:

$$\frac{1}{V} = \left\{ \frac{K_m}{V_{max}[S]} + \frac{1}{V_{max}} \right\}$$

Thus plotting the reciprocal velocity. $1/V$ against the reciprocal substrate concentration $1/[S]$ yields a straight line intersecting the ordinate at $1/V$, and the abscissa at $1/K_m$. The parameter V_{max} is the maximal velocity and K_m is the Michaelis constant, its value being equivalent to the substrate concentration at which velocity is equal to half of $V_{max}/2$.

Different types of inhibition give the different plot patterns. For instance with a Lineweaver - Burk plot, the lines will converge on the Y axis when there is competitive inhibition, so V_{max} remains constant but K_m will increase with increase in concentration of the inhibitor. But the lines will be parallel when the inhibition is uncompetitive causing decrease in value of V_{max} and K_m with increase in concentration of inhibitor. For noncompetitive inhibition, the lines will converge either on the X axis (simple noncompetitive inhibition) or above / below the X axis (mixed inhibition). Thus in non-competitive inhibition, K_m will remain constant but V_{max} will decrease with increase of inhibitor concentration.

A competitive inhibitor is a molecule which directly competes with the enzyme's true substrate for binding to the active site. On the other hand, in noncompetitive inhibition, the inhibitor binds to a site on the enzyme other than the active site, so the substrate and inhibitor are not in competition. In uncompetitive inhibition, an inhibitor binds to the enzyme – substrate complex but free enzyme is not a target of inhibition. However, in mixed inhibition, the inhibitor can bind to the enzyme at the same time as the enzyme – substrate complex. In the present case the expression for velocity of the reaction is given by

$$V = \left\{ \frac{V_{max} \times [S]}{K_m\left(\frac{1+[I]}{K_I}\right) + [S]\left(\frac{1+[I]}{K_{II}}\right)} \right\}$$

where V is the velocity, $[S]$ is the p-NPP concentration and $[I]$ is the inhibitor concentration, K_i is the inhibitory constant for the competitive part and K_{ii} is the inhibitory constant for the noncompetitive part. The enzyme inhibitor and enzyme substrate inhibitor constant were calculated from secondary plots of initial rate data by linear regression analysis. The slopes obtained from Lineweaver plots were replotted against inhibitor concentration to obtain K_i values from the x-intercepts of these replots. The intercepts obtained from Lineweaver plots were replotted against inhibitor concentration to obtain K_{ii} values from the x-intercepts of these replots.

7.3 RESULTS AND DISCUSSION

7.3.1 Stability of the compounds towards decomposition in solution

Hydrolytic stability being one of the most important conditions required to be fulfilled by metal complexes to be useful as therapeutic or bio-relevant agent,[59] we have considered it imperative to ascertain the stability of the title compounds in solution. The stability of the compounds **4.1-4.4** with respect to the loss of peroxide in solution of pH *ca.* 6, the natural pH attained by the solution on dissolving the macrocomplexes were assessed by estimating their peroxide content and monitoring the absorbance at 310 -330 nm region in the electronic spectra, at specified time intervals, for any possible change. Similarly, the stability of the mononuclear complexes, **DMo_1** and **DMo_2**, was investigated in solution of their respective natural pH values viz. pH 1.5 (**DMo_1**) and pH 3 (**DMo_2**). From the results it was evident that the peroxide content of the examined compounds and the position and intensity of the electronic spectral bands remained unchanged even after a period of 12 h. We have further tested and confirmed the stability of each of the pMo compounds in solutions over a wide range of pH values ranging from 1.2 to 3.1, 4.4 and 8.0.

Fig. 7.1 shows that the compound **PAMo**, used as a representative, is stable in solution of pH 5 as well as pH 7.

Furthermore, it is noteworthy that the ^{95}Mo and ^{13}C NMR spectra of the pMo compounds when monitored over a period of 12 h displayed no change in the spectral pattern (Fig. 7.2 and Fig. 7.3). Most importantly, the spectra remained unaltered in solution of a wide range of pH values of 1.2, 3.1 to 8.0 over a period of 12 hours. Thus, all the evidences gathered from the above investigations clearly attest to the stability of the compounds in solution.

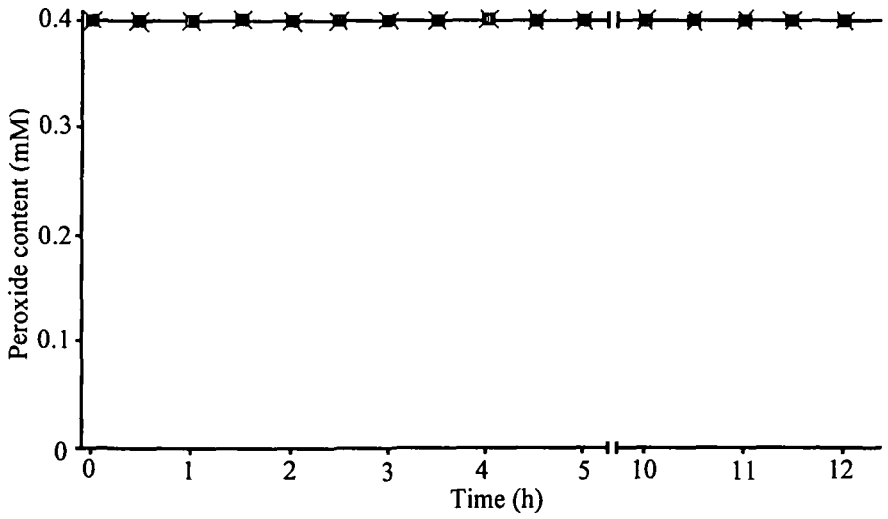

Fig. 7.1 Hydrolytic stability of compound **PAMo (4.1)** at different pH values: (■) compound solution in distilled water, pH of the solution = 5.0, (×) solution of the compound in phosphate buffer (50 mM, pH 7.0).

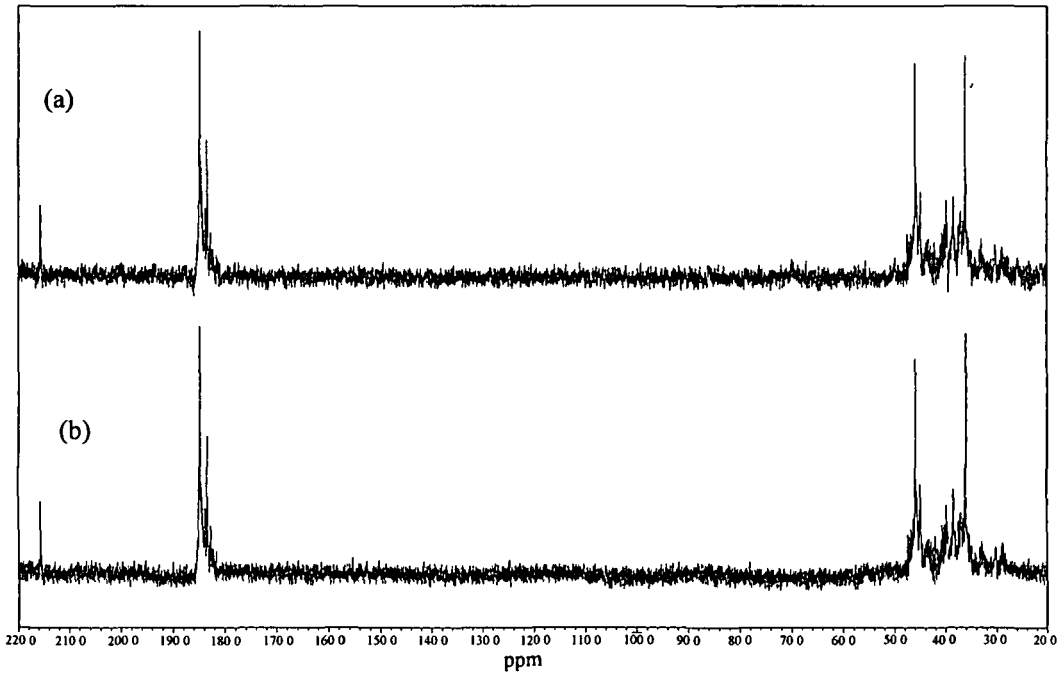

Fig. 7.2 ^{13}C NMR spectra of **PAMo (4.1)** in D_2O, recorded (a) immediately after preparation and (b) solution of (a) 12 h later, showing stability of the compound in solution.

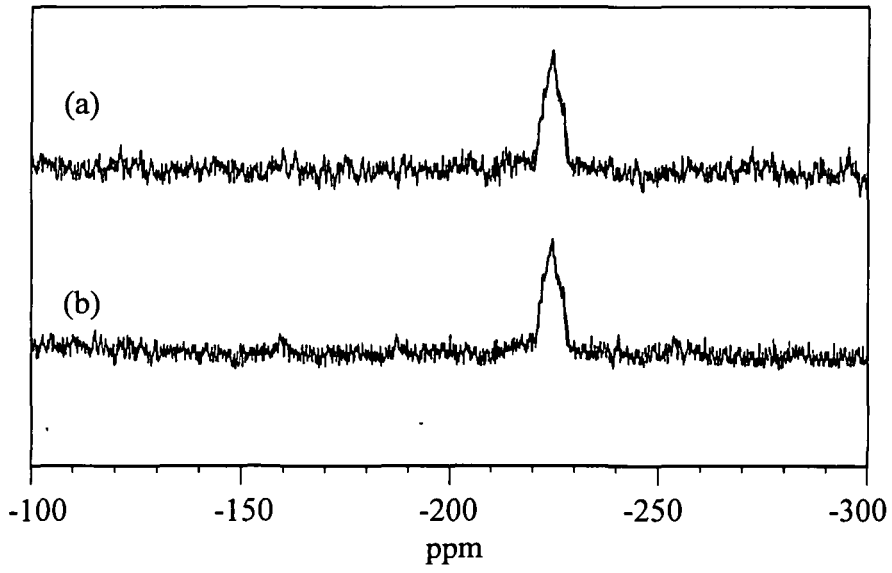

Fig. 7.3 ^{95}Mo NMR spectra of **PAMo (4.1)** in D_2O, recorded (a) immediately after preparation and (b) solution of (a) 12 h later, showing stability of the compound in solution.

7.3.2 Interaction of the peroxomolybdenum compounds with catalase

Addition of catalase to a solution of H_2O_2, its natural substrate, in phosphate buffer of pH 7.0, leads to rapid degradation of H_2O_2 with release of half equivalent of oxygen (molecular basis) as expected from the disproportionation reaction.[52] The rate of degradation of H_2O_2 with the release of oxygen was reported to be 430 μM/min from a solution of 0.1 mM concentration and the reaction requires less than 2 min for completion.[52] In the present study, the effect of catalase on the polymer bound diperoxomolybdate compounds, **4.1-4.4** as well as free monomeric diperoxomolybdates are shown in Fig. 7.4. The data presented in Table 7.1 demonstrate that on incubation with catalase at pH 7, each of the macrocomplexes degraded with a loss of peroxide with the rates of degradation varying between 10-17 μM/min. The action of catalase on each of the water soluble polymeric pMo compounds was thus observed to be relatively slower process compared to its effect on H_2O_2. As seen from the data presented in Table 7.1, the synthesized polymer bound pMo complexes are at least 70-100 times weaker as substrates to catalase compared to H_2O_2. It is noteworthy that the free pMo complexes undergo rapid degradation, with loss of peroxide within approximately five minutes of incubation, under identical condition.

The degradation of the compounds, **4.1-4.4** by catalase was further investigated by studying their UV spectra (Fig. 7.5 and Fig. 7.6) in solution. In separate experiments, each of the compounds (containing 0.4 mM of peroxide) was incubated with catalase (40 μg/mL) at 30 ^{o}C and subsequently, UV spectra of the mixture were recorded after specific time interval. From the electronic spectral analysis it was evident that the intensity of small shoulder like peak in the range of 310-330 nm owing to diperoxomolybdate species gradually decreases leaving behind a non-specific absorption below 300 nm with increasing incubation time. The rate of degradation calculated on the basis of electronic

Table 7.1 Catalase-Dependent Oxygen Release from Peroxometallates[a]

Compound	Concentration (mg/mL)	peroxide content (mM)	loss of peroxide (μM/min)
PAMo	0.137	0.4	17.81
PMAMo	0.294	0.4	17.57
PAmMo	0.327	0.4	10.34
PSMo	0.196	0.4	14.29
DMo_1[b]	0.054	0.4	37.60
DMo_2[b]	0.065	0.4	28.33

[a] The test solution contained phosphate buffer (50 mM, pH 7.0) and the catalase (40 μg/mL) which was incubated at 30 °C for 5 min.

[b] Amount of catalase = 10 μg/mL.

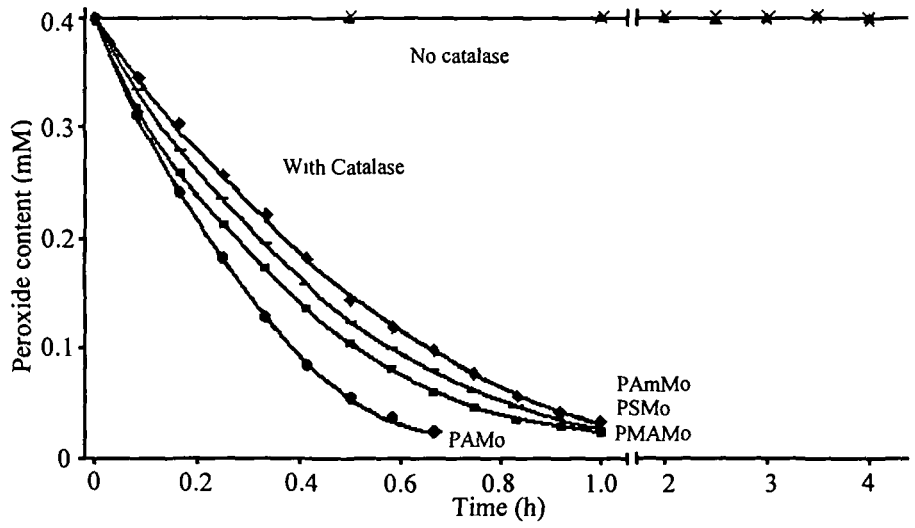

Fig. 7.4 The effect of catalase on **PAMo** (•), **PMAMo** (■), **PAmMo** (♦) and **PSMo** (-). The test solution contained phosphate buffer (50 mM, pH 7.0) and the catalase (40 μg/mL) which was incubated at 30 °C for 5 min. Compounds were then added to the reaction solution and aliquots were drawn at indicated time points and loss in peroxide content was determined. For polymeric compounds concentrations are on the basis of peroxometal loading.

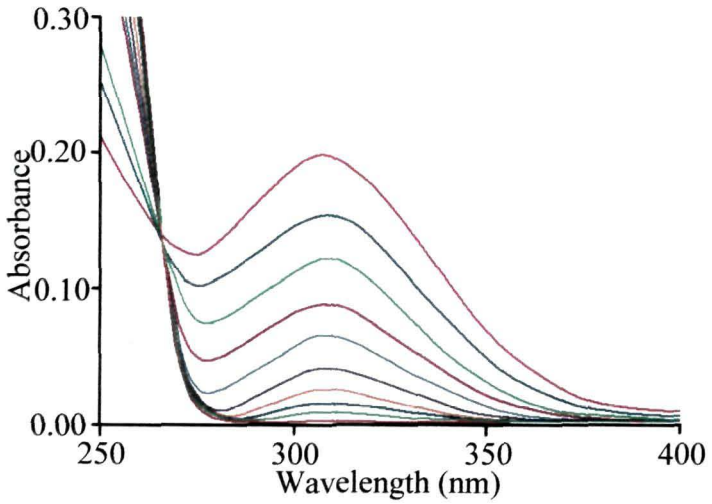

(a)

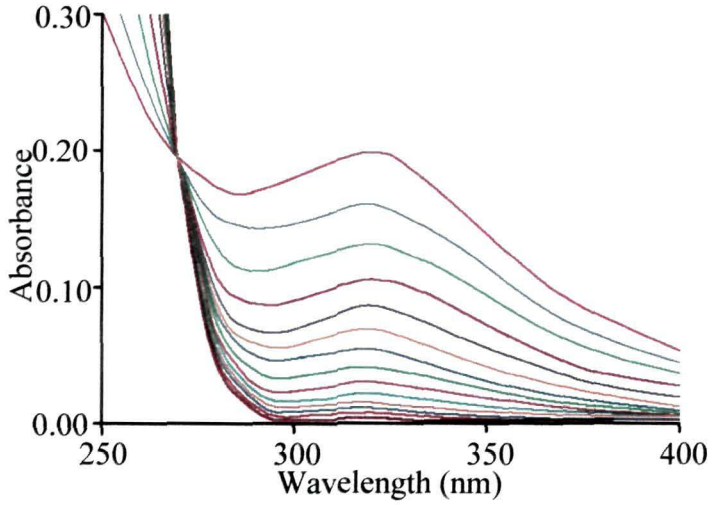

(b)

Fig. 7.5 Effect of catalase on the compounds. The spectral changes at interval of 5 min on incubation of compound with catalase in solution (a) **PAMo** (A_{311}) and (b) **PMAMo** (A_{322}). The test solution contained phosphate buffer (50 mM, pH 7.0); compound (0.4 mM of peroxide) and catalase (40 μg/mL) at 30 °C.

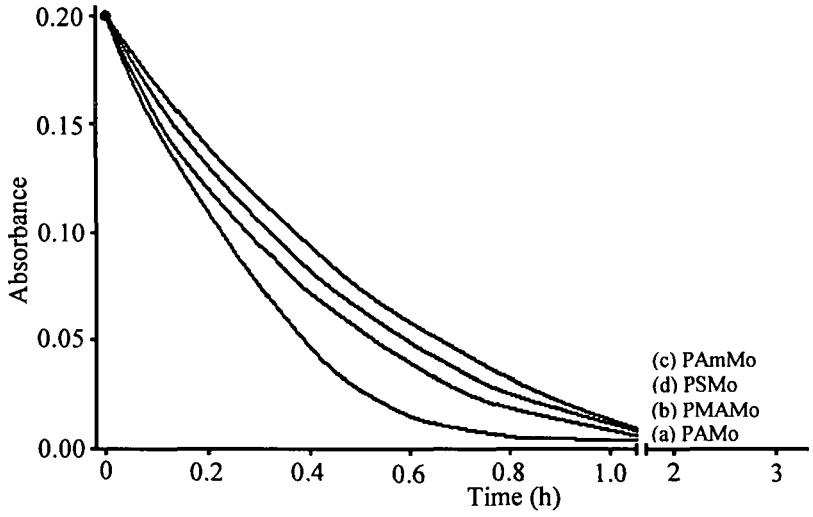

Fig. 7.6 The decrease of absorbance for the compounds (a) **PAMo** (A_{311}), (b) **PMAMo** (A_{322}), (c) **PAmMo** (A_{314}) and (b) **PSMo** (A_{320}) indicating the rate of degradation of the compounds under the effect of catalase. The reaction mixture contained phosphate buffer (50 mM, pH 7.0); compound (0.4 mM of peroxide) and catalase (40 μg/mL) at 30 °C.

spectral studies was found to be in accord with the values obtained from chemical analysis.

The total loss of peroxide from each of the compound solution was found to be *ca.* 0.4 mM which is equivalent to the concentration of co-ordinated peroxide. This indicates a ratio of 1:4 for peroxide:dinuclear pMo species (in **PAMo**) and 1:2 for mononuclear pMo (in **PMAMo, PAmMo, PSMo**) which are consistent with the estimated peroxide content of the compounds.

The tested compounds could be arranged in the following order of increasing stability towards degradation under the effect of catalase, **PAmMo > PSMo > PAMo ≈ PMAMo > > DMo_2 > DMo_1**. From the above results it may be surmised that co-ordination of peroxo ligand to Mo enhances its resistance towards degradation under the

action of catalase. Further, 2-3 fold greater ability of the peroxomolybdate in the macrocomplexes to withstand catalase action, compared to the free pMo compounds appears to be a consequence of additional stability imparted to the compounds by the polymeric support through immobilization.

7.3.3 Inhibition of activities of phosphohydrolases by peroxomolybdenum compounds

The *in vitro* phosphatase inhibitory effect of the polymer incorporated pMo compounds, **PAMo (4.1)**, **PMAMo (4.2)**, **PAmMo (4.3)**, **PSMo (4.4)** and neat mononuclear compounds, **DMo_1 (7.1)** and **DMo_2 (7.2)** along with molybdate anion as well as free ligands was examined by using p-NPP as substrate and employing standard enzyme assay system. Rabbit intestine alkaline phosphatase (ALP) and wheat thylakoid membrane acid phosphatases (ACP) were used as model enzymes. The inhibitor potential of the species were quantified by determining the half-maximal inhibitory concentration (IC_{50}) for each inhibitor which induces 50 % suppression of the original enzyme activity. Since an inhibitor species can interact with enzyme via various pathways, kinetic investigation is a major tool in enabling us to distinguish between the inhibition mechanism of enzyme catalyzed reactions. We have therefore determined the kinetic parameters, K_m and V_{max} in absence as well as in presence of peroxo metal compounds using Lineweaver-Burk double reciprocal plots. It was also necessary to assess the affinity of the enzyme for the inhibitor by evaluating the inhibitor constants. All of the tested compounds displayed affinity for the phosphohydrolases in a close order of magnitude as revealed by the values of inhibitor constants, K_I and K_{II}.

7.3.3.1 Inhibition of ALP by the peroxomolybdenum compounds

The dose dependent effects of each of the pMo compounds **4.1-4.4** and **DMo_1** and **DMo_2** in comparison to the respective free ligands are presented in Fig. 7.7. From the data obtained we find that each of the tested species, irrespective of being free or polymer bound, behaved as active inhibitor of ALP. On comparing the IC_{50} values of the polymeric compounds, in terms of their actual peroxometal loading, with those of free compounds, the inhibitors could be arranged in the following order of potency, **DMo_1 > PMAMo > DMo_2 > PAmMo > PSMo > PAMo > Na_2MoO_4**. The pMo compounds were observed to induce stronger inhibition compared to the corresponding vanadium containing analogues reported previously from our laboratory.[60] The effect of each of the polymeric ligands, without peroxometal loading and the amino acid co-ligands viz. glycine and asparagine, upon ALP activity is practically negligible under the assay conditions used and H_2O_2 had no observable effect.

Presented in Table 7.2 are the kinetic data for inhibition of ALP catalyzed hydrolysis of p-NPP by the macrocomplexes as well as free mononuclear **DMo_1** and **DMo_2**. The Lineweaver-Burk (LB) plots obtained for the compounds **4.1-4.4**, **DMo_1**, **DMo_2** and **Na_2MoO_4** are presented in Fig. 7.8 and Fig. 7.9 where $1/V$ is plotted against $1/[S]$. Kinetic measurements at several different substrate concentrations in presence of each of the inhibitors yielded straight lines with a point of intersection in the second quadrant.

The results demonstrate that with an increase in concentration of each of the polymeric inhibitor complexes, a velocity V_{max} decreases, whereas K_m remained constant. In contrast, when any of the free pMo complexes was used as inhibitor, it was found that with increasing inhibitor concentration V_{max} decreased whereas K_m value increased (Fig. 7.8 and Fig. 7.9). It has thus been established that the polymeric compounds are classical

non-competitive inhibitors of ALP. On the other hand, monomeric diperoxometallates, **DMo_1** and **DMo_2** served as mixed-type of inhibitors of the enzyme combining competitive and non-competitive modes of inhibition.

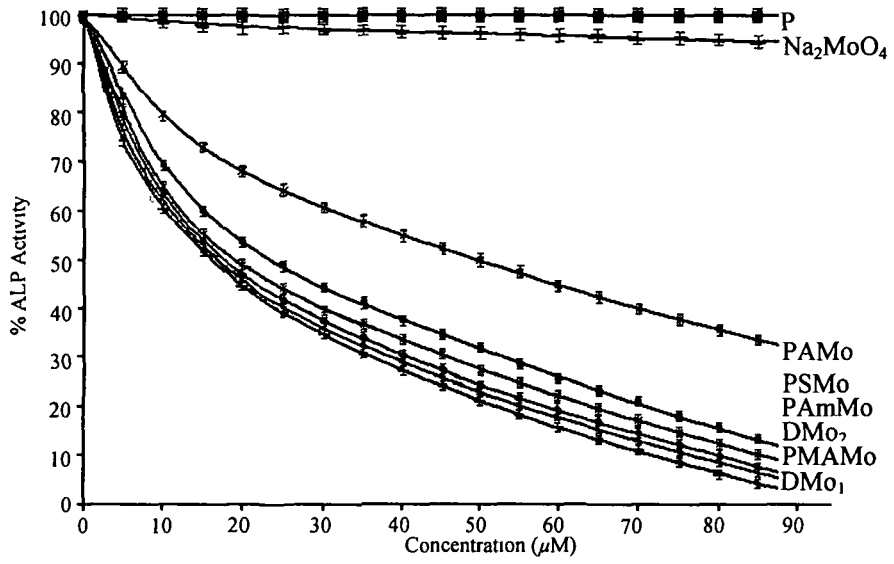

Fig. 7.7 Effect of compounds **PAMo**, **PMAMo**, **PAmMo**, **PSMo**, **DMo_1**, **DMo_2**, **Na_2MoO_4** and free polymers (**P**) on activity of ALP from rabbit intestine. The ALP catalyzed rates of hydrolysis of p-NPP at pH 10.0 were determined at 30 °C by measuring A_{405} in a reaction mixture containing ALP (3.3 μg/ml), p-NPP (2 mM) in incubation buffer (25 mM glycine + 2 mM $MgCl_2$, pH 10.0) in the absence or presence of stated concentrations of the inhibitors. Effects of the additions are represented as the percent values (rounded to integers) of control (Δp-NPP = 3.13 μM/min). The data are presented as the means ± SE from three separate experiments. For polymeric compounds concentrations are on the basis of peroxometal loading.

The inhibitor constant K_i for competitive part of inhibition was determined from the secondary plot of slope of the primary plot ($1/V$ versus $1/[S]$) against the inhibitor concentration with intercept on the inhibitor axis being $-K_i$ (Fig. 7.8 and Fig. 7.9). The value of K_{ii}, inhibitor constant for non-competitive inhibition, was obtained from a linear secondary plot of $1/V_{max}$ against the inhibitor concentration of each inhibitor, the intercept on the inhibitor axis being equivalent to $-K_{ii}$ (Fig. 7.8 and Fig. 7.9). The values of K_i and K_{ii} are presented in Table 7.2.

K_i is a measure of the affinity the inhibitor has for the free enzyme whereas K_{ii} is its affinity the inhibitor has for the enzyme-substrate complex and the ratio of K_{ii} and K_i values were used to assess the relative competitiveness of each inhibitor.[61] A larger K_{ii}/K_i value indicates a mixed type of inhibition that is relatively more competitive in its action, whereas a lower K_{ii}/K_i reflects the mixed type of inhibition that is more uncompetitive. On the other hand, when $K_{ii} = K_i$, the mode of inhibition becomes noncompetitive. For a completely competitive mode of inhibition, $K_{ii} \rightarrow \infty$ and therefore, $K_{ii}/K_i \rightarrow \infty$.[61]

For each of the macromolecular complexes value of K_i was found to be equal to K_{ii}, which is typical of a non-competitive inhibitor. For free pMo complexes, $K_{ii} > K_i$ as is the case with a mixed type of inhibitor with major mode of inhibition being of the competitive type. Data obtained from similar experiments conducted with molybdate, showed it to be competitive inhibitor of ALP, in agreement with the previous reports.[16,17,19] The K_i value determined for molybdate was 1.25 mM. From the many fold larger K_i value for molybdate relative to pMo compounds, it is evident that the pMo complexes are more potent inhibitors of ALP compared to molybdate.

Table 7.2 Half-maximal inhibitory concentration (IC_{50}) and inhibitor constants (K_i and K_{ii}) values for pMo compounds and other inhibitors against ALP

Sl. No.	Compound	$IC_{50}(\mu M)$	$K_i(\mu M)$	$K_{ii}(\mu M)$	K_{ii}/K_i	Types of inhibition
1	**PAMo**	48.64	31.72	30.31	0.95	Non-competitive
2	**PMAMo**	16.92	17.10	16.80	0.98	Non-competitive
3	**PAmMo**	18.27	19.20	18.90	0.98	Non-competitive
4	**PSMo**	24.05	25.41	25.16	0.99	Non-competitive
5	**DMo_1**	16.90	6.00	21.50	3.58	Mixed inhibition
6	**DMo_2**	17.94	7.50	24.50	3.27	Mixed inhibition
7	**Na_2MoO_4**	3208	1250	—	—	Competitive
8	Free polymer	---	---	---	---	---

Note: The ALP-catalyzed rates of hydrolysis of p-NPP at pH 10.0 were determined at 30 °C by measuring A_{405} in a reaction mixture containing ALP (3.3 μg/mL), p-NPP (2 mM) in incubation buffer (25 mM glycine + 2mM $MgCl_2$, pH10.0) in the presence of stated concentrations of the inhibitors. For polymeric compounds concentrations are on the basis of peroxometal loading.

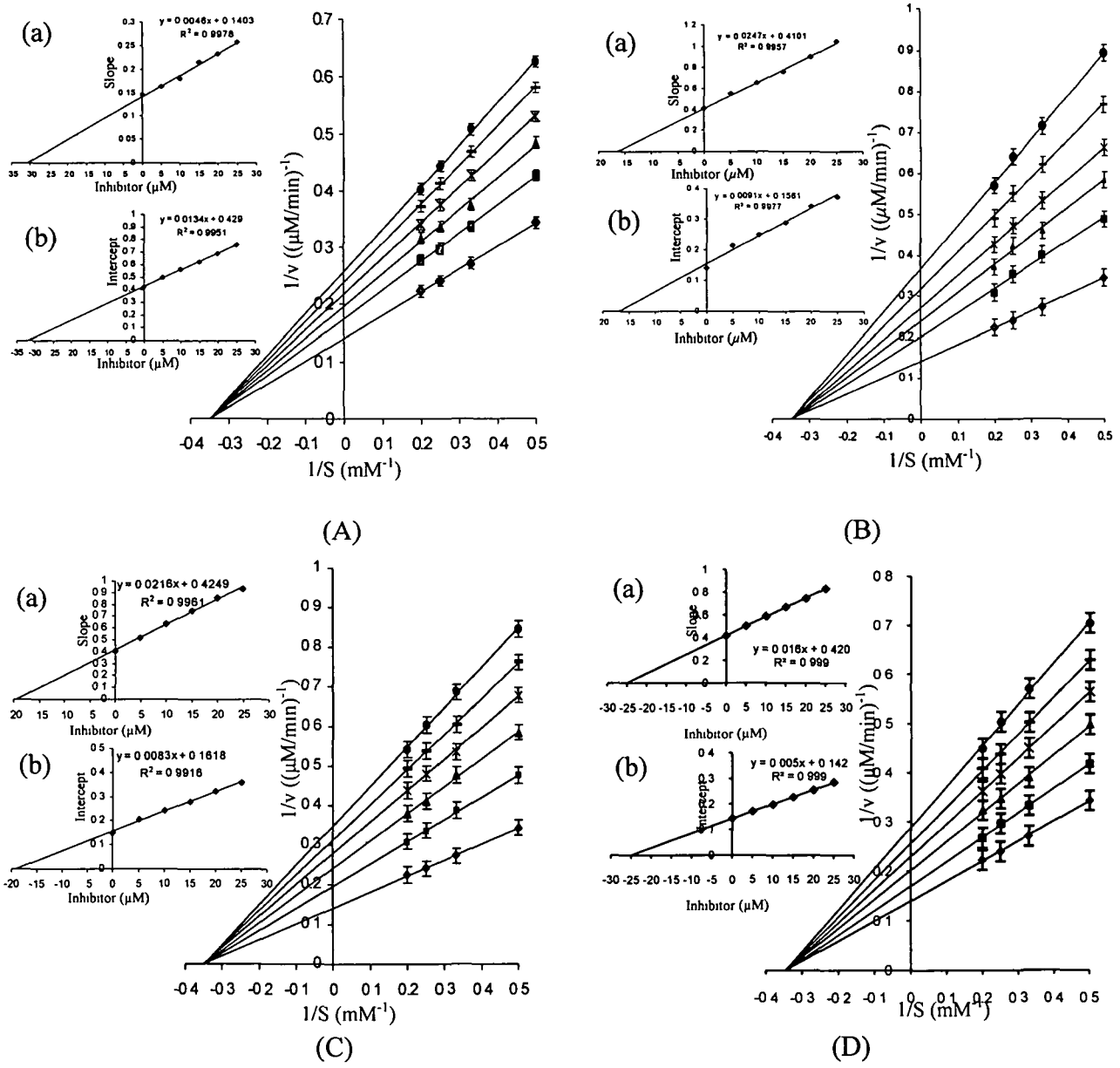

Fig. 7.8 Lineweaver-Burk plots for inhibition of ALP activity in absence and presence of (A) **PAMo**, (B) **PMAMo**,(C) **PAmMo** and (D) **PSMo**. The inset represent secondary plot of initial kinetic data of Lineweaver plot. The reaction mixture contained glycine buffer (25 mM glycine + 2 mM $MgCl_2$, pH 10.0) and p-NPP (2-5 mM). The reaction was started by adding ALP (3.3 μg/ml) to the reaction solution which was pre-incubated for 5 minutes and the rate of hydrolysis in the presence of ♦ 0 μM; ■ 5 μM; ▲ 10 μM; × 15 μM; - 20 μM; ● 25 μM inhibitors were obtained. The values are expressed as means ± SE from three separate experiments. Inset: (a) The Slopes were plotted against inhibitor concentrations and $K_i$values were obtained from the x-intercepts of these replots. (b) The vertical intercepts were plotted against inhibitor concentration and K_{ii} values were obtained from the x-intercepts of these replots. For polymeric compounds concentrations are on the basis of peroxometal loading.

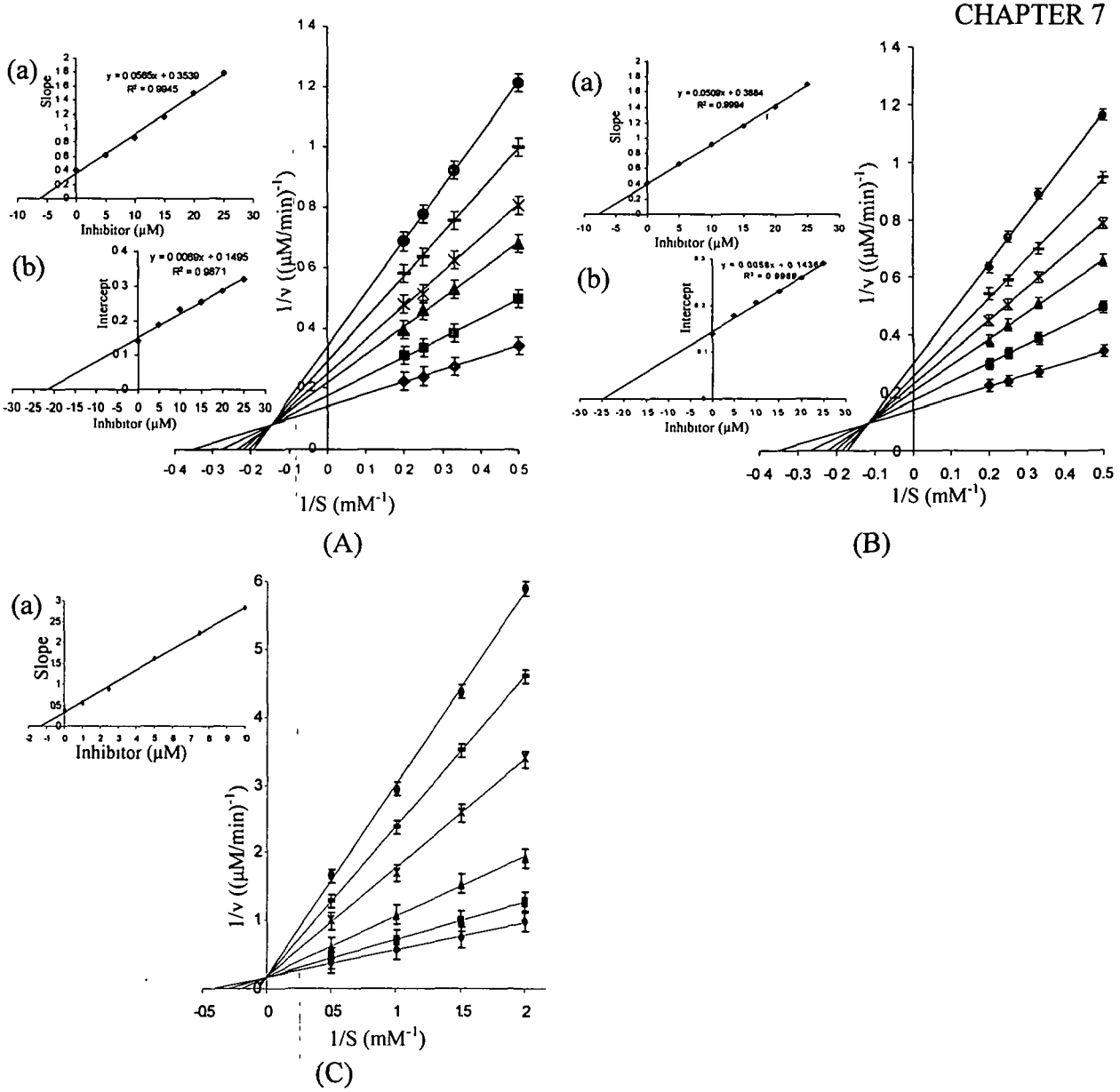

Fig. 7.9 Lineweaver-Burk plots for inhibition of ALP activity in absence and presence of (A)**DMo_1**, (B) **DMo_2** and(C) **Na_2MoO_4**. The inset represent secondary plot of initial kinetic data of Lineweaver plot. The reaction mixture contained glycine buffer (25 mM glycine + 2 mM $MgCl_2$, pH 10.0) and p-NPP (2-5 mM). The reaction was started by adding ALP (3.3 μg/ml) to the reaction solution which was pre-incubated for 5 minutes and the rate of hydrolysis in the presence of ♦ 0 μM; ■ 5μM; ▲ 10 μM; × 15 μM; - 20 μM; • 25 μM (for **DMo_1** and **DMo_2**) or ♦ 0 mM; ■ 1mM; ▲ 2.6 mM; × 5 mM; - 7.5 mM; • 10 mM (for **Na_2MoO_4**) inhibitors were obtained. The values are expressed as means ± SE from three separate experiments. Inset: (a) The Slopes were plotted against inhibitor concentrations and $K_i$values were obtained from the x-intercepts of these replots. (b) The vertical intercepts were plotted against inhibitor concentration and K_{ii} values were obtained from the x-intercepts of these replots. For polymeric compounds concentrations are on the basis of peroxometal loading.

7.3.3.2 ACP inhibition by the peroxomolybdenum compounds

The mode of inhibitory action of the polymeric pMo compounds on wheat thylakoid membrane acid phosphatase was similar to that found for the ALP as obvious from the LB plots presented in Fig. 7.11 and Fig. 7.12 and their respective kinetic data shown in Table 7.3. Considerable deviations were however noted when the values of the IC_{50} (Fig. 7.10) and inhibitor constants for the two types of enzymes were compared (Tables 7.2 and 7.3). These values for ACP were observed to be more than 20 orders of magnitude lower than those for ALP which clearly indicated a greater affinity of the complexes for the enzyme binding site of ACP compared to ALP.

From the Lineweaver-Burk plots Fig. 7.11 and Fig. 7.12 and on comparing the kinetic data it has been confirmed that polymeric pMo compounds are classical non-competitive inhibitors of ACP function whereas the free pMo compounds induce mixed-inhibition on the enzyme. The molybdate anion on the other hand shows un-competitive type of inhibition on ACP activity. It is notable that molybdate displayed un-competitive type inhibition of ACP activity under analogous conditions, in contrast to the competitive inhibition exerted on ALP. The kinetic data for the ACP inhibition by the pMo compounds indicated the following sequence which is similar to the one observed for ALP: **DMo_1 > PMAMo > DMo_2 > PAmMo > PSMo > PAMo > Na_2MoO_4.**

In this context, it is particularly interesting to note, a feature common to both the enzymes, that the IC_{50} value of the peroxo metal species anchored PMA is nearly half of that of the corresponding poly(sodium acrylate) anchored compounds in spite of these polymers having similar carboxylate functional groups as ligand sites. Pertinent here is to mention that the PA and PMA bound pV compounds also exhibited remarkable difference in their oxidant activity as well their antibacterial properties.[60] Such variations in the tested properties may be ascribed to the differences in mode of co-ordination of the metal

peroxo groups to the two polymers. In **PMAMo** and its pV containing analogue, **PMAV**[60] the diperoxo moieties are bound to the PMA chain exclusively in a monomeric fashion whereas in **PAMo** and **PAV**[60] the peroxo metals occur as dinuclear tetraperoxo species through bridging carboxylate groups of the PA chain. Consequently, ionic charge distribution and the polarity of the two compounds vary and these factors are likely to influence their availability near the enzyme active site and their ability to interact with the enzyme to different extents. It may also be relevant to note that **PMAMo** exhibited superior activity as catalyst in organic oxidations (vide Chapter 5 and 6).

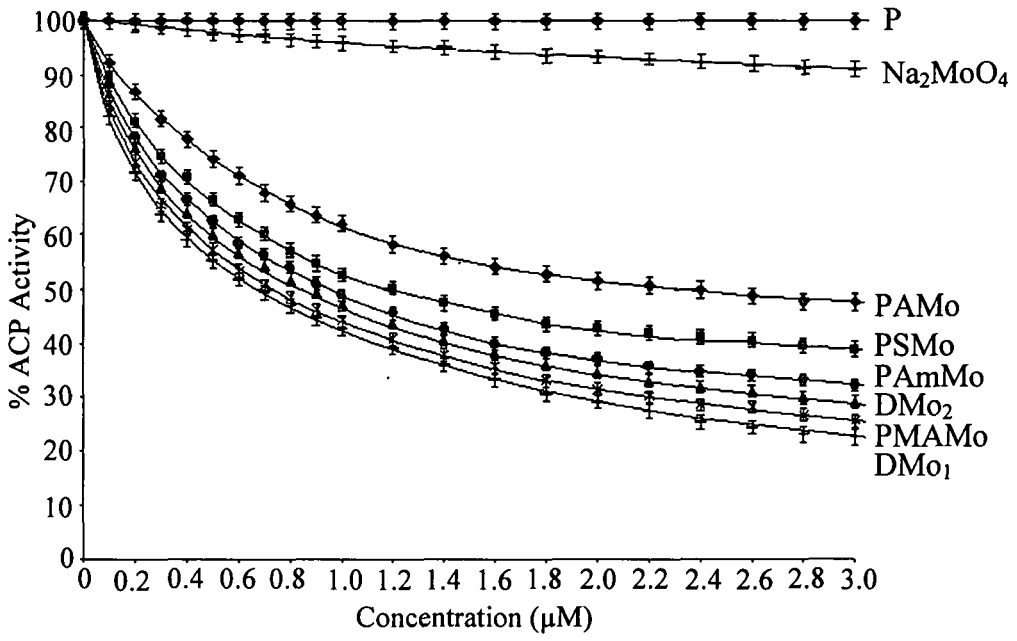

Fig. 7.10 Effect of Compounds **PAMo, PMAMo, PAmMo, PSMo, DMo_1, DMo_2, Na_2MoO_4** and free polymers (**P**) on the activity of ACP. The ACP catalyzed rates of hydrolysis of p-NPP at pH 4.6 were determined at 30 °C by measuring A_{405} in a reaction mixture containing ACP (18.38 μg/mL), p-NPP (2 mM) in acetate buffer (0.1 M, pH=4.6) in the absence or presence of stated concentrations of the inhibitors. Effects of the additions are represented as the percent values (rounded to integers) of control (Δp-NPP = 3.13 μM/min). The data are presented as the means ± SE from three separate experiments. For polymeric compounds concentrations are on the basis of peroxometal loading.

Table 7.3 Half-maximal inhibitory concentration (IC_{50}) and inhibitor constants (K_i and K_{ii}) values for pMo compounds and other inhibitors against ACP

Sl. No.	Compound	$IC_{50}(\mu M)$	$K_i(\mu M)$	$K_{ii}(\mu M)$	K_{ii}/K_i	Types of inhibition
1	**PAMo**	1.98	1.93	1.90	0.98	Non-competitive
2	**PMAMo**	0.89	0.86	0.84	0.97	Non-competitive
3	**PAmMo**	1.19	1.06	1.02	0.96	Non-competitive
4	**PSMo**	1.74	1.71	1.70	0.99	Non-competitive
5	**DMo_1**	0.67	0.61	1.95	3.19	Mixed inhibition
6	**DMo_2**	0.94	0.91	2.23	2.45	Mixed inhibition
7	**Na_2MoO_4**	377.00	250.00	---	---	Un-competitive
8	Free polymer	---	---	---	---	---

Note: The ACP catalyzed rates of hydrolysis of p-NPP at pH 4.6 were determined at 30 °C by measuring A_{405} in a reaction mixture containing ACP (18.38 μg/mL), p-NPP (2 mM) in acetate buffer (0.1 M, pH=4.6) in the presence of stated concentrations of the inhibitors (Fig. 7.11 and Fig. 7.12). For polymeric compounds concentrations are on the basis of peroxometal loading.

The afore mentioned findings from our investigation on the two types of the enzymes clearly demonstrate that there is a marked influence of the co-ligand environment on the inhibitory potency of the intact metal complexes, as well as on the mode of their inhibition of the enzymes, although the effect of the individual ligand on the ALP or ACP activity is practically negligible under the assay conditions used.

The trend emerging out of our present investigation involving effect of the title compounds on both the enzymes, ACP and ALP, reveal that the compounds tested can be grouped into two categories on the basis of their effect on the ACP and ALP hydrolysis.

The first group comprising of polymer bound metal peroxo compounds are classical non-competitive inhibitors of the phosphoproteins whereas, the free monomeric peroxomolybdates exhibits mixed inhibition indicating the presence of both competitive and non-competitive binding sites. A competitive inhibitor typically has close structural similarities to the normal substrate for the enzyme. A non-competitive inhibitor usually binds reversibly at a site other than the active site and causes a change in the overall three-dimensional shape of the enzyme that leads to a decrease in catalytic activity. Since the inhibitor binds at a different site to the substrate, the enzyme may bind to the inhibitor, the substrate or both the inhibitor and the substrate together.

Oxyanions such as vanadate,[10,16-18] molybdate and tungstate[19,20] having penta or hexa co-ordinated structures, are known to be competitive inhibitors of phosphatases which has been ascribed to their being structural analogues of phosphate.[19,20,62,63] While no exception was noted to this observation among the existing reports on ALP inhibition, in case of ACP, type of inhibition induced by these anions was found to be different to that produced by phosphate in certain cases.[12,19,47] For instance, molybdate and tungstate were observed to be non-competitive inhibitor of bovine spleen purple acid phosphatase,[64] although Gresser and co-workers[19] observed metal oxyanion inhibition of mammalian acid and alkaline phosphatases to be strictly competitive. On the other hand, Wang and co-workers reported the molybdate and vanadate to be uncompetitive and non-competitive inhibitors, respectively of the activity of wheat thylakoid membrane ACP.[47] In agreement with previous reports we have found that vanadate, molybdate and tungstate inhibit the activity of mammalian ALP in a competitive manner.[21,65,66] In the present study we observed molybdate to exert un-competitive inhibition on ACP. The information derived thus implied that different oxometallates, in spite of sharing common structural features, may differ in their mechanistic preferences in the inhibition of the various phosphatases.

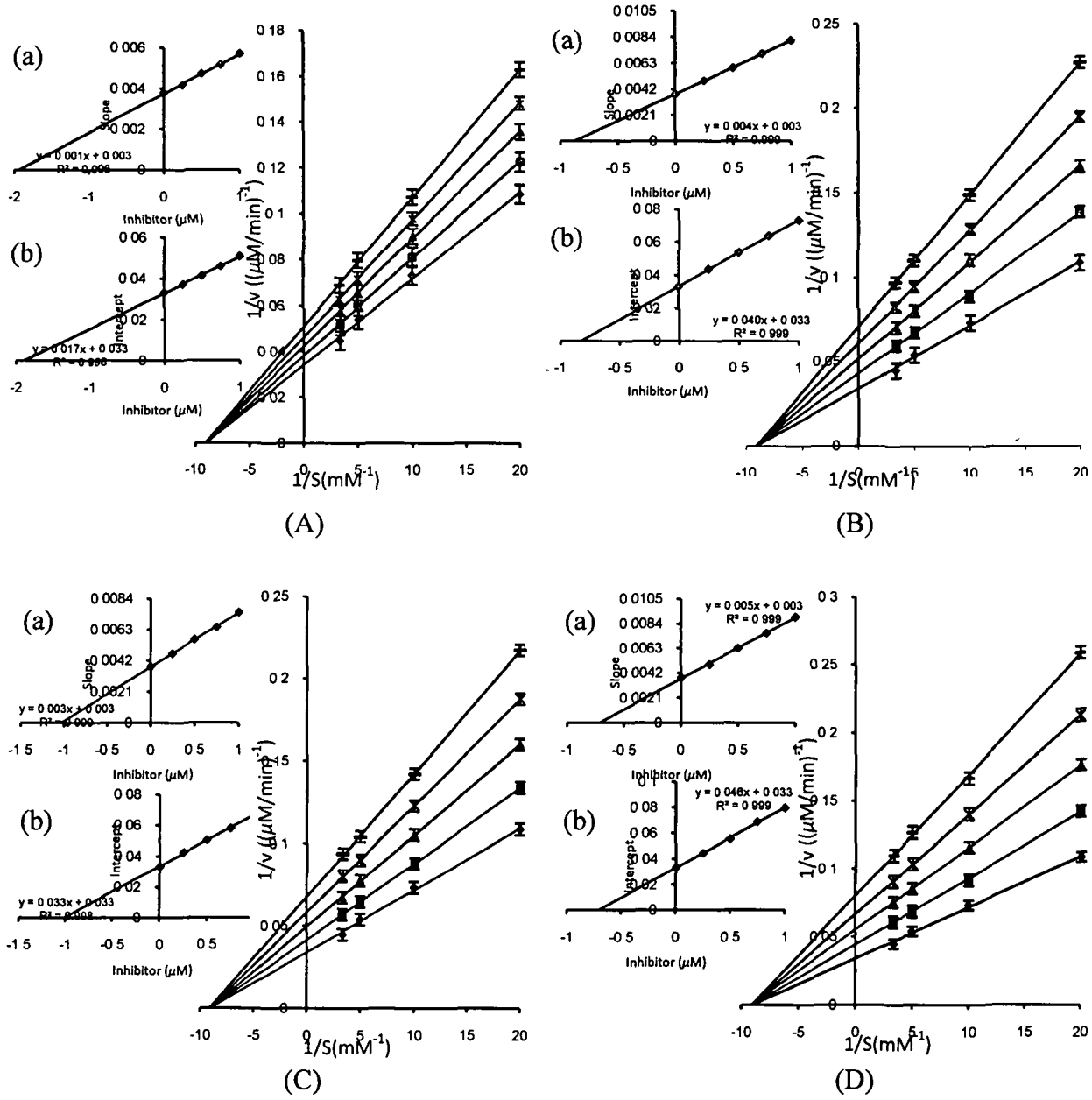

Fig. 7.11 Lineweaver-Burk plots for inhibition of ACP activity in absence and presence of (A) **PAMo**, (B) **PMAMo**, (C) **PAmMo** and (D) **PSMo**. The inset represent secondary plot of initial kinetic data of Lineweaver plot. The reaction mixture contained acetate buffer (0.1 M, pH 4.6) and p-NPP (50-300 μM). The reaction was started by adding ACP (18.38 μg/ml) to the reaction solution which was pre-incubated for 5 minutes and the rate of hydrolysis in the presence of ♦ 0 μM; ■ 0.25 μM; ▲ 0.50 μM; ⁎0.75 μM; — 1.00 μM inhibitors were obtained. The values are expressed as means ±SE from three separate experiments. Inset: (a) The Slopes were plotted against inhibitor concentrations and Ki values were obtained from the x-intercepts of these replots. (b) The vertical intercepts were plotted against inhibitor concentration and Kii values were obtained from the x-intercepts of these replots. For polymeric compounds concentrations are on the basis of peroxometal loading.

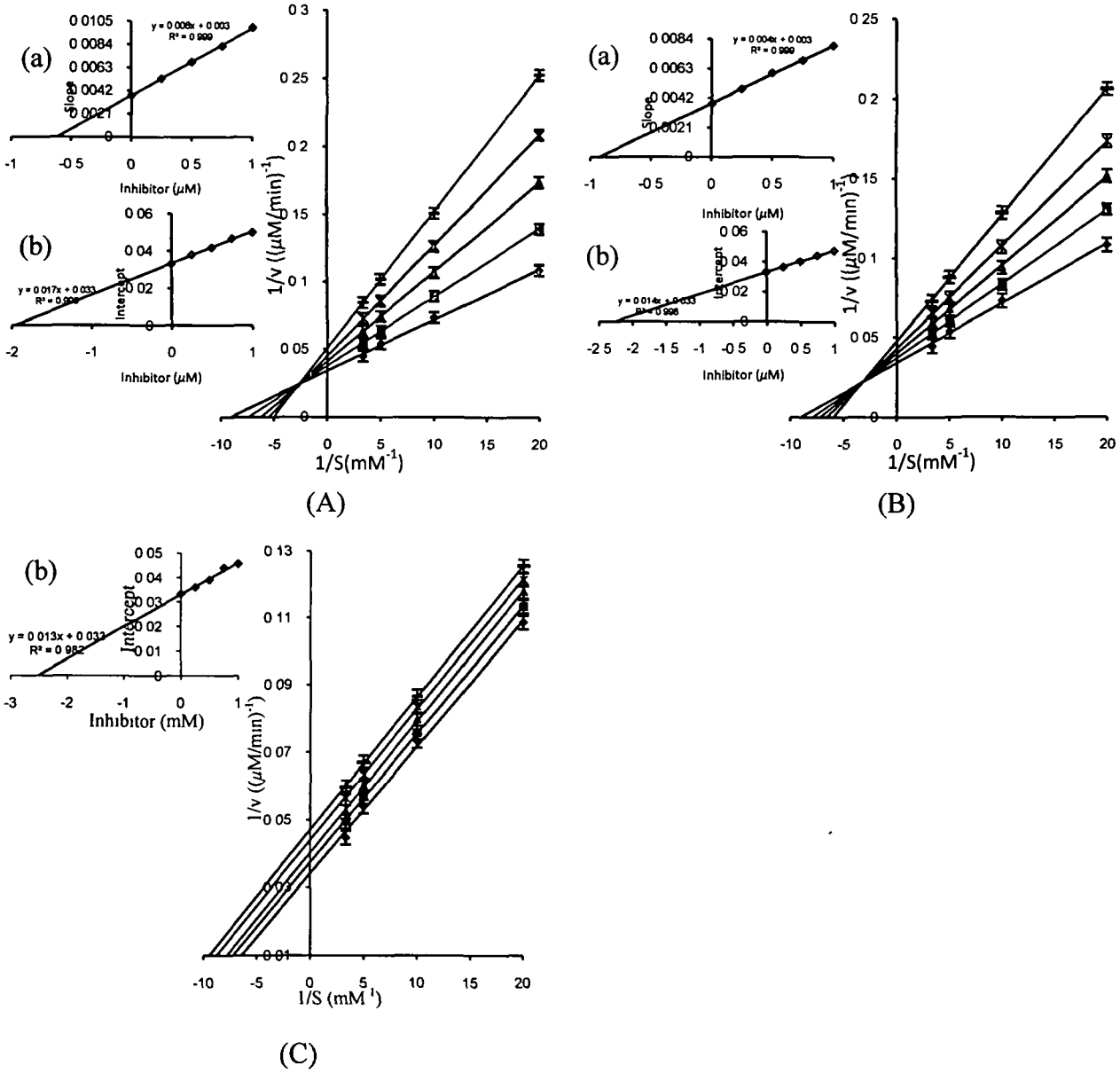

Fig. 7.12 Lineweaver-Burk plots for inhibition of ACP activity in absence and presence of (A) **DMo_1**, (B) **DMo_2** and (C) **Na_2MoO_4**. The inset represent secondary plot of initial kinetic data of Lineweaver plot. The reaction mixture contained acetate buffer (0.1 M, pH 4.6) and p-NPP (50-300 μM). The reaction was started by adding ACP (18.38 μg/ml) to the reaction solution which was pre-incubated for 5 minutes and the rate of hydrolysis in the presence of ♦ 0 μM; ■ 0.25 μM; ▲ 0.50 μM;∗ 0.75 μM; — 1.00 μM (for **DMo_1** and **DMo_2**)or ♦ 0 mM; ■ 0.25 mM; ▲ 0.50 mM; ∗ 0.75 mM; — 1.00 mM (for **Na_2MoO_4**) inhibitors were obtained. The values are expressed as means ±SE from three separate experiments. Inset: (a) The Slopes were plotted against inhibitor concentrations and Ki values were obtained from the x-intercepts of these replots. (b) The vertical intercepts were plotted against inhibitor concentration and Kii values were obtained from the x-intercepts of these replots. For polymeric compounds concentrations are on the basis of peroxometal loading.

A perusal of literature shows that there is a paucity of information on the effect of synthetic heteroligand pMo compounds on different enzyme functions including phosphatases, although inhibitory effect of synthetic peroxovanadates have been extensively investigated.[16,17,30,31,39,40,67-69] Majority of the tested synthetic pV compounds on ALP inhibitory activity were competitive in nature, however, there are examples of mixed-inhibition of Green-crab ALP by diperoxovanadate compounds with considerably large K_I and K_{II} values in milimolar range.[67,68] Earlier studies suggested that one or more of the various parameters such as oxidation state of the metal, co-ordination geometry, stability of the compounds under physiological conditions, and the nature of the phosphoproteins may be responsible in deciding the ACP or ALP inhibitory ability of different vanadium derivatives, including peroxovanadates.[17,21]

Owing to large size of the macromolecular complexes they are unlikely to be capable of approaching the enzyme active site and hence would possibly prefer to interact with the enzyme at a site away from the active site which may result in change in overall conformation of the protein and inhibition of its function in a non-competitive manner.[12] Even the non-competitive inhibition induced by molybdate and tungstate on bovine spleen purple acid phosphatase was previously ascribed to the larger size of these ions.[12] It has been further suggested that the high oxidative compounds such as molybdate and tungstate would oxidize Fe^{2+} of the enzyme ACP and oxidize it to ferric and inactivate the enzyme non-competitively.[12] The importance of redox properties of peroxo compounds has also been documented in inhibition of protein phosphatases.[16,17] It was reported earlier that peroxovanadate effectively inhibited the tyrosine phosphatase by oxidizing the critical cysteine residue in catalytic domain of the enzyme.[16,69,70] It is known that the presence of such groups in and around the active centre of the enzymes are essential for the activity and in stabilization of the quaternary structure of the enzyme.[47] Taking into

account these observations and our own findings on the oxidant activity of the complexes under investigation, it may be logical to expect that the compounds exert their inhibitory effect by interacting with the essential groups susceptible to oxidation such as –SH.[40,71] Results presented in the Chapters 5 and 6 of the present thesis have already demonstrate that each of the inhibitory pMo complexes is indeed active oxidant of organic bromides as well as sulfides. For the neat pMo compounds both the mechanisms i.e. transition state analogy as well as oxidation ability of these compounds are likely to be responsible for the mixed inhibition displayed by these compounds combining competitive and non-competitive pathways. However, being aware of the complex nature of the species involved and their reaction with the biomolecules, and in absence of direct evidence, we are constrained in commenting on the actual pathway of inhibition of the model enzymes by the tested compounds. Many experiments will clearly be necessary to unravel the exact mechanism.

7.4 CONCLUSIONS

The results of the present investigation demonstrated that pMo compounds in diverse co-ligand environment, irrespective of being monomeric or polymer supported are potent inhibitors of the function of two types of the model enzymes, rabbit intestine alkaline phosphatase (ALP) and wheat thylakoid membrane acid phosphatases (ACP). The detailed study of their inhibition kinetics revealed that the macrocomplexes and the neat monomeric compounds exert their inhibitory effect on the enzymes via distinct pathways. Each of the polymer bound peroxomolybdates tested is a non-competitive inhibitor of both the enzymes, in contrast to the mixed type of inhibition displayed by the neat complexes. Interestingly, all the tested pMo complexes were capable of inhibiting ACP activity even at sub-micromolar concentration thus showing several fold greater inhibitor affinity for ACP over ALP. Additional notable attribute of the polymer supported compounds is their enhanced resistance to degradation under the effect of the powerful enzyme catalase. This may be relevant in the cellular milieu where H_2O_2 has little chance to survive abundant catalase. There has been efforts to find stable peroxo derivatives for therapeutic application, which may be an effective alternative to H_2O_2, preferably at far lower concentrations and hence unlikely to cause cytotoxicity to the normal cells. It is remarkable that the compounds retain their structural integrity in solution not only at higher pH but also under acidic conditions. The compounds thus show prospect of being useful for *in-vivo* study even at strongly acidic condition which exist in human stomach. This feature may be significant in view of the reports that orally administered pV was ineffective as anti-diabetic drug in rats as it could not survive the strong acidity of the stomach.[59]

REFERENCES

1. Kaija, H., Patrikainen, L.O.T., Alatalo, S.L, Vaananen, H.K. & Vihko, P.T. *Acid Phosphatases* in *Dynamics of Bone and Cartilage Metabolism: Principles and Clinical Applications*, M.J. Seibel et al., eds., 2nd ed., Academic Press, USA, 2006, 165-200.

2. Tabaldi, L.A., et al. *Environ. Exp. Bot.* **59**, 43--48, 2007.

3. Cathala, G., & Brunel, C. *J. Biol. Chem.* **250**, 6040--6045, 1975.

4. Kozlenkov, A., et al. *J. Biol. Chem.* **277**, 22992--22999, 2002.

5. Whyte, M.P. *Endocr. Rev.* **15**, 439--461, 1994.

6. Wilcox, D.E. *Chem. Rev.* **96**, 2435--2458, 1996.

7. Puri, D. *Textbook of Biochemistry: A Clinically Oriented Approach*, B.I. Churchill Livingstone Pvt. Ltd., New Delhi, 2002, 174-175.

8. Holtz, K.M., & Kantrowitz, E.R. *FEBS Lett.* **462**, 7--11, 1999.

9. Bull, H., et al. *J. Clin. Pathol: Mol. Pathol.* **55**, 65--72, 2002.

10. Shechter, Y., et al. *Coord. Chem. Rev.* **237**, 3--11, 2003.

11. Lipscomb, W.N., & Strater, N. *Chem. Rev.* **96**, 2375--2434, 1996.

12. Vincent, J.B., et al. *Biochemistry* **30**, 3025--3034, 1991.

13. Donald, F.H., et al. *Biochem. Biophys. Res. Commun.* **144**, 1154--1160, 1987.

14. Ketcham, C.M., et al. *J. Biol. Chem.* **264**, 557--563, 1989.

15. Lord, D.K., et al. *Eur. J. Biochem.* **189**, 287--293, 1990.

16. Crans, D.C., et al. *Chem. Rev.* **104**, 849--902, 2004.

17. Crans, D.C. Peroxo hydroxylamido and acac derived vanadium complexes: Chemistry, biochemistry and insulinmimetic action of selected vanadium compounds, in *Vanadium Compounds Chemistry, Biochemistry, and Therapeutic Application*, A.S. Tracy, & D.C. Crans, eds., Oxford University Press, New York, 1998, 82-103.

18. Rehder, D., Bashirpoor, M., Jantzen, S., Schmidt, H., Farahbakhsh, M. & Nekola, H. Structural and functional models for biogenic vanadium compounds, in *Vanadium Compounds Chemistry, Biochemistry, and Therapeutic Application*, A.S. Tracy & D.C. Crans, eds., Oxford University Press, New York, 1998, 60-71.

19. Stankiewicz, P.J., & Gresser, M.J. *Biochemistry* **27**, 206--212, 1988.

20. Soman, G., et al. *Biochemistry* **22**, 4994--5000, 1983.

21. Louie, A.Y., & Meade, T.J. *Chem. Rev.* **99**, 2711--2734, 1999.

22. Jelikic-Stankov, M., et al. *J. Trace Elem. Med. Biol.* **21**, 8--16, 2007.

23. Kustin, K. Perspective on vanadium biochemistry, in *Vanadium Compounds Chemistry, Biochemistry, and Therapeutic Applications,* A.S. Tracy & D.C. Crans, eds., Oxford University Press, New York, 1998, 170-185.

24. Goto, Y., et al. *Biochem. Pharmacol.* **44**, 174--177, 1992.

25. Li, J., et al. *Biochemistry* **34**, 6218--6225, 1995.

26. Fraqueza, G., et al. *J. Inorg. Biochem.* **107**, 82--89, 2012.

27. McLauchlan, C.C., et al. *J. Inorg. Biochem.* **104**, 274--281, 2010.

28. Li, M., et al. *J. Inorg. Biochem.* **102**, 1846--1853, 2008.

29. Crans, D.C., et al. *Phosphorus, Sulfur Silicon Relat. Elem.* **109**, 245--248, 1996.

30. Bevan, A.P., et al. *Mol. Cell. Biochem.* **153**, 49--58, 1995.

31. Posner, B.I., et al. *J. Biol. Chem.* **269**, 4596--4604, 1994.

32. Crans, D.C., et al. *J. Am. Chem. Soc.* **111**, 7597--7607, 1989.

33. Crans, D.C., et al. *Anal. Biochem.* **188**, 53--64, 1990.

34. Williams, P.A.M., et al. *J. Inorg. Biochem.* **75**, 99--104, 1999.

35. Etcheverry, S.B., et al. *Biol. Trace Elem. Res.* **84**, 227--238, 2001.

36. Salice, V.C., et al. *Mol. Cell. Biochem.* **198**, 119--128, 1999.

37. Tracey, A.S. *J. Inorg. Biochem.* **80**, 11--16, 2000.

38. Cortizo, A.M., et al. *Biol. Trace Elem. Res.* **41**, 331--339, 1994.

39. Vescina, C.M., et al. *Biol. Trace Elem. Res.* **53**, 185--191, 1996.

40. Huyer, G., et al. *J. Biol. Chem.* **272**, 843--851, 1997.

41. Thompson, K.H., & Orvig, C. *J. Inorg. Biochem.* **100**, 1925--1935, 2006.

42. Orvig, C., et al. *J. Inorg. Biochem.* **96**, 14--27, 2003.

43. Djordjevic, C., et al. *Mol. Cell. Biochem.* **153**, 25--29, 1995.

44. Thompson, K.H., et al. *Chem. Rev.* **99**, 2561--2572, 1999.

45. Sarmah, S., et al. *Polyhedron* **23**, 1097--1107, 2004.

46. Sarmah, S., et al. *Mol. Cell. Biochem.* **236**, 95--105, 2002.

47. Fei, M.-J., et al. *J. Integr. Plant Biol.* **48**, 294--299, 2006.

48. Chelikani, P., et al. *Indian J. Clin. Biochem.* **20**, 131--135, 2005.

49. Madureira, P.A., & Waisman, D.M. *Int. J. Mol. Sci.* **14**, 3568--3594, 2013.

50. Chatterjee, N., et al. *Mech. Ageing Dev.* **132**, 230--239, 2011.

51. Giorgio, M., et al. *Nat. Rev. Mol. Cell Biol.* **8**, 722--728, 2007.

52. Ravishankar, H.N., et al. *Arch. Biochem. Biophys.* **321**, 477--484, 1995.

53. Sarmah, S., et al. *Polyhedron* **21**, 389--394, 2002.

54. Hazarika, P., et al. *Mol. Cell. Biochem.* **284**, 39--47, 2006.

55. Hazarika, P., et al. *Transition Met. Chem.* **33**, 69--77, 2008.

56. Hazarika, P., et al. *J. Enzyme Inhib. Med. Chem.* **23**, 504--513, 2008.

57. Kalita, D., et al. *Biol. Trace Elem. Res.* **128**, 200--219, 2009.

58. Ferreira, C.V., et al. *Plant Sci.* **147**, 49--54, 1999.

59. Shisheva, A., et al. *Endocrinol.* **134**, 507--510, 1994.

60. Kalita, D., et al. *React. Funct. Polym.* **68**, 876--890, 2008.

61. Barr, J.T., & Jones, P.J. *Drug Metab. Dispos.* **39**, 2381--2386, 2011.

62. Heo, Y.S., et al. *Exp. Mol. Med.* **34**, 211--223, 2002.

63. VanEtten, R.L., et al. *J. Am. Chem. Soc.* **96**, 6782--6785, 1974.

64. Garces, F.O., et al. *Macromolecules* **27**, 272--278, 1994.

65. Ravindranath, V. Animal models and molecular markers for cerebral ischemia reperfusion injury in brain, in *Methods in enzymology*, L. Packer, ed., Academic press, New York, 1994, **233**, 613.

66. Lopez, V., et al. *Arch. Biochem. Biophys.* **175**, 31--38, 1976.

67. Zhou, X.-W., et al. *Biochemistry (Moscow)* **65**, 1424--1428, 2000.

68. Zhou, X.-W., et al. *J. Protein Chem.* **18**, 735--740, 1999.

69. Tracey, A.S., Willsky, G.R. & Takeuchi, E.S. *Vanadium: Chemistry, Biochemistry, Pharmacology and Practical Application,* CRC Press and Taylor & Francis Group, Boca Raton, 2007.

70. Meister, G.E., & Butler, A. *Inorg. Chem.* **33**, 3269--3275, 1994.

71. Jonsson, C.M., et al. *Ecotoxicology* **18**, 610--619, 2009.

List of Publication

1. *Peroxomolybdate(VI) Complexes Bound to Merrifield Resin: Synthesis, Characterization and Catalytic Properties Towards Selective Oxidation of Sulfides*
   Jeena Jyoti Boruah, Siva Prasad Das, Seshadri Reddy Ankireddy, Sandhya Rani Gogoi and Nashreen S. Islam (*Green Chem.*, under revision)

2. *Polymer-anchored Peroxo Compounds of Molybdenum and Tungsten as Efficient and Versatile Catalysts for Mild Oxidative Bromination*
   Jeena Jyoti Boruah, Siva Prasad Das, Rupam Borah, Sandhya Rani Gogoi and Nashreen S. Islam
   Polyhedron **52**, 246--254, 2013. *(Werner Special Issue)*

3. *Polymer-Anchored Peroxo Compounds of Vanadium(V) and Molybdenum(VI): Synthesis, Stability, and Their Activities with Alkaline Phosphatase and Catalase*
   Jeena Jyoti Boruah, Diganta Kalita, Siva Prasad Das, Saurav Paul and Nashreen S. Islam
   Inorganic Chemistry **50**, 8046--8062, 2011.

4. *Selective oxidation of organic sulfides by mononuclear and dinuclear peroxotungsten(VI) complexes*
   Siva Prasad Das, **Jeena Jyoti Boruah**, Hiran Chetry and Nashreen S. Islam
   Tetrahedron Letters **53**, 1163--1168, 2012.

5. *New Polymer-Immobilized Peroxotungsten Compound as an Efficient Catalyst for Selective and Mild Oxidation of Sulfides by Hydrogen Peroxide*
   Siva Prasad Das, **Jeena Jyoti Boruah**, Niharika Sharma and Nashreen S. Islam
   Journal of Molecular Catalysis A: Chemical **356**, 36--45, 2012.

6. *Synthesis and Characterization of Peroxotungsten (VI) Complexes Bound to Water Soluble Macromolecules. Their Interaction with Acid and Alkaline Phosphatases*
   Siva Prasad Das, Seshadri Reddy Ankireddy, **Jeena Jyoti Boruah** and Nashreen S. Islam
   RSC Advances **2**, 7248--7261, 2012.

7. *Vasomodulatory effect of novel peroxovanadate compounds on rat aorta: Role of rho kinase and nitric oxide/cGMP pathway*
   Vivek Khanna, Manish Jain, Manoj Kumar Barthwal, Diganta Kalita, **Jeena Jyoti Boruah**, Siva Prasad Das, Nashreen S. Islam, Tangirala Ramasarma and Madhu Dikshit
   Pharmacological Research **64**, 274--282, 2011.

****